



# **Molecular Basis of Adaptation of Enteroviruses to Different Cancer Cell Lines**

Naseebh Nabih A. Baeshen

A thesis submitted for the degree of Doctor of Philosophy in Molecular Medicine

School of Biological Sciences

University of Essex

April 2015

# Table of Contents

<b>Acknowledgments .....</b>	<b>i</b>
<b>Abstract ..</b>	<b>iii</b>
<b>Abbreviations.....</b>	<b>v</b>
<b>List of Figures .....</b>	<b>ix</b>
<b>List of Tables.....</b>	<b>xiv</b>
<b>Chapter 1 Introduction .....</b>	<b>1</b>
1.1 Introduction to Virology.....	2
1.2 Picornavirus Classification and Importance.....	3
1.3 Picornavirus Structure .....	9
1.3.1 Particle Structure.....	9
1.3.2 Genome Structure and Organization.....	12
1.3.3 Picornavirus Life Cycle and Replication .....	15
1.3.3.1 Cellular Receptors.....	17
1.3.3.1.1 Integrins.....	20
1.3.3.1.2 Heparan Sulphate Proteoglycans.....	22
1.3.3.1.3 Decay-accelerating factor.....	26
1.3.3.1.4 Immunoglobulin Superfamily Receptors: ICAM.....	29
1.3.3.1.5 LDLR family .....	30
1.3.3.1.6 PSGL-1 and SCARB2 .....	31
1.3.3.1.7 Sialic Acid .....	32
1.3.4 Viral Entry .....	32
1.3.4.1 Clathrin-mediated Endocytosis (CME) .....	35
1.3.4.2 Caveolar/lipid rafts-dependent Endocytosis .....	35

1.3.4.3	Macropinocytosis.....	36
1.3.5	Particle Uncoating and Genome Release .....	36
1.3.6	Translation.....	37
1.3.7	Polyprotein processing .....	38
1.3.8	Genome Replication .....	40
1.3.9	Assembly and Maturation .....	41
1.4	Tropism of Picornaviruses .....	41
1.4.1	Picornavirus Receptors .....	42
1.4.2	Other Tropism Determinants .....	43
1.5	History of Coxsackieviruses and Their Importance .....	44
1.5.1	Coxsackievirus A9.....	46
1.5.1.1	General Properties .....	46
1.5.1.2	Cellular Receptors and Endocytosis.....	46
1.6	Echoviruses .....	47
1.6.1	Echovirus 11.....	48
1.7	Cancer.....	49
1.7.1	Cancer- An Introduction.....	49
1.8	Oncolytic Virotherapy (OV).....	50
1.8.1	History of Oncolytic Viruses.....	50
1.8.2	Potential Oncolytic Viruses in Cancer Therapy .....	51
1.9	Aims of This Thesis .....	54
<b>Chapter 2 Material and Methods .....</b>		<b>55</b>
2.1	Materials .....	56
2.1.1	Virus Strains .....	56
2.1.2	Mammalian Cell Lines .....	56

2.1.3	Tissue Culture Reagents .....	57
2.1.4	General Chemicals / Solutions .....	58
2.1.5	Chemical inhibitors .....	58
2.1.6	Antibodies .....	59
2.1.7	Plaque Overlay Medium and Crystal Violet Stain.....	59
2.1.8	Immunofluorescence Reagents.....	60
2.1.9	Extraction and Purification Techniques .....	60
2.1.10	Reverse Transcription Polymerase Chain Reaction (RT-PCR).....	61
2.1.10.1	Primers .....	61
2.1.11	Agarose Gel Electrophoresis.....	61
2.2	Methods.....	65
2.2.1	Cell Biology and Virology Techniques .....	65
2.2.1.1	Passaging Cell Lines .....	65
2.2.1.2	Cryopreservation of Mammalian Cells for Storage.....	65
2.2.1.3	Viral Plaque Assay .....	66
2.2.1.4	Viral Propagation.....	67
2.2.1.5	Plaque purification from Virus Stock.....	67
2.2.1.6	Tropism of Enteroviruses to Different Cell Lines .....	67
2.2.1.7	Flow Cytometry Analysis of CD55 Surface Expression on Different Cell Lines .....	68
2.2.1.8	Virus Blocking Assay Using Soluble Heparin .....	69
2.2.1.9	Temperature Sensitivity Assays .....	69
2.2.1.10	Virus Blocking Assays Using Chemicals .....	70
2.2.1.10.1	Metal Ions-dependence ( $\text{Ca}^{2+}$ , $\text{Mg}^{2+}$ ) .....	70

2.2.1.11	Virus Blocking Assays Using Monoclonal Antibodies (Immunofluorescence).....	70
2.2.2	Molecular Techniques .....	71
2.2.2.1	Viral RNA Purification from Tissue Cultures.....	71
2.2.2.2	Reverse transcriptase polymerase chain reaction (RT-PCR) Technique (cDNA synthesis).....	72
2.2.2.3	Agarose Gel Electrophoresis.....	75
2.2.2.4	DNA Purification from Agarose Gel (Gel Extraction).....	75
2.2.2.5	DNA Purification using PCR Purification Kit.....	76
2.2.3	Bioinformatics Techniques .....	77
2.2.3.1	DNA Sequencing and Sequence Analysis .....	77
2.2.3.2	Three-Dimensional Structure (3D).....	77
<b>Chapter 3 Enterovirus Tropism in Different Cell lines .....</b>		<b>78</b>
3.1	Introduction.....	79
3.2	Analysis of a Panel of Enteroviruses on Different Cell Lines.....	81
3.2.1	Infectivity Assay of Enteroviruses on GMK, A549, MCF7, PC3, MDA-MB- 231, HeLa, MDA-MB-435, HT-29 and RD cells.....	81
3.3	Analysis of DAF (CD55) Surface Expression on Different Cell Lines by Flow Cytometry.....	86
3.3.1	Conclusion of Cell Tropism and Receptor Expression Studies .....	91
3.4	Adaptation of an Echovirus 11 Isolate (E11 V5-7A) to A549 and HeLa Cells.....	92
3.4.1	Capsid Sequences of Echovirus 11 Strain E11 V5-7A.....	92
3.4.2	Relationship of E11 V5-7A to other E11 Isolates .....	92

3.4.3	Generation of Adapted Variants of E11 V5-7A by Passaging on A549 and HeLa Cells .....	97
3.4.4	Sequencing of Passaged E11 V5-7A .....	99
3.4.5	Sequence Analysis of Passaged E11 V5-7A.....	99
3.4.6	A549-adapted E11 V5-7A.....	101
3.4.7	Sequence alignment of E11 V5-7A with other E11 Isolates .....	106
3.4.8	HeLa-adapted E11 V5-7A .....	111
3.5	Discussion .....	118
<b>Chapter 4 Heparan Sulphate Interaction with Coxsackievirus A9 (CVA9) .....</b>		<b>125</b>
4.1	Introduction.....	126
4.2	Comprehensive Analysis of the CVA9 Mechanism of Adaptation to Heparan Sulphate Using CVA9 Griggs, CVA9 CO62 and CVA9 CO87 ....	127
4.2.1	Adaptation of CVA9 Isolates to A549 Cells .....	127
4.2.2	Sequencing of CVA9 CO87, CO62 and Griggs Plaques.....	129
4.2.3	Isolate CO87 Analysis .....	129
4.2.3.1	Inhibition of Infection of CVA9 CO87 by Soluble Heparin .....	129
4.2.3.2	Sequence Analysis of CO87 Isolate .....	132
4.2.4	Isolate CO62 Analysis .....	142
4.2.4.1	Inhibition of Infection of CVA9 CO62 by Soluble Heparin .....	142
4.2.4.2	Sequence Analysis of CO62 Isolate .....	145
4.2.5	Isolate CVA9 Griggs Analysis.....	148
4.2.5.1	Inhibition of Infection of CVA9 Griggs by Soluble Heparin .....	148
4.2.5.2	Sequence Analysis of CVA9 Griggs Variants.....	148
4.3	Mapping All Amino Acids Differences onto the 3D Structure of CVA9 .....	155

4.4	Mapping All Amino Acids Differences of CVA9 Compared to E11 onto the 3D Structure of CVA9 .....	157
4.5	Analysis of the Effect of A549-adapting Mutations .....	160
4.5.1	Location of A549-adapting Mutations .....	160
4.5.2	Integrin $\alpha_v\beta_3$ and $\alpha_v\beta_6$ Antibody Blocking of Infections .....	160
4.5.3	Metal Ion-dependence ( $\text{Ca}^{2+}$ , $\text{Mg}^{2+}$ ) .....	163
4.5.4	Temperature Sensitivity Assays .....	166
4.6	Discussion .....	169
<b>Chapter 5 General Discussion and Future Work .....</b>		<b>175</b>
5.1	General Discussion .....	176
5.2	Future Work.....	178
<b>References .....</b>		<b>180</b>
<b>Appendices .....</b>		<b>208</b>
Appendix 1 .....		209
Appendix 2.....		217

## Acknowledgments

Undertaking this PhD has been a truly life-changing experience for me and it would not have been possible to do without the support and guidance that I received from many people.

My sincere thanks and gratitude go first of all to my supervisor Professor Glyn Stanway whose guidance, patience, encouragement, constant feedback and evaluated criticism made possible all the achievements reported in this work.

I would also like to say a heartfelt thank you to my Mum, Dad and all my family members for their conscientious support and encouragement, which made this PhD possible. They are the most important people in my world and I dedicate this thesis to them.

My great appreciation and thanks go to my colleagues in the laboratory 5.14 past and present; particularly Dr. Shaia Al-Malki, Dr. Arsalan Salimi, Ehab Baghdadi, Ashjan Shami, Ali Khrid, Cheryl Eno-Ibanga and Marina Ioannou, for their help and friendly-work environment during this project. Great thanks also go to Dr. Cigdem Williams, Ms. Natalie Gray and Ms. Hannah Adams for all their help and sharing their experience during my PhD.

Special thanks go to Professor Elena Klenova for her valued advices and providing cancer cell lines. Great thanks also to Professor Nelson Fernandez and Mr. Hussain Al-Ssadh for providing cancer cell lines and who were always so helpful in numerous ways. Many thanks to Dr. Philippe Laissue for the training I have

received on the use of bioimaging facilities. Special thanks also go to Dr. Andrea Mohr for her advices and guidance on the use of flow cytometry.

Finally, I would like to thank my government for all the support I received and their scholarship.

## Abstract

Viral oncolytic therapy, a novel treatment for cancer using specially designed viruses to kill malignant cells while leaving normal cells unharmed, is currently under intense investigation. Several receptors are up-regulated in cancer cells, including decay-accelerating factor (DAF; CD55) and integrins ( $\alpha_v\beta_3$ ,  $\alpha_v\beta_6$ ) and viruses which recognise these receptors could be useful for therapy. Several echoviruses, including Echovirus 11 (E11), bind to DAF; coxsackievirus A9 (CVA9) utilizes an RGD motif to bind to integrins, particularly  $\alpha_v\beta_6$ . Some isolates of CVA9 also bind to heparan sulfate proteoglycans (HSPG). This thesis describes work designed to improve our understanding of CVA9 and echovirus cell/receptor tropism. Several echoviruses and CVA9 variants were tested in a panel of 9 cell lines. Distinct patterns of infection were seen, but did not fully correlate with receptor expression, suggesting that other determinants also help to define tropism. To investigate this further, E11 was adapted by passaging on two cell lines, A549 and HeLa. Two mutations were seen in A549-adapted virus, and both mapped to the DAF-binding footprint, suggesting changes to E11/DAF interactions. A single mutation in VP4 was seen in HeLa-adapted virus, and may affect a later stage in cell entry. To investigate CVA9 binding to HSPG, 3 isolates were propagated on A549 cells and heparin-blocked mutants were isolated. Although the isolates are diverse, the same mutation (VP3 Q59R) was seen in two isolates and probably gives a positively-charged cluster with adjacent amino acids. Other mutations were seen close to the RGD motif, where there is already a highly basic sequence. The results suggest multiple potential mechanisms for HSPG-binding. Combinations of some of the adapting mutations discovered could

significantly enhance the tropism of these viruses to specific cancer cells and optimise them as oncolytic agents.

## Abbreviations

A549	Human Lung Adenocarcinoma Epithelial Cell Line
Arf6	ADP-ribosylation Factor 6
Bp	Base pair
CAR	Coxsackievirus and Adenovirus Receptor
CCP	Clathrin-coated Pit
CCV	Clathrin-coated Vesicle
cDNA	Complementary DNA
CMC	Carboxymethyl Cellulose
CME	clathrin-mediated endocytosis
CNS	Central Nervous System
CPE	Cytopathic Effect
CVA	Coxsackie virus A
CVA9	Coxsackievirus A9
CVB	Coxsackie virus B
DAF	Decay Accelerating Factor, know as CD55
DMEM	Dulbecco's Modified Eagle's Medium
DMSO	Dimethyl Sulfoxide
DNA	Deoxyribonucleic Acid
E11	Echovirus 11
Echovirus	<u>E</u> nteric <u>C</u> ytopathogenic <u>H</u> uman <u>O</u> rphan Virus; ECHO
ECM	Extracellular Matrix
EDTA	Ethylenediaminetetraacetic Acid
eIF4GI	Eukaryotic Translation Initiation Factor 4GI

ELFO	Electrophoresis buffer
ERBV	Erbovirus
EV	Enterovirus
FACS	Fluorescence Activated Cell Sorting
FBS	Foetal Bovine Serum
FMD	Foot-and-Mouth Disease
FMDV	Foot-and-Mouth Disease Virus
GAG	Glycosaminoglycan
GMK	Green Monkey Kidney Epithelial Cells
GPI	Glycosylphosphatidyl Inositol
GRP78	Glucose-regulated Protein 78
HAV	Hepatitis A Virus
HAVcr1	Hepatitis A Virus cellular receptor 1
HeLa	Human Epithelial Cervical Cancer Cell Line ( <u>H</u> enrietta <u>L</u> acks)
HEVs	Human Enteroviruses
HFMD	Hand-Foot-and-Mouth Disease
HLA	Human Leucocyte Antigen
HPeV	Human Parechovirus
HPV	Human Papillomavirus
HRV	Human Rhinovirus
HS	Heparan Sulphate
HSPG	Heparan Sulphate Proteoglycan
HSV	Herpes Simplex Virus
ICAM-1	Intracellular Adhesion Molecule-1
IFN	Interferon

Ig	Immunoglobulin
IgG	Class G Immunoglobulin
IRES	Internal Ribosome Entry Site
Kb	Kilobase
L-protein	Leader Protein
LDLR	Low Density Lipoprotein Receptor
MAb	Monoclonal Antibody
MCF-7	Human Breast Adenocarcinoma Cell Line
MDA-MB-231	Human Breast Adenocarcinoma Cell Line
MDA-MB-435	Human Melanoma Cell Line
MHC	Major Histocompatibility Complex
mRNA	Messenger RNA
N-terminus	Amino-terminus of Protein
NEAA	Non-essential Amino Acids
ORF	Open Reading Frame
Oril	Origin of replication internal
OV	Oncolytic Virotherapy
PBS	Phosphate Buffer Saline
PC-3	Human adenocarcinoma prostate cancer cell lines
PE	Phycoerythrin, Fluorescent Dye
Pfu	Plaque Forming Unit
PSGL-1	Human P-selectin Glycoprotein Ligand-1
PV	Poliovirus
PVR	Poliovirus Receptor, know as CD155
RD	Human Rhabdomyosarcoma Cell Line

RGD	Arginine-Glycine-Aspartic acid
RNA	Ribonucleic Acid
RT	Room temperature
RT-PCR	Reverse Transcription Polymerase Chain Reaction
SA	Sialic Acid
SCARB2	Human Scavenger Receptor Class B Number 2
SCR	Short Consensus Repeat
Ss	Single Strand
SVDV	Swine Vesicular Disease Virus
TMEV	Theiler's murine encephalomyelitis virus
UTR	Untranslated Regions
VCAM-1	Vascular Cell Adhesion Molecule 1
VLDL-R	Very Low Density Lipoprotein Receptor
VP	Viral Protein
VPg	Viral Protein Genome-liked
WT	Wild Type
$\beta_2$ M	$\beta_2$ -microglobulin

## List of Figures

Figure 1.1 Phylogenetic tree showing the relationships between the 29 picornavirus genera and corresponding species in the P1 capsid region.....	6
Figure 1.2 Picornavirus particle structure. ....	11
Figure 1.3 Schematic diagram of a typical picornavirus genome. ....	14
Figure 1.4 Schematic diagram of cleavage of the picornavirus polyprotein.....	14
Figure 1.5 Summary of the picornavirus life cycle .....	16
Figure 1.6 Schematic diagram of different proteins known to be picornavirus receptors.....	19
Figure 1.7 The structure of integrin $\alpha$ and $\beta$ subunits that combine to form a heterodimer and serve as a cell-surface receptor .....	21
Figure 1.8 Schematic representation of HS structure .....	24
Figure 1.9 Structure of heparan sulphate proteoglycans .....	25
Figure 1.10 Schematic diagram of DAF structure.....	27
Figure 1.11 Interaction of DAF with EV7 and CVB3 .....	28
Figure 1.12 Summary of different endocytic mechanisms used by viruses for infection .....	34
Figure 3.1 Differences in enterovirus tropism. ....	85
Figure 3.2 Flow cytometric analysis of DAF (CD55) expression on the surface of different cell lines .....	88
Figure 3.3 Schematic diagram of DAF, $\alpha\beta 3$ and $\alpha\beta 6$ expression on different cell lines compared with cytopathic effect (CPE) observed when infected with a panel of enteroviruses .....	90

Figure 3.4 Schematic diagram of the echovirus 11 capsid proteins (VPs) in the P1 region .....	94
Figure 3.5 Molecular phylogenetic analyses of Echovirus 11 isolates by Maximum Likelihood method .....	96
Figure 3.6 A plaque assay of the original E11 (E11 V5-7A) and P3, 6 and 9 propagated on A549 and HeLa cells .....	98
Figure 3.7 Typical agarose gel electrophoresis of E11 V5-7A adapted to A549 and HeLa cells .....	100
Figure 3.8 ClustalW alignments of the E11 V5-7A amino acid sequence and the consensus sequence derived from the 4 RT-PCR fragments from the A549-passaged viruses .....	103
Figure 3.9 Histograms of the sequence analysis of the A549-adapted E11 V5-7A, P3, P6 and P9 using Chromas software .....	104
Figure 3.10 Histograms of the sequence analysis of the A549-adapted E11 V5-7A, P3, P6 and P9 using Chromas software .....	105
Figure 3.11 Alignments of the E11 V5-7A P1 sequence with other E11 isolates in the GenBank sequence database where a complete P1 sequence is available.....	Error! Bookmark not defined
Figure 3.12 Alignment of the sequence of the E11 V5-7A isolate with the E7 Wallace strain .....	Error! Bookmark not defined
Figure 3.13 The three-dimensional structure of the E11 protomer (coordinates PDB ID: 1H8T), using Rasmol software to map the mutations seen in A549-adapted E11 V5-7A.....	108
Figure 3.14 Part of the three-dimensional half-capsid structure of E11 (coordinates PDB ID: 1H8T) shown using Rasmol software .....	109

Figure 3.15 Surface projection of E7 .....	110
Figure 3.16 ClustalW alignments of the E11 V5-7A amino acid sequence and the consensus sequence derived from the 4 RT-PCR fragments from the HeLa-passaged viruses .....	114
Figure 3.17 Histograms of the sequence analysis of the HeLa-adapted E11 V5-7A, P3, P6 and P9 using Chromas software .....	115
Figure 3.18 Part of the three-dimensional half-capsid structure of E11 (coordinates PDB ID: 1H8T) shown using Rasmol software to map the mutation seen in the HeLa-adapted E11 V5-7A .....	116
Figure 3.19 Sequence alignment of the start of VP4 in all enterovirus isolates in the GenBank sequence database with R at position 16 .....	117
Figure 4.1 Heparin blocking plaque assays for some CAV9 isolates on GMK cells ..	128
Figure 4.2 Schematic diagram of the sequencing of the CVA9 isolates CO87, CO62 and Griggs capsid proteins (VPs) in the P1 region .....	130
Figure 4.3 Heparin blocking assay on A549-passaged CVA9 isolate CO87 .....	131
Figure 4.4 ClustalW Sequence alignments of the capsid region of the original CO87 and mutants (CO87N and CO87I) from plaque-purified variants isolated from CO87 adapted on A549 cells in two independent experiments .....	136
Figure 4.5 Alignment of the sequence of different plaques variants isolated from CO87 adapted on A549 cells .....	137
Figure 4.6 The three-dimensional pentameric structure of CVA9 using Rasmol software, showing the predicted positions of the CO87 mutations seen in the heparin-blocked variants .....	138

Figure 4.7 The three-dimensional pentameric structure of CVA9 using Rasmol software, showing the predicted mutation positions of the VP3 at position 59 .....	139
Figure 4.8 The three-dimensional pentameric structure of CVA9 using Rasmol software, showing the predicted mutation positions of the VP1 position 222 .....	140
Figure 4.9 A Sequence alignment of part of the VP3 protein of CO87 with other CVA9 isolates in the GenBank sequence database shown using weblogo online software .....	141
Figure 4.10 Molecular phylogenetic analysis of CVA9 isolates by Maximum Likelihood method.....	143
Figure 4.11 Heparin blocking assay on A549-passaged CVA9 isolate CO62 .....	144
Figure 4.12 ClustalW Sequence alignments of the capsid region of the original CO62 and the mutant CO62H adapted on A549 .....	146
Figure 4.13 The three-dimensional pentameric structure of CVA9 using Rasmol software, showing the predicted positions of the CO62 mutations seen in the heparin-blocked variants .....	147
Figure 4.14 Heparin blocking assay on A549-passaged CVA9 Griggs isolate .....	150
Figure 4.15 ClustalW Sequence alignments of the capsid region of the original CVA9 Griggs and mutants (GriggsN and GriggsS) from plaque-purified variants isolated from Griggs adapted on A549 cells.....	152
Figure 4.16 The three-dimensional pentameric structure of CVA9 using Rasmol software, showing the predicted positions of the Griggs mutations seen in the heparin-blocked variants .....	153
Figure 4.17 Inside view of the three-dimensional pentameric structure of CVA9.....	154

Figure 4.18 The three-dimensional pentameric structure of CVA9, showing the predicted positions of all mutations seen in adapting CVA9 isolates to A549 cells. ....	156
Figure 4.19 The three-dimensional pentameric structure of CVA9, showing the predicted positions of all mutations seen in adapting CVA9 isolates to A549 cells and all published E11 adapting mutations .....	158
Figure 4.20 Surface projection of E7 with the approximately positions of A549 adapting mutations of CVA9 shown by circles.....	159
Figure 4.21 Close up view of a pore-like structure at the 3-fold axis formed by the amino acids P2023S and D2332N.....	161
Figure 4.22 Effect of $\alpha_v\beta_6$ and $\alpha_v\beta_3$ antibodies on CVA9 infection .....	162
Figure 4.23 Infection of CVA9 in the presence and absence of calcium .....	164
Figure 4.24 Infection of CVA9 in the presence and absence of calcium plus magnesium .....	165
Figure 4.25 Temperature sensitivity assay of CVA9wt, CVA9D and P2023S on A549 cells. ....	167
Figure 4.26 Temperature sensitivity assay of CVA9wt, CVA9D and P2023S on GMK cells. ....	168
Figure 4.27 The VP1 C-terminal sequences of the CVA9 isolates used in this thesis and the previous analysis of HSPG binding, together with heparin-blocked variants were aligned using ClustalW .....	174

## List of Tables

Table 1.1	Summary of the medical and agricultural effects of some important picornaviruses .....	7
Table 1.2	Summary of molecules used by different picornaviruses.....	18
Table 2.1	Oligonucleotides that were used for RT-PCR and sequencing the overlapping fragments of CVA9 isolates/variants. ....	63
Table 2.2	Oligonucleotides that were used for RT-PCR and sequencing the overlapping fragments of echovirus 11 (E11) isolates/variants.....	64
Table 2.3	RT-PCR steps used to amplify DNA fragments spanning the enterovirus P1 region .....	74
Table 3.1	Enteroviruses present in the panel used to infect cell lines. ....	83
Table 3.2	Fluorescence intensity ratio of DAF antibody compared to the Isotype control .....	89
Table 3.3	A comparison of all mutations adapted on different cell lines .....	124
Table 4.1	Summary of heparin blocked/non-blocked isolates.....	173

# **Chapter 1**

## **Introduction**

## 1.1 Introduction to Virology

Viruses are very small infectious agents that depend on host cells and need to replicate inside cells for proliferation (Cann, 2011). Viruses can infect all cellular life forms such as bacteria, animals and plants and can cause serious disease in humans and agriculturally-important animals and plants (Carter *et al.*, 2007). Viruses are transmitted through many different routes and for human viruses these include the faecal-oral and respiratory routes, as well as transmission through fomites and through insect bites. A total understanding of the nature of viruses is needed to permit researchers to identify ways of prevention, treatment and diagnosis of virus infection, for instance through the development of efficient vaccines and anti-viral drugs (Ehrenfeld *et al.*, 2010).

In addition to their ability to cause disease, viruses can be useful and have potential applications, such as DNA delivery in gene therapy. Genetically modified viruses can also be used as anti-cancer agents (e.g herpes simplex virus and vaccinia virus) to infect and destroy specific tumor cells and leave normal cells totally unharmed (Carter *et al.*, 2007).

Picornaviruses are among the oldest known viruses. A priest shown in a temple record from 1400 BC appears to show the signs of paralytic poliomyelitis. Furthermore, poliomyelitis was first recognised as a viral disease by Karl Landsteiner and Erwin Popper in 1909, and so was one of the earliest diseases known to be caused by a virus. Foot and Mouth Disease Virus (FMDV), the first known animal virus to be identified, is also a picornavirus and was recognised even earlier, by Friedrich Loeffler and Paul Frosch in 1898 (Semler and Wimmer, 2002).

## 1.2 Picornavirus Classification and Importance

Picornaviruses are viruses that belong to the family *Picornaviridae*. The name is derived from the word “pico” which means “small”, and “RNA” referring to the ribonucleic acid (RNA) genome. Therefore "picornavirus" means small RNA virus (Carter *et al.*, 2007). The family is considered one of the largest viral families consisting of 29 genera: *Aphthovirus*, *Aquamavirus*, *Avihepatovirus*, *Avisivirus*, *Cardiovirus*, *Cosavirus*, *Dicipivirus*, *Enterovirus*, *Erbovirus*, *Gallivirus*, *Hepatovirus*, *Hunnivirus*, *Kobuvirus*, *Kunsagivirus*, *Megrivirus*, *Mischivirus*, *Mosavirus*, *Oscivirus*, *Parechovirus*, *Pasivirus*, *Passerivirus*, *Rosavirus*, *Sakobuvirus*, *Salivirus*, *Sapelovirus*, *Senecavirus*, *Sicinivirus*, *Teschovirus* and *Tremovirus* (Knowles *et al.*, 2012; Adams *et al.*, 2013). Several other viruses are unassigned and may represent new genera or species. The genetic relationship between all *Picornaviridae* genera/species and unassigned viruses is shown in Figure 1.1. The family is diverse, but 4 groups of virus can be seen which include *Enterovirus/Sapelovirus* plus some unassigned viruses; *Aphthovirus/Cardiovirus* and several other genera; *Kobuvirus/Salivirus* and other genera; *Hepatovirus/Parechovirus* and other genera (Knowles, 2014).

Picornaviruses are responsible for various diseases of both humans and animals worldwide. In human, they cause several diseases, ranging from mild infections such as skin rash and common cold infections through to more serious, acute and chronic nervous system, liver and heart problems, which may even lead to death (Table 1.1). There are more than 300 serotypes and due to their medical and economical importance they have been studied over the past years actively. Over the past thirty years, great progress has been made in understanding the

bases of their pathogenic properties and how they infect cells, as well as their epidemiology (Carter *et al.*, 2007; Lin *et al.*, 2009; Cann, 2011; Stanway, 1990 and Ehrenfeld *et al.*, 2010; Knowles *et al.*, 2012).

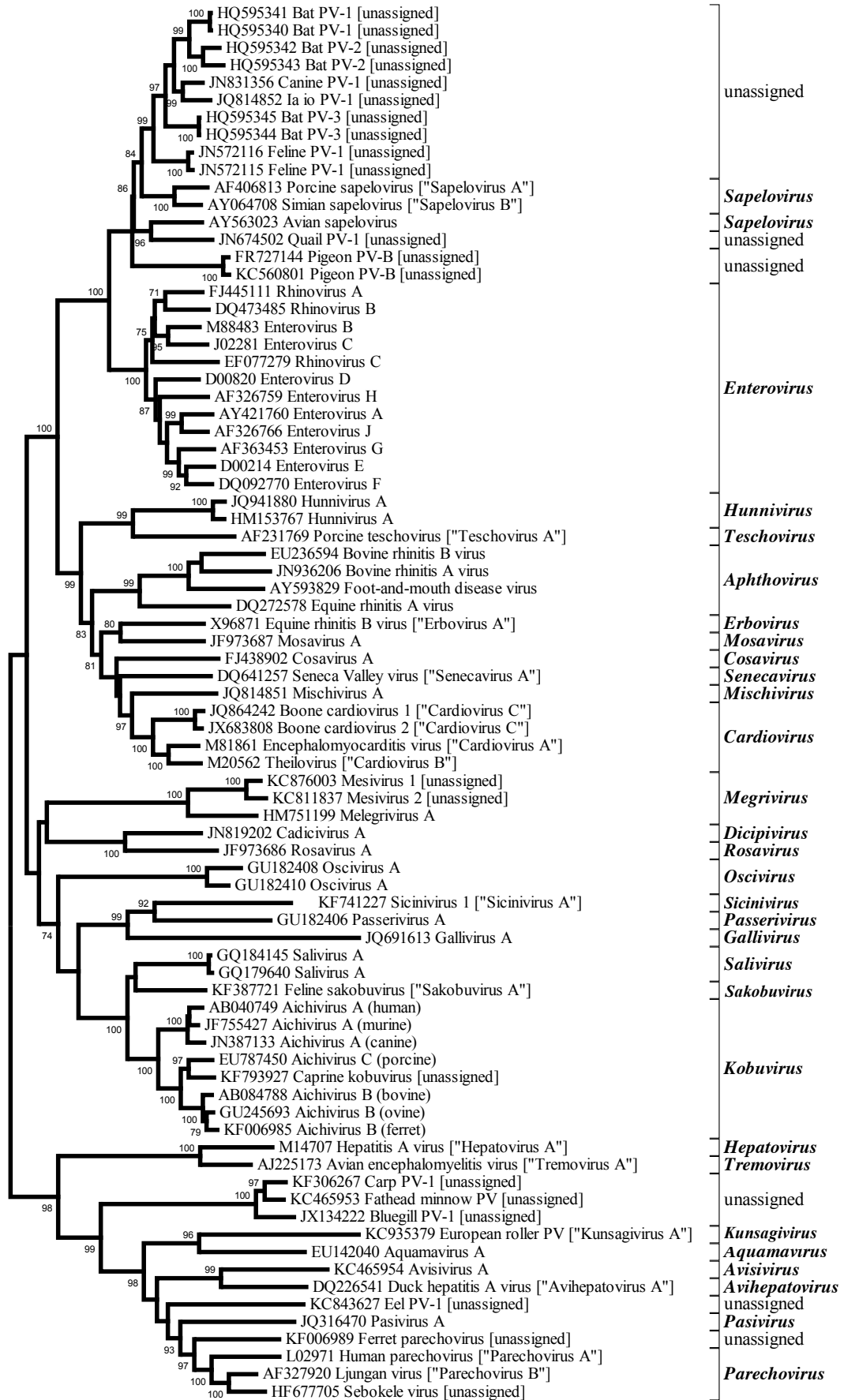


**Figure 1.1 Phylogenetic tree showing the relationships between the 29 picornavirus genera and corresponding species in the P1 capsid region.**

All the currently-recognised species, together with a number of unassigned viruses are included. The maximum-likelihood mtREV with Freqs. (+F) model, Gamma distributed with Invariant sites (G+I) as estimated in MEGA 6.06, with 1000 bootstrap replicates. Proposed new or renamed genus and species are shown between square brackets and quotation marks. Proposed new genera are indicated to the right inside quotation marks (adapted from Knowles, 2014).

(<http://www.ictvonline.org/proposals/2014.018a-dV.A.v3.Sicinivirus.pdf>).

**Table 1.1 Summary of the medical and agricultural effects of some important picornaviruses** (Carter *et al.*, 2007; Ehrenfeld *et al.*, 2010)

Genus	Examples	Diseases
<i>Enterovirus</i>	Poliovirus	Central nervous system (CNS) infections may result in: poliomyelitis, meningitis, and encephalitis.
	Enterovirus 71 (EV71)	A range of illness from mild to serious complications. It is a human pathogen which may cause severe to fatal neurological disease, especially in children. Also, hand-foot-and-mouth disease (HFMD) and severe CNS symptoms including encephalitis, aseptic meningitis and acute flaccid paralysis (poliomyelitis-like paralysis)
	Coxsackieviruses	A range of medical conditions in humans such as myocarditis (heart disease), pancreatitis, type 1 diabetes, CNS infections such as aseptic meningitis, skin rash and upper respiratory tract infections.
	Rhinoviruses (common cold viruses)	Upper respiratory tract infections (common colds) in humans.
<i>Hepatovirus</i>	Hepatitis A virus (HAV)	Infants and children: infections are undetected, asymptomatic or mild. Adults: hepatitis (liver infections).
<i>Aphthovirus</i>	Foot-and-mouth disease virus (FMDV)	Foot-and-mouth disease (FMD) in farm animals such as cattle, sheep, goats and pigs.

<i>Parechovirus</i>	Human parechovirus (HPeV)	Cause respiratory and gastrointestinal infections in children (usually mild but HPeV3 causes potentially fatal sepsis)
<i>Kobuvirus</i>	Aichi virus	Outbreaks of gastroenteritis associated with eating shellfish
<i>Teschovirus</i>	Porcine teschovirus	Enteric infections in pigs- originally an important animal but now rare
<i>Avihepatovirus</i>	Duck hepatitis virus	High mortality infection of ducklings
<i>Cardiovirus</i>	Theiler's virus Saffold virus	Mainly thought to be rodent viruses e.g. Theiler's virus causes disease similar to MS and is used as an animal model. The recently discovered Saffold virus was isolated from humans, but its significance is not known.

## 1.3 Picornavirus Structure

Picornaviruses are small (25-30 nm in diameter) particles and consist of an icosahedral protein capsid, which is non-enveloped, surrounding a single-stranded, positive sense RNA genome with approximate length from 7 kb in *Tremovirus* (*Avian encephalomyelitis virus*) to 8.8 kb in *Erbovirus* (ERBV) (Palmenberg *et al.*, 2010; Cann, 2011; King *et al.*, 2012).

### 1.3.1 Particle Structure

The picornavirus capsid is assembled from 60 protomers; each protomer contains a copy of the four structural viral proteins (VPs) known as VP1, VP2, VP3 and VP4 that are arranged to give icosahedral symmetry. VP1- VP3 (~30 kDa in mass) are on the external surface of the capsid and VP4 (~ 7 kDa) is a small protein and completely internal. VP4 and VP2 are cleaved from a precursor, VP0, and in some picornaviruses, including parechoviruses and kobuviruses, VP0 cleavage does not happen (Stanway, 1990; Ehrenfeld *et al.*, 2010; Yamashita *et al.*, 1998). These viruses only have 3 capsid proteins, VP0, VP3 and VP1. An icosahedron has 5-fold, 3-fold and 2-fold axes of symmetry (imaginary lines around which the particle can be rotated to give 5, 3 and 2 identical structures) as shown in (Figure 1.2). Each of VP1, VP2 (or VP0 in picornaviruses where VP0 is not cleaved) and VP3 share the common fold of an eight-stranded  $\beta$ -barrel (Rossmann *et al.*, 1985). The amino acid chain between the beta strands and also the amino and carboxyl terminal portions of the protein contain a series of loops, and these loops comprise the antigenic sites that are

found on the virion surface, which are responsible for the neutralisation of viral infection (Stanway *et al.*, 1990; Palmenberg *et al.*, 2010; Chen *et al.*, 2013; Williams *et al.*, 2004; Bergelson, 2010). Diversity and evolution in picornaviruses is caused mainly by variability in these regions of the capsid proteins, which is reflected in the presence of distinct serotypes. This kind of antigenic variability causes problems for the development of vaccines against these viruses.

Several picornaviruses, including rhinoviruses and polioviruses, have a deep cleft known as the “canyon” around each 5-fold axis of the icosahedron. These canyons contain the virus binding site for receptors and are lined by the C termini of VP1 and VP3 molecules (Rossmann *et al.*, 1985; Rossmann *et al.*, 2002). There is also a hydrophobic pocket with a close contact with the canyon floor and this pocket contains a small molecule called the pocket factor. This pocket is known to be the binding site for many antiviral drugs (such as WIN51711 and pleconaril). Once these bind they stabilize the capsid and inhibit the uncoating process (Bergelson, 2010; Smyth *et al.*, 2003).

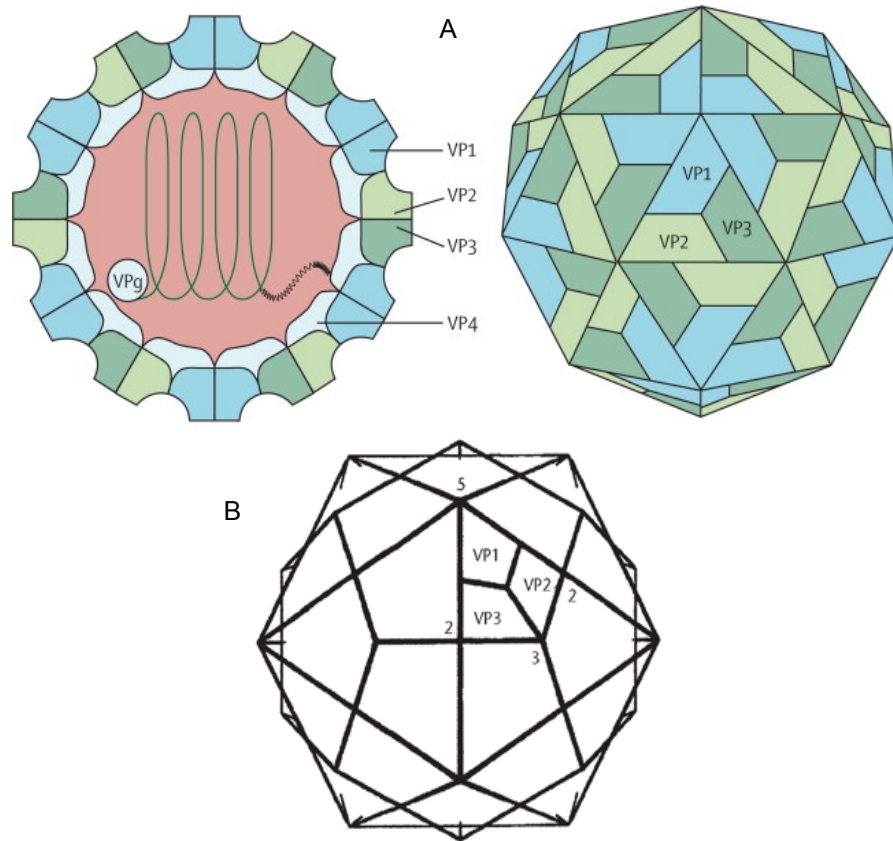


**Figure 1.2 Picornavirus particle structure.** A) The icosahedral capsid consists of 60 protomers, each protomer contains a copy of the four structural viral proteins VP1-VP4, of which VP1, VP2 and VP3 are external, while VP4 is completely internal. B) Icosahedron showing locations of 2-, 3- and 5-fold axes of symmetry and VP1-3. (Solomon *et al.*, 2010; Rowlands, 2010)

### 1.3.2 Genome Structure and Organization

The picornavirus genome is made up of a single-stranded RNA molecule, which is covalently attached to a small (20-25 amino acids) protein, VPg, at the 5' end. There is a long 5' untranslated region [5'UTR] (about 10 % of the genome size), a single open-reading frame, a 3' untranslated region [3' UTR] and a poly A tail. The structure of a typical picornavirus genome is shown in Figure 1.3. The 5'UTR contains a complex structure, the IRES (internal ribosome entry site), which is needed for translation of the virus RNA, and structures needed for RNA replication. The 3'UTR and poly A tail may also be involved in translation and replication (Lin *et al.*, 2009)

Most picornaviruses encode all proteins in a single open reading frame (ORF) (more than 2300 codons). The protein encoded is proteolytically cleaved into precursor proteins then into the final proteins (Stanway, 1990; Ehrenfeld *et al.*, 2010; King *et al.*, 2012) (Figure 1.4). Recently, a bicistronic canine picodicrovirus (genus *Dicipivirus*) with an interrupted ORF has been identified. This has an additional internal ribosome entry site (IRES) at the P1/P2 junction that separated it into two ORFs. Therefore, it is the first naturally occurring bicistronic picornavirus to be discovered (Woo *et al.*, 2012).

The picornavirus proteins are numbered from their positions in the polyprotein as follows: L, 1A (VP4), 1B (VP2), 1C (VP3), 1D (VP1), 2A, 2B, 2C, 3A, 3B (VPg), 3C, 3D, as shown in (Figure 1.3). The first precursors produced during cleavage of the polyprotein are known as P1, P2 and P3. P1 includes VP1, VP2, VP3 and VP4, the capsid (structural) and P2 and P3 include 2A, 2B, 2C, 3A, 3B, 3C, 3D,

which are non-structural proteins. L is also a non-structural protein. The non-structural proteins are involved in RNA replication and polyprotein processing.

The picornavirus RNA genome is positive sense and can function directly as an mRNA (Cann, 2011; Stanway, 1990; Ehrenfeld *et al.*, 2010). The genome has untranslated regions (UTR) at both 5' end and 3' end (5'UTR and 3'UTR, respectively). These have complex secondary structures. The UTR at the 5' end is longer and varies in length from 600 bp in the rhinoviruses to 1250 bp in the aphthoviruses. It plays a role in viral translation, virulence and possibly encapsidation. The UTR at the 3' end is shorter, about 42 bp in the rhinoviruses (HRV) to 317 bp in the avihepatovirus (DHAV), and is thought to be important for negative strand synthesis during replication; it is followed by a poly-A tail (Cann, 2011; Stanway, 1990; Ehrenfeld *et al.*, 2010). The 5' UTR contains the internal ribosome entry site (IRES). IRES elements contain cis-acting regions that recruit the translation machinery internally in the mRNA. Thus, a successful replication cycle of the picornavirus and the efficiency of infection are based on the accurate function of the IRES (Fernández-Miragall *et al.*, 2009; Martínez-Salas, 2008).

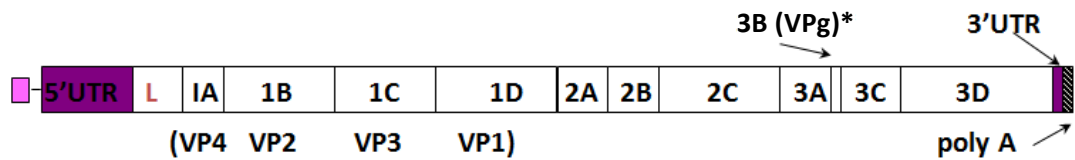


**Figure 1.3 Schematic diagram of a typical picornavirus genome.** The untranslated regions (5'UTR and 3'UTR) are shown in purple and the poly A tail in grey hatching. The single open-reading frame is in white and is made up of the regions L, 1A-D, 2A-C and 3A-D which encode the final virus proteins produced by cleavage of the single polyprotein. The pink square shows the small protein VPg which is covalently attached to the 5' end of the virus RNA. The protein-encoding regions 1A, 1B, 1C and 1D encode the proteins usually called VP4, VP2, VP3 and VP1. L is not present in all picornaviruses (Cann, 2009).

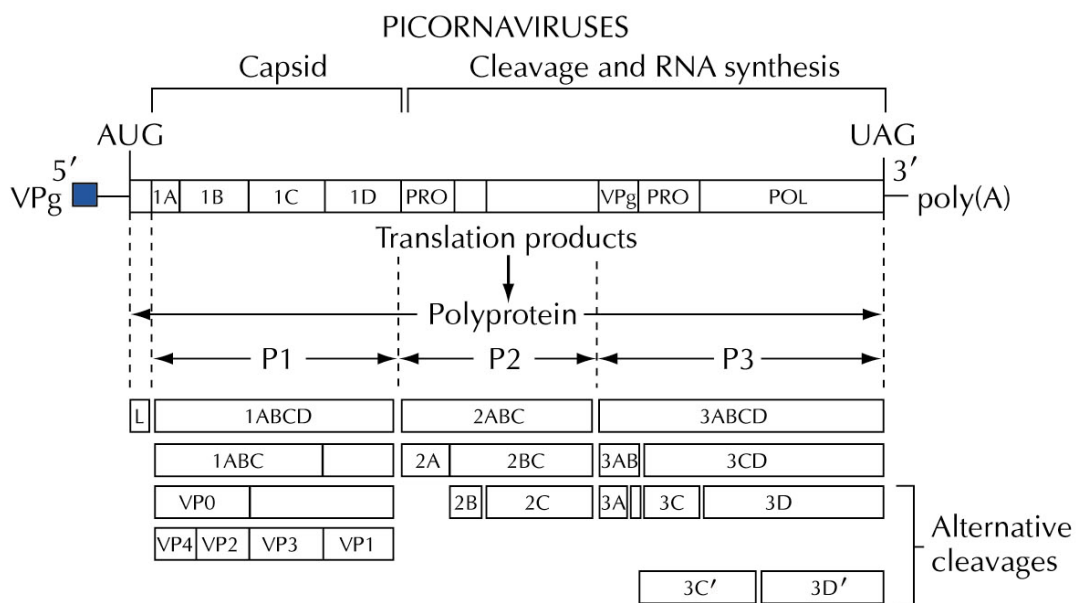


**Figure 1.4 Schematic diagram of cleavage of the picornavirus polyprotein.**

Cleavage is done by virus proteases (2A, 3C) and occurs in several steps giving a series of precursors before the final virus proteins are made. The diagram is typical for enteroviruses such as poliovirus (Cann, 2009).

### 1.3.3 Picornavirus Life Cycle and Replication

The replication cycle of picornavirus shows some variation between species. However, for a typical picornavirus it occurs in the host cell cytoplasm (Figure 1.5), and starts upon attachment and receptor binding of a virus at the host cell surface, followed by the entry of the virus (DePalma *et al.*, 2008; Wanger *et al.*, 2008). The genome is uncoated, then translated, followed by the polyprotein cleavage to produce individual viral proteins. Then, RNA replication occurs on membrane vesicles; assembly of the virus particle then happens and the replication cycle ends with the release of newly formed viral particles from the cell (DePalma *et al.*, 2008). A number of changes to the cell are made by the virus during infection, including host cell translation shut-off which reduces competition for cell resources and prevents anti-virus responses (Lin *et al.*, 2009).

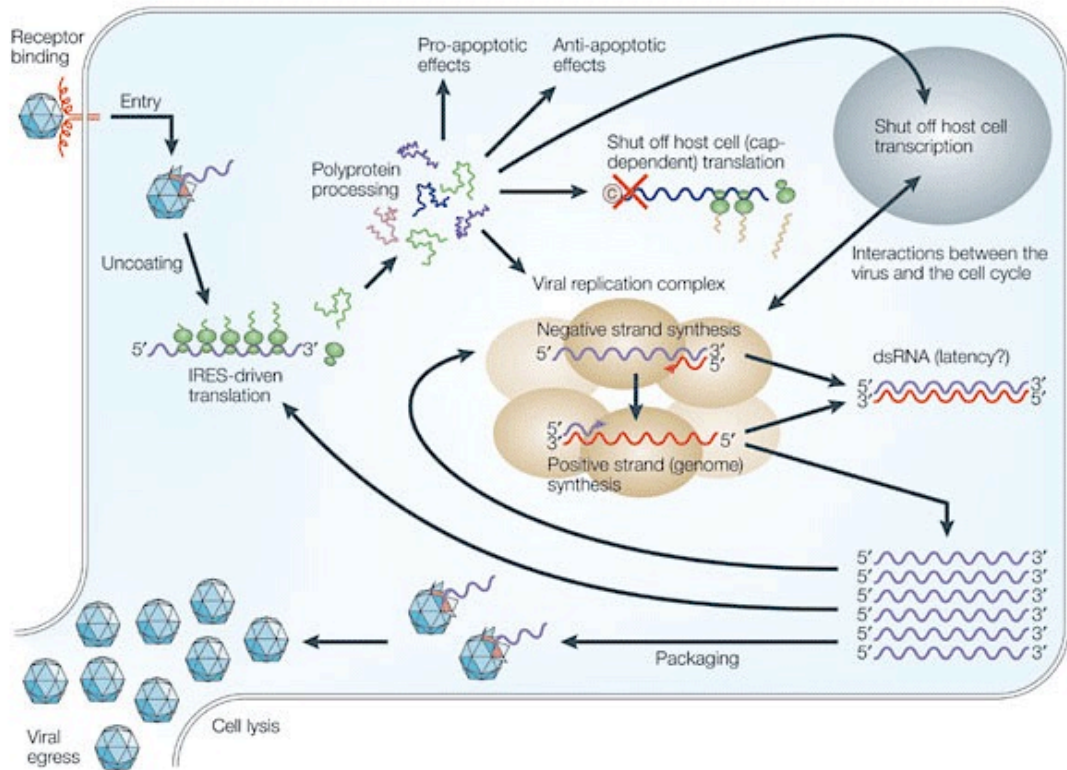


**Figure 1.5 Summary of the picornavirus life cycle.** The main events in the replication process are started by attachment and receptor binding, and include virus entry, uncoating, IRES-driven translation, polyprotein processing, -ve (red) and +ve (purple) strand synthesis by the virus replication complex, which gives multiple +ve strand copies, assembly, maturation, packing and viral release (Whitton *et al.*, 2005).

### 1.3.3.1 Cellular Receptors

Viruses take advantage of receptors on the cell surface, which are internalised and take the virus into the cell. It is a key step in infection and possibly a drug target, as well as being an important determinant of host, tissue tropism and pathogenesis, as only cells expressing the required receptor can be infected. Picornaviruses bind to a range of specific cell surface receptors and studies have identified at least 12 receptors that are utilized by different picornaviruses for cell entry. These are: integrins (several types), low density lipoprotein receptor (LDLR), heparan sulphate proteoglycans (HSPG), Decay-accelerating factor (DAF; CD55), Intracellular adhesion molecule-1 (ICAM-1), Coxsackie-adenovirus receptor (CAR), Poliovirus receptor (PVR; CD155), HAV-cr1 (Hepatitis A virus cellular receptor 1), human P-selectin glycoprotein ligand-1 (PSGL-1), the human scavenger receptor class B number 2 (SCARB2) and sialic acid as shown in (Figure 1.5) (Mercer *et al.*, 2010; Ehrenfeld *et al.*, 2010; Semler and Wimmer, 2002). Molecules such as  $\beta$ 2 microglobulin and GRP78 may also be receptors/co-receptors or involved in events after virus binding (Ward *et al.*, 1998; Triantafilou *et al.*, 2002). A summary of different receptors used by picornaviruses is shown in Table 1.2 and a schematic of many of them in Figure 1.6. All these molecules that viruses bind to are related to other cellular functions, such as cell-cell recognition, ion transport, and binding to the extracellular matrix (ECM). These molecules are glycoconjugates (glycoproteins, glycolipids, proteoglycans), and the carbohydrate moieties can play a key role in virus binding (Mercer *et al.*, 2010).

Table 1.2 Summary of molecules used by different picornaviruses (Ehrenfeld *et al.*, 2010; Stanway, 2013)

Viruses	Receptors													
	DAF	HSPG	B2-Microglobulin	Sialic acid	ICAM-1	CAR	PVR	LDLR	$\alpha$ v $\beta$ 3	$\alpha$ v $\beta$ 6	$\alpha$ 2 $\beta$ 1	PSGL-1	SCARB2	HAVcr-1
Most Echo	✓	✓	✓		x	x	x	x	x	x	✓			
CVA21	✓			✓		x	x	x						
CVA24				✓		x	x	x						
CVBs	✓	✓			x	x	x	x						
CVA9	x	✓	✓	x	x	x	x	x	✓	✓	x	x	x	x
EV70	✓			✓	x	x	x	x			x			
EV71		✓		✓		x	x	x	x	x	x	✓	✓	
E9						x	x	x	✓	✓				
E1						x	x	x			✓			
HPeV		✓				x	x	x	✓					
RV		✓		✓		x	x	✓						
HAV						x	x	x						✓
PV						x	✓	x						
EMCV		✓		✓		x	x	x						
FMDV		✓				x	x	x	✓	✓*				

✓- used as a receptor; x- not used as a receptor; blank- not tested; \* FMDV also interacts with other RGD-dependent integrin.  
 CVA- coxsackievirus A, CVB- coxsackievirus B, EV- enterovirus, E- echovirus, HPeV- human parechovirus, RV- rhinovirus, HAV- hepatitis A virus, FMDV- foot and mouth disease virus, EMCV- Theiler's murine encephalomyelitis viruses.

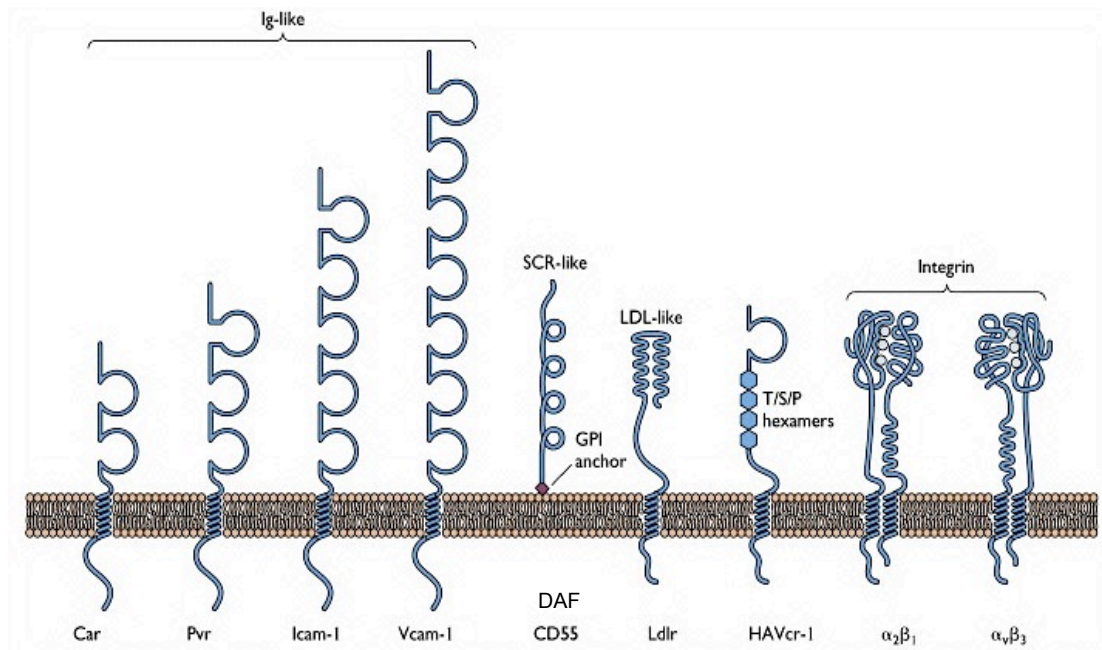


**Figure 1.6 Schematic diagram of different proteins known to be picornavirus receptors.** Members of the Ig superfamily: CAR, coxsackie–adenovirus receptor; PVR, poliovirus receptor; ICAM-1, intracellular adhesion molecule type 1 and VCAM-1, vascular cell adhesion molecule type 1. Integrins  $\alpha_2\beta_1$  and  $\alpha_V\beta_3$  (like integrin  $\alpha_V\beta_3$ , integrin  $\alpha_V\beta_6$  is RGD dependent and is probably the preferred receptor for several picornaviruses with an RGD motif); DAF (CD55), decay-accelerating factor; GPI, glycosylphosphatidylinositol; HAVcr-1, hepatitis A virus cellular receptor 1; LDL-like, low density lipoprotein; LDLR, low density lipoprotein receptor; SCR-like, short consensus repeat; T/S/P, threonine/serine/proline. (Taken from Flint *et al.*, 2009)

### 1.3.3.1.1 Integrins

Integrins are large, heterodimeric cell surface glycoproteins composed of two non-covalently associated subunits called  $\alpha$  and  $\beta$  (Figure 1.6, 1.7). There are a variety of heterodimers made from 18  $\alpha$ - and 8  $\beta$ - subunits that can be combined to form at least 24 distinct  $\alpha\beta$  combinations in humans (Hynes, 2002; Takada *et al.*, 2007). They bind to several different ligands including extracellular matrix proteins such as collagens, laminins, fibronectin and vitronectin. They are named for their roles in integrating the intracellular cytoskeleton with the extracellular matrix and involved in cell adhesion, cell-cell interactions and stimulation of signal transduction (Ehrenfeld *et al.*, 2010; Semler and Wimmer, 2002; Williams *et al.*, 2004; Berinstein *et al.*, 1995).

Integrins can be used by several picornaviruses, such as E1, FMDV, E9, CVA9 and HPeV1 (Nelsen-Salz *et al.*, 1999; Williams *et al.*, 2004; Seitsonen *et al.*, 2010). The  $\alpha_2\beta_1$  integrin (VLA-2; collagen and laminin receptor) binds to E1 in a non-RGD-dependent way involving the  $\alpha_2$  I domain (Xing *et al.*, 2004). In contrast, the other picornaviruses contain an RGD (Arg-Gly-Asp) motif in their VP1 C-terminus, or in the case of FMDV in the VP1 GH loop, and this is recognised by one or more RGD-dependent integrins, mainly  $\alpha_v$  integrins such as  $\alpha_v\beta_3$  and  $\alpha_v\beta_6$  (Williams *et al.*, 2004; Vuorinen *et al.*, 1999; Ehrenfeld *et al.*, 2010; Merilähti *et al.*, 2012). Moreover, studies show that FMDV (Aphthovirus) utilizes the integrins  $\alpha_v\beta_1$ ,  $\alpha_v\beta_3$ ,  $\alpha_v\beta_6$  and  $\alpha_v\beta_8$  as receptors to initiate infection via the RGD motif located on the VP1 GH loop (Berinstein *et al.*, 1995; Jackson *et al.*, 2000a, 2002, 2004).

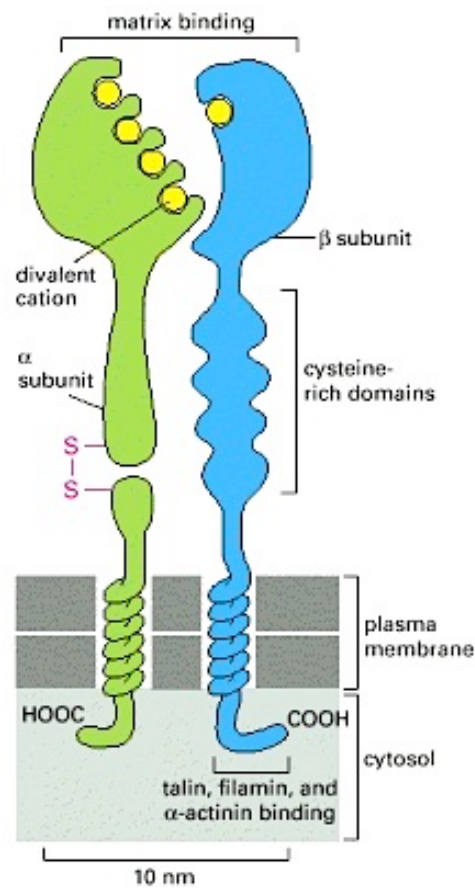


**Figure 1.7** The structure of integrin  $\alpha$  and  $\beta$  subunits that combine to form a heterodimer and serve as a cell-surface receptor. The  $\alpha$  and  $\beta$  subunits are linked together via noncovalent bonds. The  $\alpha$  subunit contains four divalent cation-binding sites. The extracellular part of the  $\beta$  unit has a single divalent cation-binding site and a cysteine-rich region (Taken from Alberts *et al.*, 2002).

### 1.3.3.1.2 Heparan Sulphate Proteoglycans

Heparan sulphate (HS) is a family of linear polysaccharides found on the surface of mammalian cells and in extracellular matrix (Figure 1.8 and Figure 1.9) (Reijmers *et al.*, 2013; Häcker *et al.*, 2005). HS is a glycosaminoglycan (GAG), which are unbranched polysaccharides consisting mainly of a repeating disaccharide unit [GlcA-GlcNAc]<sub>n</sub>, where GlcA stands for glucuronic acid and GlcNAc is N-acetylglucosamine. Some of the disaccharides are modified by sulphation making HS highly negatively charged. HS is attached to core proteins (proteoglycans) giving heparan sulphate proteoglycans (HSPG). These proteoglycans are mainly syndecans and glypicans. HSPG has a potential role in the differentiation processes, the regulation of cell growth and transformation and cell adhesion (Barth *et al.*, 2006; Häcker *et al.*, 2005; Christianson and Belting, 2014; Byrnes *et al.*, 1998). HSPG is also known to serve as a cellular receptor for several viruses such as certain echovirus serotypes, coxsackievirus B3 (CVB3), foot-and-mouth disease virus (FMDV) and swine vesicular disease virus (SVDV) (Goodfellow *et al.*, 2001; Zautner *et al.*, 2006; Jackson *et al.*, 1996; Romero *et al.*, 2004). In most cases, HSPG is considered as an initial receptor which increases the efficiency of another receptor to facilitate the attachment to the host cell surface (Romero *et al.*, 2004).

A treatment of cells with heparinase 1, or treating virus with heparin, blocks the binding of viruses to the cell surface if the virus uses this molecule (Goodfellow *et al.*, 2001). Heparin is a commercial derivative of heparan sulphate; both share identical sugar chain structure but differ in degree of sulphation. It is used as a cheaper and more available alternative of heparan sulphate in virus interaction

studies. HS interactions with cellular and virus proteins are naturally electrostatic; therefore, positively charged amino acid residues interact with the negatively charged sulphate. Bonding may be due to a linear epitope or due to cluster of positively charged amino acids on the virus surface (Romero *et al.*, 2004). FMDV is known to use an RGD motif to interact with integrins, yet some FMDV serotypes can use HSPG as a receptor, particularly after cell culture adaptation (Jackson *et al.*, 2000b). Interestingly, non-RGD-dependent/non-HSPG-dependent variants of FMDV can also be isolated, suggesting that FMDV can use other receptors in addition to integrins and HSPG (Berryman *et al.*, 2013)

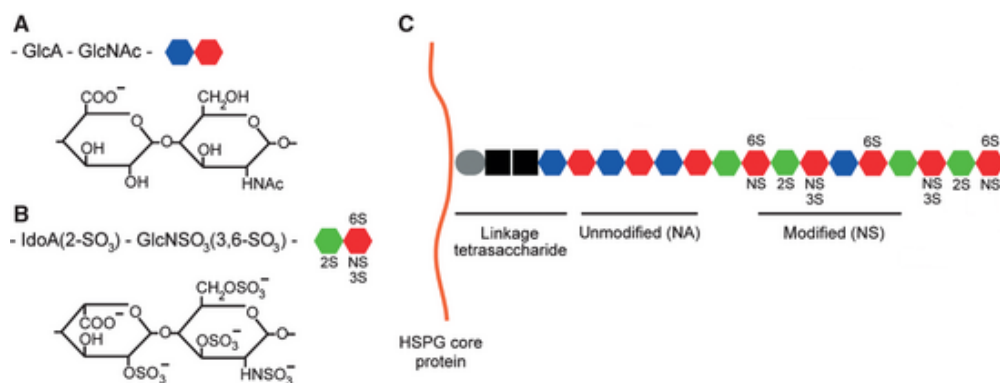


**Figure 1.8 Schematic representation of HS structure.** (A) Unmodified disaccharide consisting of GlcA and GlcNAc, simplified as a blue and red symbol, respectively. (B) Modified disaccharide consisting of a C5-epimerized IdoA (green symbol) sulfated at the C2-position and GlcNAc sulfated at the N-, C3- and C6-position. (C) An HSPG core protein with an HS chain attached to it, via a linkage tetrasaccharide (Modified from Reijmers *et al.*, 2013).

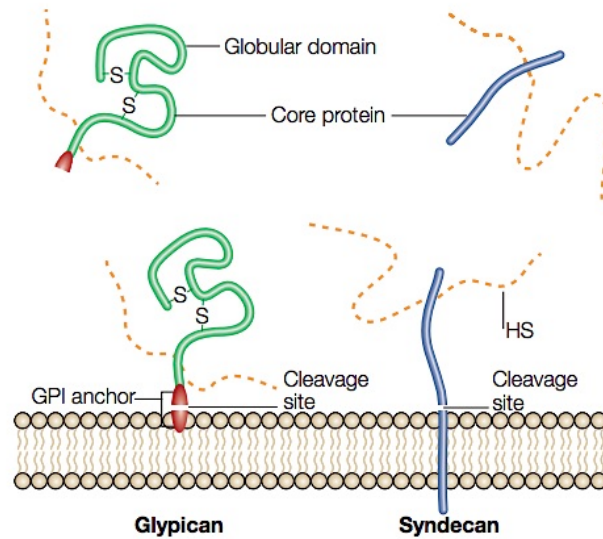


**Figure 1.9 Structure of heparan sulphate proteoglycans.** Glypicans contain an N-terminal globular domain that is stabilized by disulphide bonds. Attachment sites for glycosaminoglycans (GAGs) are located near the C terminus, to which a glycosylphosphatidylinositol (GPI) anchor is attached that links the core protein to the cell membrane. The GPI anchor can be cleaved to shed the heparan sulphate (HS) proteoglycan from the cell surface. Syndecans are type I transmembrane proteins with up to five GAG attachment sites. Syndecans can also be shed by proteolytic cleavage. (Häcker *et al.*, 2005)

### 1.3.3.1.3 Decay-accelerating factor

Decay-accelerating factor (DAF; CD55) is a 70-kDa extracellular glycoprotein and is expressed on the surface of almost all cells (Figure 1.5, 1.10, 1.11). It serves as a cellular receptor for CVB, CVA21 and many echoviruses (E3, 6, 7, 11, 12, 13, 19, 21, 24, 25, 29, 30, and 33) (Clarkson *et al.*, 1995; He *et al.*, 2002; Newcombe *et al.*, 2004; Shafren *et al.*, 1998). In the uninfected cell it plays a role in down-regulation of complement activity by accelerating the decay of C3 and C5 convertases enzymes. DAF comprises of five domains from the N-terminus including four short consensus repeats (SCRs), with approximately 60 amino acid residues, and a C- terminal serine/Threonine-rich region, with approximately 70 amino acids, and is attached to the cell surface by a glycosylphosphatidyl inositol (GPI) anchor (Clarkson *et al.*, 1995; Shafren *et al.*, 1998; Plevka *et al.*, 2010; Novoselova *et al.*, 2012). DAF does not bind in the virion canyon but folds around the virus surface near the 2-fold axis of symmetry (Ehrenfeld *et al.*, 2010). The binding of DAF to EV7, EV12 and CVB3 uses different combinations of SCRs and slightly different parts of the virus surfaces are involved (Plevka *et al.*, 2010) (Figure 1.10). Viruses which use DAF have the ability of causing hemagglutination (HA) of human red blood cells, which is linked with DAF binding, and DAF interactions can be recognised in this way. E11 is one of the best-studied viruses in terms of DAF binding and several strains have been shown to interact with DAF, through inhibition of infection by anti-DAF monoclonal antibodies or by soluble DAF (Stuart *et al.*, 2002).

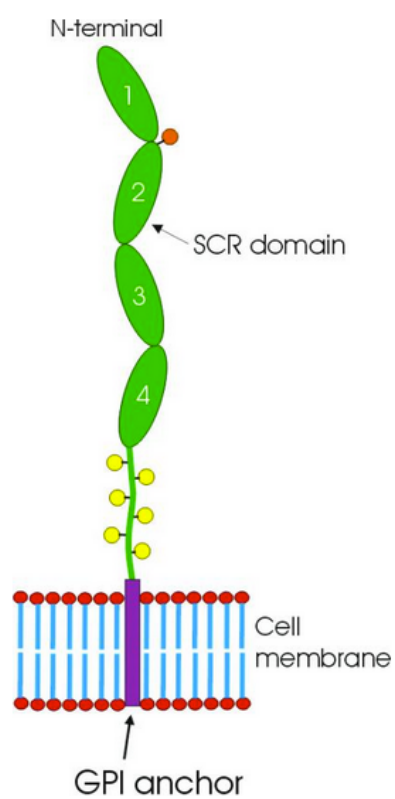


**Figure 1.10 Schematic diagram of DAF structure.** The green ellipses represent the 4 SCR domains. The yellow circles are O-linked and the orange circles are N-linked carbohydrate moieties. GPI, glycosylphosphatidylinositol (Taken from He *et al.*, 2002)

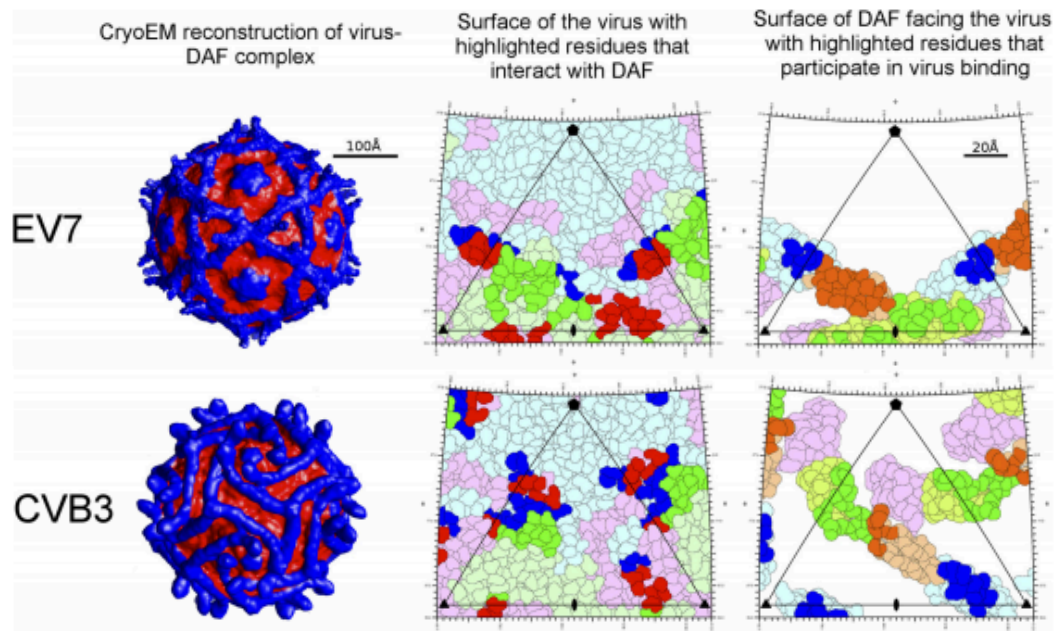


**Figure 1.11 Interaction of DAF with EV7 and CVB3.** Surface-rendered view of each virus complexed with DAF, with all density at a radius of 160 Å shown in blue, which corresponds mostly to DAF density. (Middle) Outer surface of the virus, viewed from outside the virus and subdivided into small areas representing individual amino acids, with residues in VP1 shown in blue, those in VP2 shown in green, and those in VP3 shown in pink. Residues in contact with DAF are coloured similarly, but in darker shades. (Right) Inner surface of DAF, viewed from inside the particle (with SCR1 residues in pink, SCR2 residues in green, SCR3 residues in orange, and SCR4 residues in blue), with DAF residues contacting the virus shown in darker shades. The asymmetric unit is indicated by a black triangular outline (Taken from Plevka *et al.*, 2010).

#### 1.3.3.1.4 Immunoglobulin Superfamily Receptors: ICAM

##### ICAM-1

Intracellular adhesion molecule-1 (ICAM-1) belongs to the immunoglobulin superfamily (IgSF) and has five extracellular Ig-like domains (Figure 1.5). It is present in the membrane of leukocytes and endothelial cells, thus providing adhesion between them (Vuorinen *et al.*, 1999; Rossmann *et al.*, 2002; Xiao *et al.*, 2001; Semler and Wimmer, 2002). It is a cell surface molecule that is recognized as the receptor for the major group of human rhinoviruses (~90 serotypes such as HRV3, HRV14 and HRV16), as well as CVA21. The interaction between ICAM-1 and rhinoviruses is via the N-terminal domain that inserts into the centre of the virus canyon (Olson *et al.*, 1993).

##### CAR

Coxsackievirus and adenovirus receptor (CAR) is the common receptor for both Coxsackievirus B (CVB) and adenoviruses (Bergelson *et al.*, 1997). CAR is a cell surface glycoprotein (46-kDa) with two extracellular immunoglobulin Ig-like domains (Figure 1.5). It is expressed in many human tissues and in the developing central nervous system. It functions as a cell adhesion molecule. CAR is recognized as a receptor by all six CVB serotypes for both the attachment and infection of cells. In many adenoviruses, it acts as a receptor to mediate the initial attachment of the virus to the cell surface, while the entry of virus is mediated by an integrin. In CVBs it is known to bind to the virus canyon and causes formation

of the A particle, an intermediate in uncoating of the virus (Ehrenfeld *et al.*, 2010, Rossmann *et al.*, 2002).

## **PVR**

Poliovirus receptor (PVR; CD155) is a transmembrane glycoprotein with three extracellular immunoglobulin Ig-like domains (Figure 1.5). Its cellular functions are not yet clearly understood but it seems these are related to cell-cell interactions, extracellular matrix proteins interactions, cell migration and NK cell function. It acts as a receptor for all three serotypes of poliovirus and the first N-terminal Ig-like domain (D1) of PVR seems to be responsible for virus binding and infection by binding within the canyon. Studies indicate that PVR is the only receptor that is associated with PV attachment and infection and so it is a critical determinant of PV infection. Most poliovirus isolates cannot recognise mouse PVR and mouse cells cannot be infected. Transgenic mice expressing human PVR can be infected, showing that PVR is a host tropism determinant (He *et al.*, 2000; Racaniello *et al.*, 1996; Ehrenfeld *et al.*, 2010; Semler and Wimmer, 2002).

### **1.3.3.1.5 LDLR family**

Member of the low-density lipoprotein receptor (LDLR) family vary greatly in sizes (up to 600 kD). LDLR structures are very repetitive and one receptor molecule can make contact with many capsid proteins, which may stabilised the virion against pH-induced conformational changes (Figure 1.5) (Semler and Wimmer,

2002; Ehrenfeld *et al.*, 2010; Tuthill *et al.*, 2010). There are two types of receptor in the family: low-density lipoprotein receptor (LDLR) and very low-density lipoprotein receptor (VLDLR). These receptors carry cysteine-rich N-terminal repeats “Cys-repeats” to which the minor group of human rhinoviruses (HRV1A, -1B, -2, -23, -24, -25, -29, -30, -31, -44, -47, -49 and -62) attach and soluble forms of LDLR can block virus binding to cultured cells (Uncapher *et al.*, 1991; Marlovits *et al.*, 1997). The receptor binds to a star-shaped prominence around the 5-fold axis symmetry of the virus and not within the canyon. LDLR functions to deliver virus to the endosomal compartment where the uncoating process is started as part of the endosomal acidification (Semler and Wimmer, 2002; Ehrenfeld *et al.*, 2010; Tuthill *et al.*, 2010).

#### **1.3.3.1.6 PSGL-1 and SCARB2**

Two transmembrane proteins, human P-selectin Glycoprotein Ligand-1 (PSGL-1) and human Scavenger Receptor Class B-2 (SCARB2), have been both identified as cellular receptors for Enterovirus 71 (EV71) (Tan *et al.*, 2013; Yamayoshi *et al.*, 2013). PSGL-1 is a sialomucin membrane protein expressed in leukocytes, which is important in the tethering and rolling of leukocytes for their recruitment from blood vessels into inflamed tissues. It seems to be involved in the viremic phase of EV71 infection but is not thought to be a major receptor as transgenic mice expressing human PSGL-1 are not more susceptible to EV71 infection (Liu *et al.*, 2012). SCARB2 is a type III double-transmembrane protein located primarily in endosomes but also expressed on the cell surface, it has been reported that it plays an important role in the maintenance of lysosomes. It is also

expressed in neurons in the central nervous system (Tan *et al.*, 2013; Liu and Rossmann, 2014; Yamayoshi *et al.*, 2013). It appears to be the essential EV71 receptor (Yamayoshi *et al.*, 2013).

#### **1.3.3.1.7 Sialic Acid**

Sialic acid (SA) is known as neuraminic acid and usually linked to glycoproteins and gangliosides. It functions as a receptor for cell attachment and entry of many viruses and can be a determinant of tropism and pathogenicity. These viruses include influenza viruses, EV71, EV70, Theiler's virus and EMCV (Matrosovich *et al.*, 2013; Yang *et al.*, 2009; Alexander *et al.*, 2002; Tuthill *et al.*, 2010). SAs are highly present and expressed and are attached at terminal ends of *N*- and *O*-glycans as well as glycolipids. The most common sialic acid in humans is  $\alpha$ 5-*N*-acetylneuraminic acid (Neu5Ac). Studies showed that EV70 binds Neu5Ac as an  $\alpha$ 2,3-linkage to galactose, while CVA24 variant is able to use both  $\alpha$ 2,3- and  $\alpha$ 2,6-linked Neu5Ac as receptors (Zocher *et al.*, 2014; Ströh and Stehle, 2014).

#### **1.3.4 Viral Entry**

Following attachment, viruses must be internalised and uncoat. This process usually involves a cellular endocytosis pathway (Mercer *et al.*, 2010). A number of endocytosis pathways for internalisation have been identified (Figure 1.12), for example, macropinocytosis, clathrin-mediated endocytosis (CME), caveolin-mediated mechanisms, caveolar/lipid raft-dependent and others that remain

poorly understood (Mercer *et al.*, 2010; Heikkilä *et al.*, 2010; Sieczkarski and Whittaker, 2002; Merilahti *et al.*, 2012).

The most important advantage of using endocytosis for internalization is that endocytosis can avoid leaving any evidence of virus entry on the surface of the cell, which could be recognised by the immune system. In addition, the virus can be delivered to a cell compartment where uncoating of the genome and replication can start. Some viruses such as herpes simplex virus 1 (HSV-1) and human immunodeficiency virus 1 (HIV-1) have the ability of entering directly but they often prefer to use endocytic pathway for productive entry (Mercer *et al.*, 2010). Some mechanisms are pinocytic and promoting the uptake of fluid, solutes and small particles; while, some viruses are internalized by on-going endocytic activities. Endocytosis can also be virus-triggered. Phagocytosis is typically restricted to large particles and few cell types (Mercer *et al.*, 2010).

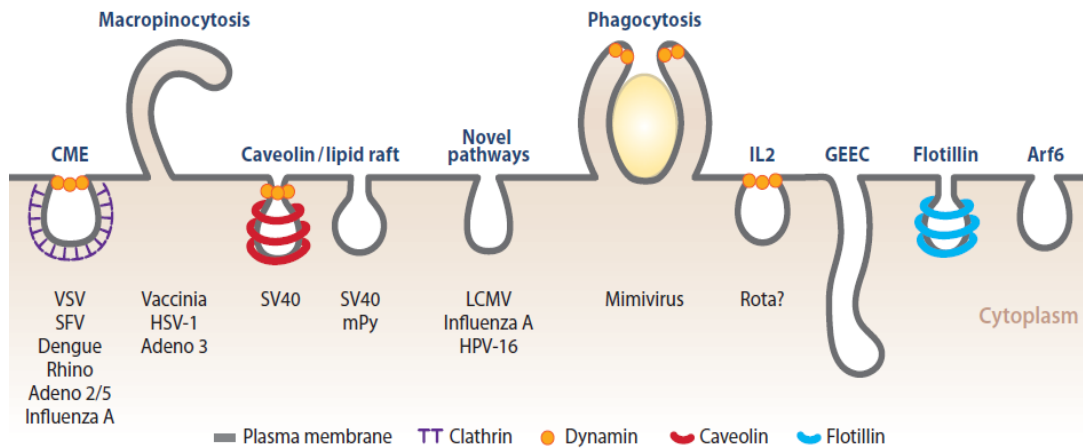


**Figure 1.12 Summary of different endocytic mechanisms used by viruses for infection.** These include clathrin-mediated endocytosis (CME), macropinocytosis, phagocytosis, caveolar/raft-mediated mechanisms and several novel mechanisms. Some of these pathways are via dynamin-2 as indicated by the beads around the neck of the endocytic indentations. Phagocytosis is restricted to a few cell types. There are several possible internalization pathways such as IL-2, the GEEC pathway, and the flotillin- and ADP-ribosylation factor 6 (Arf6)-dependent pathways that normally carry specific cellular cargo. (Taken from Mercer *et al.*, 2010)

#### **1.3.4.1 Clathrin-mediated Endocytosis (CME)**

CME is one of the most common pathways for virus entry (Mercer *et al.*, 2010). Clathrin is assembled on the inside face of the plasma membrane, forming invaginated pits which then become clathrin-coated vesicles (CCVs). Other essential molecules that also interact with clathrin are Eps15, amphiphysin and the AP2 adapter proteins and the dynamin GTP. Clathrin plays a key role in the internalization of several viruses, such as some adenoviruses, vesicular stomatitis virus (VSV), influenza virus and semliki forest virus (SFV), which were identified previously in clathrin-coated pits (CCPs) in the plasma membrane at early stages of internalization by transmission electron microscope (TEM) (Mercer *et al.*, 2010; Sieczkarski and Whittaker, 2002). FMDV is internalised through this pathway (Berryman *et al.*, 2005) and a recent study indicates that HPeV1 is endocytosed via the clathrin-mediated pathway (Merilahti *et al.*, 2012).

#### **1.3.4.2 Caveolar/lipid rafts-dependent Endocytosis**

Caveolae seem to be used for entry by several viruses including polyomavirus and simian virus 40 (SV40). They are characterised by the formation of primary endocytic vesicles which depends on cholesterol, lipid rafts (cholesterol-rich microdomains) and a complex signalling pathway including tyrosine kinases and phosphatases. Dynamin is essential in the caveolar pathway to close off the neck of the vesicle (Mercer *et al.*, 2010; Sieczkarski and Whittaker, 2002).

### 1.3.4.3 Macropinocytosis

Macropinocytosis is considered to be a non-specific mechanism for internalization, not related to a specific receptor. During this process fluids and membrane are internalized into large vacuoles leading to plasma membrane ruffling. Endocytic vesicles occur as a response to cell stimulation of actin and microfilaments. The ruffles form as lamellipodia (planer folds), filopodia or blebs and are closed at the membrane ruffling sites forming a large vesicle known as a macropinosome. The formed closed vacuoles are no longer attached to the plasma membrane. Macropinosomes have the ability to become acidified and interact with early endosomes, and the same is true of vesicles produced by several different entry pathways (Sieczkarski and Whittaker, 2002; Mercer and Helenius, 2009). Echovirus 1 and coxsackievirus B are picornavirus examples of entering the cell via the macropinocytosis pathway (Mercer and Helenius, 2009).

### 1.3.5 Particle Uncoating and Genome Release

In this stage, the process of uncoating happens when the virus particle is disrupted to some extent and naked RNA is transmitted to the cytoplasm of the host cell. This can be as a result of changes in the pH (due to endosomal acidification) or some other less understood processes (Tuthill *et al.*, 2010; Smyth and Martin, 2002).

A "pore" runs through the capsid at the 5-fold axis (Rossmann *et al.*, 1985). At the base of this pore there is myristate residue, which is covalently linked to the N-terminus of VP4. There is also a concentration of hydrophobic protein regions,

e.g. the N-terminus of VP1. Following interaction with the receptor, these hydrophobic residues are exposed and interact with the cell or endosomal membrane. Originally, this was thought to allow the RNA to pass through the pore and the membrane to enter the cytoplasm. However, it now seems that in enteroviruses the RNA is released by changes, which make an opening at the 2-fold axis (Wang *et al.*, 2012). VP4 is released from the capsid during uncoating and it has been shown recently that this protein can form multimers which have pore forming ability, which may be related to entry (Panjwani *et al.*, 2014). A mutation in VP4 has been shown to prevent infection at a step after receptor binding (Moscufo *et al.*, 1993).

### **1.3.6 Translation**

Following the release of genomic RNA, translation in picornaviruses is initiated by the internal ribosome entry site (IRES) element located in the 5'UTR. The genomic RNA acts as mRNA and is translated to a single polyprotein which is the precursor of the viral protein. The IRES is formed of approximately 450 nt from the whole 5'UTR (~ 600 to 1300 nts) and is made up of several RNA secondary structures (Ehrenfeld *et al.*, 2010; Tuthill *et al.*, 2010; Wanger *et al.*, 2008). Picornavirus IRES are divided into five types: type I e.g. enteroviruses; type II e.g. aphthoviruses; type III in hepatoviruses; type IV a hepatitis C (HCV)-like IRES element found e.g. in teschoviruses; type V e.g. kobuviruses (Lin *et al.*, 2009).

### 1.3.7 Polyprotein processing:

The success of viral replication depends on the activity of proteases encoded within the polyprotein to process it into mature viral protein. The proteases used are: 2A, 3C and leader protein (L) (Figure 1.4).

#### 2A

2A protein shows considerable differences amongst picornaviruses genera and is found within the P2 region. For instance, in enteroviruses 2A protein is a trypsin-like, cysteine protease which is responsible for *cis* cleavage at its N terminus between VP1 and 2A, which is the first step in polyprotein processing (Stanway and Hyypia, 1999; Hughes and Stanway, 2000). 2A is also involved in shut-off of host-cell macromolecular synthesis, which reduces competition and enhances virus replication. 2A does this by cleaving the eIF4GI (eukaryotic translation initiation factor 4GI) component of the cap-binding complex during infection, which leads to reduction of host cell translation (Stanway and Hyypia, 1999; Hughes and Stanway, 2000; Semler and Wimmer, 2002). A number of other cellular proteins are cleaved by 2A such as eIF4GII, eIF-4F and dystrophin (Lin *et al.*, 2009; Porter, 1993). In many picornaviruses, 2A protein is linked with an unusual C-terminal activity, where during translation no peptide bond is made between the G and P of a NPGP motif (ribosome skipping) (Hughes and Stanway, 2000). Other picornaviruses lack either of these types of protein and 2A does not seem to be involved in cleavage/ribosome skipping.

### 3C

The 3C protein, found within the P3 region, is the main protease in all picornaviruses and is responsible for the majority of cleavage. In some cases this is as the precursor 3CD. It is active in both *cis* and *trans* cleavage (Semler and Wimmer, 2002; Porter, 1993). 3C is structurally and functionally related to the large trypsin-like serine proteases (Porter, 1993). 3C also cleaves cell proteins such as eIF4A1, which lead to the shut off of host translation (Lin *et al.*, 2009).

### Leader (L) Protein

The L protein is distinct structurally and functionally among picornavirus and is only present in some picornaviruses. L protein is encoded at the N-terminus of the polyprotein in several picornaviruses including aphthoviruses, cardioviruses, erboviruses, tescovirus, sencavirus and kobuviruses (Hughes and Stanway, 2000). In aphthoviruses and erboviruses L is a papain-like protease. The L protein of aphthoviruses cleaves between its own C-terminus and the N-terminus of VP4; this is the only known cleavage of this enzyme on the viral polyprotein. However, it also cleaves eIF4GI (eukaryotic translation initiation factor 4GI), thus preventing the host cell from translating its own capped mRNA, in a similar manner to 2A in enteroviruses and rhinoviruses (Lin *et al.*, 2009; Hughes and Stanway, 2000; Semler and Wimmer, 2002).

### 1.3.8 Genome Replication

In picornaviruses there are several activities that occur during genome replication. In the initial step, the positive strand viral RNA is copied to produce multiple copies of minus strands RNA, which are then used as templates for positive strand RNA replication (Carter *et al.*, 2007; Lin *et al.*, 2009). Picornaviruses have a peptide called VPg, a small protein of about 23 residues, and the first step of viral RNA replication is synthesis of uridylylated VPg. Firstly, a tyrosine residue at position 3 (Tyr-3) is modified by the viral RNA-dependent RNA polymerase (3Dpol) to produce uridylylated VPg (VPg-pU-pU). This process is called uridylylation. Secondly, the VPg-pU-pU is then used as a primer to produce full-length genomic RNA. The mechanism that is involved in VPg-pU-pU formation is termed 'slide back', in which a single adenylated residue located in the loop of an RNA stem-loop structure, called the cre motif (cis-acting replication element) or oril (origin of replication internal), is used as the template for VPg uridylylation (Pathak *et al.*, 2007; Shen *et al.*, 2008; Lin *et al.*, 2009). RNA replication occurs on replication complexes, derived from different host cell membranes in different picornaviruses. These concentrate the components needed for replication and possibly also protects the dsRNA, which is present during RNA synthesis from being recognised by cell defence mechanisms (Nagy and Pogany, 2012).

### **1.3.9 Assembly and Maturation**

This step is mainly completed by packing the viral genome into the capsid. Capsid assembly first starts by cleavage of the polyprotein into three proteins P1, P2 and P3. P1 forms the subunit of the virus capsid VP0, VP1, and VP3. The VP0, VP1 and VP3 assembled into 6S promoters. Five of these promoters are assembled into a 14S pentamer and 12 pentamers are assembled to form a 150S particle. The final stage involves insertion of the RNA into empty capsid. At this stage, the maturation happens and the precursor of VP0 is cleaved to VP2 and VP4 and then the virion is a mature. The release of virus from the host cell is mostly by cell lysis (Semler and Wimmer, 2002).

## **1.4 Tropism of Picornaviruses**

Viruses are often highly specific for particular organisms, for instance poliovirus will only infect humans and closely related primates and the same is true of human rhinoviruses. Enterovirus 71 also seems to be specific for humans (Wang and Yu, 2014). Sometimes viruses can alter their tropism and an example of this in picornaviruses is SVDV (swine vesicular disease virus), which is closely related to the primate virus CVB5 but has accumulated several mutations, which are presumably involved in this change in host (Jimenez-Clavero *et al.*, 2005).

The pathogenicity of enteroviruses is highly complex due to variation in the genetic background of populations and immunological aspects, and this is difficult to study due to restrictions to investigations in higher primates. This inspired scientists to develop animal models for studies of the important pathogens such

as human enterovirus 71 (HEV71), major-group human rhinoviruses (HRVs) and some coxsackieviruses A (CVAs) (Wang *et al.*, 2011; Zaini *et al.*, 2012). New born mice have been used as animal models as these seem to be susceptible to some enteroviruses, but cannot be infected after a few days. This model was used to define CVB and CVA isolates as these have different effects in new born mice (Stanway and Hyypia, 1999). EV71 adapted to grow in adult mice have also been used to study disease caused by this virus (Wang and Yu, 2014).

As well as host tropism, viruses can have different tissue tropism and this can be important in pathogenesis, for example in poliovirus virulence. Several regions of the virus genome have been shown to be help to define host and tissue tropism.

#### **1.4.1 Picornavirus Receptors**

The interaction between the virus and its specific cellular receptor is a key determinant of cell tropism and pathogenicity. Viruses may use multiple attachment receptors and/or co-receptors for entry and several conformational changes may occur. Viral tropism, virulence and development of diseases can be affected by any of these changes (Schneider-Schaulies, 2000). Transgenic mice expressing the human form of CD155, the poliovirus receptor, are an example of where receptor interactions play a role in defining host tropism. Poliovirus does not recognize the mouse CD155 and so mice are not infected with poliovirus, but the transgenic mice are infected and are important in research and vaccine testing (Ren and Racaniello, 1992). Transgenic mice expressing SCARB2 can be infected with EV71 and so are useful models (Wang and Yu, 2014).

Studies show that in recombinants between coxsackieviruses A9 and B3 (CVA9, CVB3), which show different pathogenicity in new-born mice, this correlated with the P1 region and so probably involved receptor interactions (Harvala *et al.*, 2002).

Adaptation of viruses to different cell lines or different hosts often involves changes in the capsid proteins, which map to known receptor binding domains. For instance, E11 has been adapted to several cell lines and mutations tend to map either to known DAF binding domains and change the DAF binding phenotype, or to the canyon region where it is suggested that interactions with an unknown receptor are affected (Stuart *et al.*, 2002; Rezaikin *et al.*, 2009; Novoselov *et al.*, 2012).

#### **1.4.2 Other Tropism Determinants**

##### **5'UTR**

Previous studies have identified that the 5'UTR of enteroviruses is a key factor in tissue tropism and viral pathogenesis. For instance, several sites in the 5'UTR of all 3 poliovirus serotypes are cited as neurovirulent/attenuation determinants (Minor, 1996). Also, the 5'UTR of CVB1 and CVB3 were shown to include cardiovirulent determinants (Lin and Shih, 2014). Attenuating mutations in the enterovirus 5'UTR influence translation efficiency in different cells, which might be a major factor affecting tropism (Harvala *et al.*, 2005; Svitkin *et al.*, 1988).

## **Non-Structural Proteins**

The aphthovirus, FMDV is one of the most important animal diseases worldwide and the natural hosts are mainly cattle, goats and sheep. Studies show that deletions in the non-structural protein 3A were related to attenuation for cattle of FMDV serotypes O and C and also contribute to high virulence of swine FMDV serotype O (Núñez *et al.*, 2001). Another example, is that amino acid changes in the 2C protein of HRV-16 can increase the cytopathic effect and level of viral RNA production seen when this virus infects mouse cells (Harris and Racaniello, 2005).

### **1.5 History of Coxsackieviruses and Their Importance**

Coxsackievirus was named according to a village called Coxsackie in New York State, USA. In 1948, Gilbert Dalldorf discovered the coxsackieviruses while investigating an outbreak of poliomyelitis in the US. Isolation of unrecognized agents from the faeces of two suspected polio cases was done. The first coxsackievirus was identified when faecal specimens were injected into suckling mice and paralysis was induced (Dalldorf, 1950; Carter *et al.*, 2007; James, 1952). Coxsackieviruses are divided into 2 groups, Coxsackie A viruses and Coxsackie B viruses (CVA and CVB) according to their pathogenic effects in new-born mice. CAVs infect skeletal muscle causing flaccid paralysis, while CBVs, detected in several tissues including the central nervous system causing spastic paralysis (Harvala *et al.*, 2005).

Coxsackieviruses belong to the genus *Enterovirus* in the family of *Picornaviridae*. The genus *Enterovirus* is classified into 12 species: *Enterovirus A*, *Enterovirus B*, *Enterovirus C*, *Enterovirus D*, *Enterovirus E*, *Enterovirus F* and *Enterovirus G*, *Enterovirus H*, *Enterovirus J*, *Rhinovirus A*, *B* and *C*, mainly based on genetic relationships (Knowles *et al.*, 2012; Adams *et al.*, 2013). Coxsackieviruses do not form one group of viruses on this basis, as some belong to *Enterovirus A* (some CVAs), *Enterovirus B* (CVA9 and CVBs) and *Enterovirus C* (poliovirus and some CVAs). This is one reason why enteroviruses are no longer assigned to either the Coxsackievirus or echovirus groups and new viruses are just given an enterovirus number e.g. EV70, EV71 etc.

Coxsackieviruses are an important and large group that cause a wide range of illnesses in humans, including aseptic meningitis, respiratory and undifferentiated febrile illness, herpangina, hand-foot-and-mouth disease, and acute haemorrhagic conjunctivitis, myocarditis (Brooks *et al.*, 2007). Initial replication of enteroviruses in the body usually occurs in the cells of the respiratory or gastrointestinal tracts. Thereafter, the viruses can reach the bloodstream and cause viraemia, which occasionally leads to infection of secondary target organs such as the central nervous system (CNS), heart, skin, liver and pancreas (Vuorinen *et al.*, 1999).

## 1.5.1 Coxsackievirus A9

### 1.5.1.1 General Properties

Coxsackievirus A9 (CVA9); is part of the species *Enterovirus B* (Knowles *et al.*, 2012; Adams *et al.*, 2013). CVA9 is one of the 10 most commonly-isolated enteroviruses and causes infections of the central nervous system, myocarditis and respiratory infections (Heikkilä *et al.*, 2009; Williams *et al.*, 2004).

### 1.5.1.2 Cellular Receptors and Endocytosis

CVA9 utilizes integrins as primary receptors for cell attachment. They use integrin  $\alpha_v\beta_3$  in target cell recognition but  $\alpha_v\beta_6$  is probably more important (Heikkilä *et al.*, 2010; Williams *et al.*, 2004; Vuorinen *et al.*, 1999). The interaction between CVA9 and cell surface integrins  $\alpha_v\beta_3$  and  $\alpha_v\beta_6$  is via an arginine-glycine-aspartic acid (RGD) motif in the C terminus of capsid protein VP1 (Heikkilä *et al.*, 2009; Heikkilä *et al.*, 2010; Williams *et al.*, 2004). Although the RGD is an important motif in CVA9 infection, particularly in cell lines expressing integrin  $\alpha_v\beta_6$ , there also seem to be RGD-independent receptors in some cell lines as an RGD deletion mutant can still infect many cell lines and in some cases the deletion has little effect on infection (Hughes *et al.*, 1995; Merilahti *et al.*, 2012). RGD motifs have been found in many other picornaviruses such as human parechoviruses (HPeVs), foot-and-mouth disease virus (FMDV) and echovirus 9 (E9).  $\beta_2$ -microglobulin ( $\beta_2$ -M, a subunit of histocompatibility complex class I [MHC-I]) and GRP78 (glucose-regulated protein 78-kDa) are used as co-receptors in the internalization process, and possibly play roles in post-

attachment step in several picornaviruses including CVA9 (Triantafilou *et al.*, 2002; Heikkilä *et al.*, 2009; Heikkilä *et al.*, 2010; Huttunen *et al.*, 2014; Shakeel *et al.*, 2013). Studies indicate that the internalisation of CVA9 appears to depend on  $\beta$ 2-M, dynamin and the Arf6 pathway but are independent of the clathrin and caveolin-1 pathways (Heikkilä *et al.*, 2009; Heikkilä *et al.*, 2010; Merilahti *et al.*, 2012).

Several picornaviruses, including different species of the genus *Enterovirus*, interact with heparan sulphate proteoglycan (HSPG) and HSPG serves as a co-receptor for some strains of CVA9. Analysis of the HSPG-binding domain suggested that an arginine (R) at position 132 in VP1 in the folded form clusters around the 5-fold axis of symmetry and produces a positively-charged area allowing interactions with HSPG (McLeish *et al.*, 2012).

## 1.6 Echoviruses

Echoviruses (E) are members of the *Enterovirus* genus and are a group of pathogens can infect the human enteric tract (Brooks *et al.*, 2007; Stuart *et al.*, 2002b; Novoselov *et al.*, 2012; Sobo *et al.*, 2011). The term ECHO is an acronym for Enteric Cytopathogenic Human Orphan, where orphan means that the disease that is caused by echoviruses was not known when the name was invented (Brooks *et al.*, 2007; Stuart *et al.*, 2002b). There are 28 serotypes (E1-E33, but E8 [now thought to be the same as E1], E10 [a rheovirus], E22, E23 [both parechoviruses] and E28 [rheovirus] were reclassified as different viruses). Echoviruses are now known to cause a range of illness. Most infections are

either asymptomatic or show only mild symptoms such as diarrhea, common colds and mild ocular disease, but more serious infections are possible, from aseptic meningitis, paralysis, encephalitis, myocarditis and hemorrhagic conjunctivitis (Brooks *et al.*, 2007; Sobo *et al.*, 2011).

To date, a variety of cell surface receptors have been identified for echoviruses. Decay-accelerating factor (DAF; CD55) appears to be a major echovirus receptor, binding many echovirus serotypes, including E3, 6, 7, 11, 12, 13, 19, 21, 24, 25, 29, 30 and 33 (Powell *et al.*, 1998). Echovirus serotype 1 binds a subunit of the very late antigen (VLA-2)  $\alpha_2\beta_1$  integrin and uses it as a receptor. Integrin  $\alpha_v\beta_3$  has been reported to serve as a receptor for E9 (Nelsen-Salz *et al.*, 1999). Also, human leucocyte antigen (HLA) class I molecules may be involved in the attachment and entry of E11 into susceptible cells (Razaikin *et al.*, 2009). HSPG seem to be involved in some cases (Goodfellow *et al.*, 2001; McLeish *et al.*, 2012).

### **1.6.1 Echovirus 11**

Echovirus 11 (E11); belongs to the genus *Enterovirus B* in the family of *Picornaviridae* (Knowles *et al.*, 2012; Adams *et al.*, 2013). Most isolates of E11 are hemagglutinating and utilize DAF as a primary cell surface receptor, although non-DAF binding variants can be isolated (Novoselov *et al.*, 2012; Stuart *et al.*, 2002b).

## **1.7 Cancer**

### **1.7.1 Cancer- An Introduction**

Cancer is considered one of the most dangerous diseases worldwide. Cancer is a group of different diseases characterized by uncontrolled cell proliferation in the human body leading to rapid growth of abnormal tissue. Tumours are described as benign if they are unable to invade normal tissue while a malignant tumour invades tissue and has the potential to metastasize (King and Robins, 2006). According to the Cancer Research UK report in 2012, around 22% of all human deaths in the UK are due to cancer, and around 46% of all cancer deaths are caused by lung, bowel, breast and prostate cancers (Cancer Research UK report, 2012).

Cancer is usually treated with chemotherapy, radiotherapy, immunotherapy, surgery resection (used in combination with chemo- or radio- therapy) or other methods. The choice of therapy that should be used to treat the cancer depends on the stage and location of the tumour, also the general state of the patient (King and Robins, 2006). Unfortunately, many cancer patients suffer from these aggressive treatments as they are not specific for malignant cells and cause side effects; they are also expensive and not always successful. Consequently, new and efficient therapies are urgently needed for the prevention and treatment of cancer.

## 1.8 Oncolytic Virotherapy (OV)

Oncolytic (onco=cancer; lytic=killing) Virotherapy or cancer-killing viruses, is a novel treatment for cancer by using viruses, either genetically engineered or naturally occurring. These are specially designed to infect and destroy malignant cells, directly by virus replication inside the cells then lysing the cells, or indirectly by induction of apoptosis, while leaving normal cells largely unharmed (Berry *et al.*, 2008; Reddy *et al.*, 2007; Nakhaeil *et al.*, 2005; Meerani and Yao, 2010). A successful virus replication in cancer cells leads to release of newly formed infectious virus particles and as a result the virus will infect neighbouring tumor cells. In general, cancer cells often lack interferon (IFN) or tumour suppressor pathways, and as a result cancer cells maybe more susceptible to infections (Nakhaeil *et al.*, 2005; Murphy *et al.*, 2012). In addition, molecules that used as cell-surface receptors by viruses are often up-regulated in cancer cells (Berry *et al.*, 2008; Allen *et al.*, 2013; Liu *et al.*, 2014; Koretz *et al.*, 1992). Thus, oncolytic viruses can specifically infect, replicate within and destroy cancer cells (Murphy *et al.*, 2012).

### 1.8.1 History of Oncolytic Viruses

Experiments with animals in the 1920s proved that viruses were successful in infecting and lysing experimental murine tumours (Mullen and Tanabe, 2002). Several reports followed in the 1950s demonstrating oncolysis of murine tumours by Newcastle disease virus (NDV) and influenza virus. In the late 1940s and early 1950s, studies of oncolytic viruses in human cancer cases were initiated.

The most famous of these studies was one reported from the National Cancer Institute in 1956, in which wild-type adenoviruses of different serotypes were injected into patients with cervical carcinomas (Mullen and Tanabe, 2002). More than half of the patients given live virus showed tumour regression without evidence of toxicity, on the other hand the control patients given inactivated virus exhibited no response. However, the initial tumour regression was followed by tumour progression in all patients. This apparent lack of long-term anti-tumour efficacy led investigators to abandon this type of therapy in the 1970s and 1980s (Mullen and Tanabe, 2002). However, in 2005 a reappearance of the oncolytic virus idea led to a genetically modified oncolytic adenovirus H101 (Kelly and Russell, 2007). Advances in cancer biology, molecular genetics and virology in the second half of the 20<sup>th</sup> century set the stage for the current enthusiasm for the therapeutic potential of oncolytic viruses. There are two main approaches to oncolytic viral therapy; one of them is the direct treatment of tumours with replicating oncolytic viral vectors alone or in combination with therapeutic transgene delivery, chemotherapy or radiotherapy. The other is the indirect enhancement of anti-tumour immunity via the modulation of the immune response, as manifested with viral oncolysate vaccines, and tumour-protective monoclonal antibodies (Mullen and Tanabe, 2002).

### **1.8.2 Potential Oncolytic Viruses in Cancer Therapy**

A number of viruses have been identified and used as oncolytic virotherapy, such as: vesicular stomatitis virus (VSV), sindbis virus, adenoviruses, reovirus, measles virus, herpesviruses and Newcastle disease virus (Reddy *et al.*, 2007;

Kelly and Russell, 2007; Au *et al.*, 2007; Murphy *et al.*, 2012). In addition, several enteroviruses from the *Picornaviridae* family have been investigated for this purpose, for example poliovirus, coxsackievirus A21 (CVA21) and Echovirus 1 (E1) (Berry *et al.*, 2008; Reddy *et al.*, 2007; Kelly and Russell, 2007). These show effective oncolytic activity *in vivo* against human neuroblastoma, malignant melanoma and ovarian tumours, respectively (Berry *et al.*, 2008; Au *et al.*, 2007; Toyoda *et al.*, 2007; Shafren *et al.*, 2004). Recently, poliovirus has shown promise for treating several cancer cell lines, as it replicates efficiently inside cells. For example, an attenuated oncolytic poliovirus with a manipulated *cre* element that is needed for replication (Toyoda *et al.*, 2007).

CVA21 gives common cold symptoms. It targets and destroys susceptible cells via a specific cellular receptor complex comprising of ICAM-1 and DAF then subsequent cell lysis. It has been suggested that CVA21-mediated oncolysis of malignant melanomas may be a promising new approach to treatment of metastatic melanoma. The major advantages for the selection of CVA21 as a potential oncolytic agent lie in its mild pathogenicity in humans. Also CVA21 offers the ability to prepare highly purified virions directly from genetically characterized full-length infectious cDNA clones (Au *et al.*, 2007; Shafren *et al.*, 2004). Echovirus 1 is another potential oncolytic enterovirus that shows a high level of tropism for human cancer cells including ovarian cancer cells. Lytic infection of E1 is initiated via Integrin  $\alpha_2\beta_1$  that is widely expressed on ovarian cancer and has high levels on the cell surface (Shafren *et al.*, 2005).

A successful virotherapy of cancer using oncolytic enteroviruses requires the expression of viral receptors on the cell surface that is necessary for the

attachment of viruses and cellular interactions (Berry *et al.*, 2008). In fact, numerous virus receptors are up-regulated in cancer cells, for example decay-accelerating factor (DAF), intercellular adhesion molecule-1 (ICAM-1) and  $\alpha_2\beta_1$  are expressed in several human prostate cancer cells. DAF is over-expressed in melanomas, breast cancer and colorectal carcinoma. Heparan sulphate proteoglycans (HSPGs) are over-expressed on human breast cancers. Some integrins, for example  $\alpha\beta_6$  is up-regulated on pancreatic cancers (Berry *et al.*, 2008; Allen *et al.*, 2013; Liu *et al.*, 2014; Koretz *et al.*, 1992; Shafren *et al.*, 2004; Lim *et al.*, 2015)

Oncolytic virotherapy offers prostate cancer patients a novel treatment, especially those with tumours at stages that are resistant to other cancer therapies, as some studies suggest that patients with advanced prostate cancer showed an increase in DAF expression on prostate tumour epithelial cells unlike non-malignant prostate epithelium (Berry *et al.*, 2008; Loberg *et al.*, 2005).

It has been suggested that the direct lysis of tumour cells by oncolytic viruses is the measurement of the technique's efficiency (Meerani and Yao, 2010). Importantly, inhibition of the immune response may be useful, so the virus is not eliminated. However, another point of view suggests that the lysis of tumour cells relies on the activation of the immune response against cancer proliferation, by boosting the immune response even if it then neutralizes the virus (Meerani and Yao, 2010). Oncolytic virotherapy has been shown to be safe and has generated clinical responses in tumours that are resistant to chemotherapy or radiotherapy (Eager and Nemunaitis, 2001).

## 1.9 Aims of This Thesis

The aims of this thesis were to identify cell tropism determinants of enteroviruses, to contribute to an understanding of how viruses could be targeted more efficiently to different cancer cells. This was approached by:

- Analyzing the ability of different echoviruses and CVA9 variants to infect cancer cells.
- Adapting E11 to cancer cell lines and finding the sequence changes present and to determine if other possible mechanisms can be used by adapting this virus onto different cancer cell line.
- Identifying the mechanisms that CVA9 can use to bind to HSPG.

## **Chapter 2**

### **Materials and Methods**

## 2.1 Materials

### 2.1.1 Virus Strains

Several virus isolates were used in this work as followed:

- Coxsackievirus A9 wild-type (CVA9wt; Griggs strain), Coxsackievirus A9 S2871R (CVA9; genetically engineered mutant), Coxsackievirus A9 P2023S (CVA9; genetically engineered mutant). These were derived from a Coxsackievirus A9 Griggs cDNA clone (Hughes *et al.*, 1995).
- CVA9D (A549-adapted mutant), CVA9B (A549-adapted mutant), these were produced by passaging the Griggs strain on A549 cells (Williams, 2002).
- Coxsackievirus A9 clinical isolates CO62, CO79, CO85 and CO87 (Chang *et al.*, 1992).
- Several enterovirus isolates (Echovirus 11, Echovirus 15, Echovirus 20, Echovirus 30, Echovirus 6, EV-06, CVA9-1884, were obtained from Dr. Merja Roivainen, THL, Helsinki, Finland.

### 2.1.2 Mammalian Cell Lines

Several mammalian cell lines were used:

- GMK- Green Monkey Kidney epithelial cell line
- A549- Human epithelial lung adenocarcinoma cell line
- MCF-7- Human breast adenocarcinoma cell line
- PC-3- Human adenocarcinoma prostate cancer cell line
- HeLa- Human epithelial cervical cancer cell line

- MDA-MB-435- Human melanoma cell line
- MDA-MB-231- Human breast adenocarcinoma cell line
- HT-29- Human epithelial colorectal adenocarcinoma cell line
- RD- Human rhabdomyosarcoma cell line

These were obtained originally from ATCC and provided by Dr Merja Roivainen, THL, Helsinki, Finland (GMK); Dr Sisko Tauriainen, University of Turku, Finland (A549, RD); Dr Andrea Mohr (HT-29); Professor Nelson Fernandez (MCF-7, HeLa) and Professor Elena Klenova (PC-3, MDA-MB-435, MDA-MB-231) (University of Essex).

### **2.1.3 Tissue Culture Reagents**

Cells were cultured in:

- DMEM- Dulbecco's Modified Eagle's Medium. High Glucose (4.5 g/L) with L-Glutamine (Biosera)
- RPMI-1640 Medium- Roswell Park Memorial Institute (Sigma)
- McCoy's 5A (modified) medium (1x) (Gibco)
- FBS- Fetal Bovine Serum (Research grade, Sigma)
- NEAA- MEM Non-essential Amino Acid Solution (100x) (Sigma)
- Gentamicin solution (50mg/mL) (Sigma)
- Penicillin-Streptomycin solution (100x) (Sigma)
- Trypsin-EDTA (1x liquid, 0.25% Trypsin 1mM) (Gibco)

- Accutase solution (1x Accutase enzymes in Dulbeco's PBS, 0.5 mM EDTA) (Sigma)
- PBS- Phosphate Buffered Saline tablets (1x) (Fisher). 1 tablet of PBS was dissolved in 100 ml of water then autoclaved.

#### **2.1.4 General Chemicals / Solutions**

- DMSO- Dimethyl sulfoxide Hybri-Max,  $\geq 99.7\%$  (Sigma)
- EDTA-Ethylenediaminetetraacetic Acid anhydrous (Sigma)
- TBS- Tris Buffered Saline (made up of 20 mM Tris+150 mM NaCl) (Sigma), and adjusted to pH 7.5 then autoclaved.
- Calcium chloride  $\text{CaCl}_2$  (Sigma). A 20 mM of solution was prepared and adjusted to pH 7.5 then autoclaved.
- Calcium plus magnesium chloride ( $\text{MgCl}_2$ ) (Sigma). A 20 mM of solution was prepared and adjusted to pH 7.5 then autoclaved.

#### **2.1.5 Chemical inhibitors**

- Heparin sodium salt, from porcine intestinal mucosa (Sigma) - heparin was dissolved in water to give a 50 mg/ml solution and filter sterilised using a 20 nm filter.

### 2.1.6 Antibodies

- Monoclonal Anti-Integrin  $\alpha_v\beta_6$  antibody, produced in mouse (MAB2077Z, Millipore)
- Purified Mouse IgG2a,  $\kappa$  Isotype Ctrl Antibody for  $\alpha_v\beta_6$  (400201, biolegend).
- Monoclonal Anti-Integrin  $\alpha_v\beta_3$  antibody, produced in mouse (MAB1976Z, Millipore).
- Purified Mouse IgG1,  $\kappa$  Isotype Ctrl Antibody for  $\alpha_v\beta_3$  (401401, biolegend).
- Monoclonal Anti-Coxsackievirus A9 antibody, produced in mouse (MAB947, Millipore).
- PE anti-human CD55 Antibody (clone JS11, biolegend).
- PE Mouse IgG1,  $\kappa$  Isotype Ctrl (400113, biolegend).
- Secondary Antibody: Goat anti-mouse IgG [Alexa fluor 555] (Lifetechnologies).

### 2.1.7 Plaque Overlay Medium and Crystal Violet Stain

- Agarose (general purpose, Fisher)
- CarboxyMethyl Cellulose (CMC, Sigma).
  - A 2 % CMC/agarose overlay was produced by adding 2.0 g of CMC and 2.0 g of agarose to 100 ml of distilled water then autoclaved.
  - A 2 % Liquid CMC overlay was produced by adding 2.0 g to 100 ml of distilled water then autoclaved

- A 0.1% w/v solution of Crystal Violet was produced by dissolving 0.5 g of Crystal Violet powder (ACROS Organics, Fisher) in 495 ml of distilled water + 5 ml of absolute ethanol.

### **2.1.8 Immunofluorescence Reagents**

- 4 % Formaldehyde (FA): 40 % formaldehyde (Fisher) was diluted with x1 PBS to give a 4% solution.
- Washing buffer: 100 mM glycine was prepared by dissolving 0.751 g of glycine (Fisher) in 100 ml of 1x PBS.
- Permeabilization buffer: 250 µl of Triton X-100 (0.25 %) (Fisher) was mixed with 100 ml of 1x PBS.
- Blocking Solution: 2 % FBS, 1 % Bovine Serum Albumin (BSA) (Sigma), 0.05 % TWEEN<sup>®</sup> 20 (Sigma), 1x PBS.
- Antibody diluents: 1 % BSA, 0.05 % TWEEN<sup>®</sup> 20, 1x PBS
- VECTASHIELD HardSet Mounting Medium with DAPI (Vector Laboratories).

### **2.1.9 Extraction and Purification Techniques**

A variety of extraction and purification kits were used for purifying DNA, viral RNA or PCR products (Qiagen). These include:

- QIAGEN- QIAquick PCR purification kit (50), using a microcentrifuge.
- QIAGEN- QIAquick Gel Extraction kit (50), using a microcentrifuge.

- QIAGEN- QIAamp Viral RNA Mini Kit (50), for purification of viral RNA (Spin Protocol) from tissue cultures.

### **2.1.10 Reverse Transcription Polymerase Chain Reaction (RT-PCR)**

- SuperScript III one-Step RT-PCR System with Platinum *Taq* DNA polymerase kit (Lifetechnologies).

#### **2.1.10.1 Primers**

Oligonucleotides (Table 2.2 and Table 2.3) were used for RT-PCR and sequencing. They were obtained from Fisher on a 50 nmole scale and dissolved in sterile distilled water to give a 100  $\mu$ M solution.

#### **2.1.11 Agarose Gel Electrophoresis**

- Agarose (general purpose, Fisher)
- TopVision Low Melting Point Agarose (Thermo scientific)
- Loading mixture for a 5 mm agarose gel lane: 1  $\mu$ l GeneRuler 1 Kb DNA ladder (0.5  $\mu$ g/ $\mu$ l), 1  $\mu$ l 6x DNA loading dye, were mixed and the volume was made up to 6  $\mu$ l with nuclease-free water (Thermo scientific).
- Loading buffer (5x): 25 ml of glycerol, 100  $\mu$ l of 0.5 M EDTA pH 8 and 0.2 g of bromophenol blue were mixed and volume made up to 50 ml with sterile distilled water. For some DNA isolations, loading buffer without bromophenol

blue was used to avoid co-purification of DNA/bromophenol blue and make bands migrating to the approximate bromophenol blue position more visible.

Loading buffer was added to DNA samples at a ratio of 1:5.

- SafeView Nucleic Acid Stain (NBS Biologicals) was used at 5  $\mu$ l/ 50 ml gel.
- ELFO buffer (50x): A mixture of 242 g Tris base and 100 ml of 0.5 M EDTA (pH 8.0) was adjusted to pH 7.7 with glacial acetic acid and made up to 1 L with water.

**Table 2.1 Oligonucleotides that were used for RT-PCR and sequencing the overlapping fragments of CVA9 isolates/variants.**

<b>Virus</b>	<b>Primers name</b>	<b>Orientation (5'-3' →, 3'-5' ←)</b>	<b>Primers sequence (5' → 3')</b>	<b>Length (bp)</b>
<b>CVA9-wt</b>	OL2055	Fragment 1-Fwd →	AGT CCT CCG GCC CCT GAA TG	20
	OL2079	Fragment 1-Rev ←	CTT CCA CCA CCA CCC CAC CGA	21
	OL2080	Fragment 2-Fwd →	GTG TGC TAA CGT GGT GGT GGG GT	23
	OL2081	Fragment 2-Rev ←	AGG TTC TTC ACT TCT CCT GGG ATG	24
	OL2082	Fragment 3-Fwd →	CTA TGC CGA CAC CGC ATC CAC	21
	OL2083	Fragment 3-Rev ←	TGG CTT CTT CCA CAT CCC CTT G	22
	OL2145	Fragment 4-Fwd →	ACG TGT TGG TAT CAG ACT GGT ATG	24
	OL2146	Fragment 4-Rev ←	CTT CCG TCC AGA AAA TGC TGG GGT	24
	OL2147	Fragment 5-Fwd →	TCG ACA AGA CCC CGG AAC AAC CCT	24
	OL2148	Fragment 5-Rev ←	TCG TGC TCA CAA GGA GGT CTC T	22
<b>CO87</b>	OL2055	Fragment 1-Fwd →	AGT CCT CCG GCC CCT GAA TG	20
	OL2101	Fragment 1-Rev ←	GTG AAC TCA TAT GCC TTG TCC CCA	24
	OL2102	Fragment 2-Fwd →	CAG GGG TGT CTG TTG GTC GTG TG	23
	OL2103	Fragment 2-Rev ←	ACG CGA TCA GGA ACT TGC CTG TTG	24
	OL2104	Fragment 3-Fwd →	CAC ACC CTA CTG GGG GAG ATT CT	23
	OL2105	Fragment 3-Rev ←	ACG CGC CGG CGC ATT TCC TTC TGT	24
	OL2106	Fragment 4-Fwd →	GAT TAT GTA TGT ACC ACC CGG TGG A	25
	OL2107	Fragment 4-Rev ←	GTT TCC CAC ATA CAC GGC CCC TG	23
<b>CO62</b>	OL2055	Fragment 1-Fwd →	AGT CCT CCG GCC CCT GAA TG	20
	OL2094	Fragment 1-Rev ←	CAC CGT TAG CCA TTG CAG TAG AG	23
	OL2095	Fragment 2-Fwd →	AGT TCC ACC AAG GGT GGC TGC TG	23
	OL2096	Fragment 2-Rev ←	TCT TCG GGG GGT TTG CTC CTG GT	23
	OL2097	Fragment 3-Fwd →	CTA CGC GCA TTG GTC AGG CAG T	22
	OL2098	Fragment 3-Rev ←	GTT CCC TTC CGT CCA GAA GAT ACT G	25
	OL2099	Fragment 4-Fwd →	AGC ACA AGA CAT GCC AGT GTT GAC A	25
	OL2100	Fragment 4-Rev ←	GTT CCC CAC GTA AGC AGC ACC TG	23

**Table 2.2 Oligonucleotides that were used for RT-PCR and sequencing the overlapping fragments of echovirus 11 (E11) isolates/variants.**

<b>Virus</b>	<b>Primers name</b>	<b>Orientation (5'-3' →, 3' - 5' ←)</b>	<b>Primers sequence (5' → 3')</b>	<b>Length (bp)</b>
<b>a. E11 general</b>	OL2053	Fragment 1-Fwd →	TTA AAA CAG CCT GTG GGT TG	20
	OL2054	Fragment 1-Rev ←	ACC CAA AGT AGT CGG TTC CGC	21
	OL2055	Fragment 2-Fwd →	AGT CCT CCG GCC CCT GAA TG	20
	OL2056	Fragment 2-Rev ←	AGG GAA TTT CCA CCA CCA NCC	21
	OL2057	Fragment 3-Fwd →	CAT GTG TGC CTT GGA TTA GYC ARA C	25
	OL2058	Fragment 3-Rev ←	GTC CCT GTT GTA RTC YTC CCA	21
	OL2171	Fragment 1/2-Fwd →	GTT TCG CTC CAC ACA ATC CCA GTG	24
	OL2172	Fragment 1/2-Rev ←	CAG ATG GTG AGT TGA GGG CAG GCA	24
	OL2173	Fragment 2/3- Rev ←	GAA GAT CAG CCA ACC CAA CCA GAT G	25
	OL2174	Fragment 2/3- Fwd →	TCA TTG CAA GCT GAC ACG AAG CAC A	25
<b>b. E11 V5-7A</b>	OL2208	Fragment 1-Fwd →	TGG CTG CTT ATG GTG ACG ATC GAG	24
	OL2209	Fragment 1-Rev ←	TGC CGA CTC CAA CTC CCA TTC CGG CA	26
	OL2210	Fragment 2-Fwd →	TGG GGT GTA GCG ATG TTA ACG GGG T	25
	OL2211	Fragment 2-Rev ←	AGG AGG ACT GCA GAC CCA CGT CCC A	25
	OL2212	Fragment 3-Fwd →	CTA CGC CCA CTG GTC GGG TAG TGT CA	26
	OL2213	Fragment 3-Rev ←	GAC CTA GTT GGG TTC CCT GGT CCT	24
	OL2214	Fragment 4-Fwd →	AGC AGC ATG CGT GTA CAT GGG AG	23
	OL2215	Fragment 4-Rev ←	CAG TTT TGC CAA TCG TTG TGT GTC GCC A	28

## **2.2 Methods**

### **2.2.1 Cell Biology and Virology Techniques**

#### **2.2.1.1 Passaging Cell Lines**

GMK, A549, MDA-MB-435, MDA-MB-231, HeLa and RD cells monolayer were grown in 50 ml (25 cm<sup>2</sup>) tissue culture flasks in DMEM supplemented with 10% FCS, 1 % NEAA and 50 µg/ml Gentamicin or 5 µg/ml Penicillin-Streptomycin. PC3 and MCF-7 cells were maintained in RPMI-1640 containing 10% FCS and 50 µg/ml Gentamicin or 5 µg/ml Penicillin-Streptomycin. HT-29 cells were maintained in McCoy's 5A medium supplemented with 10% FCS and 5 µg/ml Penicillin-Streptomycin.

To propagate the cells the entire growth medium was discarded carefully from flasks, then the cells were washed gently twice with 1x PBS, 300-500 µl of Trypsin-EDTA or Accutase were added and the cells were placed on a rocking platform shaker at room temperature for 3 minutes until all cells were detached. In order to culture the cells in flasks, 4 ml of growth medium was added to the cell suspension and 1 ml aliquots were then placed into flasks containing 3 ml of fresh medium, then the flasks were incubated at 37°C in 5% CO<sub>2</sub> and passaged after an ~80-100 % confluent cells monolayer was observed (3-5 days).

#### **2.2.1.2 Cryopreservation of Mammalian Cells for Storage**

Freezing: cells were washed twice with 1x PBS and detached by 300-500 µl of Trypsin-EDTA or Accutase. Then were re-suspended in 90 % FBS and 10 % DMSO before being transferred to labeled cryovials (Nunc). The cryovials were

then wrapped in cotton wool and frozen at  $-80^{\circ}\text{C}$  for 48 hours. For long-term storage, the cells were transferred into liquid nitrogen.

Thawing: frozen cells were removed from  $-80^{\circ}\text{C}$  freezer or liquid nitrogen and immediately transferred to a  $37^{\circ}\text{C}$  water-bath for a minute, then cells were transferred to a flask containing 4 ml of DMEM and incubated at  $37^{\circ}\text{C}$  5%  $\text{CO}_2$  incubator. Next day, the growth of cells was checked and the old medium was replaced with 4 ml of fresh DMEM.

### **2.2.1.3 Viral Plaque Assay**

Plaque assays were performed in  $25\text{ cm}^2$  tissue culture flasks. Confluent cell monolayers was obtained 3-4 days after splitting cells, medium was discarded and 100  $\mu\text{l}$  of each diluted virus were added to 1 ml of fresh growth medium then the flasks were placed on a rocking platform for 45 minutes at room temperature. The infected cells were covered with 4 ml of overlay made from warm DMEM ( $56^{\circ}\text{C}$ ) and a 2 % solution of CMC and agarose (melted in a boiling water bath) at a ratio of 1:3 (CMC/ agarose : DMEM). The flasks were then incubated at  $37^{\circ}\text{C}$  in a 5%  $\text{CO}_2$  incubator for 3 days or until plaques had formed. Once the plaques were observed, the overlay medium was removed gently by washing twice with 1x PBS, and 0.1 % Crystal Violet stain was added. After 5 minutes the flasks were washed with PBS and the plaques were counted. In order to perform the plaque assays in 6-well plates, cells were treated the same way as above with a slight difference in the CMC overlay (2 % CMC without agarose was used) with a ratio of (1:2 / CMC:DMEM).

#### **2.2.1.4 Viral Propagation**

In order to propagate the virus, the medium was discarded from the confluent monolayers of cells and 1 ml of fresh growth medium was added. Then, 10 µl of virus sample was added and placed on a rocking platform for 1 hour to allow each virus particle to adsorb to a cell and initiate a spreading infection. After that, 3 ml of media was added and the flasks incubated at 37 °C in a 5% CO<sub>2</sub> incubator for 3-4 days to allow cytopathic effect (CPE) to progress. Virus was then released by freeze-thawing three times and then 1 ml aliquots of these infected cells were placed in microcentrifuge tube and stored at -80 °C.

#### **2.2.1.5 Plaque purification from Virus Stock**

In order to pick plaques, a plaque assay was performed. When plaques have fully developed, individual and rounded plaques were marked then a sterile micropipette tip was pushed to the center of plaque through the CMC/agarose overlay. The plaque was scratched and about 10 µl of fluid in the vicinity was withdrawn then transferred to a microcentrifuge tube contained 200 µl of fresh growth medium. The mixture was briefly vortexed and 100 µl was transferred to a fresh monolayer of cell to propagate the picked plaques (section 2.2.1.4).

#### **2.2.1.6 Tropism of Enteroviruses to Different Cell Lines**

To study the cytopathic effects (CPE) of a panel of viruses on GMK, A549, MCF7, PC3, MDA-MB-231, HeLa, MDA-MB-435, HT-29 and RD, cells were

grown in 24-well plates for 2 days. All media were removed and 5 µl of undiluted samples of enteroviruses (CVA9, CVA9D, Echo11, Echo15, Echo20, Echo30, CVA9-1884, Echo6, EV-06, CVB) were added to 500 µl of growth medium to each well. Then plates were placed on a rocking platform for 45 minutes at room temperature. After that, 1 ml of growth medium was added to each well and incubated at 37 °C in a 5% CO<sub>2</sub> incubator, then plates were monitored periodically. When all the cells in some wells seemed to be detached, cells were washed gently with 1x PBS and stained with 0.1 % Crystal Violet.

#### **2.2.1.7 Flow Cytometry Analysis of CD55 Surface Expression on Different Cell Lines**

Expression of DAF (Decay accelerating factor; CD55) on the cell surface was analyzed by flow cytometry using a specific monoclonal antibody (PE labelled anti human CD55 [clone JS11], Biolegend). A PE labelled isotype antibody was used as a control (IgG1, k, Biolegend). Sub-confluent monolayers of cells were washed with PBS and detached using (Trypsin-EDTA) then harvested in 10 ml of DMEM. Cells were visualised and counted using a hemocytometer under a microscope and re-suspended at  $5 \times 10^5$  cells per ml in DMEM. Then cells were centrifuged for 5 min at 1300 rpm. Cells were re-suspended in 95 µl of DMEM after pelleting and then incubated with the appropriate mAb; 5 µg/ml of anti-human CD55 antibody (primary antibody), 5 µg/ml of Isotype control (IgG1, k) and mock-treated (cells only). Then cells were incubated in the dark at 4 °C for 20 min. After that, 1 ml of DMEM were added, cells were pelleted, then re-

suspended in 200  $\mu$ l of DMEM, vortexed, and then analyzed with FACS Calibur flow cytometry (Becton Dickinson; BD Accuri™ C6).

#### **2.2.1.8 Virus Blocking Assay Using Soluble Heparin**

Cells were grown in 25 cm<sup>2</sup> flasks to ~ 100 % confluence. 90  $\mu$ l of virus dilution were incubated with 10  $\mu$ l of 50 mg/ml of heparin at room temperature for 20 minutes. 90  $\mu$ l of virus plus 10  $\mu$ l of water was used as a control. Then, the virus mixtures were added to 1 ml of medium and added to the cell monolayer. Incubation continued for 1 hour on a rocking platform at room temperature. After this time, the infected cells were overlaid with a 2 % solution of CMC/agarose in DMEM (flasks) or a 2 % solution of liquid CMC in DMEM (plates), then incubated at 37°C in a 5% CO<sub>2</sub> incubator for 3-4 days. Upon plaque formation, cells were stained with 0.1 % Crystal Violet.

#### **2.2.1.9 Temperature Sensitivity Assays**

The temperature sensitivity of viruses was measured by adding diluted viruses (CVA9, CVA9D and P2023S) to cell monolayers (A549 and GMK cells) and carrying out a plaque assay but incubating at different temperatures i.e. 34°C, 37°C and 40°C, for 3 days. Upon obtaining the plaques the cells were stained with 0.1% Crystal Violet.

## **2.2.1.10 Virus Blocking Assays Using Chemicals**

### **2.2.1.10.1 Metal Ions-dependence ( $\text{Ca}^{2+}$ , $\text{Mg}^{2+}$ )**

Virus binding to cells in the presence or absence of calcium chloride ( $\text{CaCl}_2$ , [20 mM]) or calcium plus magnesium chloride [20 mM of  $\text{CaCl}_2$  and  $\text{MgCl}_2$ ], both in TBS, was performed in A549 cells in 6-well plates. Confluent monolayers were washed twice with TBS, TBS- $\text{CaCl}_2$  or TBS- $\text{CaCl}_2/\text{MgCl}_2$ , then 100  $\mu\text{l}$  of diluted viruses (CVA9-wt, S2871R and P2023S) were added to the cells for 1 hour on a rocking platform at room temperature. Then the buffers and unbound virus were discarded and cells were washed twice with same buffers and plaque assay was performed in the presence of growth medium.

### **2.2.1.11 Virus Blocking Assays Using Monoclonal Antibodies (Immunofluorescence)**

For the virus blocking assays using anti-human-integrin mAbs, sub-confluent A549 cells were grown on sterile coverslips in 6-well plates for 1 day. DMEM was discarded and 500  $\mu\text{l}$  of fresh DMEM were placed in each well. Cells were pretreated with 1.0  $\mu\text{g}$  of mAb against integrin  $\alpha_v\beta_6$ ,  $\alpha_v\beta_3$  or isotype controls for 30 minutes at 37 °C prior to the infection. Then 100  $\mu\text{l}$  of  $10^3$  PFU/ml stock of virus were added to each well and incubated at 4 °C for 30 min before 2 ml of fresh DMEM was added into wells. Then cells were incubated for 6 hours at 37°C in a  $\text{CO}_2$  incubator. After that, all media were removed and cells were gently washed twice with 1x PBS and dried at room temperature before being fixed. 1 ml of cold 4 % formaldehyde (FA) was added onto the cells and they were incubated at

room temperature on rocking platform for 20 minutes, then the cells were washed twice with 100 mM glycine prepared in 1x PBS for 5 minutes (to eliminate any FA residues, thus stopping the fixation reaction), then permeabilized for 20 minutes with 0.25 % Triton X-100. This was followed by a single wash with 1x PBS for 10 minutes and then the cells were treated with blocking solution for 30 minutes on a rocking platform. Primary antibody (anti-CVA9) was at titre of 1:112 (diluted with antibody diluent) and coverslips were inverted onto 50 µl pools of antibody solution that were placed on parafilm in a humid chamber and incubated at least 2 hours to overnight (16 hrs) at 4°C. The next day, cells were gently washed with 1x PBS for 10 minutes. The secondary antibody (Alexa fluor 555-labelled anti-mouse IgG) was diluted at (1:200), added to the cells and incubated in the dark for 2 hours at 4 °C. Cells then were washed with 1x PBS and mounted using mounting media containing DAPI on glass slides. The slides were examined and observed by fluorescence microscopy using a BX41 microscope. The numbers of red-fluorescent cells in 20 random fields were counted.

## **2.2.2 Molecular Techniques**

### **2.2.2.1 Viral RNA Purification from Tissue Cultures**

Total viral RNA was extracted from cell-culture supernatant containing viral particles using a QIAamp Viral RNA Mini Kit (QIAGEN). A volume of 560 µl of Buffer AVL was mixed with 5.6 µl carrier tRNA in a 1.5 ml microcentrifuge tube. 140 µl of cell-culture supernatant virus was added to the Buffer AVL–carrier RNA and mixed by pulse-vortexing for 15 s, then incubated at room temperature for 10 min and briefly centrifuged to remove drops from the inside of the lid. After that,

560 µl of ethanol (100%) was added to the sample and mixed by pulse-vortexing for 15 s. After mixing, the tube was briefly centrifuged to remove drops from inside the lid. Then 630 µl of the solution was added to the QIAamp Mini column in a 2 ml collection tube and centrifuged at 8000 rpm for 1 min. Then the tube containing the filtrate was discarded and the QIAamp Mini column was placed into a clean 2 ml collection tube. Then the rest of the sample was loaded onto the spin column and centrifuged. 500 µl of Buffer AW1 was added and centrifuged. Then the spin column was placed in a clean 2 ml collection tube and the tube containing the filtrate was discarded. 500 µl of Buffer AW2 was added and centrifuged at full speed at 14,000 rpm for 3 min and then centrifuged at full speed for 1 min (to eliminate any residue of AW2 buffer). Finally, the QIAamp Mini column was placed into a clean 1.5 ml microcentrifuge tube and 60 µl of Buffer AVE was added to the centre of the filter to elute the sample and the column and tube was centrifuged (1 min). Viral RNA is stable for up to one year when stored at  $-20^{\circ}\text{C}$  or  $-70^{\circ}\text{C}$ .

#### **2.2.2.2 Reverse transcriptase polymerase chain reaction (RT-PCR) Technique (cDNA synthesis)**

RT-PCR was performed to generate overlapping fragments spanning the P1 region of enteroviruses, using the Superscript III One-Step RT-PCR System with Platinum *Taq* (Lifetechnologies). cDNA was generated and amplified from 5 µl of the purified RNA, 1 µl of a 100 mM solution of each desired forward and reverse primers (Table 2.1/2.2), 1 µ RT-*Taq* mix, 25 µl 2x reaction mix and the volume made up to 50 µl with nuclease-free water. The RT-PCR reactions were gently

mixed and run in an Applied Biosystems GeneAmp 9700 thermal cycler as described in (Table 2.3). The amplicons were purified using a QIAquick Gel Extraction kit (QIAGEN) and sequenced commercially by Source Bioscience Lifesciences (Nottingham, U.K.).

**Table 2.3 RT-PCR steps used to amplify DNA fragments spanning the enterovirus P1 region**

Steps of the reaction	Temperature (°C)	Time	Cycles
cDNA synthesis and pre-denaturation	50	30 mins	x1
	94	2 mins	x1
Denaturation	94	30 sec	} x35-40
Annealing	45-50	1 min	
Extension and	68	1 min/kb	
Final Extension	68	5 min	x1
	4	∞	

### **2.2.2.3 Agarose Gel Electrophoresis**

For small analytical gels, 0.5 g of agarose was mixed with 50 ml of 1x ELFO buffer, then heated in a microwave until completely dissolved. This was left to cool at room temperature. 5 $\mu$ l of safeView was added to the cooled gel which was then poured slowly into the casting tray, and then the comb was inserted. Then the gel was allowed to solidify at room temperature.

5  $\mu$ l of DNA sample was mixed with 1  $\mu$ l 5x clear loading buffer and loaded to the gel. 5  $\mu$ l of 1 kb ladder was added to the first lane. Electrophoresis was carried out at a voltage of 100-150 V for 20-30 minutes. Then the gel was visualized under UV light and an image was taken using a gel documentation and analysis system (SYNGENE InGenius3/ GeneSys software)

### **2.2.2.4 DNA Purification from Agarose Gel (Gel Extraction)**

TopVision Low Melting Point agarose gel was used for nucleic acid recovery after electrophoresis and to purify specific PCR/ DNA fragments. The agarose gel was prepared, run and visualized as usual, and then the desired DNA fragment was excise of the gel with a clean scalpel blade under UV light and placed in 1.5 ml microcentrifuge tube. DNA was purified from the gel using a QIAquick Gel Extraction kit. The procedure was done according to the protocol that was provided by the supplier (Qiagen, 2006). 300  $\mu$ l of QG buffer was added per 100 mg of gel. Then the tube was incubated in a water bath at 50 °C for 15-20 minutes or until the gel slice had completely dissolved. 100  $\mu$ l of isopropanol was added to the sample and mixed, then the mixture was transferred to the QIAquick

spin column, which was placed in a 1.5 ml tube and centrifuged at 14,000 rpm for 1 minute. The flow-through was discarded. 500 µl of QG buffer was added again to the spin column which was centrifuged for another minute. Then, the spin column was washed by adding 750 µl of PE buffer and centrifuging for a minute. Once again the flow-through was discarded and the spin column was re-centrifuged for an additional minute. Then the QIAquick spin column was transferred into a new sterile 1.5ml tube. 50 µl of EB buffer was added to the column to elute the DNA followed by centrifugation at 14,000 rpm for 1 minute. The purified DNA was analyzed by gel electrophoresis or stored at -20°C.

#### **2.2.2.5 DNA Purification using PCR Purification Kit**

In order to purify specific PCR products where a single band was obtained and gel separation by gel electrophoresis was not required, a QIAquick PCR purification kit were used. 5 volumes of Buffer PBI were added to 1 volume of the PCR sample and mixed gently. To bind DNA, the sample was applied to the QIAquick column and then centrifuged for 30–60 s. Then the flow-through was discarded and the QIAquick column was placed again into the same collection tube. To wash, 0.75 ml Buffer PE was added to the QIAquick column and centrifuged for 30–60 s. Then the flow-through was discarded and the QIAquick column was placed again into the same collection tube and centrifuged for an additional 1 min. The QIAquick column was placed then in a clean 1.5 ml microcentrifuge tube. To elute DNA, 50 µl Buffer EB or water was added to the centre of the QIAquick membrane and centrifuged for 1 min. Then DNA samples were stored at -20°C or analyzed on an agarose gel.

## 2.2.3 Bioinformatics Techniques

### 2.2.3.1 DNA Sequencing and Sequence Analysis

DNA fragments were sequenced commercially by Source BioScience LifeSciences. The fragments were sequenced in both orientations, using the primers used for amplification.

- Chromas Lite: ([http://technelysium.com.au/?page\\_id=13](http://technelysium.com.au/?page_id=13)) was used to open the .ab1 files to check any disagreements between the sequences. The sequences were assembled manually into a complete sequence, which was then translated into protein sequences using the ExPASy online tool (<http://web.expasy.org/translate/>). Sequence alignments were performed using the online (<http://www.genome.jp/tools/clustalw/>) tool ClustalW (Larkin *et al.*, 2007). Database searches were performed using NCBI BLAST (<http://blast.ncbi.nlm.nih.gov/Blast.cgi>).
- Weblogo (<http://weblogo.berkeley.edu/logo.cgi>) was used to produce sequence logos.
- MEGA6 (<http://www.megasoftware.net/>) was used to produce phylogenetic trees.

### 2.2.3.2 Three-Dimensional Structure (3D)

Amino acid positions of interest were plotted onto the structure of the CVA9 (coordinates provided by Professor David Stuart; Hendry *et al.*, 1999) or E11 pentamer (1H8T, Stuart *et al.*, 2002) using the program RASMOL version 2.7.4.2. (<http://rasmol.org/FAQ.html>).

## **Chapter 3**

### **Enterovirus Tropism in Different Cell lines**

### 3.1 Introduction

Most of the enteroviruses can be responsible for similar mild diseases but can also cause diverse symptoms (Brooks *et al.*, 2007). The pathogenicity of enteroviruses is highly complex due to variation in the genetic background of populations and immunological aspects, and this is difficult to study due to restrictions to investigations in higher primates. This inspired scientists to develop animal models for studies of the important pathogen human enterovirus 71 (HEV71) (Wang *et al.*, 2011; Zaini *et al.*, 2012). Transgenic mice expressing the human form of CD155, the poliovirus receptor, have also been important in research and vaccine testing (Ren and Racaniello, 1992). Previous studies have identified that the 5'UTR and 3'UTR of enteroviruses are key factors in tissue tropism, and viral pathogenesis (Lin and Shih, 2014).

The interaction between a virus and its cellular receptor is also potentially a key determinant of cell tropism and disease. Recombinants between coxsackieviruses A9 and B3 (CVA9, CVB3), which show different pathogenicity in new-born mice, showed that this usually correlated with the P1 region and so probably involved receptor interactions (Lin and Shih, 2014; Harvala *et al.*, 2002).

In addition, enteroviruses are currently being explored as possible oncolytic agents (Berry *et al.*, 2008; Patel *et al.*, 2013; Au *et al.*, 2007). An understanding of virus-receptor interactions might help to design specific viruses for cancer therapy. Cancer cells show over-expression of some cell-surface molecules and as these include molecules used by some enteroviruses as receptors, these viruses could be potentially be potent oncolytic agents (Allen *et al.*, 2013; Liu *et al.*, 2014; Koretz *et al.*, 1992).

This chapter describes an extensive series of experiments to investigate the cell tropism determinants of enteroviruses. A panel of enteroviruses was used to infect different cell lines to identify which cell types can be selectively infected. This was followed by FACS examination using a specific monoclonal antibody to detect the expression of DAF (CD55), as this receptor previously believed to be utilized by several of the echoviruses present in the panel (Clarkson *et al.*, 1995; Bergelson *et al.*, 1994; He *et al.*, 2002; Powell *et al.*, 1998). Finally, one virus, echovirus 11 (E11 V5-7A), was propagated on two cell lines; A549 and HeLa, to investigate if adapting mutations were observed.

## **3.2 Analysis of a Panel of Enteroviruses on Different Cell Lines**

### **3.2.1 Infectivity Assay of Enteroviruses on GMK, A549, MCF7, PC3, MDA-MB-231, HeLa, MDA-MB-435, HT-29 and RD cells**

To analyse the cell tropism of enteroviruses towards a range of cancer cells, we performed a screen of enteroviruses. A panel of enteroviruses was used on GMK, A549, MCF-7, PC-3, MDA-MB-231, HeLa, MDA-MB-435, HT-29 and RD cells. Cell monolayers were infected with 10 enteroviruses: CVA9wt, CVA9D, CVA9B, CVA9-1884, Echo 6, Echo 11 (E11 V5-7A), Echo 15, Echo 20, Echo 30 and EV-06. These are described more fully in Table 3.1.

Infected cell monolayers were incubated for 4-5 days then plates were washed gently with PBS before being stained with Crystal Violet. The results are shown in (Figure 3.1). It can be seen that the mock (uninfected) wells have a monolayer of cells in each case. All the viruses in the panel caused complete or partial destruction of the monolayers in at least one of the cell lines, apart from EV-06. None of the viruses had a clear effect on MDA-MB-231 or MDA-MB-435 cells but there were signs of possible CPE in MDA-MB-231 caused by Echo 20 and CVA9B, and similar signs on MDA-MB-435 caused by Echo 20 and CVA9wt.

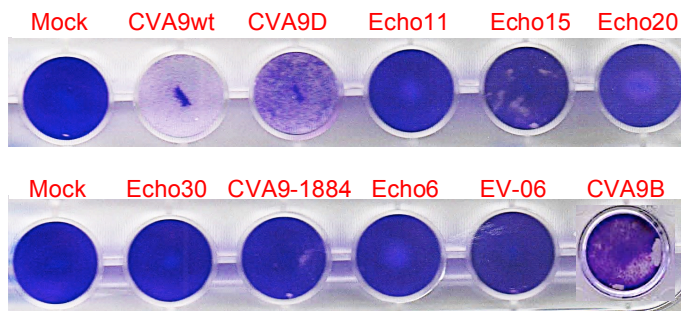
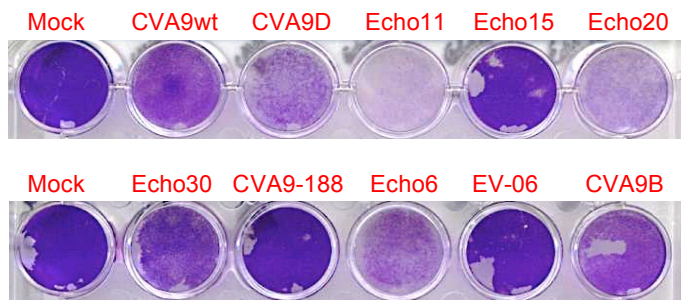
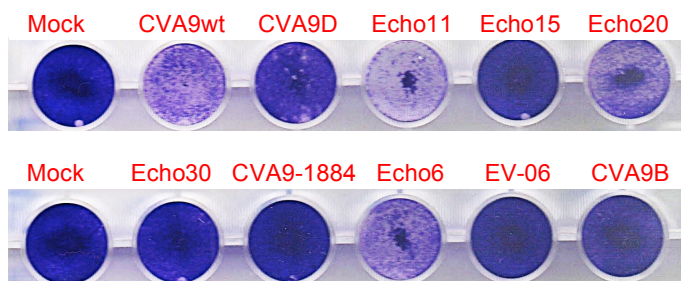
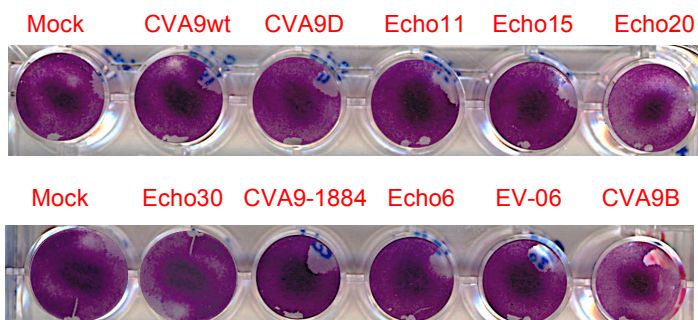
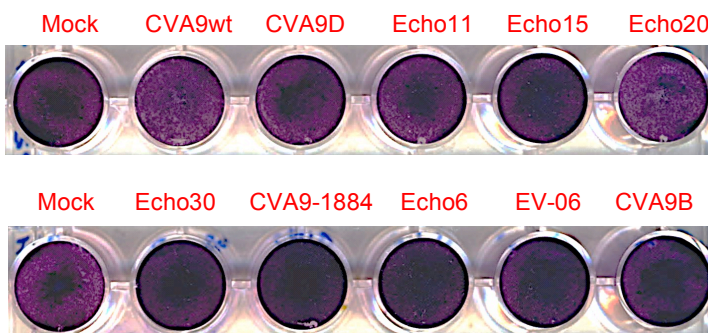
On the other hand, most of the panel had a large effect on RD cells, except EV-06. As this sample did not have a clear effect on any of the cell lines, it may be that the virus concentration was low or the virus had become inactivated. None of the tested echoviruses infect GMK cells, although a few plaques were seen in the Echo 15 sample. Most echoviruses killed the A549 cells. This shows that enteroviruses can have different tropism for cells. Both CVA9wt and the A549-adapted strain CVA9D caused extensive cell death in GMK, A549, RD and HT-29

cells. However, as expected the A549 adapted mutant infects these cells more efficiently than CVA9wt, but caused less death of GMK cells. CVA9D also had a much larger effect than CVA9wt on PC3 cells. Surprisingly, the other CVA9 isolate, CVA9-1884 did not infect any of the cell lines except PC-3 and RD cells, while CVA9B, did not infect HeLa, MBA-MD-435 or HT-29 cells. This shows that there can be differences in cell tropism within an enterovirus type.

Echo 6, 11 (E11 V5-7A) and 20 had a clear effect on A549, MCF-7, HT-29 and RD cells, while less effect could be seen on PC-3 and HeLa cells, except that Echo 11 (E11 V5-7A) was more effective than Echo 6 and Echo 20 on PC-3 cells.

**Table 3.1 : Enteroviruses present in the panel used to infect cell lines.**

Name	Description	Source
<b>CVA9wt</b>	CVA9 Griggs strain recovered from cDNA clone but later found to have S287R mutation in VP1.	Hughes <i>et al.</i> , 1995
<b>CVA9D</b>	CVA9 Griggs adapted on A549 cells and containing a mutation at position D233N in VP2	Williams, 2002
<b>CVA9B</b>	CVA9 Griggs adapted on A549 cells and containing mutations at position T73A in VP3 and S287R in VP1	Williams, 2002
<b>CVA9-1884</b>	Clinical isolate of CVA9-1884	Finland *
<b>Echo 11</b>	Clinical isolate of E 11 (strain V5-7A)	Finland *
<b>Echo 15</b>	Clinical isolate of E 15	Finland *
<b>Echo 20</b>	Clinical isolate of E 20	Finland *
<b>Echo 30</b>	Clinical isolate of E 30	Finland *
<b>Echo 6</b>	Clinical isolate of E 6	Finland *
<b>EV-06</b>	Clinical enterovirus isolate, type unknown	Finland *
* Clinical isolates were provided by Dr. Merja Roivainen, THL, Finland.		

**GMK****A549****MCF-7****MDA-MB-231****MDA-MB-435**

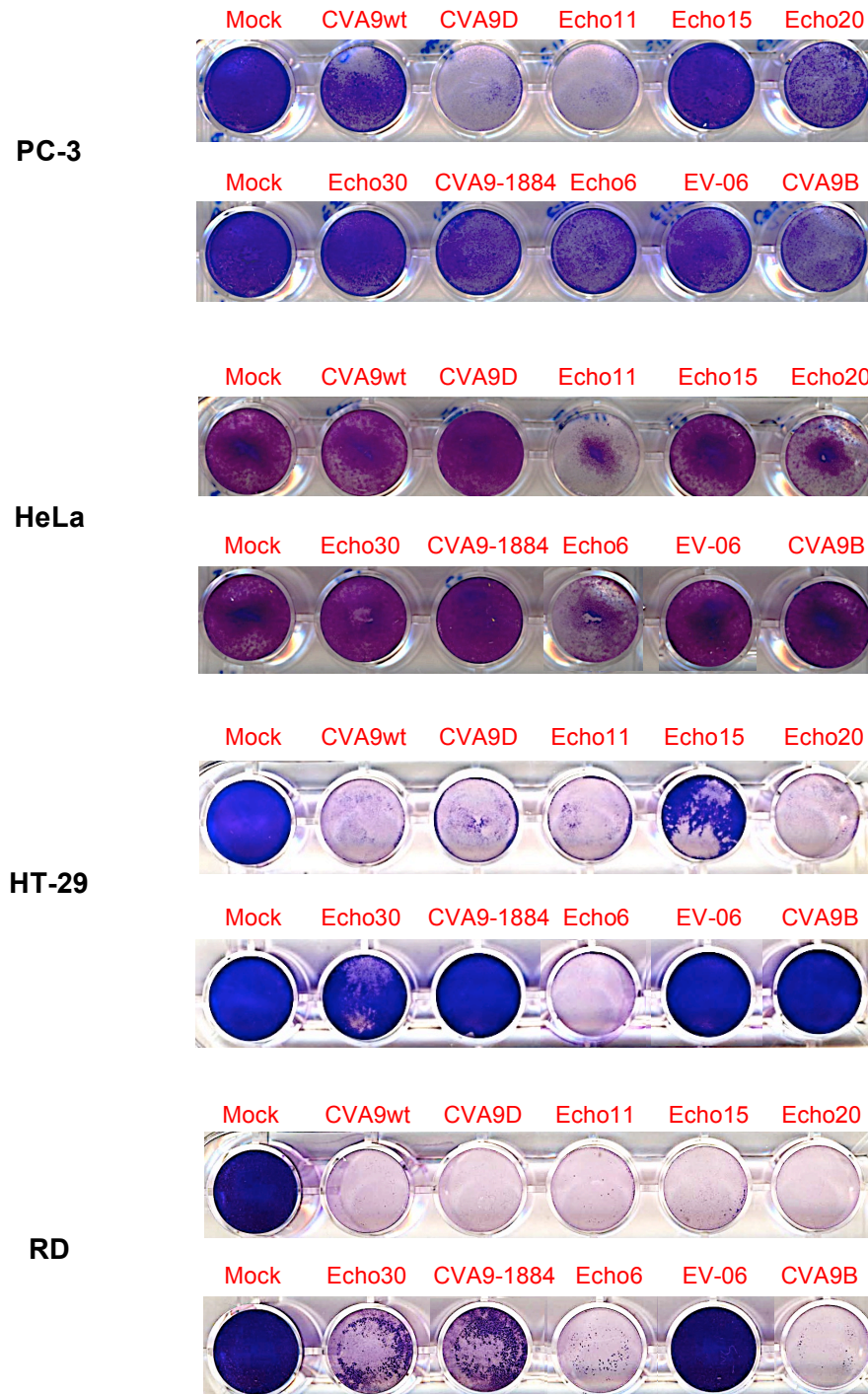


**Figure 3.1 Differences in enterovirus tropism;** shown by the growth of a panel of 10 enterovirus isolates or mutants. Monolayers of cells in 24-well plates were mock-infected or incubated with 5  $\mu$ l of undiluted samples in 500  $\mu$ l of medium of CVA9 strains or several echoviruses for 45 min at room temperature (section 2.2.1.6). 1 ml of growth medium was added to each well and the plates were transferred to a 37°C (5% CO<sub>2</sub>) incubator and incubated for 4-5 days before being stained with Crystal Violet. Each cell line was tested 3 times and the results obtained were consistent in each case.

### 3.3 Analysis of DAF (CD55) Surface Expression on Different Cell Lines by Flow Cytometry

Viral capsid interactions with the host cell surface by binding to its receptor decay-accelerating factor (DAF; CD55) are a major determinant of the cellular infectivity of echovirus 11 (Stuart *et al.*, 2002a,b; Rezaikin *et al.*, 2009). A number of other echoviruses are also known to utilize DAF as a receptor such as echovirus 3, 6, 7, 11, 12, 13, 19, 21, 24, 25, 29, 30 and 33 (Clarkson *et al.*, 1995; Bergelson *et al.*, 1994; Ward *et al.*, 1994; Bhella, *et al.*, 2004; He *et al.*, 2002; Powell *et al.*, 1998).

A flow cytometric (FACS analysis) study was done to investigate whether DAF (CD55) is expressed on the cell surface of the different cell lines in our panel and so could be used as a receptor to initiate echoviruses infections. 5 µg/ml of PE anti-human CD55 antibody and 5 µg/ml of PE mouse Isotype control (IgG1, k) were used. Then samples were analysed with a FACS (BD Accuri C6). The results was analysed and gated by FlowJo software. As shown in Figure 3.2, flow cytometry analysis indicates that GMK cells show a little-to-no DAF expression. Expression on RD cells is very low. A549 and HeLa expressed abundant levels of cell surface DAF, whilst PC-3, MDA-MB-231, MCF-7, HT-29 and MDA-MB-435 expressed low levels of surface DAF (Table 3.2). It has previously been reported that RD, HeLa, HT-29 and PC-3 cells express DAF, in agreement with the results shown in Figure 3.2 (Pasch *et al.*, 1999; Gullberg *et al.*, 2010; Nasu *et al.*, 1998; Berry, *et al.*, 2008). There is no published information on GMK, MCF-7, MDA-MB-231 and MDA-MB-435 cells.

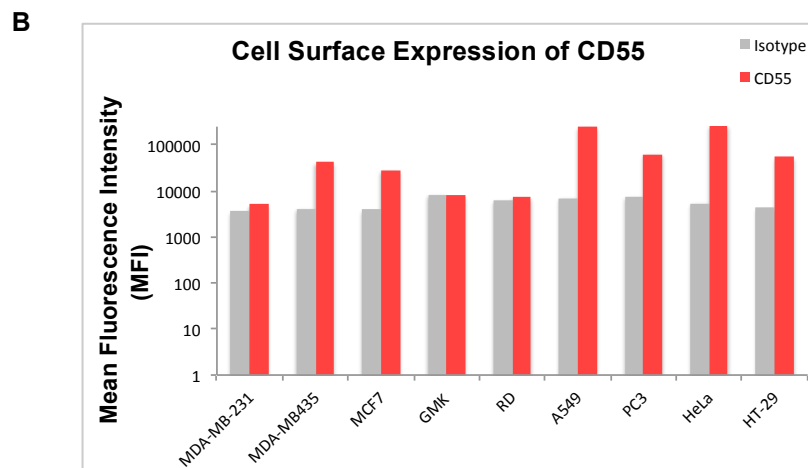
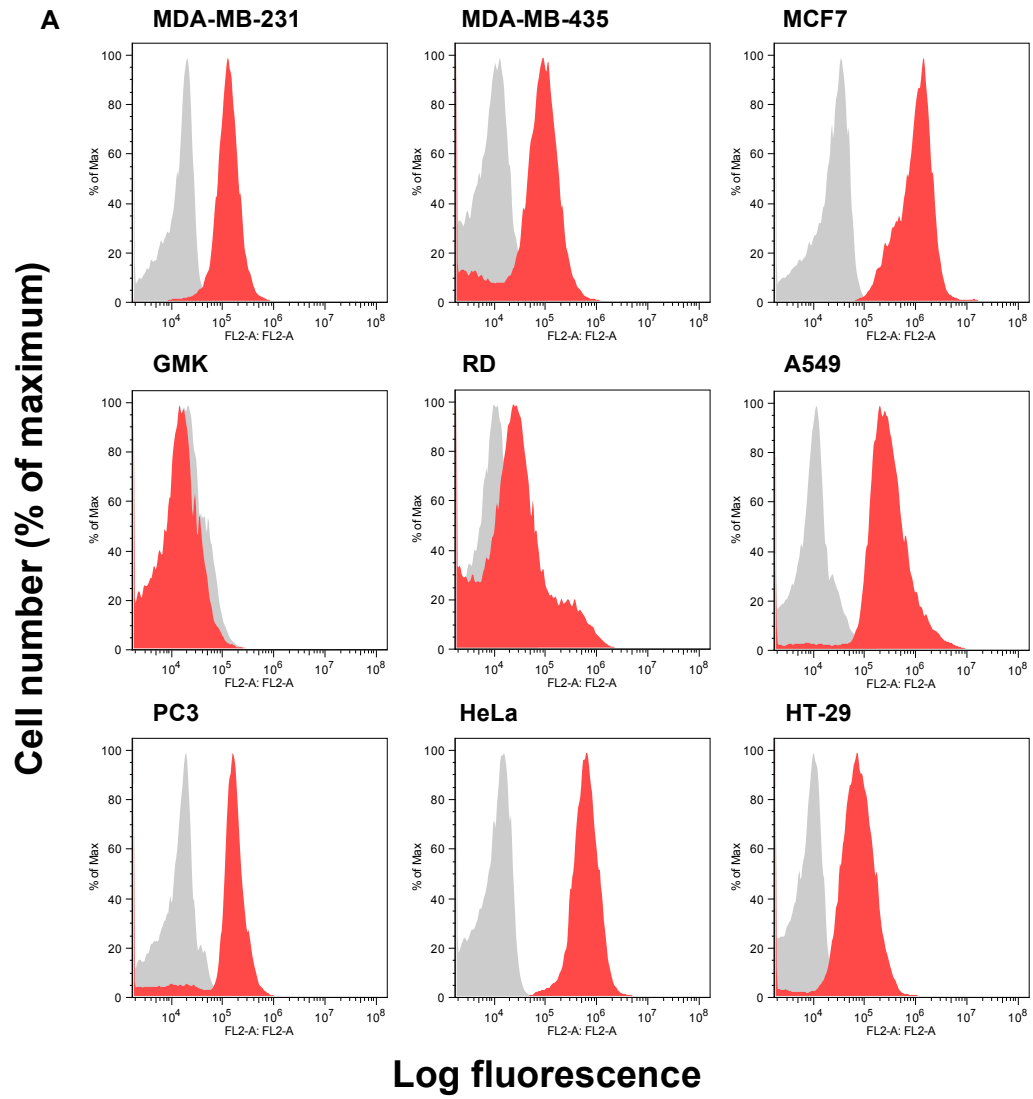


**Figure 3.2 Flow cytometric analysis of DAF (CD55) expression on the surface of different cell lines.** Cells were at a density of  $5 \times 10^5$  cells per ml. (A) Histograms show detection of 5  $\mu\text{g/ml}$  PE mouse IgG1 Isotype controls (grey plots) and detection of DAF by 5  $\mu\text{g/ml}$  PE anti-human CD55 antibody (red plots). Results were generated and gated with a FACS (BD Accuri C6) then analyzed and gated by FlowJo software. (B) A chart shows a comparison of the Isotype and anti-CD55 antibody on different cell lines (logarithmic scale, base 10).

**Table 3.2 Fluorescence intensity ratio of DAF antibody compared to the Isotype control.** Ratios are used to define categories of expression for use in Figure 3.3.

< 1= no expression, then 1 - 5, 5 -15, > 15 increasing levels of expression.

<b>Cells</b>	<b>Isotype (IgG1)</b>	<b>DAF (CD55)</b>	<b>Ratio</b>
<b>MDA-MB-231</b>	3554	5086	<b>1.43</b>
<b>MDA-MB435</b>	4122	42347	<b>10.27</b>
<b>MCF7</b>	3864	28631	<b>7.41</b>
<b>GMK</b>	8341	8012	<b>0.96</b>
<b>RD</b>	6304	7371	<b>1.17</b>
<b>A549</b>	7046	247000	<b>35.05</b>
<b>PC3</b>	7511	63969	<b>8.51</b>
<b>HeLa</b>	5436	266000	<b>48.93</b>
<b>HT-29</b>	4301	54098	<b>12.57</b>

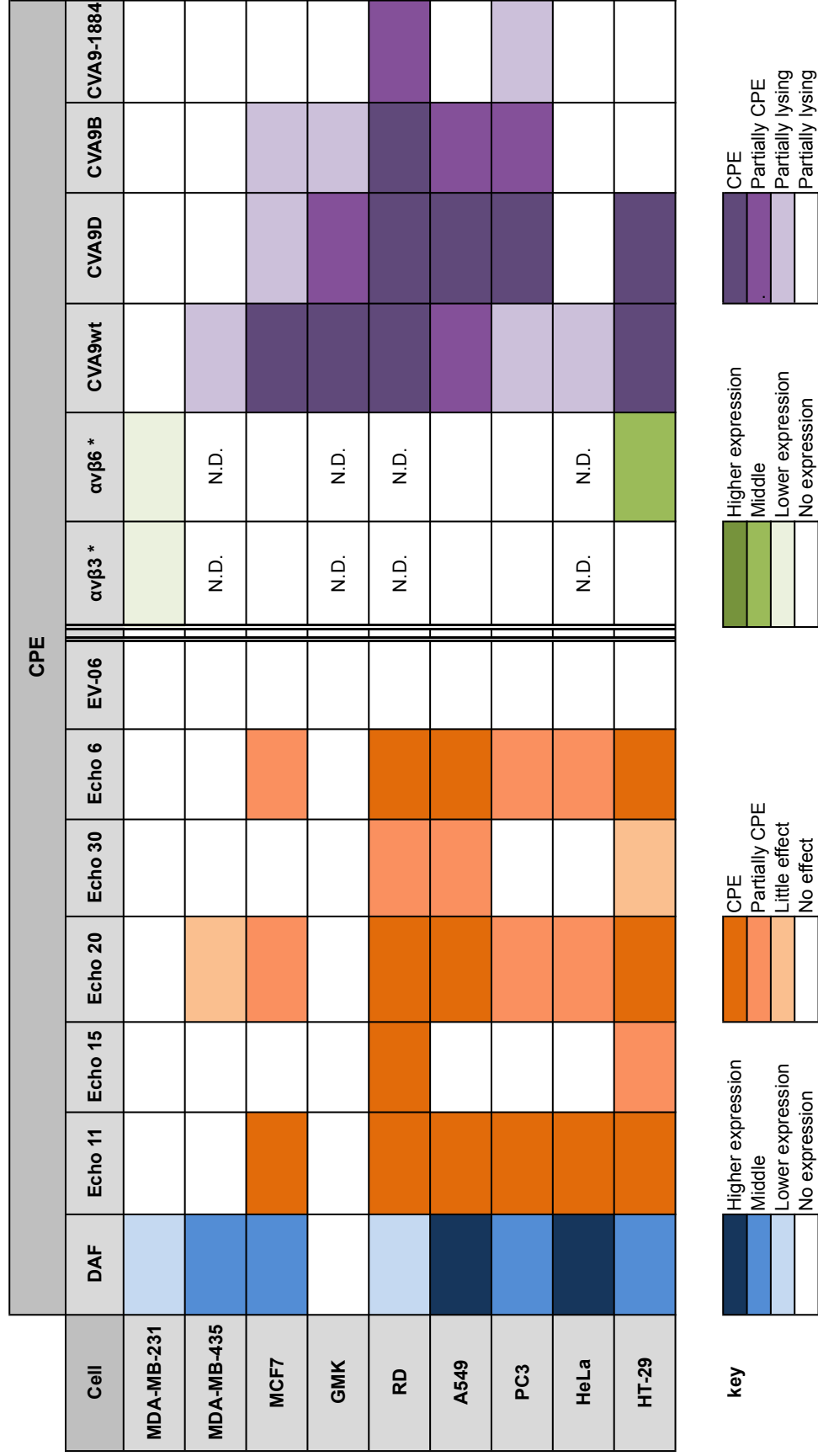


**Figure 3.3 Schematic diagram of DAF,  $\alpha\beta 3$  and  $\alpha\beta 6$  expression on different cell lines compared with cytopathic effect (CPE) observed when infected with a panel of enteroviruses. DAF expression is based on fluorescence intensity ration in Table 3.2. \*  $\alpha\beta 3$  and  $\alpha\beta 6$  expression is based on an analysis by Goodman *et al.*, 2012.**

It can be seen that there is only a slight correlation between expression of the receptor and the observed virus CPE, except for echoviruses and GMK cells where there is no DAF expression and no CPE caused by any echoviruses. MDA-MB-231 and MDA-MB-435 cells express low but significant levels of DAF but are not killed by most of the echoviruses. On the other hand, RD cells express little DAF but are killed efficiently by all the echoviruses except EV-06. MDA-MB-231 cells are reported to express both  $\alpha_v\beta_3$  and  $\alpha_v\beta_6$  (Goodman *et al.*, 2012) but are not killed by most of the CVA9 strains. MCF-7, A549 and PC-3 cells are reported to express no  $\alpha_v\beta_3$  and  $\alpha_v\beta_6$  and are infected by several of the CVA9 strains.

### 3.3.1 Conclusion of Cell Tropism and Receptor Expression Studies

The reported receptors used by echoviruses (DAF) and CVA9 (integrin  $\alpha_v\beta_6/\alpha_v\beta_3$ ) seem to show very different expression patterns. DAF is expressed on all the cell lines tested, except GMK. While  $\alpha_v\beta_6/\alpha_v\beta_3$  are not widely expressed according to the work of Goodman *et al.*, 2012. In both cases we find that receptor expression does not correlate well with the ability of echoviruses or CVA9 to infect the cells. This suggests that other receptors or other factors may be involved in defining cell tropism. In the case of CVA9, it is already known that mutants lacking the RGD motif can be infectious, which implies that the virus can use non-integrin receptors for entry (Hughes *et al.*, 1995). Similarly, adaptation of echoviruses to different cell lines can involve loss DAF binding (Stuart *et al.*, 2002b; Rezaikin *et al.*, 2009; Novoselov *et al.*, 2012).

### **3.4 Adaptation of an Echovirus 11 Isolate (E11 V5-7A) to A549 and HeLa Cells**

Previous studies have identified echovirus 11 mutants associated with adaptation into HT-29, Vero and RD cells (Stuart *et al.*, 2002b; Rezaikin *et al.*, 2009; Novoselov *et al.*, 2012). To extend our understanding of adaptation to other cell lines, we propagated Echovirus 11 (E11 V5-7A strain) on HeLa and A549 cells.

#### **3.4.1 Capsid Sequences of Echovirus 11 Strain E11 V5-7A**

The E11 V5-7A strain had not been sequenced previously, so initially sequence analysis of the P1 region was performed. Pan-enterovirus (5'UTR and VP2 primers) and primers based on conserved regions in an echovirus 11 alignments (Table 2.2a) were used for RT-PCR and sequencing (Figure 3.4). Four overlapping fragments were generated and sequenced using the same primers in both orientations. The whole sequence was then assembled and translated to give the amino acid sequence using the Expasy online tool (Artimo *et al.*, 2012).

#### **3.4.2 Relationship of E11 V5-7A to other E11 Isolates**

The predicted P1 amino acid sequence of E11 V5-7A was aligned with the sequence of all echovirus 11 isolates in the GenBank sequence database with a complete P1 sequence available. A maximum likelihood method tree was generated using MEGA6 (Figure 3.5). It can be seen that E11 V5-7A clusters

relatively closely with a few other isolates. These originate from several European countries including Finland, Hungary and Romania (Chevaliez *et al.*, 2004; Lukashev *et al.*, 2004) and the isolations were made from 1986- 2011. It is more distant from a cluster of strains which are mainly cell-line adapted variants of the Russian strain 7611 isolated in 1993 (Rezaikin *et al.*, 2009; Novoselov *et al.*, 2012). E11 V5-7A is also distant from the 1953 E11 prototype Gregory and adapted variants.

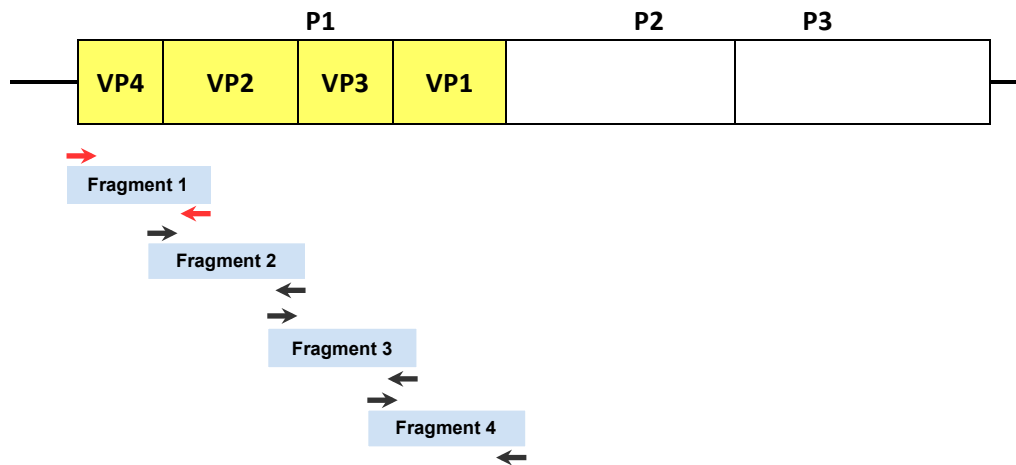


**Figure 3.4 Schematic diagram of the echovirus 11 capsid proteins (VPs) in the P1 region.** Overlapping fragments were generated using pan-enterovirus primers (red arrows) and primers based on E11 alignments (black arrows).

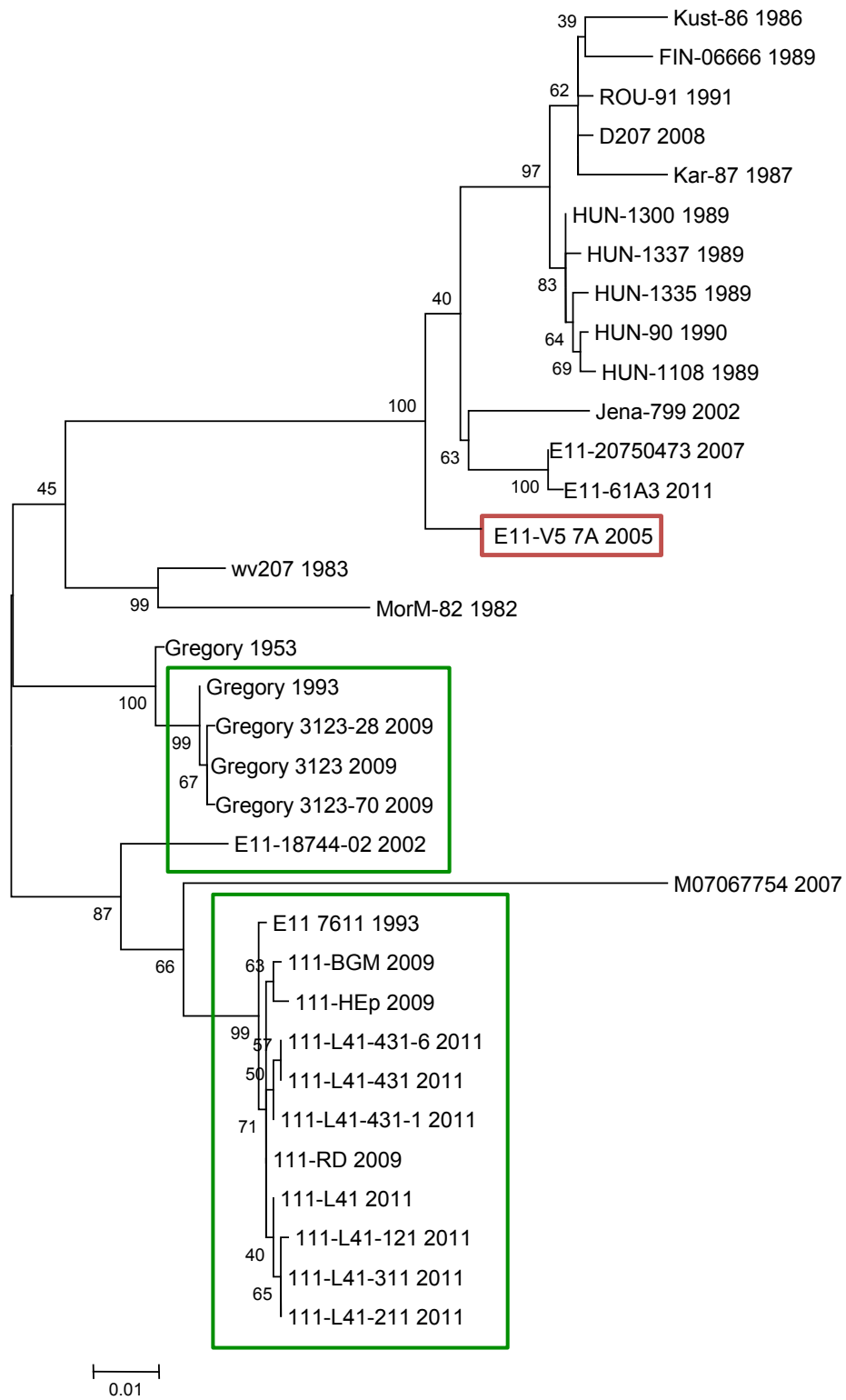


**Figure 3.5 Molecular phylogenetic analyses of Echovirus 11 isolates by Maximum Likelihood method.** The evolutionary history was inferred by using the Maximum Likelihood method based on the JTT matrix-based model (Jones *et al.*, 1992). The dendrogram shows phylogenetic relationships between sequenced E11 V5-7A isolate (red square) and the E11 isolates (green square indicated the isolates obtained by Rezaikin *et al.*, 2009; Novoselov *et al.*, 2012) of the GenBank sequence database for which complete P1 sequences are available. The analysis involved 34 amino acid sequences. Numbers at nodes shown next to the branches correspond to the percentage of replicates tree in which the associated taxa clustered together in the bootstrap test (1000 replicates). The tree is drawn to scale, with branch lengths measured in the number of substitutions per site. Evolutionary analyses were conducted in MEGA6 (Tamura *et al.*, 2013).

### **3.4.3 Generation of Adapted Variants of E11 V5-7A by Passaging on A549 and HeLa Cells**

We propagated 5 µl of the original E11 V5-7A stock on 25 cm<sup>2</sup> flasks containing monolayers of A549 and HeLa cells supplemented with 5 ml of DMEM culture medium. These showed a complete cytopathic effect (CPE) at the first passage on these cells, which developed after 3 days post-infection. Infected cells were freeze-thawed three times to release the virus and then 5 µl of the culture was added to fresh cell monolayers. The process was then repeated until nine passages. Passage 3, 6 and 9 (P3, P6 and P9) were analysed using a plaque assay (Figure 3.6). It can be seen that surprisingly the amount of virus presented at each passage level decreased. For the virus passaged on A549 cells there was a slight increase in plaque size from the original to P9. A much clearer increase was seen for the virus passaged on HeLa cells. The original pinprick plaques become much larger by P6 and P9.

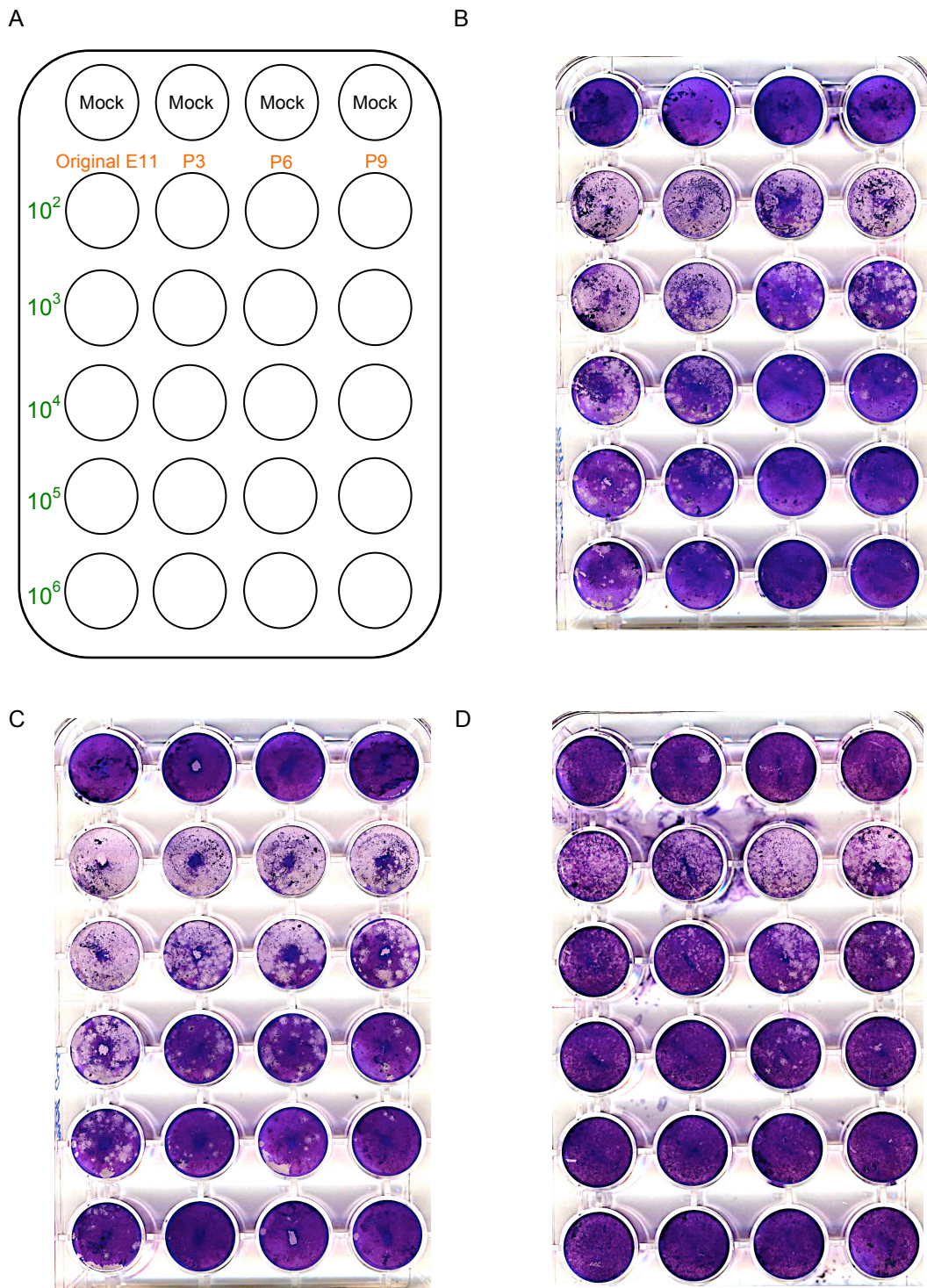


**Figure 3.6 A plaque assay of the original E11 (E11 V5-7A) and P3, 6 and 9 propagated on A549 and HeLa cells. (A) Schematic diagram describing the panel organization. A plaque assay comparing E11 V5-7A with P3, P6 and P9: (B) A549-adapted virus tested on A549 cells (C) HeLa-adapted virus tested on A549 cells (D) HeLa-adapted virus tested on HeLa cells.**

#### **3.4.4 Sequencing of Passaged E11 V5-7A**

Viral RNAs were isolated from E11 V5-7A adapted A549 and HeLa cells (P3, P6 and P9) then amplification was carried out by RT-PCR using specific primers (Table 2.2b) to give overlapping fragments. These primers were designed from the sequence generated from E11 V5-7A to improve the quality of the RT-PCR and sequencing. RT-PCR samples were separated by agarose gel electrophoresis and the amplicons were purified using a QIAquick Gel Extraction kit. The purified fragments were at position ~900 bp, ~880 bp, ~800 bp and ~780 bp respectively as expected (Figure 3.7). Then total DNA fragments were collected and sent for sequencing commercially by Source BioScience LifeSciences.

#### **3.4.5 Sequence Analysis of Passaged E11 V5-7A**

Sequences from passages 3, 6 and 9 were assembled and the capsid encoding-region sequence was translated into protein sequences using the ExPASy online tool. Then alignment comparisons were performed using the online tool ClustalW (*Larkin et al.*, 2007). There was no difference between the original E11 V5-7A sequence and the sequence recovered for P3 and P6. However, for E11 V5-7A adapted to A549 cells, two mutations appeared in P9. For E11 V5-7A adapted to HeLa cells, one mutation appeared in P9.

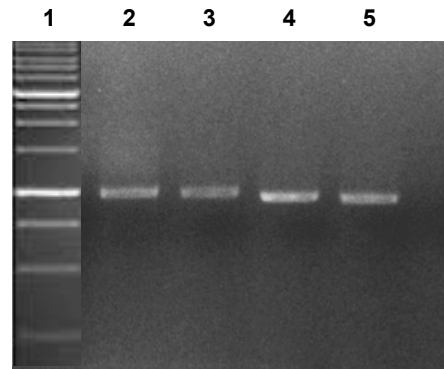


**Figure 3.7 Typical agarose gel electrophoresis of E11 V5-7A adapted to A549 and HeLa cells.** cDNAs were amplified by RT-PCR then DNA was isolated with a QIAquick Gel Extraction kit. This example shows the result for P9 on A549 cells.

Lane 1: 1 Kb ladder, Lane 2: fragment 1 (a band of ~900), Lane 3: fragment 2 (a band of ~880), Lane 4: fragment 3 (a band of ~800), Lane 5: fragment 4 (a band of ~780).

### 3.4.6 A549-adapted E11 V5-7A

The alignment of the A549-adapted viruses is shown in Figure 3.8. The two amino acids differences are G1452S (G at position 145 in VP2 changed to S) and E593V (E at position 59 in VP3 changed to V). The first mutation was due to a GGT to AGT change and the second mutation was due to GAG to GTG.

Furthermore, a visual inspection of the original E11 V5-7A; and passages 3, 6 and 9 in these regions was performed by using Chromas software to open the AB1 files for each sequence (Figure 3.9 and 3.10). The histograms for the G1452S region showed only GGT for the original E11 V5-7A and P3, but there was apparent heterogeneity of the viral populations at P6 and P9. At P6 there was a small amount of AGT and the first nucleotide was read by the sequencer as G. At P9, AGT mostly replaced GGT and the first nucleotide was read by the sequencer as A. Some GGT was still present (Figure 3.9).

The situation for the E593V region was slightly different as a small amount of the mutant sequence GTG was already seen at P3. This increased slightly at P6 and the central T of the codon becomes the larger peak at P9 (Figure 3.10).

>VP4

E11 V5-7A MGTQVSTQKTGAHETGLNASGNSVIHYTNINYYKDAASNSANRQDFTQDPGKFTEPVKDI 60
E11 A549-P3 MGTQVSTQKTGAHETGLNASGNSVIHYTNINYYKDAASNSANRQDFTQDPGKFTEPVKDI 60
E11 A549-p6 MGTQVSTQKTGAHETGLNASGNSVIHYTNINYYKDAASNSANRQDFTQDPGKFTEPVKDI 60
E11 A549-P9 MGTQVSTQKTGAHETGLNASGNSVIHYTNINYYKDAASNSANRQDFTQDPGKFTEPVKDI 60
\*\*\*\*\*

>VP2

E11 V5-7A MIKSM PALNSPSAE ECGYSDRVSITLGNSTITTTQECANVVVAYGRWPEYLSDEEATAED 120
E11 A549-P3 MIKSM PALNSPSAE ECGYSDRVSITLGNSTITTTQECANVVVAYGRWPEYLSDEEATAED 120
E11 A549-p6 MIKSM PALNSPSAE ECGYSDRVSITLGNSTITTTQECANVVVAYGRWPEYLSDEEATAED 120
E11 A549-P9 MIKSM PALNSPSAE ECGYSDRVSITLGNSTITTTQECANVVVAYGRWPEYLSDEEATAED 120
\*\*\*\*\*

E11 V5-7A QPTQPDVATCRFYTLESVTWERESPGWWWKFPDALKDMGLFGQNMYYHYLGRAGYTIHVQ 180
E11 A549-P3 QPTQPDVATCRFYTLESVTWERESPGWWWKFPDALKDMGLFGQNMYYHYLGRAGYTIHVQ 180
E11 A549-p6 QPTQPDVATCRFYTLESVTWERESPGWWWKFPDALKDMGLFGQNMYYHYLGRAGYTIHVQ 180
E11 A549-P9 QPTQPDVATCRFYTLESVTWERESPGWWWKFPDALKDMGLFGQNMYYHYLGRAGYTIHVQ 180
\*\*\*\*\*

145

E11 V5-7A CNASKFHQGC LLVVCVPEAEMGCS DVNGVVNEHGI SEGETAKKFSATASNGTHTVQSI VT 240
E11 A549-P3 CNASKFHQGC LLVVCVPEAEMGCS DVNGVVNEHGI SEGETAKKFSATASNGTHTVQSI VT 240
E11 A549-P6 CNASKFHQGC LLVVCVPEAEMGCS DVNGVVNEHGI SEGETAKKFSATASNGTHTVQSI VT 240
E11 A549-P9 CNASKFHQGC LLVVCVPEAEMGCS DVNGVVNEHGI SEGETAKKFSATASNGTHTVQSI VT 240
\*\*\*\*\*

E11 V5-7A NAGMGVGVGNLTIYPHQWINLR TNNSATI VMPYINSVPMDNMFRRHNF TLMII PFVSLDY 300
E11 A549-P3 NAGMGVGVGNLTIYPHQWINLR TNNSATI VMPYINSVPMDNMFRRHNF TLMII PFVSLDY 300
E11 A549-P6 NAGMGVGVGNLTIYPHQWINLR TNNSATI VMPYINSVPMDNMFRRHNF TLMII PFVSLDY 300
E11 A549-P9 NAGMGVGVGNLTIYPHQWINLR TNNSATI VMPYINSVPMDNMFRRHNF TLMII PFVSLDY 300
\*\*\*\*\*

>VP3

E11 V5-7A SSDASTYVPI TVTVAPMCAEYNGLR LATS LQGLPVMNTPGSNQFLTSDDFQSPSAMPQFD 360
E11 A549-P3 SSDASTYVPI TVTVAPMCAEYNGLR LATS LQGLPVMNTPGSNQFLTSDDFQSPSAMPQFD 360
E11 A549-P6 SSDASTYVPI TVTVAPMCAEYNGLR LATS LQGLPVMNTPGSNQFLTSDDFQSPSAMPQFD 360
E11 A549-P9 SSDASTYVPI TVTVAPMCAEYNGLR LATS LQGLPVMNTPGSNQFLTSDDFQSPSAMPQFD 360
\*\*\*\*\*

59

E11 V5-7A VTPELDIPGEVKNLMEIAEVD SVVPVNNV E GKLDTMDIFRIPVQSGNQQTQVFGFQVQP 420
E11 A549-P3 VTPELDIPGEVKNLMEIAEVD SVVPVNNV E GKLDTMDIFRIPVQSGNQQTQVFGFQVQP 420
E11 A549-P6 VTPELDIPGEVKNLMEIAEVD SVVPVNNV E GKLDTMDIFRIPVQSGNQQTQVFGFQVQP 420
E11 A549-P9 VTPELDIPGEVKNLMEIAEVD SVVPVNNV E GKLDTMDIFRIPVQSGNQQTQVFGFQVQP 420
\*\*\*\*\*

E11 V5-7A GLDSVFKHTLLGEILNYYAHWSG SVKLT FVFCGSAMATGKFL LAYSPPGANAPKTRKDAM 480
E11 A549-P3 GLDSVFKHTLLGEILNYYAHWSG SVKLT FVFCGSAMATGKFL LAYSPPGANAPKTRKDAM 480
E11 A549-P6 GLDSVFKHTLLGEILNYYAHWSG SVKLT FVFCGSAMATGKFL LAYSPPGANAPKTRKDAM 480
E11 A549-P9 GLDSVFKHTLLGEILNYYAHWSG SVKLT FVFCGSAMATGKFL LAYSPPGANAPKTRKDAM 480
\*\*\*\*\*

E11 V5-7A LGTHVVWDVGLQSSCVLCIPWISQ THYRLVHQDEYTSAGNVTCWYQTGIVVPAGTPTSCS 540
E11 A549-P3 LGTHVVWDVGLQSSCVLCIPWISQ THYRLVHQDEYTSAGNVTCWYQTGIVVPAGTPTSCS 540
E11 A549-P6 LGTHVVWDVGLQSSCVLCIPWISQ THYRLVHQDEYTSAGNVTCWYQTGIVVPAGTPTSCS 540
E11 A549-P9 LGTHVVWDVGLQSSCVLCIPWISQ THYRLVHQDEYTSAGNVTCWYQTGIVVPAGTPTSCS 540
\*\*\*\*\*

>VP1

E11 V5-7A IMCFVSACNDFSVRLLKDTPFIEQSALLQGDVVEAIESAVARVADTISSGPTNSQAVPAL 600
E11 A549-P3 IMCFVSACNDFSVRLLKDTPFIEQSALLQGDVVEAIESAVARVADTISSGPTNSQAVPAL 600
E11 A549-P6 IMCFVSACNDFSVRLLKDTPFIEQSALLQGDVVEAIESAVARVADTISSGPTNSQAVPAL 600
E11 A549-P9 IMCFVSACNDFSVRLLKDTPFIEQSALLQGDVVEAIESAVARVADTISSGPTNSQAVPAL 600
\*\*\*\*\*

E11 V5-7A TAVETGHTSQVVPGDTMQTRHVKNYHSRSESTIENFLSRAACVYMGEYTTNTDETKRFA 660
E11 A549-P3 TAVETGHTSQVVPGDTMQTRHVKNYHSRSESTIENFLSRAACVYMGEYTTNTDETKRFA 660
E11 A549-P6 TAVETGHTSQVVPGDTMQTRHVKNYHSRSESTIENFLSRAACVYMGEYTTNTDETKRFA 660
E11 A549-P9 TAVETGHTSQVVPGDTMQTRHVKNYHSRSESTIENFLSRAACVYMGEYTTNTDETKRFA 660
\*\*\*\*\*

```

E11 V5-7A      NWTINARRMVQMRKLEMFTYVRFDVEVTFVITSKDQGTQLGQDMPPLTHQIMYIPPGG 720
E11 A549-P3   NWTINARRMVQMRKLEMFTYVRFDVEVTFVITSKDQGTQLGQDMPPLTHQIMYIPPGG 720
E11 A549-P6   NWTINARRMVQMRKLEMFTYVRFDVEVTFVITSKDQGTQLGQDMPPLTHQIMYIPPGG 720
E11 A549-P9   NWTINARRMVQMRKLEMFTYVRFDVEVTFVITSKDQGTQLGQDMPPLTHQIMYIPPGG 720
*****

E11 V5-7A      PIPKSTTDYAWQTSTNPSIFWTEGNAPPRMSIPFVSI GNAYSNFYDGWSHFSQNGVYGYN 780
E11 A549-P3   PIPKSTTDYAWQTSTNPSIFWTEGNAPPRMSIPFVSI GNAYSNFYDGWSHFSQNGVYGYN 780
E11 A549-P6   PIPKSTTDYAWQTSTNPSIFWTEGNAPPRMSIPFVSI GNAYSNFYDGWSHFSQNGVYGYN 780
E11 A549-P9   PIPKSTTDYAWQTSTNPSIFWTEGNAPPRMSIPFVSI GNAYSNFYDGWSHFSQNGVYGYN 780
*****

E11 V5-7A      TLNNMGQLYMRHVNGPSPLPMTSTVRVYFKPKHKVKAWVPRPPRLCQYKNASTVNFSSSTNI 840
E11 A549-P3   TLNNMGQLYMRHVNGPSPLPMTSTVRVYFKPKHKVKAWVPRPPRLCQYKNASTVNFSSSTNI 840
E11 A549-P6   TLNNMGQLYMRHVNGPSPLPMTSTVRVYFKPKHKVKAWVPRPPRLCQYKNASTVNFSSSTNI 840
E11 A549-P9   TLNNMGQLYMRHVNGPSPLPMTSTVRVYFKPKHKVKAWVPRPPRLCQYKNASTVNFSSSTNI 840
*****

E11 V5-7A      TDKRNSITYIPDTVKPDVSNH 861
E11 A549-P3   TDKRNSITYIPDTVKPDVSNH 861
E11 A549-P6   TDKRNSITYIPDTVKPDVSNH 861
E11 A549-P9   TDKRNSITYIPDTVKPDVSNH 861
*****

```

**Figure 3.8 ClustalW alignments of the E11 V5-7A amino acid sequence and the consensus sequence derived from the 4 RT-PCR fragments from the A549-passaged viruses (E11 A549-P3, E11 A549-P6 and E11 A549-P9). The amino acid differences are seen in P9, G145S in VP2 and E59V in VP3 (marked with blue and pink respectively).**

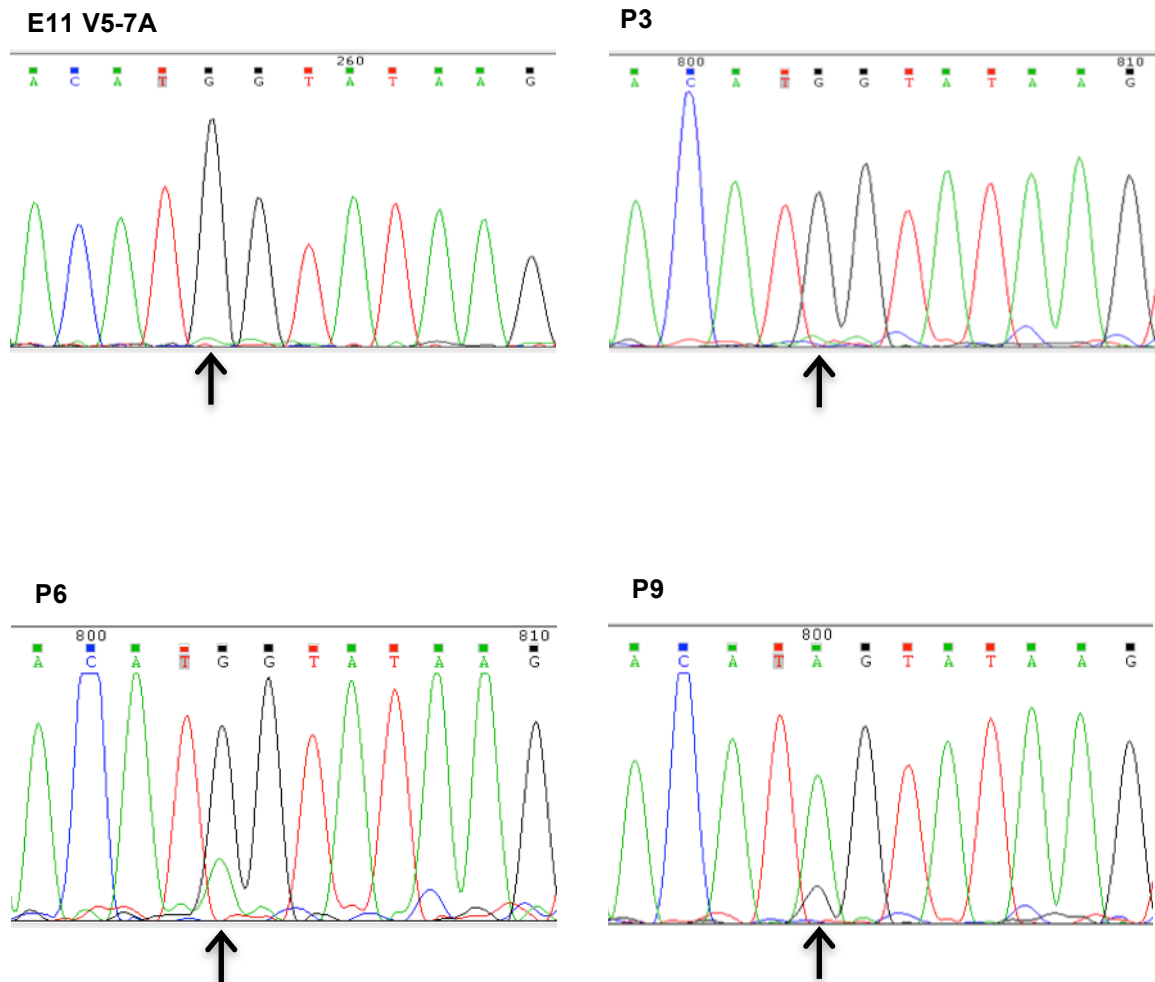


**Figure 3.9** Histograms of the sequence analysis of the A549-adapted E11 V5-7A, P3, P6 and P9 using Chromas software. The arrows indicate the nucleotide change to give G1452S (G to A). Result shows that there is a single peak in the E11 V5-7A sequence and P3, whereas, two peaks appeared at the same position in P6 and P9, indicating heterogeneity of the viral population.

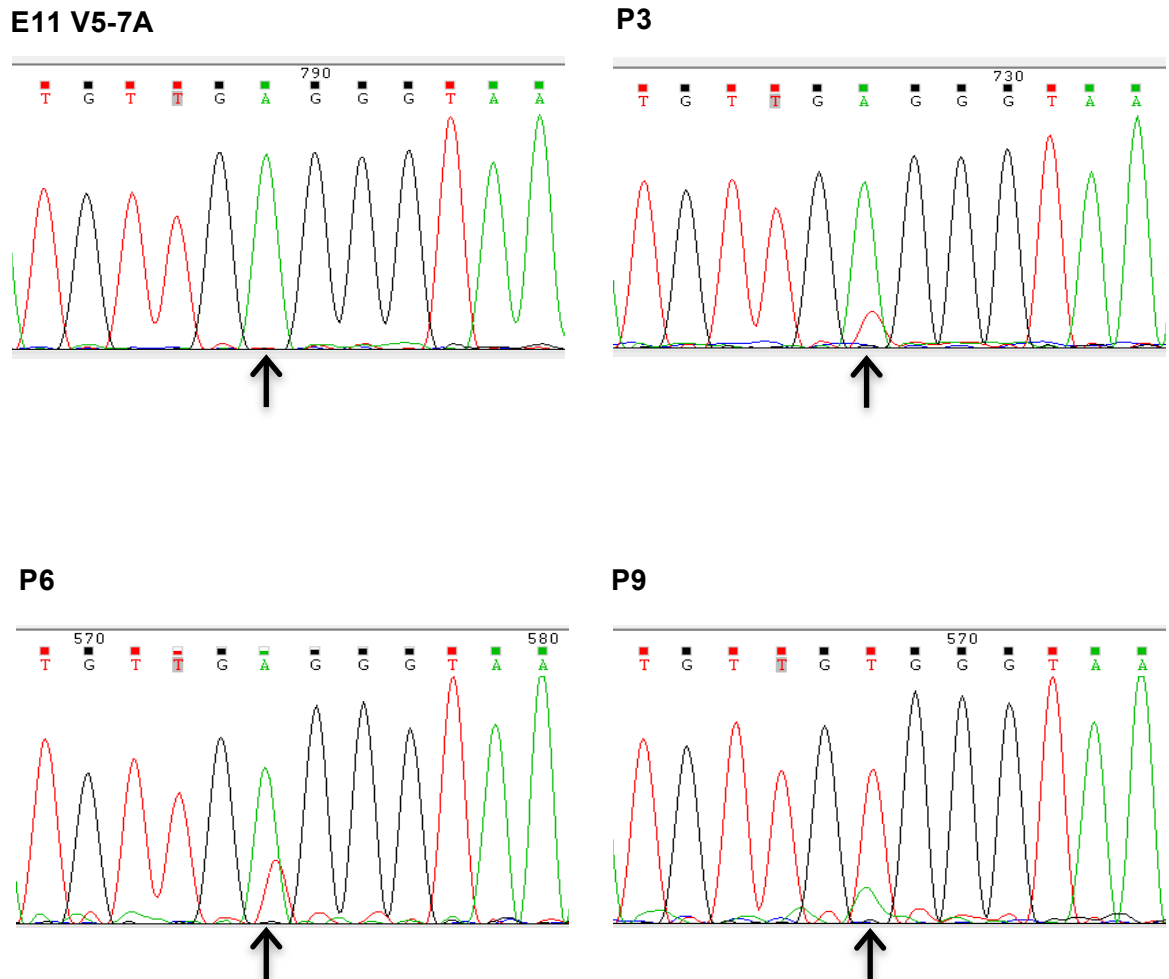


**Figure 3.10** Histograms of the sequence analysis of the A549-adapted E11 V5-7A, P3, P6 and P9 using Chromas software. The arrows indicate the nucleotide change to give E593V (A to T). Results shows that there is a single peak in the E11 V5-7A sequence, whereas, two peaks appeared at the same position in P3, P6 and P9, indicating heterogeneity of the viral population.

### 3.4.7 Sequence alignment of E11 V5-7A with other E11 Isolates

The same E11 isolate sequences used for the phylogenetic tree (Figure 3.5) were aligned with the E11 V5-7A sequence (Appendix 1). Predicted secondary structural domains based on the E7 X-ray crystallography structure are marked on the alignment (Plevka *et al.*, 2010). The most variable regions are: part of the VP2 puff, between  $\beta$ E and  $\alpha\beta$ 1, and between  $\alpha\beta$ 1 and  $\alpha\beta$ 2; the VP3 Knob domain in the  $\alpha$ Z2/ $\alpha$ Z2 region; the C-terminus of VP3 and N-terminus of VP1; the  $\alpha$ Z2 of VP1 and the VP1  $\beta$ B-  $\beta$ C loop; the VP1  $\beta$ D-  $\beta$ E loop; the VP1 C-terminus. The puff and knob are very exposed on the cell surface as is the VP1  $\beta$ B-  $\beta$ C loop, and  $\beta$ D-  $\beta$ E and are therefore probably more flexible and can tolerate changes, as well as possibly being under immune system selection, even though these are all E11 isolates. The termini of the protein are mainly internal but unstructured and therefore changes can be tolerated (Plevka *et al.*, 2010). Also marked on the alignment are amino acids likely to be involved in the DAF footprint, based on an alignment with E7 (Appendix 2), where the footprint has been defined (Plevka *et al.*, 2010; Yoder *et al.*, 2012). The footprint shows that 3 DAF SCR domains (SCR2-4) bind to E7, SCR2 to part of VP1, SCR3 mainly to the VP2 puff and SCR4 mainly to the VP3 knob domain. E7 and E11 V5-7A are closely related and the overall surface structure is likely to be similar, although there are several amino acid differences in the puff and knob domains.

The VP2 G145S mutation is in the puff domain and VP3 E59V is in the knob domain (Appendix 1). The G145S is in the predicted binding site for DAF SCR3. The E59V is in the DAF SCR4 binding site. This VP2 145 site, as shown in Appendix 1, shows some variations between different E11 isolates and S145 is

seen in 14 isolates, while 17 have G and three have A. The VP3 59 site also shows some variations between E11 isolates, although only one (kust-86) has a V.

The mutations were mapped onto the E11 coordinates (PDB ID: 1H8T) (Stuart *et al.*, 2002b), together with other mutations seen in E11 adaptation experiments on the other cell lines (Figure 3.11 and 3.12). These mutations fall into two groups, one closer to the 5-fold axis and at the north side of the canyon, the other one further from the 5-fold axis and at the south rim of the canyon. The A549-adapted E11 V5-7A mutations fall into the second group, which are associated with the DAF binding domains. G1452S clusters with several other previously seen mutations (Stuart *et al.*, 2002b; Rezaikin *et al.*, 2009; Novoselov *et al.*, 2012). E593V is further away from other mutations. As expected from the sequence alignment when both mutations are plotted onto the DAF binding footprint (Figure 3.13) of a surface projection of E7 (Yoder *et al.*, 2012), G1452S maps to the binding site for DAF SCR3 and E593V to the SCR4 binding site.

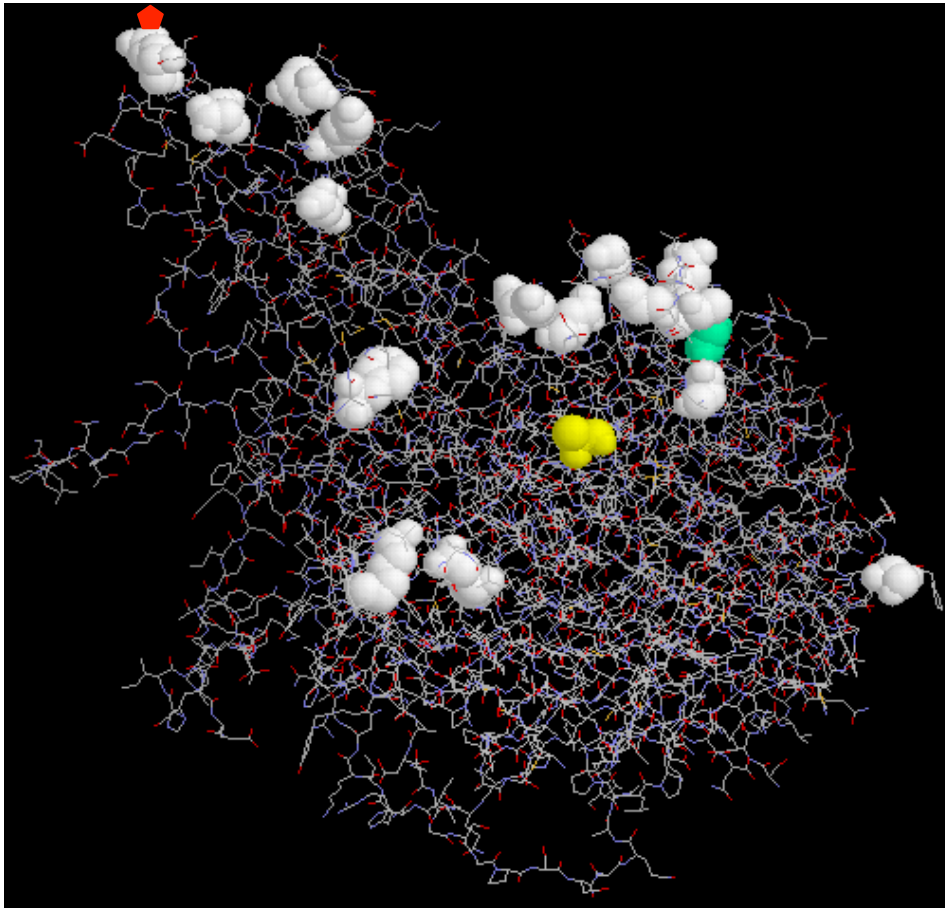


**Figure 3.11** The three-dimensional structure of the E11 protomer (coordinates PDB ID: 1H8T), using Rasmol software to map the mutations seen in A549-adapted E11 V5-7A. VP2 position 145 is shown in spacefill, green. VP3 position 59 shown in spacefill, yellow. Other mutations associated with adaptation to other cell lines are shown in spacefill, white (Stuart *et al.*, 2002b; Rezaikin *et al.*, 2009; Novoselov *et al.*, 2012). The position of the 5-fold axis is shown by a red pentagon.

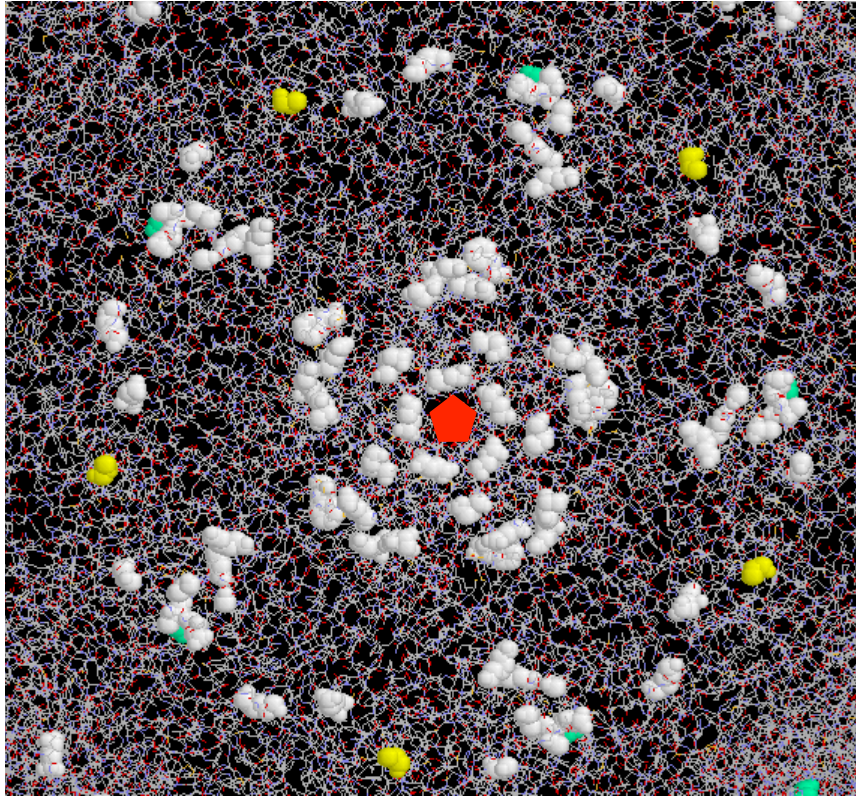


**Figure 3.12** Part of the three-dimensional half-capsid structure of E11 (coordinates PDB ID: 1H8T) shown using Rasmol software. The results show five copies of VP2 position 145 (shown in spacefill, green) and VP3 position 59 (shown in spacefill, yellow). Other mutations associated with adaptation to other cell lines are shown in spacefill white. A red pentagon is centered on the 5-fold axis (Stuart *et al.*, 2002b; Rezaikin *et al.*, 2009; Novoselov *et al.*, 2012).

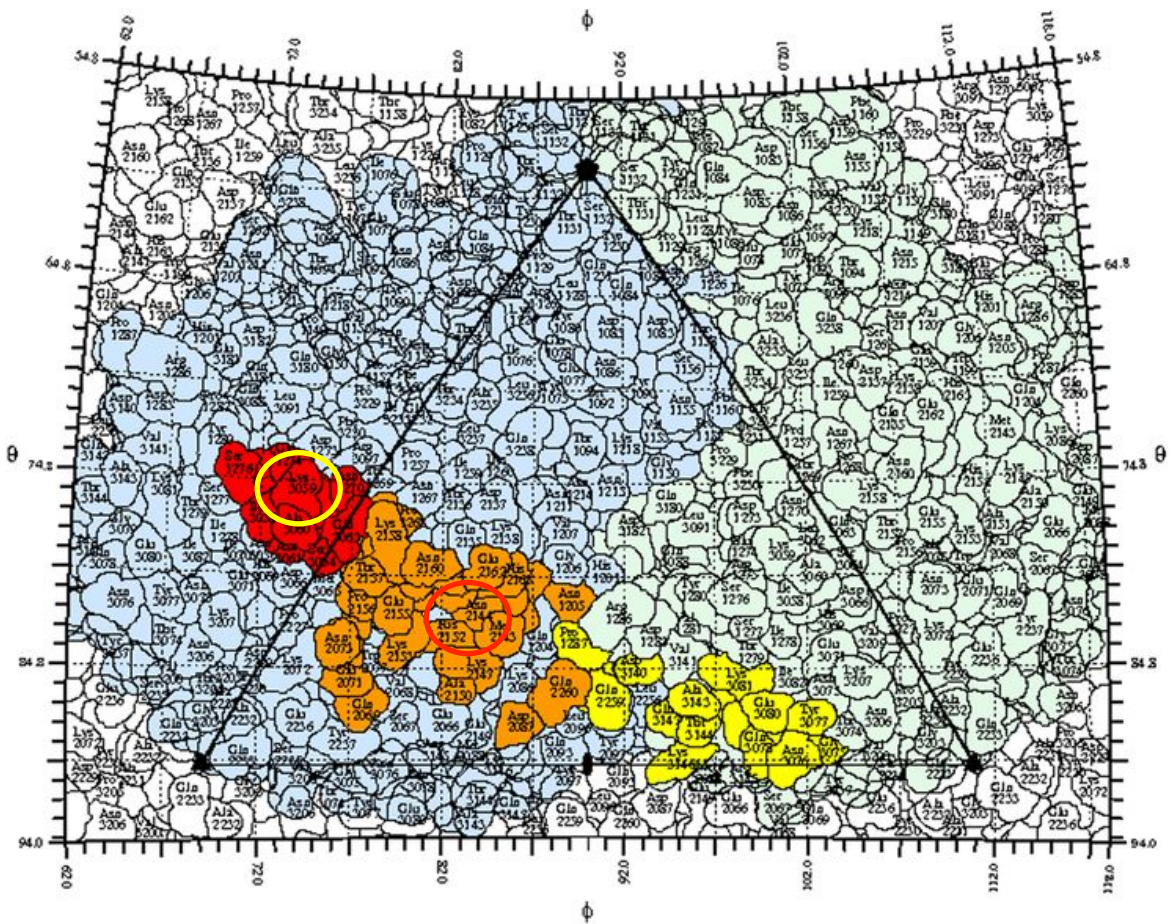


**Figure 3.13** Surface projection of E7 (Yoder *et al.*, 2012), showing the location of the amino acids which bind to DAF domains SCR2 (yellow), SCR3 (orange) and SCR4 (red). The predicted positions of the amino acid mutations seen in the P9 passage of A549-adapted E11 V5-7A are shown as a yellow circle (E593V) and a red circle (G1452S).

### 3.4.8 HeLa-adapted E11 V5-7A

E11 V5-7A was also propagated on HeLa cells for 9 passages as for A549 cells (Section 3.4.3). The HeLa-adapted virus P3, P6 and P9 were then sequenced and the alignments were compared to E11 V5-7A sequence (Figure 3.14). One amino acid change was seen in P9, at VP4 position 16 (G164R, G at position 16 in VP4 changed to R). The mutation was due to a GGA to AGA change.

A visual inspection of the original E11 V5-7A and passages (3, 6 and 9) in this region was performed by using Chromas software to open the AB1 files for each sequence (Figure 3.15). The histograms showed only GGA for E11 V5-7A and E11 V5-7A-P3, but there was apparent heterogeneity of the viral populations at P6 and P9. At P6 there was a small amount of AGA and the first nucleotide was read by the sequencer as G. At P9, there seems to be approximately equal amounts of AGA and GGA and the first nucleotide was read by the sequencer as A in the negative sense but G in the positive sense (Figure 3.15).

The G164R mutation is probably located on the inner surface of the capsid, but this position is not visible by X-ray crystallography. The nearest amino acid whose position is known is position 15 and this was used and mapped onto the E11 (coordinates PDB ID: 1H8T) (Stuart *et al.*, 2002b), as shown in Figure 3.16. All E11 isolates shown in the alignment in Figure 3.11 have G16, and no variations appeared between different E11 isolates. R at this position is not seen frequently in other enteroviruses. An alignment of the sequences of all enteroviruses in the database with R at position 16 is shown in Figure 3.17. It is seen in the Nancy CBV3 strain, some isolates of E14, E2 and E9 and in a few untyped viruses isolated from cases of acute flaccid paralyses (*Enterovirus B*). It

is also seen in some CVA6 (*Enterovirus A*) isolates. Interestingly, a mutation of G164R was associated with increased virulence in a CBV3 strain (Ramsingh and Collins, 1995).

**>VP4** 16  
E11 V5-7A MGTQVSTQKTGAHETGLNASGNSVIHYTNINYYKDAASNSANRQDFTQDPGKFTEPVKDI 60  
E11 HeLa-P3 MGTQVSTQKTGAHETGLNASGNSVIHYTNINYYKDAASNSANRQDFTQDPGKFTEPVKDI 60  
E11 HeLa-P6 MGTQVSTQKTGAHETGLNASGNSVIHYTNINYYKDAASNSANRQDFTQDPGKFTEPVKDI 60  
E11 HeLa-P9 MGTQVSTQKTGAHETGLNASGNSVIHYTNINYYKDAASNSANRQDFTQDPGKFTEPVKDI 60  
\*\*\*\*\*

**>VP2**  
E11 V5-7A MIKSMPALNSPSAECCGYSDRVSITLGNSTITTTQECANVVVAYGRWPEYLSDEEATAED 120  
E11 HeLa-P3 MIKSMPALNSPSAECCGYSDRVSITLGNSTITTTQECANVVVAYGRWPEYLSDEEATAED 120  
E11 HeLa-P6 MIKSMPALNSPSAECCGYSDRVSITLGNSTITTTQECANVVVAYGRWPEYLSDEEATAED 120  
E11 HeLa-P9 MIKSMPALNSPSAECCGYSDRVSITLGNSTITTTQECANVVVAYGRWPEYLSDEEATAED 120  
\*\*\*\*\*

E11 V5-7A QPTQPDVATCRFYTLESVTWERESPGWWWKFPDALKDMGLFGQNMYYHYLGRAGYTIHVQ 180  
E11 HeLa-P3 QPTQPDVATCRFYTLESVTWERESPGWWWKFPDALKDMGLFGQNMYYHYLGRAGYTIHVQ 180  
E11 HeLa-P6 QPTQPDVATCRFYTLESVTWERESPGWWWKFPDALKDMGLFGQNMYYHYLGRAGYTIHVQ 180  
E11 HeLa-P9 QPTQPDVATCRFYTLESVTWERESPGWWWKFPDALKDMGLFGQNMYYHYLGRAGYTIHVQ 180  
\*\*\*\*\*

E11 V5-7A CNASKFHQGCLLVVCPPEAEMGCSDVNGVNEHGI SEGETAKKFSATASNGTHTVQSI VT 240  
E11 HeLa-P3 CNASKFHQGCLLVVCPPEAEMGCSDVNGVNEHGI SEGETAKKFSATASNGTHTVQSI VT 240  
E11 HeLa-P6 CNASKFHQGCLLVVCPPEAEMGCSDVNGVNEHGI SEGETAKKFSATASNGTHTVQSI VT 240  
E11 HeLa-P9 CNASKFHQGCLLVVCPPEAEMGCSDVNGVNEHGI SEGETAKKFSATASNGTHTVQSI VT 240  
\*\*\*\*\*

E11 V5-7A NAGMGVGVGNLTIYPHQWINLR TNNSATIVMPYINSVPMDNMFRRHNF TLMII PFVSLDY 300  
E11 HeLa-P3 NAGMGVGVGNLTIYPHQWINLR TNNSATIVMPYINSVPMDNMFRRHNF TLMII PFVSLDY 300  
E11 HeLa-P6 NAGMGVGVGNLTIYPHQWINLR TNNSATIVMPYINSVPMDNMFRRHNF TLMII PFVSLDY 300  
E11 HeLa-P9 NAGMGVGVGNLTIYPHQWINLR TNNSATIVMPYINSVPMDNMFRRHNF TLMII PFVSLDY 300  
\*\*\*\*\*

**>VP3**  
E11 V5-7A SSDASTYVPITVTVAPMCAEYNGRLRLATSLQGLPVMNTPGSNQFLTSDDFQSPSAMPQFD 360  
E11 HeLa-P3 SSDASTYVPITVTVAPMCAEYNGRLRLATSLQGLPVMNTPGSNQFLTSDDFQSPSAMPQFD 360  
E11 HeLa-P6 SSDASTYVPITVTVAPMCAEYNGRLRLATSLQGLPVMNTPGSNQFLTSDDFQSPSAMPQFD 360  
E11 HeLa-P9 SSDASTYVPITVTVAPMCAEYNGRLRLATSLQGLPVMNTPGSNQFLTSDDFQSPSAMPQFD 360  
\*\*\*\*\*

E11 V5-7A VPELDIPGEVKNLMEIAEVD SVVPVNNVEGKLD TMDIFRIPVQSGNQQTQVFGFQVQP 420  
E11 HeLa-P3 VPELDIPGEVKNLMEIAEVD SVVPVNNVEGKLD TMDIFRIPVQSGNQQTQVFGFQVQP 420  
E11 HeLa-P6 VPELDIPGEVKNLMEIAEVD SVVPVNNVEGKLD TMDIFRIPVQSGNQQTQVFGFQVQP 420  
E11 HeLa-P9 VPELDIPGEVKNLMEIAEVD SVVPVNNVEGKLD TMDIFRIPVQSGNQQTQVFGFQVQP 420  
\*\*\*\*\*

E11 V5-7A GLDSVFKHTLLGEILNYYAHWSGSVKLTFVFCGSAMATGKFL LAYSPPGANAPKTRKDAM 480  
E11 HeLa-P3 GLDSVFKHTLLGEILNYYAHWSGSVKLTFVFCGSAMATGKFL LAYSPPGANAPKTRKDAM 480  
E11 HeLa-P6 GLDSVFKHTLLGEILNYYAHWSGSVKLTFVFCGSAMATGKFL LAYSPPGANAPKTRKDAM 480  
E11 HeLa-P9 GLDSVFKHTLLGEILNYYAHWSGSVKLTFVFCGSAMATGKFL LAYSPPGANAPKTRKDAM 480  
\*\*\*\*\*

E11 V5-7A LGTHVVWDVGLQSSCVLCIPWISQTHYRLVHQDEYTSAGNVTCWYQTGIVVPAGTPTSCS 540  
E11 HeLa-P3 LGTHVVWDVGLQSSCVLCIPWISQTHYRLVHQDEYTSAGNVTCWYQTGIVVPAGTPTSCS 540  
E11 HeLa-P6 LGTHVVWDVGLQSSCVLCIPWISQTHYRLVHQDEYTSAGNVTCWYQTGIVVPAGTPTSCS 540  
E11 HeLa-P9 LGTHVVWDVGLQSSCVLCIPWISQTHYRLVHQDEYTSAGNVTCWYQTGIVVPAGTPTSCS 540  
\*\*\*\*\*

**>VP1**  
E11 V5-7A IMCFVSACNDFSVRLLKDTPFIEQSALLQGDVVEAIESAVARVADTISSGPTNSQAVPAL 600  
E11 HeLa-P3 IMCFVSACNDFSVRLLKDTPFIEQSALLQGDVVEAIESAVARVADTISSGPTNSQAVPAL 600  
E11 HeLa-P6 IMCFVSACNDFSVRLLKDTPFIEQSALLQGDVVEAIESAVARVADTISSGPTNSQAVPAL 600  
E11 HeLa-P9 IMCFVSACNDFSVRLLKDTPFIEQSALLQGDVVEAIESAVARVADTISSGPTNSQAVPAL 600  
\*\*\*\*\*

E11 V5-7A TAVETGHTSQVVPGD TMQTRHVKNYHSRSESTIENFLSRAACVYMGEYTTNTDETKRFA 660  
E11 HeLa-P3 TAVETGHTSQVVPGD TMQTRHVKNYHSRSESTIENFLSRAACVYMGEYTTNTDETKRFA 660  
E11 HeLa-P6 TAVETGHTSQVVPGD TMQTRHVKNYHSRSESTIENFLSRAACVYMGEYTTNTDETKRFA 660  
E11 HeLa-P9 TAVETGHTSQVVPGD TMQTRHVKNYHSRSESTIENFLSRAACVYMGEYTTNTDETKRFA 660  
\*\*\*\*\*

```

E11 V5-7A      NWTINARRMVQMRKLEMFTYVRFDVEVTFVITSKDQGTQLGQDMPPLTHQIMYIPPGG 720
E11 HeLa-P3   NWTINARRMVQMRKLEMFTYVRFDVEVTFVITSKDQGTQLGQDMPPLTHQIMYIPPGG 720
E11 HeLa-P6   NWTINARRMVQMRKLEMFTYVRFDVEVTFVITSKDQGTQLGQDMPPLTHQIMYIPPGG 720
E11 HeLa-P9   NWTINARRMVQMRKLEMFTYVRFDVEVTFVITSKDQGTQLGQDMPPLTHQIMYIPPGG 720
*****

E11 V5-7A      PIPKSTTDYAWQTSTNPSIFWTEGNAPPRMSIPFVSI GNAYSNFYDGWSHFSQNGVYGYN 780
E11 HeLa-P3   PIPKSTTDYAWQTSTNPSIFWTEGNAPPRMSIPFVSI GNAYSNFYDGWSHFSQNGVYGYN 780
E11 HeLa-P6   PIPKSTTDYAWQTSTNPSIFWTEGNAPPRMSIPFVSI GNAYSNFYDGWSHFSQNGVYGYN 780
E11 HeLa-P9   PIPKSTTDYAWQTSTNPSIFWTEGNAPPRMSIPFVSI GNAYSNFYDGWSHFSQNGVYGYN 780
*****

E11 V5-7A      TLNNMGQLYMRHVNGPSPLPMTSTVRVYFKPKHKV KAWVPRPPRLCQYKNASTVNFSSSTNI 840
E11 HeLa-P3   TLNNMGQLYMRHVNGPSPLPMTSTVRVYFKPKHKV KAWVPRPPRLCQYKNASTVNFSSSTNI 840
E11 HeLa-P6   TLNNMGQLYMRHVNGPSPLPMTSTVRVYFKPKHKV KAWVPRPPRLCQYKNASTVNFSSSTNI 840
E11 HeLa-P9   TLNNMGQLYMRHVNGPSPLPMTSTVRVYFKPKHKV KAWVPRPPRLCQYKNASTVNFSSSTNI 840
*****

E11 V5-7A      TDKRNSITYIPDTVKPDVSNH 861
E11 HeLa-P3   TDKRNSITYIPDTVKPDVSNH 861
E11 HeLa-P6   TDKRNSITYIPDTVKPDVSNH 861
E11 HeLa-P9   TDKRNSITYIPDTVKPDVSNH 861
*****

```

**Figure 3.14 ClustalW alignments of the E11 V5-7A amino acid sequence and the consensus sequence derived from the 4 RT-PCR fragments from the HeLa-passaged viruses (E11 HeLa-P3, E11 HeLa-P6 and E11 HeLa-P9). The amino acid difference is seen in P9, G164R in VP4 (marked with red).**

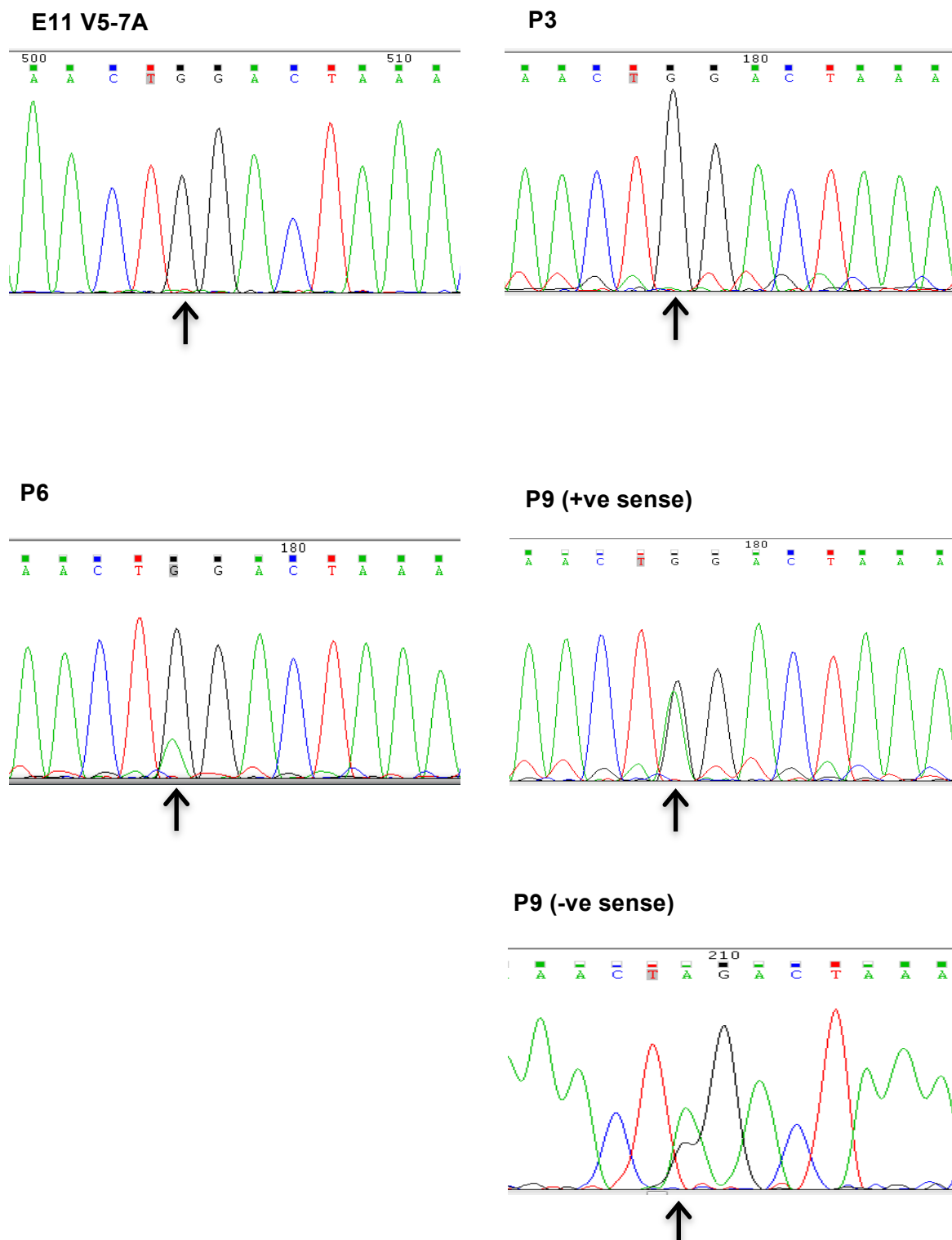


**Figure 3.15** Histograms of the sequence analysis of the HeLa-adapted E11 V5-7A, P3, P6 and P9 using Chromas software. The arrows indicate the nucleotide change to give G164R (G to A). Result shows that there is a single peak in E11 V5-7A sequence and P3, whereas, two peaks appeared at the same position in P6 and P9, indicating heterogeneity of the viral population.

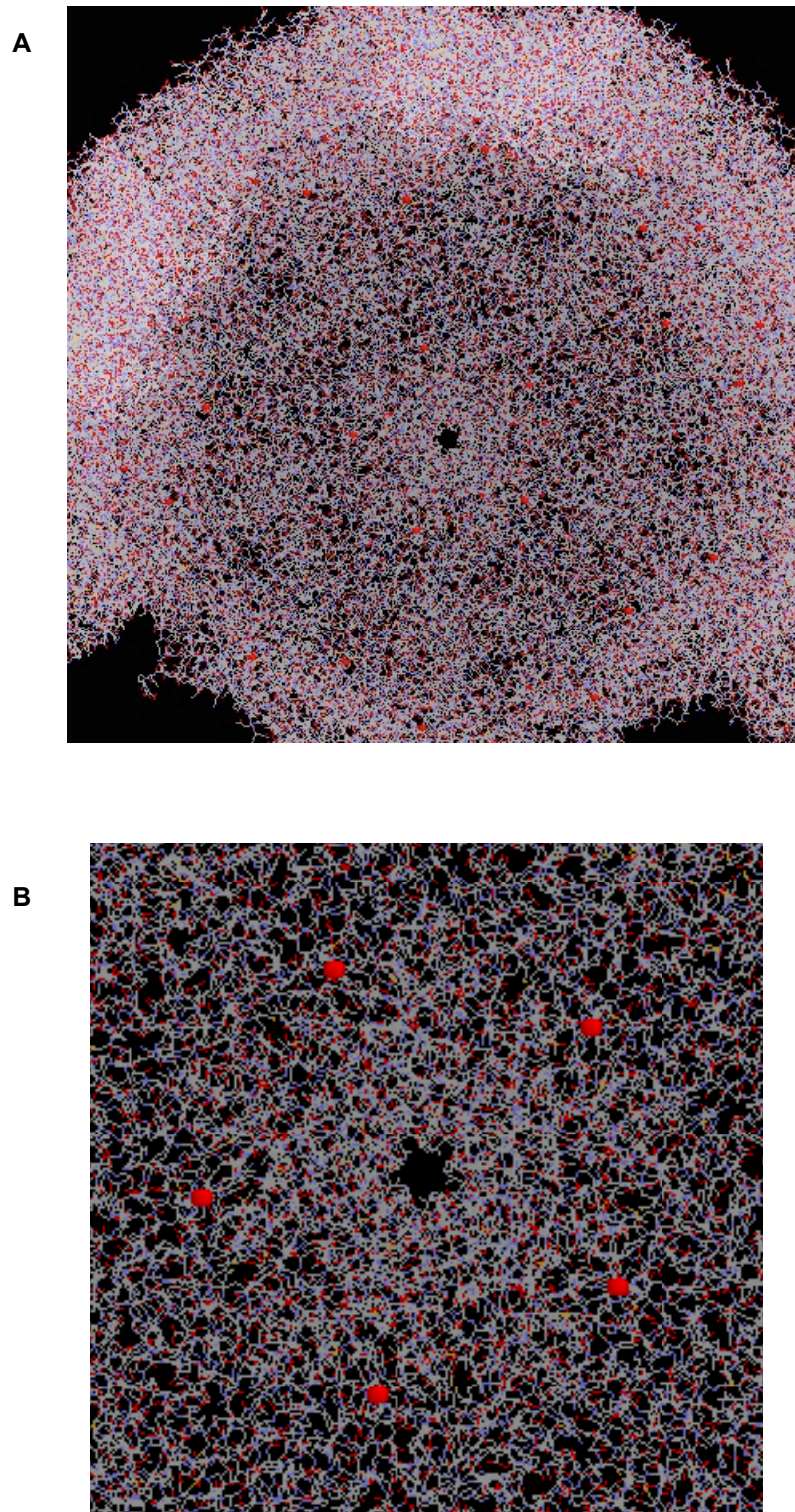


**Figure 3.16** Part of the three-dimensional half-capsid structure of E11 (coordinates PDB ID: 1H8T) shown using Rasmol software to map the mutation seen in the HeLa-adapted E11 V5-7A. A) Inside view of VP4. B) Zoom in showing five copies of the VP4 position 15, which is the nearest visible amino acid to our mutation at position 16 shown, in spacefill, red.

E11 V5-7A (G164R)	MGTQVSTQKTGAHETRLNASGNSVIHYTNI
CVA6	MGAQVSTQKSGSHETRVNATEGSTINFTNI
CVA6 3018	MGAQVSTQKSGSHETRVNATEGSTINFTNI
CVA6 BJXC09-239	MGAQVSTQKSGSHETRVNATEGSTINFTNI
CVA6 Eps	MGAQVSTQKSGSHETRVNATEGSTINFTNI
CVA6 GD406	MGAQVSTQKSGSHETRVNATEGSTINFTNI
CVA6 ICO00045	MGAQVSTQKSGSHETRVNATEGSTINFTNI
CVA6 M-027	MGAQVSTQKSGSHETRVNATEGSTINFTNI
CVA6 P-2220	MGAQVSTQKSGSHETRVNATEGSTINFTNI
CVA6 V-15558	MGAQVSTQKSGSHETRVNATEGSTINFTNI
CVA9 Fin/1/83	MGAQVSTQKTGAHETRLSATGNSIIHYTNI
CVB3 Nancy	MGAQVSTQKTGAHETRLNASGNSIIHYTNI
CVB3 Cd01/Kw/2004	MGAQVSTQKTGAHETRLNASGNSIIHYANI
E14 08-07-0579	MGAQVSTQKTGAHETRLNAQGSSVIHYTNI
E14 08-07-0909	MGAQVSTQKTGAHETRLNAQGNsvIHYTNI
E14 08-08-0907	MGAQVSTQKTGAHETRLNAQGNsvIHYTNI
E14 08-08-0912	MGAQVSTQKTGAHETRLNAQGNsvIHYTNI
E2 Cornelis	MGAQVSSQKVGahETKLNTGNNSTINyTNI
E9 KwamE001	MGAQVSTQKTGAHETRLNASGSSIIHYTNI
E9 KwNs/03/3158	MGAQVSTQKTGAHETRLNASGSSIIHYTNI
EV 09szk135	MGAQVSTQKSGSHETRVNATEGSTINFTNI
EV 09szk142	MGAQVSTQKSGSHETRVNATEGSTINFTNI
EV B-CAM1924	MGAQVSTQKTGAHETRLNAQGNsvIHYTNI
EV INDIS-U406	MGAQVSTQKSGSHETRVNATEGSTINFTNI

**Figure 3.17** Sequence alignment of the start of VP4 in all enterovirus isolates in the GenBank sequence database with R at position 16. E2 Cornelis has K (like R a basic amino acid) at this position. CVA6 belongs to the species *Enterovirus A*, while the other viruses belong to *Enterovirus B*.

### 3.5 Discussion

The interaction of a virus with specific receptors on the cell surface may be one of the determinants of virus host range, tissue tropism and pathogenicity. Decay accelerating factor (DAF, CD55) is known to serve as a receptor for several echoviruses and mutations in DAF binding sites have been associated with adaptation to several cell lines (Stuart *et al.*, 2002a,b; Rezaikin *et al.*, 2009; Novoselov *et al.*, 2012). CVA9 binds to integrin  $\alpha_v\beta_6$  in cell entry, although other molecules also appear to be involved (Heikkila *et al.*, 2009; Huttunen *et al.*, 2014). Both DAF and  $\alpha_v\beta_6$  are up-regulated in some cancer cells and so echoviruses and CVA9 are potentially useful for oncolytic therapy (Berry *et al.*, 2008; Allen *et al.*, 2013; Bandyopadhyay and Raghavan, 2009; Koretz *et al.*, 1992). A deep understanding of how viruses infect cells, for instance, how viruses may interact with cell surface receptors and enter the cells, is vital to establish an efficient cancer treatment based on these interactions.

A panel of enteroviruses was used originally to investigate possible viruses that could target cancer cells and how receptor expression may influence infection. Three echoviruses E6, E11 (E11 5V-7A) and E20 caused a partial or complete CPE on A549, MCF-7, PC-3, HeLa, HT-29 and RD cancer cells, but not GMK, MDA-MB-231 or MDA-MB-435 cells that did not show significant effects. Of these, E11 5V-7A had the greatest effect on all the susceptible cell lines, particularly PC-3 cells where complete killing was seen, while E6 and E20 had a more limited effect. Two other echoviruses, E15 and E30 were less effective in cell killing. It is not clear whether these differences are due to specific molecules features, such as receptor tropism, or due to differences in the amount of

infectious virus in the sample.

The CVA9 mutants showed a similar tropism to the echoviruses, as again there was no effect on MDA-MB-231 and MDA-MB-435 (except that CVA9wt had a slight effect) cells, while A549, HT-29 and RD cells were permissive. There are some differences, however. The main one is that GMK cells can be killed by CVA9, but is resistant to the echoviruses. In addition, MCF-7 cells are killed by E6, E11 and E20, but it was observed previously that CVA9 does not kill these cells (Ivanova *et al.*, unpublished). The results in Figure 3.1 show some killing by CVA9wt but sequence analysis indicated that the sample used had acquired an S2871R mutation and infection can be blocked by heparin. This suggests that the ability to infect MCF-7 cells depends on this mutation, which allows binding to heparan sulphate. The few plaques obtained from the CVA9D mutant could also be blocked by heparin (data not shown). Infection of MCF-7 cells by E6, E11 (E11 5V-7A) and E20 is not blocked by heparin (data not shown) suggesting that infection does not depend on heparan sulphate (data not shown). Another difference between the echoviruses and CVA9 is that HeLa cells seem to be more susceptible to the echoviruses. The data suggest that relatively similar viruses, such as echoviruses and CVA9, both members of *Enterovirus B*, can show different cell tropism. This is emphasized by differences in the CVA9 mutants on some of the cell lines such as A549 and PC-3 cells.

To find if receptor distribution may be responsible for differences in cell tropism, a flow cytometric analysis (FACS) was performed (Figure 3.2). This showed that DAF is expressed on the cell surface of most of the cancer cell lines but not the green monkey kidney cell line (GMK). This suggests that the failure to infect GMK

cells could be due to the absence of DAF. However, it may also be that the DAF antibody used does not recognise the form of DAF found on monkey cells. It would be interesting to propagate the echoviruses on GMK cells to find if adapted mutants appear and therefore to possibly identify host tropism determinants. A similar experiment was performed on the green monkey kidney cell line (BGM) (Rezaikin *et al.*, 2009). Adapting mutations were observed in VP1 at the 5' axis and at the north rim of the canyon, which are not close to the region that binds to DAF. This suggests that adaptation involves a different receptor rather than DAF. The fact that MDA-MB-231 and MDA-MB-435 cells express DAF but are not infected by the echoviruses suggests that there are other blocks to infection. These could be receptors interactions or intracellular events. CVA9 tropism also does not correlated with expression of integrin  $\alpha_v\beta_3$  or  $\alpha_v\beta_6$  as published by Goodman *et al.*, 2012.

The enterovirus entry pathways and tissue tropism may notably depend on the expression of specific cellular receptor on the plasma membrane and the receptor-binding site on the virion surface. However, the situation is more complex in some echoviruses and seems not to be depending on single cell surface molecule. Several types of cell surface molecules are known to contribute with E11 infection into susceptible cells. In addition to DAF, another molecule, HLA class I associated  $\beta_2$ -microglobulin is known to be involved in the E11 internalization process in rhabdomyosarcoma (RD) cells (Chevaliez *et al.*, 2008; Ward *et al.*, 1998; Novoselov *et al.*, 2012). Moreover, another unknown 44 kDa glycoprotein molecule was previously identified in human and simian origin cell lines by monoclonal antibody and immunoaffinity purification (Novoselov *et al.*, 2012). It has also been reported that an antibody to integrin  $\alpha_v\beta_3$  can block

the infection of E11 on GMK cells (Ylipaasto *et al.*, 2010; Novoselov *et al.*, 2012).  $\beta$ 2-microglobulin also seems to be involved in the entry of CVA9 and another molecule GRP78 could also be needed (Heikkila *et al.*, 2009; Triantafilou *et al.*, 2002). Any of these molecules could be absent in the cells which could not be infected.

The 5'UTR has also been shown to influence cell tropism of poliovirus and CVBs (La Monica and Racaniello, 1989; Lin and Shih, 2014). Non-structural proteins 2B and 3A influence host tropism of rhinoviruses (Harris and Racaniello, 2005). In addition, the assay used to assess tropism of echoviruses and CVA9 was based on visible cell death. It has been reported that CVB2 can infect cells in a non-cytolytic way but a mutation in VP1 gives a mutant that gives a lytic infection (Gullberg *et al.*, 2010). It could be that cells which were not killed were infected. This could be investigated by detecting virus infection by immunofluorescence, but as the aim of the work is to develop viruses capable of killing specific cancer cells, it was decided to concentrate on the cells which were killed.

Since the most promising virus was E11, (strain 7V-5A), which killed the A549, MCF-7, PC-3 and HeLa cancer cells, but not GMK cells (Figure 3.1), this was chosen for further study. The capsid encoding-region of E11 7V-5A was sequenced to identify the basis of the phenotype. Furthermore, E11 was propagated on A549 and HeLa cell lines and mutations were observed after the 9 passage.

For adapted E11 5V-7A on HeLa cells, this resulted in a single nucleotide substitution at position 16 in VP4 causing a replacement of Glycine with Arginine. Previous studies indicated that the same VP4-16 (G164R) substitution occurred

in CVB4. Here it caused an increase in virulence and it was suggested that as the N-terminus of VP4 is known to occur on the inner surface of the virion of picornaviruses and interacts with the flexible N-terminus of the other capsid proteins causing an intertwined network within the virion, this might affect its stability and/or tropism (Ramsingh and Collins, 1995). Moreover, a mutation that was introduced into the VP4 coding sequence of poliovirus can affect cell entry, host range and pathogenicity. This mutation at position 28 did not affect the stability of the particle or its interaction with receptor but blocked a late stage in entry showing that VP4 is involved in entry (Moscufo *et al.*, 1993). The precise function of VP4 is not fully understood, but is related to entry through the myristate at the N-terminus that presumably interacts with cell membranes. VP4 has recently been shown to form pores in cell membranes (Davis *et al.*, 2008; Panjwari *et al.*, 2014). Changes in VP4 could therefore be important in entry by allowing more efficient interactions with the different membrane environment in different cell lines.

As only approximately 50% of the virus RNA in HeLa P9 has the mutation, it will be important in the future to isolate viruses containing the mutant and original VP4 position 16 sequences to confirm that G164R gives the large plaque phenotype. This mutation was not observed in the other E11 (E11 V5-7A) adaptation experiments previously reported (summarised in Table 3.3) and is therefore a novel adapting mutation. It will be interesting to adapt CVA9 to HeLa cells, where it grows poorly, to see if a similar mutation would be selected.

Subsequently, after passaging E11 V5-7A on A549 cells two mutations were identified at P9. These are both in regions likely to be involved in DAF binding

based on the structure of the E7-DAF complex (Plevka *et al.*, 2010), G145S in the SCR3 binding domains and E59V in the SCR4 binding domain. Previous work (Table 3.3) reported that adaptation to cell lines is due to changes in the VP2 puff and VP3 knob domains. In some cases, this causes a loss of DAF binding, such as position 165 in VP2 seems to be an important amino acid in DAF binding. Propagating E11 on L41 cells gave a T1652A mutant that cannot bind to DAF, and propagating this mutant on RD cells selected an A1652T which could bind to DAF (Novoselov *et al.*, 2012). Propagating E11 on HEp-2, HEF and HT-29 cells also led to changes in VP2 (A1562T, T1652M and S1352G, N1642D respectively), which are probably responsible for the DAF<sup>-</sup> phenotype (Rezaikin *et al.*, 2009; Stuart *et al.*, 2002b). It would be interesting to analyse the DAF phenotype of the A549 mutants, especially as these mutations have not been observed in previous experiments.

Some adapted viruses also showed mutations in VP1 and it was proposed that this allowed binding to a different receptor which interacted with the canyon, possibly an immunoglobulin superfamily member. Two of these mutations may also allow binding to heparan sulphate, Q1321K and Q1291R (Stuart *et al.*, 2002b; Rezaikin *et al.*, 2009). It was reported that CVA9 and some echoviruses with a basic amino acid at CVA9 VP1 position 132 and the equivalent position in echoviruses gave a cluster of positive charges due to the symmetry of the virus as position 132 is at the 5-fold axis (McLeish *et al.*, 2012). Both Q129R and Q132K are mutations to a basic amino acid close to the 5-fold axis.

**Table 3.3 A comparison of all mutations seen when E11 is adapted to different cell lines.** Our mutations are shaded by blue; the mutations seen by other research groups are shaded by yellow. DAF<sup>+</sup> and DAF<sup>-</sup> mutants with these mutations are shown as + or - (Stuart *et al.*, 2002b; Novoselov *et al.*, 2012; Rezaikin *et al.*, 2009).

Cell lines	Mutations			
	VP4	VP2	VP3	VP1
<b>A549</b>		G145S <sup>?</sup>	E59V <sup>?</sup>	
<b>HeLa</b>	G16R <sup>?</sup>			
<b>HT-29</b>		N164D <sup>-</sup>		E83D <sup>-</sup>
<b>RD</b>		A165T <sup>+</sup>		
<b>Vero</b>		G139R <sup>+</sup>		E78Q <sup>+</sup> K88E <sup>+</sup> Q132K <sup>+</sup> F240L <sup>+</sup> K259E <sup>+</sup>
<b>HEF</b>		S135G <sup>-</sup> T165M <sup>-</sup>		
<b>BGM</b>				K88E <sup>+</sup> Q129R <sup>+</sup>
<b>Hep-2</b>		A156T <sup>-</sup>		K88E <sup>-</sup> N265S <sup>-</sup>
<b>L41</b>		T165A <sup>-</sup> S233L <sup>-</sup>	Q86R <sup>-</sup>	K286R <sup>-</sup>

## **Chapter 4**

# **Heparan Sulphate Interaction with Coxsackievirus A9 (CVA9)**

## 4.1 Introduction

Receptor binding is a crucial event during viral infection and tissue tropism. Heparan sulphate proteoglycans (HSPGs) are found at the cell surface and in the extracellular matrix (ECM) (Sarrazin, *et al.*, 2011; Zhu *et al.*, 2011). HSPG has been reported to be a receptor for several viruses including herpes simplex viruses (HSV), swine vesicular disease virus (SVDV), human papillomavirus 16 (HPV16), Theiler's murine encephalomyelitis virus (TMEV), Enterovirus 71 (EV-71), foot-and-mouth disease viruses (FMDV) and human rhinoviruses (HRV -89 and -54) (Shieh *et al.*, 1992; Escibano-Romero *et al.*, 2004; Knappe *et al.*, 2007; Reddi and Lipton, 2002; Tan *et al.*, 2013; Jackson *et al.*, 2003; Vlasak *et al.*, 2005; Khan *et al.*, 2007). Several enteroviruses have been reported to bind to HSPG, but the basis of this binding has not usually been explored (Israelsson *et al.*, 2010; Goodfellow *et al.*, 2001). Adaptations of viruses to cell cultures have been frequently associated with gaining the ability to bind to HSPG by at least a single amino acid substitution (Fry *et al.*, 1999, Maree *et al.*, 2011; Bai *et al.*, 2014).

In CVA9, it has been found that an amino acid difference at position 132 in VP1 is associated with HSPG binding through symmetry-related clusters of positive charges (McLeish *et al.*, 2012). Non-binding isolates tested (CO62, CO87 and Griggs) have a threonine (T) at this position, while HSPG-binding isolates (CO79 and CO85) have the positively charged amino acid arginine (R) (McLeish *et al.*, 2012). Variants of some other *Enterovirus B* species viruses were found to have a similar polymorphism that correlated with HSPG binding.

The aim of this chapter is to find whether there are any other mechanisms which CVA9 can use to bind to HSPG. We performed an extensive analysis of the adaptation of the non-binding CVA9 isolates CO62, CO87 and Griggs to the A549 cell line.

## **4.2 Comprehensive Analysis of the CVA9 Mechanism of Adaptation to Heparan Sulphate Using CVA9 Griggs, CVA9 CO62 and CVA9 CO87**

### **4.2.1 Adaptation of CVA9 Isolates to A549 Cells**

Previous studies identified 4 isolates (CO62, CO79, CO85 and CO87) of CVA9 that differ in their ability to use HSPG as a receptor. CO62 and CO87 do not bind to HSPG and the infections were not blocked in the presence of heparin, which is an analogue of heparan sulphate, while CO79 and CO85 bind to HSPG and the infections were inhibited in the presence of heparin (Figure 4.1). Most of the previous experiments were performed on GMK cells (McLeish *et al.*, 2012). To extend these results, non-binding CVA9 isolates CO87, CO62 and Griggs were propagated twice on the A549 cell line. Virus was analysed for heparin blocking after the second passage. As no significant reduction in plaque numbers was seen in any case, individual plaques were picked, propagated once in A549 cells, and then tested for heparin blocking (see sections 4.2.3, 4.2.4 and 4.2.5). This allowed heparin-blocked viruses to be identified.

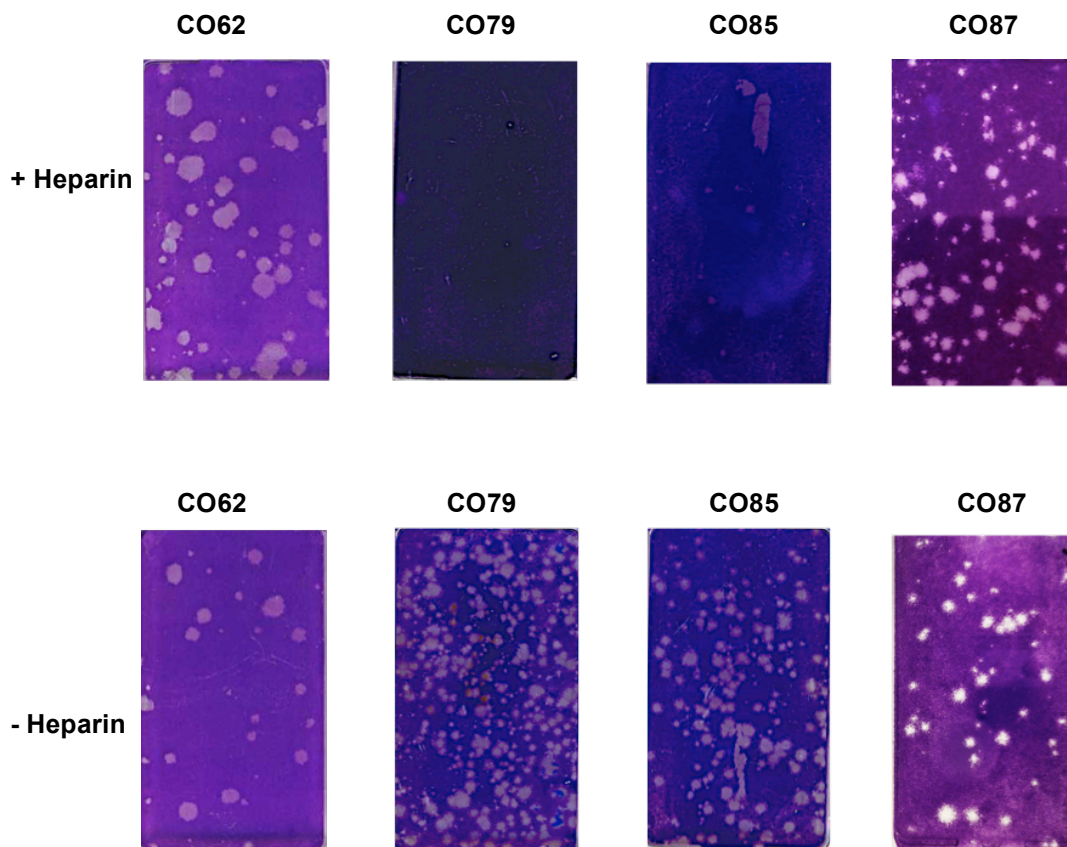


**Figure 4.1 Heparin blocking plaque assays for some CAV9 isolates on GMK cells.** The top line shows the result of treatment with heparin (90  $\mu$ l of  $10^2$  diluted virus and 10  $\mu$ l of 50 mg/ml heparin). The bottom line shows mock-treated virus (90  $\mu$ l of  $10^2$  diluted virus and 10  $\mu$ l of water). Virus-heparin mixture or the mock-treated control were incubated for 30 min then added to monolayers of GMK cells and then incubated for 1 hr. Cells were overlaid with CMC/agarose/medium then incubated for 3 days then stained with Crystal Violet. Two isolates (CO79 and CO85) are blocked by heparin, but the other isolates CO62 and CO87 are not blocked.

## **4.2.2 Sequencing of CVA9 CO87, CO62 and Griggs Plaques**

Viral RNAs were isolated from picked/passaged plaques from CVA9 isolates CO87, CO62 and Griggs (P1 and P2) then amplification was carried out by RT-PCR using specific primers (Table 2.1) to give 4 overlapping fragments (Figure 4.2). The amplicons were purified using a QIAquick Gel Extraction kit after agarose gel electrophoresis. The purified fragments of CO87, CO62 and Griggs were at position ~950 bp, ~900 bp, ~950 bp and ~800 bp respectively as expected (data not shown). Then total DNA fragments were collected and sent for sequencing commercially by Source BioScience LifeSciences.

## **4.2.3 Isolate CO87 Analysis**

### **4.2.3.1 Inhibition of Infection of CVA9 CO87 by Soluble Heparin**

The second passage of the propagated CO87 (CO87P2) was tested in a plaque assay in the presence and absence of heparin. The results are shown in Figure 4.3. There was some reduction in the number of plaques obtained suggesting that some of the virus population has acquired the ability to bind the HSPG. This was confirmed by the results of testing one of the passaged plaques (CO87N) picked from the CO87P2. Infection is blocked and inhibited by heparin. In contrast, a second plaque (CO87PL1) showed no blocking. Similar results were obtained from another plaque (CO87I) picked during an independent A549 adaptation experiment (data not shown).

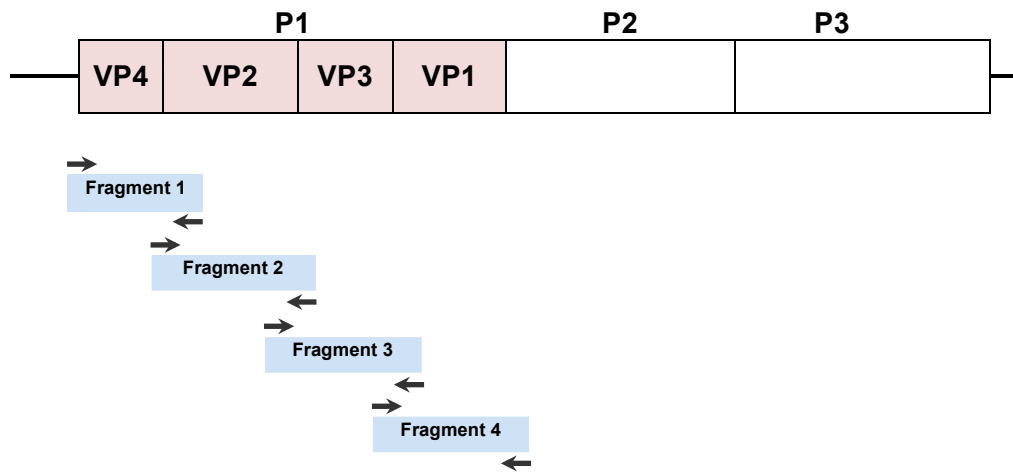


**Figure 4.2 Schematic diagram of the sequencing of the CVA9 isolates CO87, CO62 and Griggs capsid proteins (VPs) in the P1 region.** Overlapping fragments were generated using primers based on the available CO87, CO62 and Griggs sequences (Chang *et al.*, 1989; McLeish *et al.*, 2012).

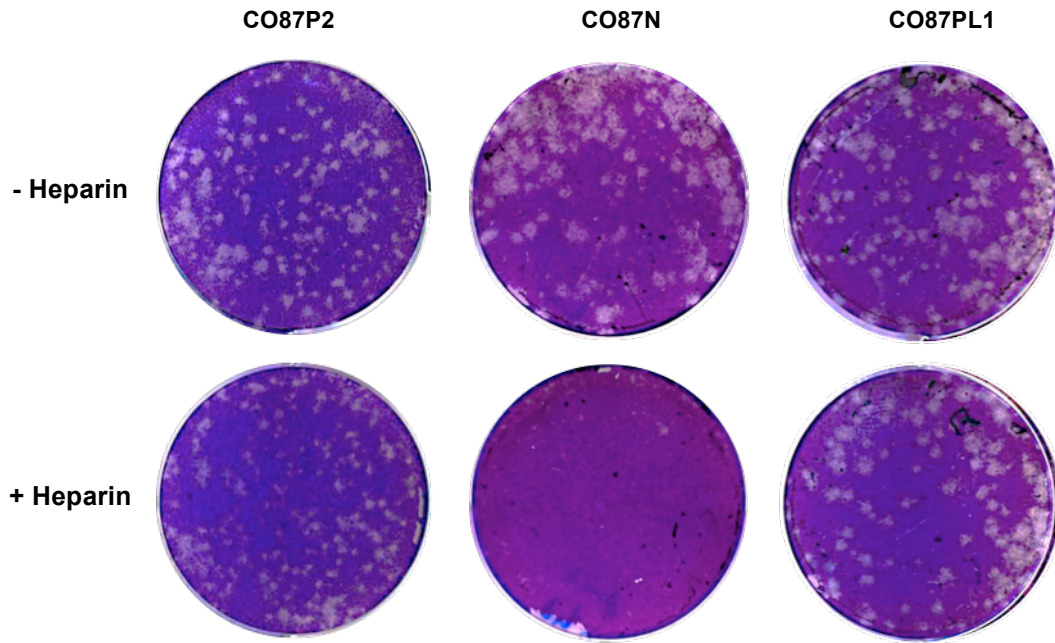


**Figure 4.3 Heparin blocking assay on A549-passaged CVA9 isolate CO87.** CO87P2 (passaged twice), CO87N (plaque-purified from CO87P2) and CO87PL1 (also plaque-purified from CO87P2). The top line shows mock-treated virus (90  $\mu$ l of  $10^2$  diluted virus and 10  $\mu$ l of water). The bottom line shows the treatment with heparin (90  $\mu$ l of  $10^2$  diluted virus and 10  $\mu$ l of 50 mg/ml heparin). Virus-heparin mixture or the mock-treated control were incubated for 30 min then added to monolayers of A549 cells and then incubated for 1 hr. Cells were overlaid with CMC/agarose/medium then incubated for 3 days then stained with Crystal Violet. It can be seen that infections of CO87N can be completely blocked by heparin compared with CO87P2 and CO87PL1.

#### 4.2.3.2 Sequence Analysis of CO87 Isolate

The plaque purified viruses CO87N and CO87I were analysed by sequencing the P1 capsid encoding-region. Then alignment comparisons were performed using the online tool ClustalW (Larkin *et al.*, 2007). As shown in Figure 4.4, the sequence alignment of the A549-CO87 adapted variant CO87N shows only one mutation which appeared at position 59 in VP3 (Q593R). CO87I shows the same mutation plus two more mutations, one at position 163 in VP2 (Q1632R) and one at position 222 in VP1 (R2221K). It is interesting that all three mutations in CO87I involve positively-charged amino acid residues as gaining a positive charge after gives a virus capable of binding to HSPG (McLeish *et al.*, 2012; Maree *et al.*, 2010). One of the mutations R2221K is not a gain of a positive charge, but both Q593R and Q1632R give an extra positive charge. None of the mutations are surrounded by other positively-charged amino acids in the amino acid sequence and none gives a linear HSPG binding site of the type 'BBXB' or 'BBBXXB', where 'B' is any one of the basic amino acids and 'X' is a neutral or hydrophobic amino acid (Cardin and Weintraub, 1989).

The Q593R mutation was seen in both heparin-blocked variants and as this is the only mutation seen in CO87N, it is likely that this is enough to give the heparin-blocked phenotype. This was supported by an analysis of the Q593R region from several different plaques (CO87N1, CO87N2, CO87N3 and CO87N4) isolated during the first A549 adaptation experiment. All these had the same Q593R mutation. An independent adaptation experiment was performed by M. Ivanova on A549 cells and two plaque-purified variants (CO87M1 and CO87M2) blocked

by heparin were sequenced in the complete P1 region. Both had only one mutation, Q593R (Figure 4.5).

An analysis of the location of the mutations seen in the three-dimensional structure, based on the CVA9 Griggs crystal structure was performed (Hendry *et al.*, 1999) (Figure 4.6). The T1321R mutation shown to give heparin blocking in the CO79 and CO85 isolates is also plotted (McLeish *et al.*, 2012). None of the mutations is close to the T1321R mutation at the 5-fold axis and none is close to either the 3-fold axis or 2-fold axis. So the symmetry-clustering mechanism (McLeish *et al.*, 2012) does not seem to be involved. The surrounding amino acids in the structure were therefore analysed. The amino acid at position Q1632R has no adjacent positive charges close enough to form a cluster (data not shown). However, the amino acid at position Q593R has two adjacent positively-charged amino acids which are located at position 275 (arginine, R) and 276 (lysine, K) to form a positively-charged cluster (Figure 4.7). Moreover, the amino acid analysis at position R2221K indicates that there are two adjacent positively-charged amino acids located at position 223 (histidine, H) and 84 (lysine, K) in VP1 (Figure 4.8).

An alignment of the sequence of CO87 with other CVA9 isolates based on the GenBank sequence database was done for the VP3 position 59 region and is presented using weblogo online software (Crooks *et al.*, 2004; Schneider and Stephens, 1990) as in Figure 4.9. It can be seen that VP3 position is polymorphic and just under half of the isolates have R at this position, while half have Q and a small number have H. The VP1 position 275 and 276, which are close to VP3 59, are R and K in virtually all CVA9 isolates and so any isolate with R at VP3 59

should have a positively-charged cluster as in the CO87 variants. This may mean that several CVA9 isolates potentially can bind to HSPG. In addition, VP3 position 80 is also polymorphic, but this is not close to position 59 and there is no correlation between VP3 59R and either K or Q at position 80 (data not shown).

**>VP4**  
 C087 MGAQVSTQKTGAHETSLSATGGSVIHYTNINYYKDAASNSANRQDFTQDPSKFTPEVKDV 60  
 C087N MGAQVSTQKTGAHETSLSATGGSVIHYTNINYYKDAASNSANRQDFTQDPSKFTPEVKDV 60  
 C087I MGAQVSTQKTGAHETSLSATGGSVIHYTNINYYKDAASNSANRQDFTQDPSKFTPEVKDV 60  
 \*\*\*\*\*

**>VP2**  
 C087 MIKSLPALNSPTVEECGYSDRVRSITLGNSTVTTQECANVVVGYGRWPTYLRDDEATAED 120  
 C087N MIKSLPALNSPTVEECGYSDRVRSITLGNSTVTTQECANVVVGYGRWPTYLRDDEATAED 120  
 C087I MIKSLPALNSPTVEECGYSDRVRSITLGNSTVTTQECANVVVGYGRWPTYLRDDEATAED 120  
 \*\*\*\*\*

C087 QPTQPDVATCRFYTLDSIKWEKGSVGVWVWKFPEALSDMGLFGQNMQYHYLGRAGYTIHVQ 180  
 C087N QPTQPDVATCRFYTLDSIKWEKGSVGVWVWKFPEALSDMGLFGQNMQYHYLGRAGYTIHVQ 180  
 C087I QPTQPDVATCRFYTLDSIKWEKGSVGVWVWKFPEALSDMGLFGQNMQYHYLGRAGYTIHVQ 180  
 \*\*\*\*\*

C087 CNASKFHQGCLLVVCPPEAEMGGAVVGQAFPSAALANGDKAYEFTSTTQGD<sup>163</sup>TKIQTVVH 240  
 C087N CNASKFHQGCLLVVCPPEAEMGGAVVGQAFPSAALANGDKAYEFTSTTQGD<sup>163</sup>TKIQTVVH 240  
 C087I CNASKFHQGCLLVVCPPEAEMGGAVVGQAFPSAALANGDKAYEFTSTTQGD<sup>163</sup>TKIQTVVH 240  
 \*\*\*\*\*:\*\*\*\*\*

C087 NAGMGVGVGNLTIFPHQWINLRTNNSATIIVMPYVNSVPMNMFHRYNFTLMVIPVFKLDY 300  
 C087N NAGMGVGVGNLTIFPHQWINLRTNNSATIIVMPYVNSVPMNMFHRYNFTLMVIPVFKLDY 300  
 C087I NAGMGVGVGNLTIFPHQWINLRTNNSATIIVMPYVNSVPMNMFHRYNFTLMVIPVFKLDY 300  
 \*\*\*\*\*

**>VP3**  
 C087 ADTASTYVPIITVTVAPMCAEYNGLRRLAQAGLPTMNTPGSTQFLTSDDFQSPCALPQFDV 360  
 C087N ADTASTYVPIITVTVAPMCAEYNGLRRLAQAGLPTMNTPGSTQFLTSDDFQSPCALPQFDV 360  
 C087I ADTASTYVPIITVTVAPMCAEYNGLRRLAQAGLPTMNTPGSTQFLTSDDFQSPCALPQFDV 360  
 \*\*\*\*\*

**59**  
 C087 TPMSDIPGEVKNLMEIAEVDSVVPVNNV<sup>59</sup>DTTDQMEMFRIPVTTINAPLQQQVFGRLRQPG 420  
 C087N TPMSDIPGEVKNLMEIAEVDSVVPVNNV<sup>59</sup>DTTDQMEMFRIPVTTINAPLQQQVFGRLRQPG 420  
 C087I TPMSDIPGEVKNLMEIAEVDSVVPVNNV<sup>59</sup>DTTDQMEMFRIPVTTINAPLQQQVFGRLRQPG 420  
 \*\*\*\*\*:\*\*\*\*\*

C087 LDSVFKHTLLGEILNYYAHWSGSMKLTFFVFCGSAMATGKFLIAYSPPGANPPKTRKDAML 480  
 C087N LDSVFKHTLLGEILNYYAHWSGSMKLTFFVFCGSAMATGKFLIAYSPPGANPPKTRKDAML 480  
 C087I LDSVFKHTLLGEILNYYAHWSGSMKLTFFVFCGSAMATGKFLIAYSPPGANPPKTRKDAML 480  
 \*\*\*\*\*

C087 GTHIIWDIGLQSSCVLCPWISQTHYRLVQQDEYTSAGFVTCWYQTGMIVPPGTPNSSSI 540  
 C087N GTHIIWDIGLQSSCVLCPWISQTHYRLVQQDEYTSAGFVTCWYQTGMIVPPGTPNSSSI 540  
 C087I GTHIIWDIGLQSSCVLCPWISQTHYRLVQQDEYTSAGFVTCWYQTGMIVPPGTPNSSSI 540  
 \*\*\*\*\*

**>VP1**  
 C087 MCFASACNDFSVRMLRDTPFISQDNKLQGDVEEAIERAVVHVADTVRSGPNSSESIPALT 600  
 C087N MCFASACNDFSVRMLRDTPFISQDNKLQGDVEEAIERAVVHVADTVRSGPNSSESIPALT 600  
 C087I MCFASACNDFSVRMLRDTPFISQDNKLQGDVEEAIERAVVHVADTVRSGPNSSESIPALT 600  
 \*\*\*\*\*

C087 AVETGHTSQVTPSDTMQTRHVKNYHSRSESTIENFLGRSACVYMEEYKTTDEDTNKKFVA 660  
 C087N AVETGHTSQVTPSDTMQTRHVKNYHSRSESTIENFLGRSACVYMEEYKTTDEDTNKKFVA 660  
 C087I AVETGHTSQVTPSDTMQTRHVKNYHSRSESTIENFLGRSACVYMEEYKTTDEDTNKKFVA 660  
 \*\*\*\*\*

C087 WPINTRQMVQMRRKLEMFTYLRFDMEVTFVITSRQDPGTTLAQDMPVLTHQIMYVPPGGP 720  
 C087N WPINTRQMVQMRRKLEMFTYLRFDMEVTFVITSRQDPGTTLAQDMPVLTHQIMYVPPGGP 720  
 C087I WPINTRQMVQMRRKLEMFTYLRFDMEVTFVITSRQDPGTTLAQDMPVLTHQIMYVPPGGP 720  
 \*\*\*\*\*

C087 IPAKVDDYAWQTSTNPSIFWTEGNAPARMSIPFISIGNAYSNFYDGWSNFDQKGSYGNT 780  
 C087N IPAKVDDYAWQTSTNPSIFWTEGNAPARMSIPFISIGNAYSNFYDGWSNFDQKGSYGNT 780  
 C087I IPAKVDDYAWQTSTNPSIFWTEGNAPARMSIPFISIGNAYSNFYDGWSNFDQKGSYGNT 780  
 \*\*\*\*\*

```

                222
CO87      LNNLGHIYVRHVSGSSSPYPITSTIRIYFKPKHTRAWVPRPPRLCQYEKAFSVDVFPVPT 840
CO87N    LNNLGHIYVRHVSGSSSPYPITSTIRIYFKPKHTRAWVPRPPRLCQYEKAFSVDVFPVPT 840
CO87I    LNNLGHIYVKHVSGSSSPYPITSTIRIYFKPKHTRAWVPRPPRLCQYEKAFSVDVFPVPT 840
          *****:*****
          :*****

CO87      DTRKDINTVVSVQRKRRGDLSALNTH 867
CO87N    DTRKDINTVVSVQRKRRGDLSALNTH 867
CO87I    DTRKDINTVVSVQRKRRGDLSALNTH 867

          *****

```

**Figure 4.4 ClustalW Sequence alignments of the capsid region of the original CO87 and mutants (CO87N and CO87I)** from plaque-purified variants isolated from CO87 adapted on A549 cells in two independent experiments. The amino acid differences are seen at positions Q59R in VP3 (both variants), R222K in VP1 and Q163R in VP2 (CO87I only).

```

CO87N      TPSMDIPGEVKNLMEIAEVDSVVPVNNVRDTTDQMEMFRIPVTINAPLQQQVFGRLRQPG
CO87N1     TPSMDIPGEVKNLMEIAEVDSVVPVNNVRDTTDQMEMFRIPVTINAPLQQQVFGRLRQPG
CO87N2     TPSMDIPGEVKNLMEIAEVDSVVPVNNVRDTTDQMEMFRIPVTINAPLQQQVFGRLRQPG
CO87N3     TPSMDIPGEVKNLMEIAEVDSVVPVNNVRDTTDQMEMFRIPVTINAPLQQQVFGRLRQPG
CO87N4     TPSMDIPGEVKNLMEIAEVDSVVPVNNVRDTTDQMEMFRIPVTINAPLQQQVFGRLRQPG
CO87I      TPSMDIPGEVKNLMEIAEVDSVVPVNNVRDTTDQMEMFRIPVTINAPLQQQVFGRLRQPG
CO87M1 ♦    TPSMDIPGEVKNLMEIAEVDSVVPVNNVRDTTDQMEMFRIPVTINAPLQQQVFGRLRQPG
CO87M2 ♦    TPSMDIPGEVKNLMEIAEVDSVVPVNNVRDTTDQMEMFRIPVTINAPLQQQVFGRLRQPG
*****

```

**Figure 4.5 Alignment of the sequence of different plaques variants isolated from CO87 adapted on A549 cells.** Results from part of VP3 indicate that the amino acid R appears at the same position in all the different isolates.

♦ Experiment was performed by M. Ivanova. The complete P1 sequences were obtained and only this mutation was seen.

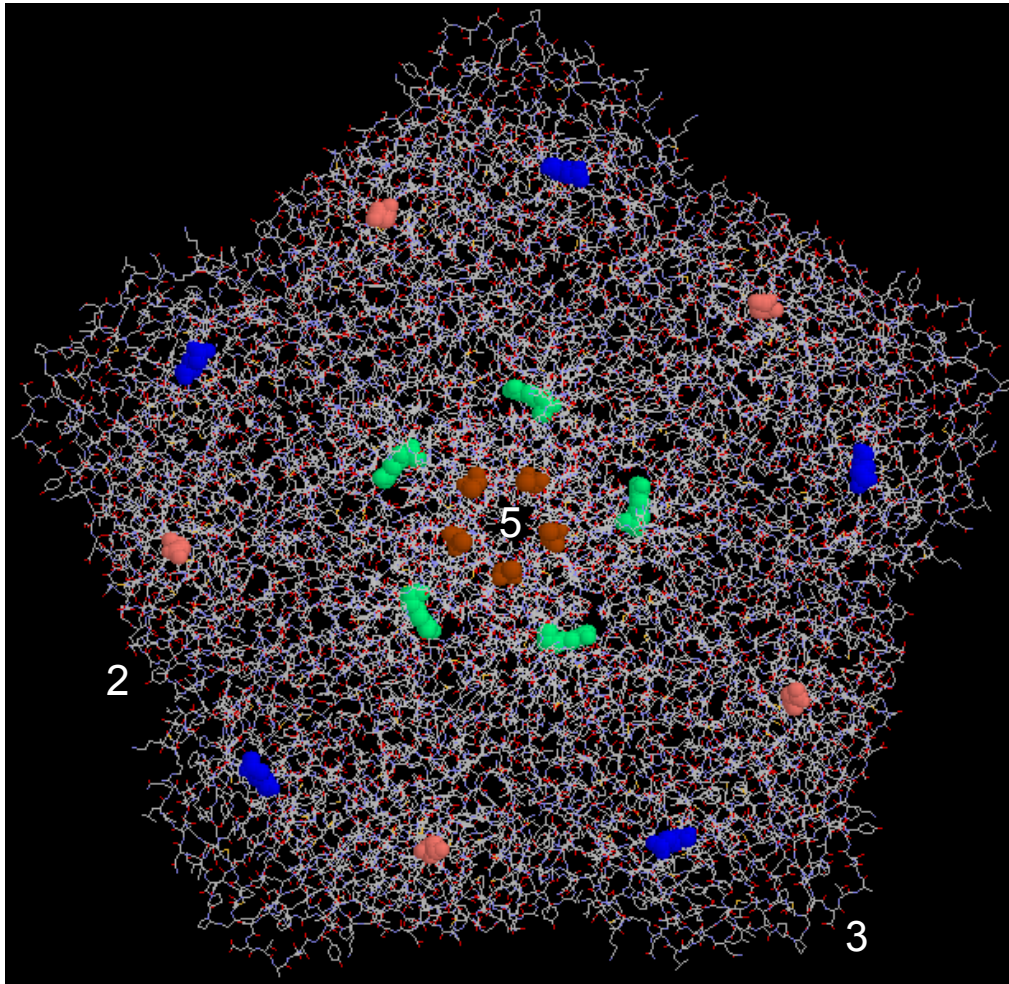


**Figure 4.6** The three-dimensional pentameric structure of CVA9 using Rasmol software, showing the predicted positions of the CO87 mutations seen in the heparin-blocked variants. VP3 position 59 is shown in spacefill, blue. VP2 position 163 is shown in spacefill, salmon. VP1 position 222 is shown in spacefill, green. VP1 position 132, which clusters at the 5-fold axis is shown in spacefill, brown. Numbers indicate the 2- 3- and 5- fold axis.

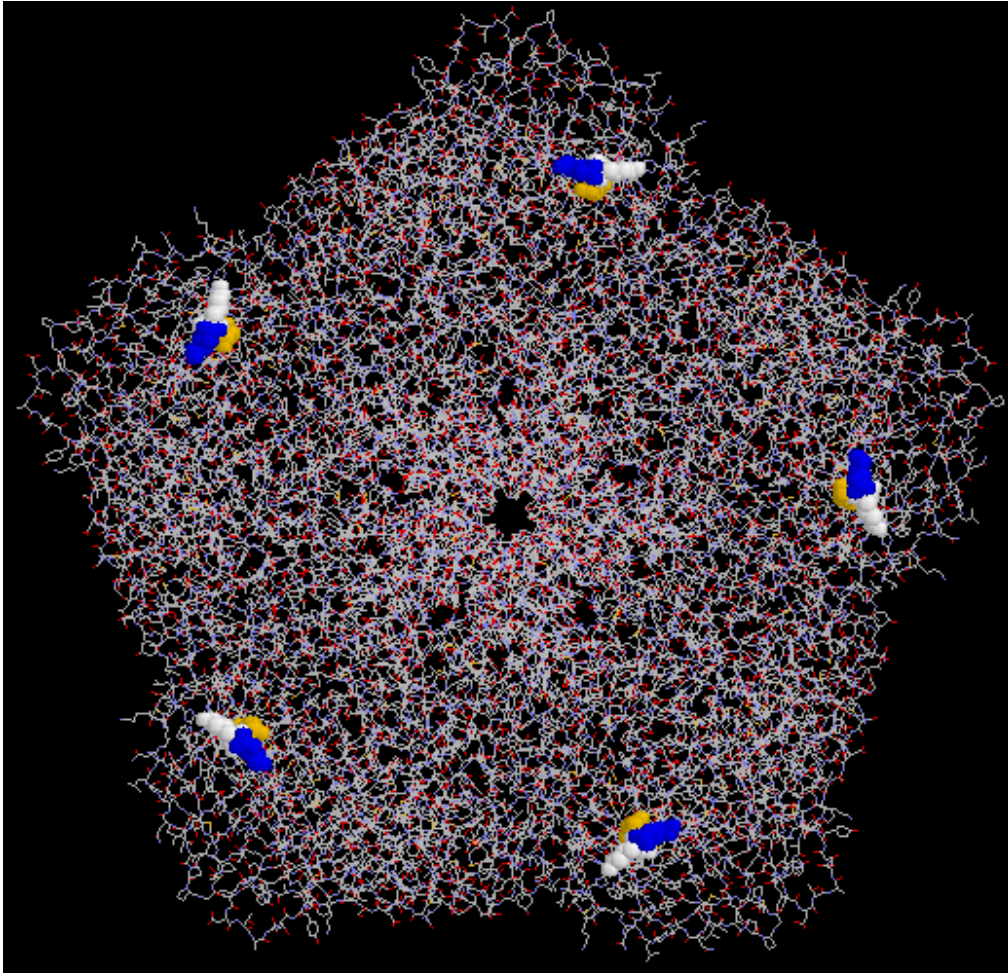


**Figure 4.7** The three-dimensional pentameric structure of CVA9 using Rasmol software, showing the predicted mutation positions of the VP3 at position 59 (blue) and the surrounding positively-charged amino acids giving a cluster. These are lysine (K) at position 276 (white) and arginine (R) at position 275 (yellow) in VP1.

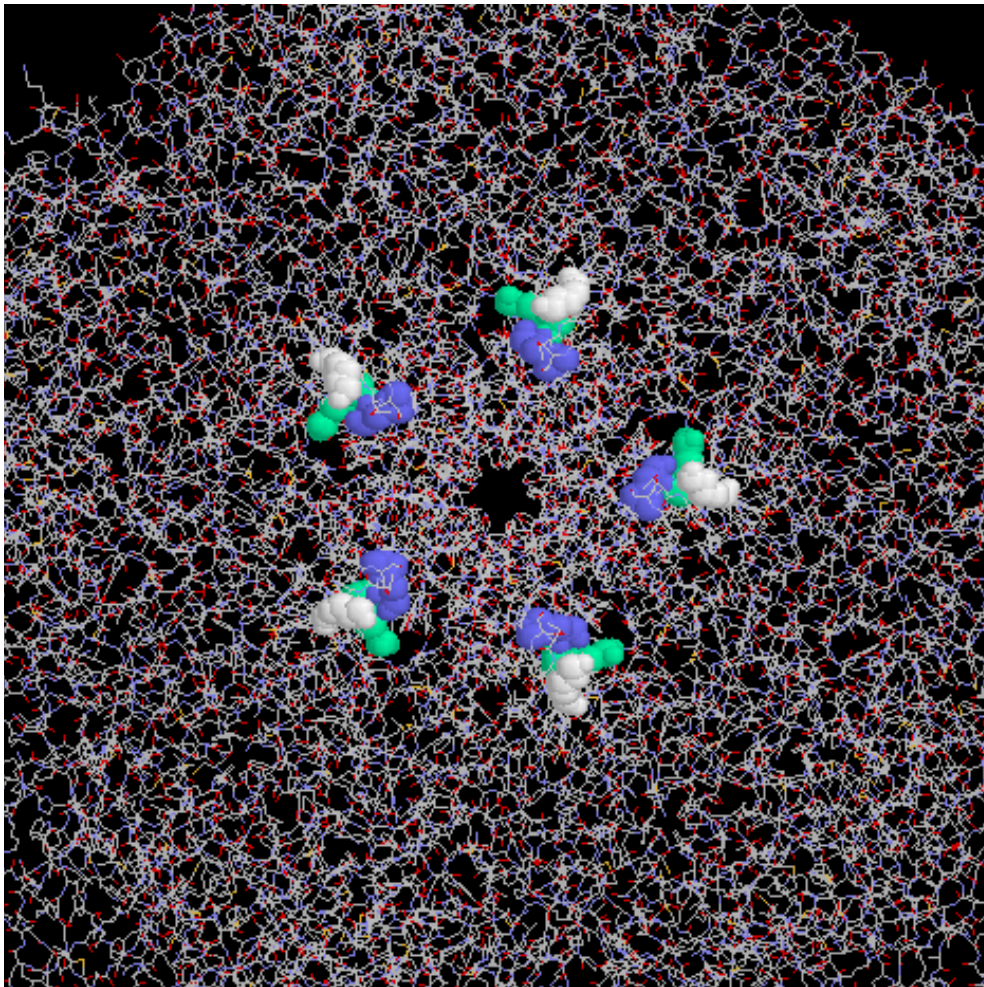


**Figure 4.8** The three-dimensional pentameric structure of CVA9 using Rasmol software, showing the predicted mutation positions of the VP1 position 222 (green) and the surrounding basic amino acids, these are histidine (H) at position 223 (purple) and lysine (K) at position 84 (white) in VP1.

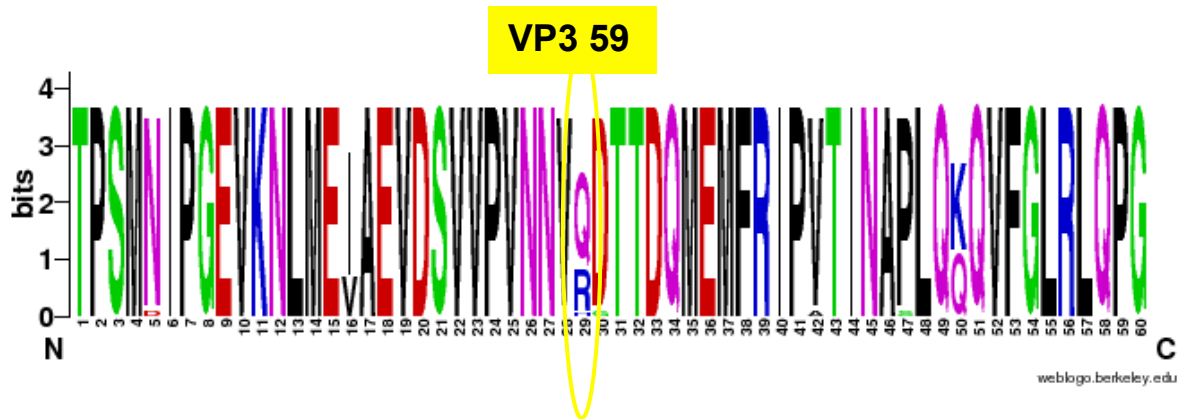


**Figure 4.9 A** Sequence alignment of part of the VP3 protein of CO87 with other CVA9 isolates in the GenBank sequence database shown using weblogo online software (Crooks *et al.*, 2004; Schneider and Stephens, 1990). 60 amino acids are analysed, centered on position 59. The data for this logo involved 25 amino acid sequences and the height of each single-letter amino acid code is related to the number of times the amino acid occurs at that position.

#### **4.2.4 Isolate CO62 Analysis**

##### **4.2.4.1 Inhibition of Infection of CVA9 CO62 by Soluble Heparin**

CO62, another isolate, which is not blocked by heparin, was also passaged twice on A549 cells. CO62 and CO87 are strains isolated in 1962 and 1987 respectively and are relatively diverse from one another (Figure 4.10). The sequence differences present may mean that adaptation to HSPG use can occur by a different mechanism.

The propagated CO62 (CO62P2) was tested in a plaque assay in the presence and absence of heparin. The results are shown in (Figure 4.11). The population is not blocked extensively by heparin, but plaque purification gave plaques that could be blocked. One of these (CO62H) was chosen for sequence analysis. Interestingly, the plaque passaged CO62 isolate (CO62H) is able to infect and kill cells and its infection is blocked by heparin. In contrast, a second plaque (CO62PL3) showed no blocking.

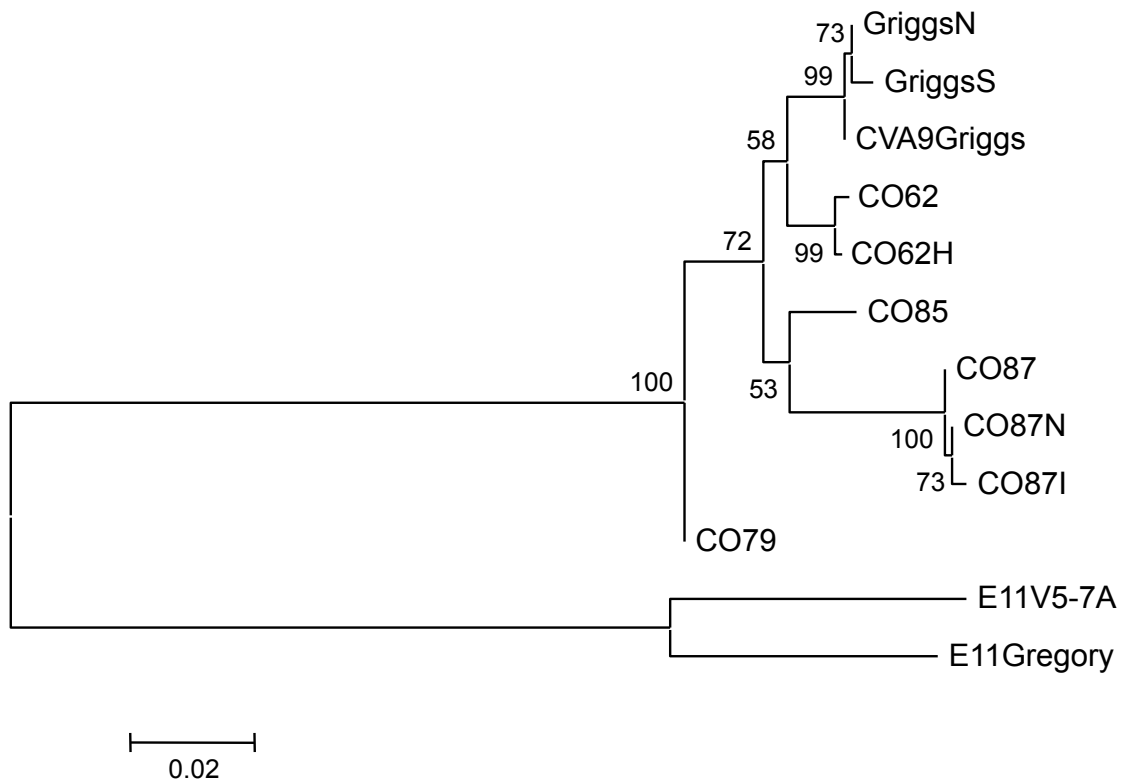


**Figure 4.10 Molecular phylogenetic analysis of CVA9 isolates by Maximum Likelihood method.** The evolutionary history was inferred by using the Maximum Likelihood method based on the JTT matrix-based model (Jones *et al.*, 1992). The dendrogram shows phylogenetic relationships between the complete P1-region sequences of CVA9 isolates and two E11 isolates (used as an out-group). The analysis involved 12 amino acid sequences. Numbers at nodes shown next to the branches correspond to the percentage of replicates tree in which the associated taxa clustered together in the bootstrap test (1000 replicates). The tree is drawn to scale, with branch lengths measured in the number of substitutions per site. Evolutionary analyses were conducted in MEGA6 (Tamura *et al.*, 2013).

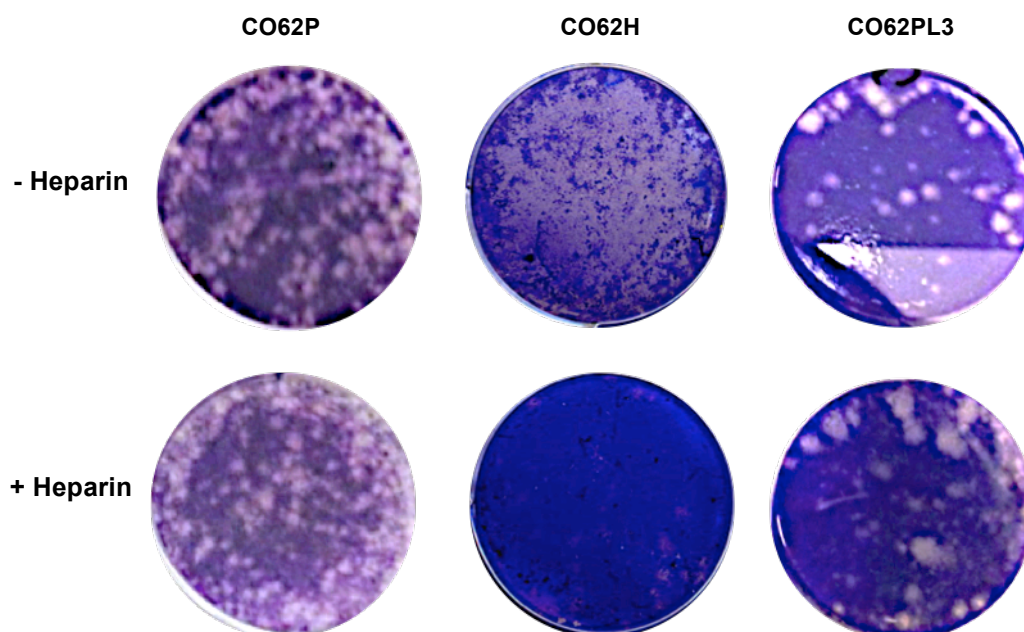


**Figure 4.11 Heparin blocking assay on A549-passaged CVA9 isolate CO62.** CO62P2 (passaged twice), CO62H (plaque-purified from CO62P2) and CO62PL3 (also plaque-purified from CO62P2). The top line shows mock-treated virus (90  $\mu$ l of  $10^2$  diluted virus and 10  $\mu$ l of water). The bottom line shows the treatment with heparin (90  $\mu$ l of  $10^2$  diluted virus and 10  $\mu$ l of 50 mg/ml heparin). Virus-heparin mixture or mock-treated control were incubated for 30 min then added to monolayers of A549 cells and then incubated for 1 hr. Cells were overlaid with CMC/agarose/medium then incubated for 3 days then stained with Crystal Violet. It can be seen that infections of CO62H can be completely blocked by heparin compared with CO62P2 and CO62PL3.

#### 4.2.4.2 Sequence Analysis of CO62 Isolate

The plaque purified virus CO62H was analysed by sequencing the P1 capsid encoding-region. As shown in Figure 4.12, the sequence alignment of the A549-CO62 adapted variant CO62H shows four mutations compared to the original CO62 sequence at position: 121 in VP2 (W121C), 59 in VP3 (Q593R), 72 in VP3 (A723V) and 286 in VP1 (Q2861R).

An analysis of the location of the mutations seen in the three-dimensional structure, based on the CVA9 Griggs crystal structure was performed (Hendry *et al.*, 1999) (Figure 4.13). The T132R mutation shown to give heparin blocking in the CO79 and CO85 isolates is also plotted (McLeish *et al.*, 2012). The amino acid at position W121C in VP2 is most likely not significant to HSPG binding as it is not on the surface of the pentamer. The same mutation, Q59R in VP3, which was seen in the CO87 variants was also found in CO62H. Another VP3 mutation, A723V is located in the same area, but is not adjacent to Q593R. The amino acid at position Q286R in VP1 cannot be visualised due to the flexible nature of this region (Hendry *et al.*, 1999), the closest visible amino acid VP1 position 284 is therefore shown. This maps quite closely to Q593R and it is possible that Q2861R is also close. This may mean that the predicted basic cluster of Q593R, K2751 and R2761 is bigger in CO62H. Q2861R is also very close to the RGD motif, which in CO62 has two basic amino acids before it. The CO62H sequence RSRRRGD is not a linear HSPG binding domain but is highly basic and so this may be able to bind to HSPG.

```

      >VP4
CO62      MGAQVSTQKTGAHETSLNATGNSVIHYTNINYYKDAASNSANRQDFTQDPSKFTPEVKDV 60
CO62H     MGAQVSTQKTGAHETSLNATGNSVIHYTNINYYKDAASNSANRQDFTQDPSKFTPEVKDV 60
          *****

      >VP2
CO62      MIKSLPALNSPTVEECGYSDRVRISITLGNSTITTQECANVVVGYGRWPTYLRDDEATAED 120
CO62H     MIKSLPALNSPTVEECGYSDRVRISITLGNSTITTQECANVVVGYGRWPTYLRDDEATAED 120
          *****

CO62      QPTQPDVATCRFYTLDSIKWEKGSVGVWWWKFEALSDMGLFGQNMQYHYLGRAGYTIHVQ 180
CO62H     QPTQPDVATCRFYTLDSIKWEKGSVGVWWWKFEALSDMGLFGQNMQYHYLGRAGYTIHVQ 180
          *****

      121
CO62      CNASKFHQGWLLVVCVPEAEMGGAVVGQAFPSTAMANGDKAYEFTSETQSDQTKVQTAVH 240
CO62H     CNASKFHQGWLLVVCVPEAEMGGAVVGQAFPSTAMANGDKAYEFTSETQSDQTKVQTAVH 240
          *****

CO62      NAGMGVGVGNLTIFPHQWINLRNTNSATIIVMPYINSVPMDNMFRHYNFTLMVIPVKLDY 300
CO62H     NAGMGVGVGNLTIFPHQWINLRNTNSATIIVMPYINSVPMDNMFRHYNFTLMVIPVKLDY 300
          *****

      >VP3
CO62      ADTASTYVPIIVTVAPMCAEYNGRLRLAQAQGLPTMNTPGSTQFLTSDDFQSPCALPQFDV 360
CO62H     ADTASTYVPIIVTVAPMCAEYNGRLRLAQAQGLPTMNTPGSTQFLTSDDFQSPCALPQFDV 360
          *****

      59      72
CO62      TPSMNIPGEVKNLMEIAEVDSVVPVNNVQDTTDDQMEMFRIPATINAPLQQQVFGRLRQPG 420
CO62H     TPSMNIPGEVKNLMEIAEVDSVVPVNNVQDTTDDQMEMFRIPATINAPLQQQVFGRLRQPG 420
          *****

CO62      LDSVFKHTLLGEILNYYAHWSGSMKLTFFVFCGSAMATGKFLIAYSPPGANPPKTRKDAML 480
CO62H     LDSVFKHTLLGEILNYYAHWSGSMKLTFFVFCGSAMATGKFLIAYSPPGANPPKTRKDAML 480
          *****

CO62      GTHIIWDIGLQSSCVLCVPWISQTHYRLVQQDEYTSAGYVTCWYQTMGIVPPGTPNSSSI 540
CO62H     GTHIIWDIGLQSSCVLCVPWISQTHYRLVQQDEYTSAGYVTCWYQTMGIVPPGTPNSSSI 540
          *****

      >VP1
CO62      MCFASACNDFSVRMLRDTPFISQDNKLGQDVVEEAINRAIVHVADTMRSGPSNSESVPALT 600
CO62H     MCFASACNDFSVRMLRDTPFISQDNKLGQDVVEEAINRAIVHVADTMRSGPSNSESVPALT 600
          *****

CO62      AVETGHTSQVTPSDTMQTRHVKNYHSRSESTVENFLGRSACVYMEEYKTTDNDNTNKKFVA 660
CO62H     AVETGHTSQVTPSDTMQTRHVKNYHSRSESTVENFLGRSACVYMEEYKTTDNDNTNKKFVA 660
          *****

CO62      WPINTKQMVQMRRLKEMFTYLRFDMEVTFVITSRQDPGTTLAQDMPVLTHQIMYVPPGGP 720
CO62H     WPINTKQMVQMRRLKEMFTYLRFDMEVTFVITSRQDPGTTLAQDMPVLTHQIMYVPPGGP 720
          *****

CO62      IPAKVDDYAWQTSTNPSIFWTEGNAPARMSIPFISIGNAYSNFYDGWSNFDQKGSYGNT 780
CO62H     IPAKVDDYAWQTSTNPSIFWTEGNAPARMSIPFISIGNAYSNFYDGWSNFDQKGSYGNT 780
          *****

CO62      LNNLGHIVVRHVGSSSPHPITSTIRVYFKPKHTRAWVPRPRLCQYKKAFSVDFTPPTIT 840
CO62H     LNNLGHIVVRHVGSSSPHPITSTIRVYFKPKHTRAWVPRPRLCQYKKAFSVDFTPPTIT 840
          *****

      286
CO62      DTRKDINTVTMMQSRRRGDMSTLNTH 867
CO62H     DTRKDINTVTMMQSRRRGDMSTLNTH 867
          *****

```

**Figure 4.12 ClustalW Sequence alignments of the capsid region of the original CO62 and the mutant CO62H adapted on A549. The amino acid differences seen are: W121C in VP2 (grey), Q59R in VP3 (purple) and A72V in VP3 (blue) and Q286R in VP1 (red).**

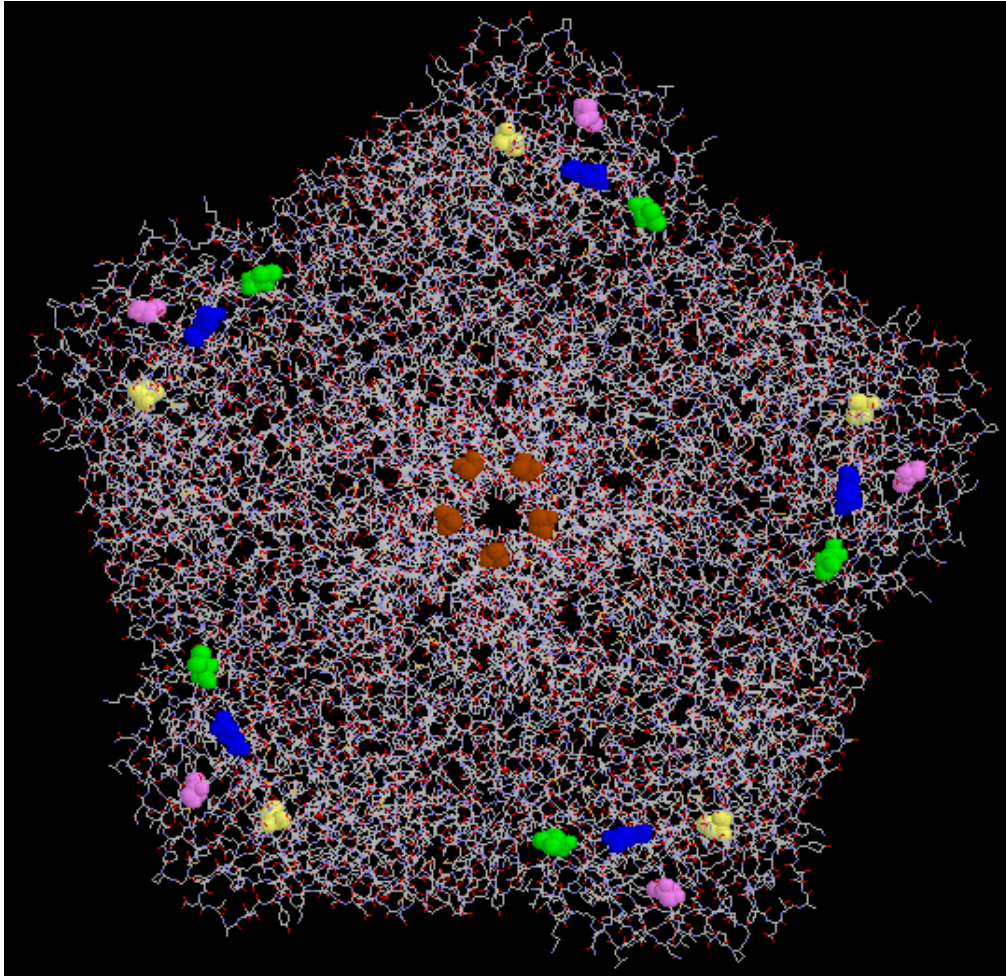


**Figure 4.13** The three-dimensional pentameric structure of CVA9 using Rasmol software, showing the predicted positions of the CO62 mutations seen in the heparin-blocked variants. VP3 position 59 is shown in spacefill, blue. VP2 position 121 is shown in spacefill, yellow. VP3 position 72 is shown in spacefill, pink. VP1 position 284 is shown in spacefill, green (the closest position to 286). VP1 position 132, which clusters at the 5-fold axis, is shown in spacefill, brown.

## **4.2.5 Isolate CVA9 Griggs Analysis**

### **4.2.5.1 Inhibition of Infection of CVA9 Griggs by Soluble Heparin**

The second passage of the propagated Griggs (GriggsP2) was tested in a plaque assay in the presence and absence of heparin. The results are shown in (Figure 4.14). Again the population was not greatly affected by heparin, but a variant (GriggsN) plaque-purified from the population was blocked. A separate adaptation experiment was performed and another heparin-blocked variant (GriggsS) was isolated (data not shown). In contrast, a second plaque (GriggsPL5) showed no blocking.

### **4.2.5.2 Sequence Analysis of CVA9 Griggs Variants**

The plaque purified viruses GriggsN and GriggsS were analysed by sequencing the P1 capsid encoding-region. As shown in Figure 4.15, the sequence alignment of the A549-Griggs adapted variant GriggsN shows a single mutation, located just before the RGD motif, of S2871R. GriggsS has four mutations at position: 76 in VP3 (A763V), 234 in VP3 (D2343N), 11 in VP1 (V111I) and the same mutation seen in GriggsN, 287 in VP1 (S2871R). As S2871R is the only mutation in GriggsN, this is probably also the key mutation giving the heparin-blocked phenotype in GriggsS. In addition, the S2871R mutation was observed previously in some mutants adapted to A549 cells and an engineered mutant containing only this mutation was blocked by heparin (Williams, 2002). None of the other mutations seen in GriggsS involve a basic amino acid and are unlikely to be contributing to the heparin-blocking. In addition, V111I is on the inside of the

particle (4.17). An analysis of the location of the mutations seen in the three-dimensional structure, based on the CVA9 Griggs crystal structure was performed (Hendry *et al.*, 1999) (Figure 4.16 and 4.17). The T132R mutation shown to give heparin blocking is also plotted (McLeish *et al.*, 2012). The effect of S2871R could be due to the linear RRRR sequence, which is highly basic.

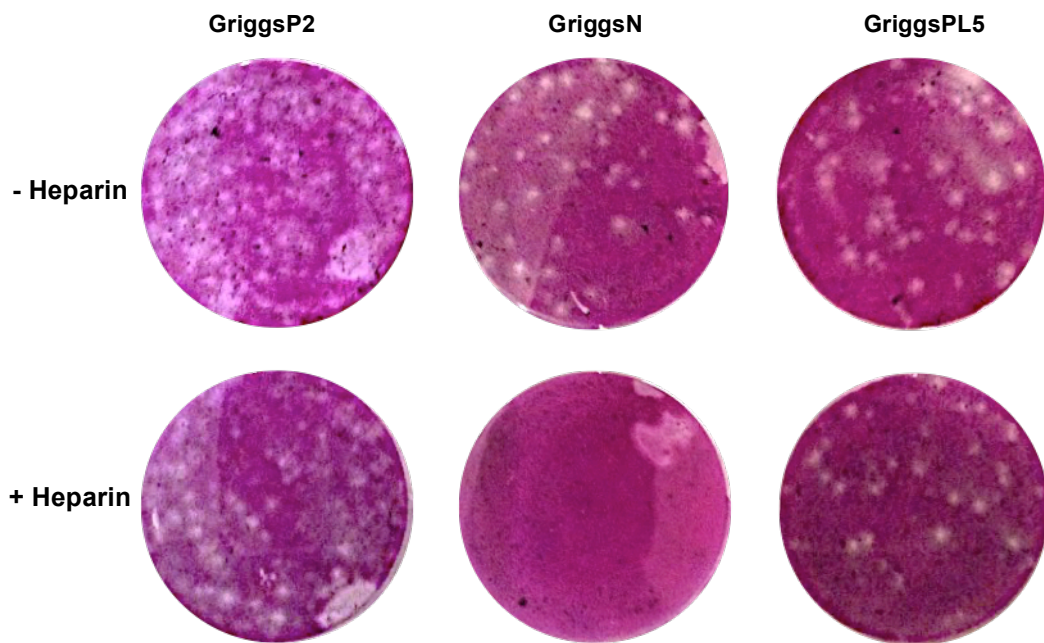


**Figure 4.14 Heparin blocking assay on A549-passaged CVA9 Griggs isolate.** GriggsP2 (passed twice), GriggsN (plaque-purified from GriggsP2) and Griggs PL5 (also plaque-purified from GriggsP2). The top line shows mock-treated virus (90  $\mu$ l of  $10^2$  diluted virus and 10  $\mu$ l of water). The bottom line shows the treatment with heparin (90  $\mu$ l of  $10^2$  diluted virus and 10  $\mu$ l of 50 mg/ml heparin). Virus-heparin mixture or the mock-treated control were incubated for 30 min then added to monolayers of A549 cells and then incubated for 1 hr. Cells were overlaid with CMC/agarose/medium then incubated for 3 days then stained with Crystal Violet. It can be seen that infections of GriggsN can be completely blocked by heparin compared with GriggsP2 and GriggsPL5.

>VP4  
 Griggs MGAQVSTQKTGAHETSLSAAGNSIIHYTNINYYKDAASNSANRQDFTQDPSKFTPEVKDV 60  
 GriggsN MGAQVSTQKTGAHETSLSAAGNSIIHYTNINYYKDAASNSANRQDFTQDPSKFTPEVKDV 60  
 GriggsS MGAQVSTQKTGAHETSLSAAGNSIIHYTNINYYKDAASNSANRQDFTQDPSKFTPEVKDV 60  
 \*\*\*\*\*

>VP2  
 Griggs MIKSLPALNSPTVEECGYSDRVRSITLGNSTITTQECANVVVGYGRWPTYLRDDEATAED 120  
 GriggsN MIKSLPALNSPTVEECGYSDRVRSITLGNSTITTQECANVVVGYGRWPTYLRDDEATAED 120  
 GriggsS MIKSLPALNSPTVEECGYSDRVRSITLGNSTITTQECANVVVGYGRWPTYLRDDEATAED 120  
 \*\*\*\*\*

Griggs QPTQPDVATCRFYTLDSIKWEKGSVGVWWKFPPEALSDMGLFGQNMQYHYLGRAGYTIHVQ 180  
 GriggsN QPTQPDVATCRFYTLDSIKWEKGSVGVWWKFPPEALSDMGLFGQNMQYHYLGRAGYTIHVQ 180  
 GriggsS QPTQPDVATCRFYTLDSIKWEKGSVGVWWKFPPEALSDMGLFGQNMQYHYLGRAGYTIHVQ 180  
 \*\*\*\*\*

Griggs CNASKFHQGCLLVVCPPEAEMGGAVVGQAFSATAMANGDKAYEFTSATQSDQTKVQTAIH 240  
 GriggsN CNASKFHQGCLLVVCPPEAEMGGAVVGQAFSATAMANGDKAYEFTSATQSDQTKVQTAIH 240  
 GriggsS CNASKFHQGCLLVVCPPEAEMGGAVVGQAFSATAMANGDKAYEFTSATQSDQTKVQTAIH 240  
 \*\*\*\*\*

Griggs NAGMGVGVGNLTIYPHQWINLRTNNSATIVMPYINSVPMNMFHRYNFTLMVIPVFKLDY 300  
 GriggsN NAGMGVGVGNLTIYPHQWINLRTNNSATIVMPYINSVPMNMFHRYNFTLMVIPVFKLDY 300  
 GriggsS NAGMGVGVGNLTIYPHQWINLRTNNSATIVMPYINSVPMNMFHRYNFTLMVIPVFKLDY 300  
 \*\*\*\*\*

>VP3  
 Griggs ADTASTYVPI TVTVAPMCAEYNGRLRLAQAGLPTMNTPGSTQFLTSDDFQSPCALPQFDV 360  
 GriggsN ADTASTYVPI TVTVAPMCAEYNGRLRLAQAGLPTMNTPGSTQFLTSDDFQSPCALPQFDV 360  
 GriggsS ADTASTYVPI TVTVAPMCAEYNGRLRLAQAGLPTMNTPGSTQFLTSDDFQSPCALPQFDV 360  
 \*\*\*\*\*

76  
 Griggs TPSMNI PGEVKNLMEIAEVDSVVPVNNVQD TTDQMEMFRI PVTINAPLQQQVFGRLRQPG 420  
 GriggsN TPSMNI PGEVKNLMEIAEVDSVVPVNNVQD TTDQMEMFRI PVTINAPLQQQVFGRLRQPG 420  
 GriggsS TPSMNI PGEVKNLMEIAEVDSVVPVNNVQD TTDQMEMFRI PVTINAPLQQQVFGRLRQPG 420  
 \*\*\*\*\*

Griggs LDSVFKHTLLGEILNYYAHWSGSMKLT FVFCGSAMATGKFLIAYSPPGANPPKTRKDAML 480  
 GriggsN LDSVFKHTLLGEILNYYAHWSGSMKLT FVFCGSAMATGKFLIAYSPPGANPPKTRKDAML 480  
 GriggsS LDSVFKHTLLGEILNYYAHWSGSMKLT FVFCGSAMATGKFLIAYSPPGANPPKTRKDAML 480  
 \*\*\*\*\*

Griggs GTHIIWDIGLQSSCVLCPWISQTHYRLVQQDEYTSAGYVTCWYQTGMIVPPGTPNSSSI 540  
 GriggsN GTHIIWDIGLQSSCVLCPWISQTHYRLVQQDEYTSAGYVTCWYQTGMIVPPGTPNSSSI 540  
 GriggsS GTHIIWDIGLQSSCVLCPWISQTHYRLVQQDEYTSAGYVTCWYQTGMIVPPGTPNSSSI 540  
 \*\*\*\*\*

234 >VP1 11  
 Griggs MCFASACNDFSVRMLRDTPFISQDNKLGDVVEEAIERAVVHVADTMRSGPNSASVPALT 600  
 GriggsN MCFASACNDFSVRMLRDTPFISQDNKLGDVVEEAIERAVVHVADTMRSGPNSASVPALT 600  
 GriggsS MCFASACNDFSVRMLRDTPFISQDNKLGDVVEEAIERAVVHVADTMRSGPNSASVPALT 600  
 \*\*\*\*\*

Griggs AVETGHTSQVTPSDTMQTRHVKNYHSRSESTVENFLGRSACVYMEEYKTTDNDVNKKFVA 660  
 GriggsN AVETGHTSQVTPSDTMQTRHVKNYHSRSESTVENFLGRSACVYMEEYKTTDNDVNKKFVA 660  
 GriggsS AVETGHTSQVTPSDTMQTRHVKNYHSRSESTVENFLGRSACVYMEEYKTTDNDVNKKFVA 660  
 \*\*\*\*\*

Griggs WPINTKQMVQMRRKLEMFTYLRFDMEVTFVITSRQDPGTTLAQDMPVLTHQIMYVPPGGP 720  
 GriggsN WPINTKQMVQMRRKLEMFTYLRFDMEVTFVITSRQDPGTTLAQDMPVLTHQIMYVPPGGP 720  
 GriggsS WPINTKQMVQMRRKLEMFTYLRFDMEVTFVITSRQDPGTTLAQDMPVLTHQIMYVPPGGP 720  
 \*\*\*\*\*

Griggs IPAKVDDYAWQTSTNPSIFWTEGNAPARMSIPFISIGNAYSNFYDGWSNFDQRGSYGNT 780  
 GriggsN IPAKVDDYAWQTSTNPSIFWTEGNAPARMSIPFISIGNAYSNFYDGWSNFDQRGSYGNT 780  
 GriggsS IPAKVDDYAWQTSTNPSIFWTEGNAPARMSIPFISIGNAYSNFYDGWSNFDQRGSYGNT 780  
 \*\*\*\*\*

```

Griggs      LNNLGHIYVRHVGSSPHPITSTIRVYFKPKHTRAWVPRPPRLCQYKKAFSVDFTPIT 840
GriggsN     LNNLGHIYVRHVGSSPHPITSTIRVYFKPKHTRAWVPRPPRLCQYKKAFSVDFTPIT 840
GriggsS     LNNLGHIYVRHVGSSPHPITSTIRVYFKPKHTRAWVPRPPRLCQYKKAFSVDFTPIT 840
            *****
            287
Griggs      DTRKDINTVTTVAQSRRRGDMSTLNTH 867
GriggsN     DTRKDINTVTTVAQRRRGDMSTLNTH 867
GriggsS     DTRKDINTVTTVAQRRRGDMSTLNTH 867
            *****

```

**Figure 4.15 ClustalW Sequence alignments of the capsid region of the original CVA9 Griggs and mutants (GriggsN and GriggsS) from plaque-purified variants isolated from Griggs adapted on A549 cells. The amino acid differences are seen at positions A76V in VP3 (blue), D234N in VP3 (yellow) and V11I in VP1 (grey) (GriggsS only) and S287R in VP1 (purple) (both variants).**

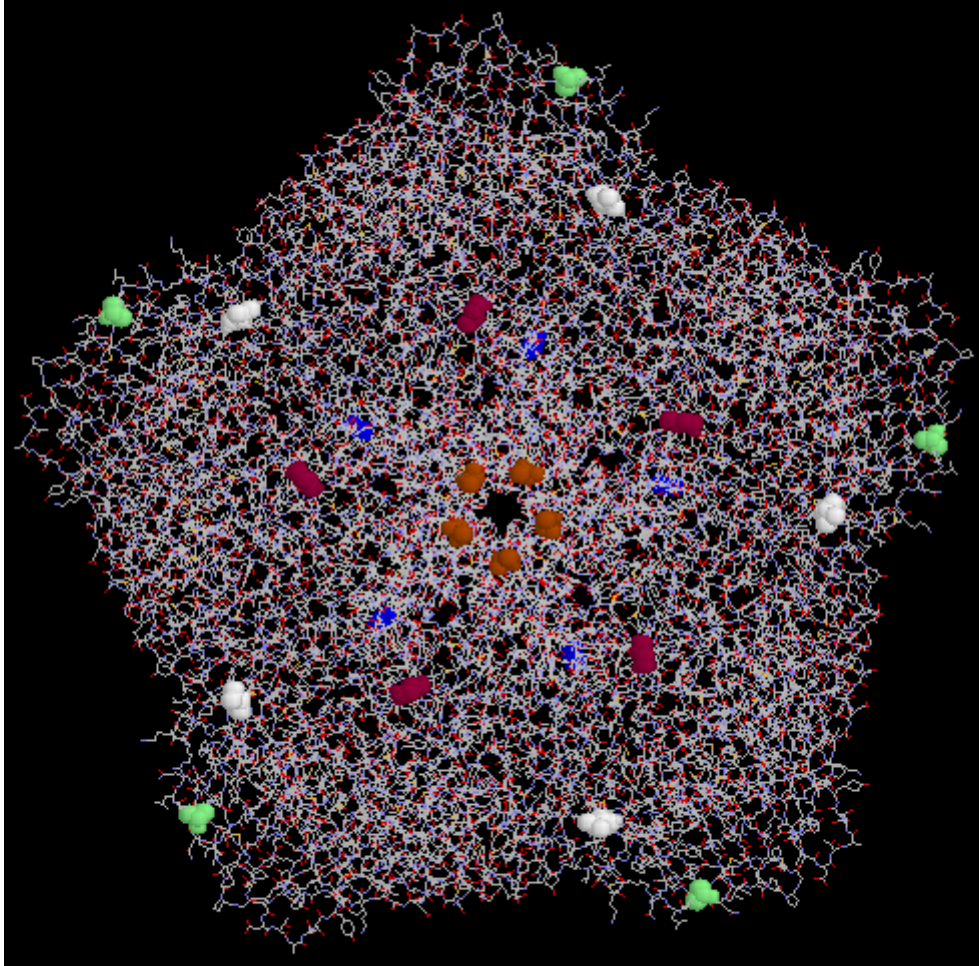


**Figure 4.16** The three-dimensional pentameric structure of CVA9 using Rasmol software, showing the predicted positions of the Griggs mutations seen in the heparin-blocked variants. VP3 position 76 is shown in spacefill, green. VP3 position 234 is shown in spacefill, magenta. VP1 position 11 is shown in spacefill, blue. VP1 position 284 is shown in spacefill, white (the closest position to 287). VP1 position 132, which clusters at the 5-fold axis is shown in spacefill, brown.

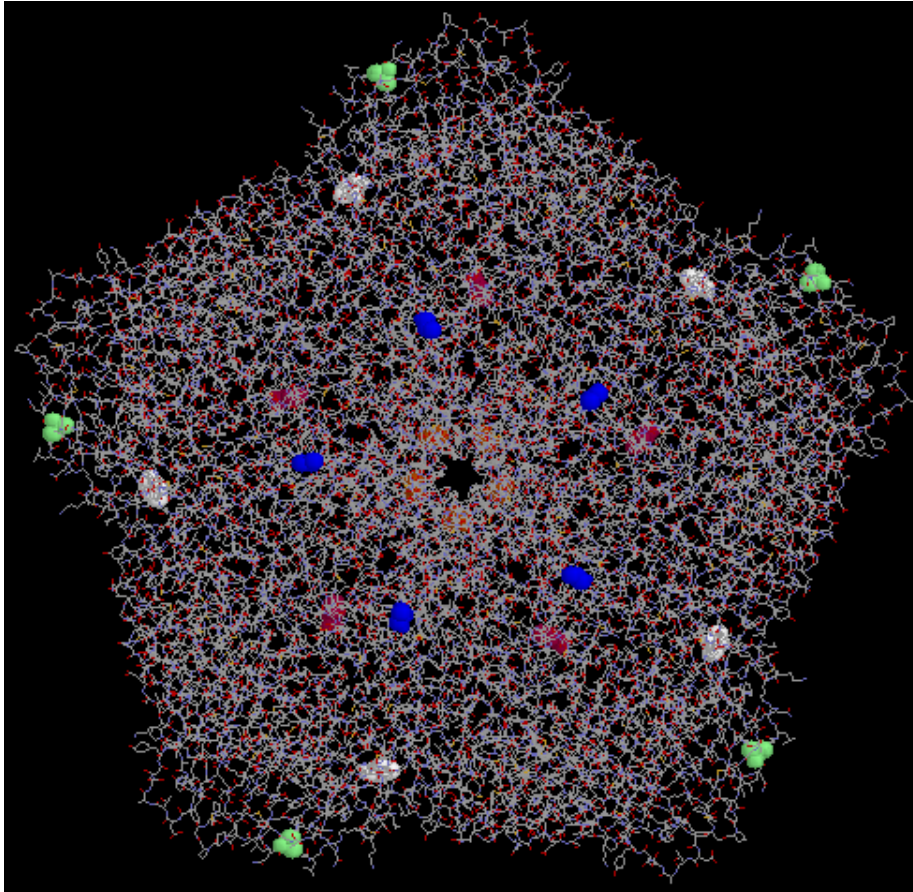


**Figure 4.17** Inside view of the three-dimensional pentameric structure of CVA9 using Rasmol software, showing the predicted positions of the Griggs mutations seen in the heparin-blocked variants, showing VP1 position 11 (spacefill, blue).

### **4.3 Mapping All Amino Acids Differences onto the 3D Structure of CVA9**

A summary of all the mutations seen in adapting CVA9 isolates to A549 cells is shown in Figure 3.18. The previously identified T1321R, which has a heparin binding/blocking phenotype, is also shown. The novel Q593R mutation is located very far from T1321R. However, the Q2861R and S2871R mutations may be involved close to Q593R. Two mutations, D2343N and R2221K, are in the canyon region. Several of the mutations, including Q593R and Q2861R/S2871R (based on the 2841 position which is the closest amino acid that can be visible in the structure) form a line parallel to the pentamer edge. Several of the mutations are probably not involved in HSPG binding, but could have an effect on binding to other receptors as the canyon is known to be the binding site of receptors in several picornaviruses (Rossmann *et al.*, 2002).

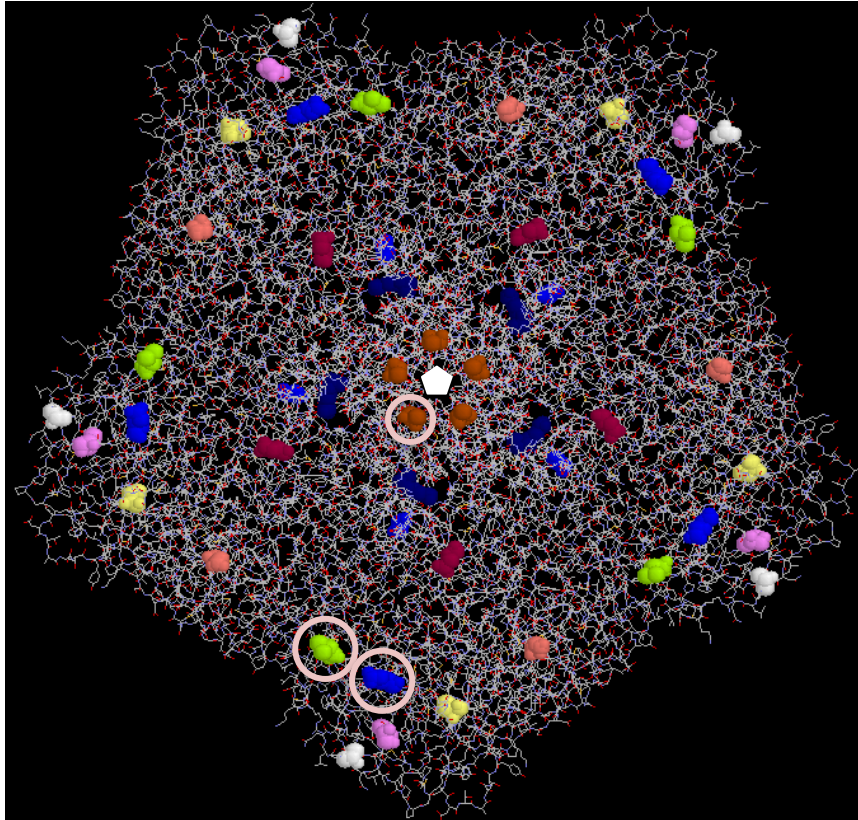


**Figure 4.18** The three-dimensional pentameric structure of CVA9, showing the predicted positions of all mutations seen in adapting CVA9 isolates to A549 cells.

VP3 position 76 (white)

VP3 position 234 (magenta)

VP1 position 11 (light blue)

VP1 position 284 (green, the closest position to 286 and 287)

VP1 position 132, which clusters at the 5-fold axis (brown)

VP2 position 121 (yellow)

VP3 position 59 (blue)

VP3 position 72 (pink)

VP1 position 222 (dark blue)

VP2 position 163 (salmon)

A white pentagon shows the position of the 5-fold axis. Circles show the positions of mutations linked to the heparin blocked phenotype. Mutations were mapped using Rasmol software.

#### **4.4 Mapping All Amino Acids Differences of CVA9 Compared to E11 onto the 3D Structure of CVA9**

As several E11 adapting mutations (Chapter 3) were found close to the pentamer edge, the CVA9 A549 mutations and E11 mutations were mapped onto the CVA9 structure (Figure 4.19). The mutations are mainly in different regions, with several CVA9 mutations surrounding the 3-fold axis. The 2332 mutation seen in previous work (Williams, 2002) at the 3-fold axis is, however, seen in CVA9 and in E11 adapted to L41 cells. Interestingly, mutation at VP3 position 59 was observed in E11 V5-7A adapted to A549 cells (E593V), and in CVA9 CO87 and CO62 adapted to A549 cells (Q593R).

The other A549-adapting mutation in E11 V5-7A (G145S) as well as other E11 adapting mutations are close to CVA9 Q1632R. To investigate a possible CVA9 interaction with DAF or DAF-related molecules, the CVA9 mutations were mapped onto the E7 surface (Yoder *et al.*, 2012) (Figure 4.20). Four CVA9 mutations map in or close to the known E7 DAF binding regions.

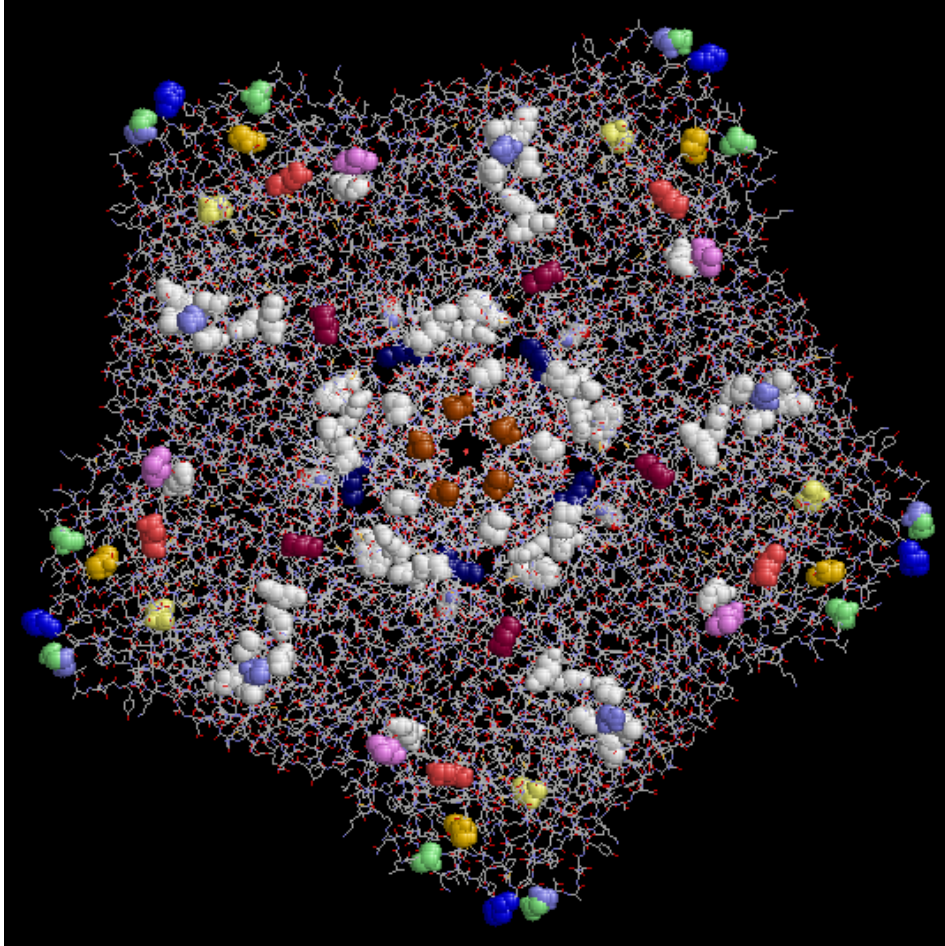


**Figure 4.19** The three-dimensional pentameric structure of CVA9, showing the predicted positions of all mutations seen in adapting CVA9 isolates to A549 cells and all published E11 adapting mutations (Stuart *et al.*, 2002b; Rezaikin *et al.*, 2009; Novoselov *et al.*, 2012) (chapter 3). Mutations were mapped using Rasmol software. The E 11 mutations are shown in white. CVA9 mutations are: VP3 position 59 (salmon)  
 VP1 position 284 (pink, the closest position to 286 and 287)  
 VP3 position 76 (green)  
 VP3 position 234 (burgundy)  
 VP1 position 11 (grey, on inside surface)  
 VP1 position 132 (brown)  
 VP2 position 121 (yellow)  
 VP3 position 72 (dark yellow)  
 VP1 position 222 (dark blue)  
 VP2 position 163 (pale blue)  
 VP2 position 233 (green/pale blue)  
 VP3 position 202 (blue)

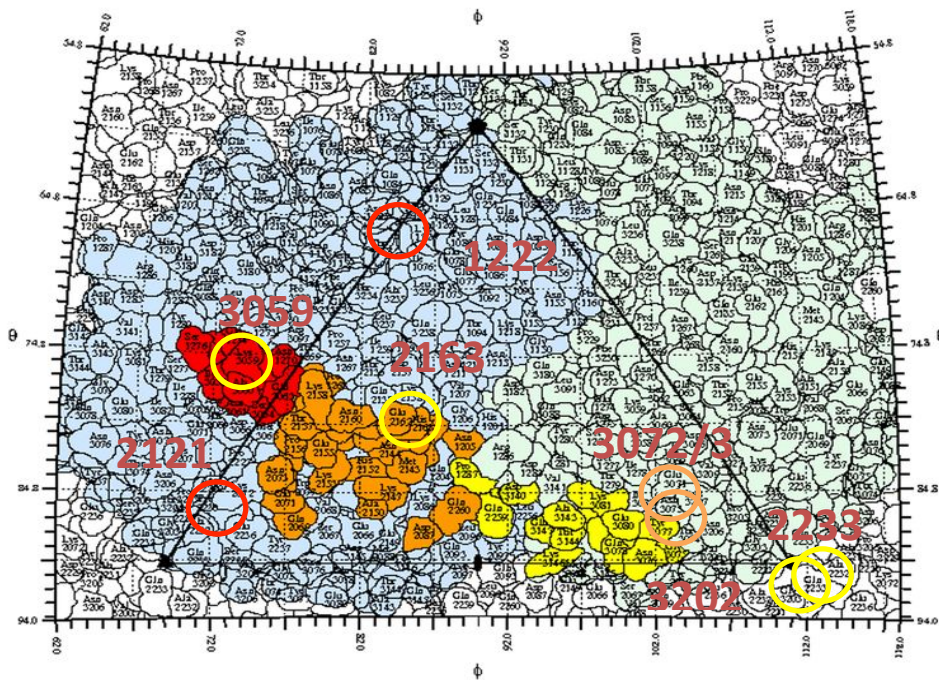


**Figure 4.20** Surface projection of E7 (Yoder *et al.*, 2012), with the approximate positions of A549 adapting mutations of CVA9 shown by circles. The numbering used is different from that used in the rest of this chapter to make it consistent with the numbering in the projection. For instance, 3059 marks the position of the Q593R mutation. The CVA9 2233, 3073, 3202 mutations were found in previous A549 adaptation experiments (Williams, 2002).

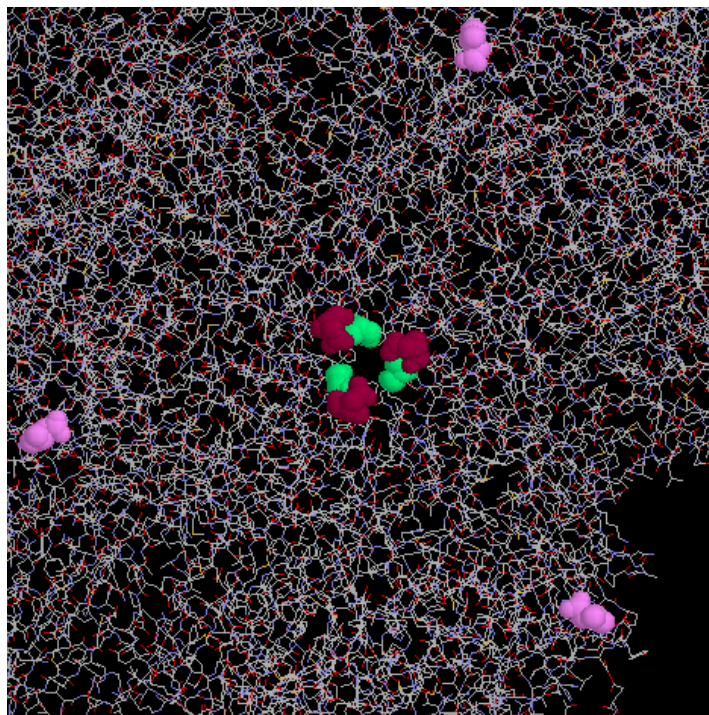
## 4.5 Analysis of the Effect of A549-adapting Mutations

### 4.5.1 Location of A549-adapting Mutations

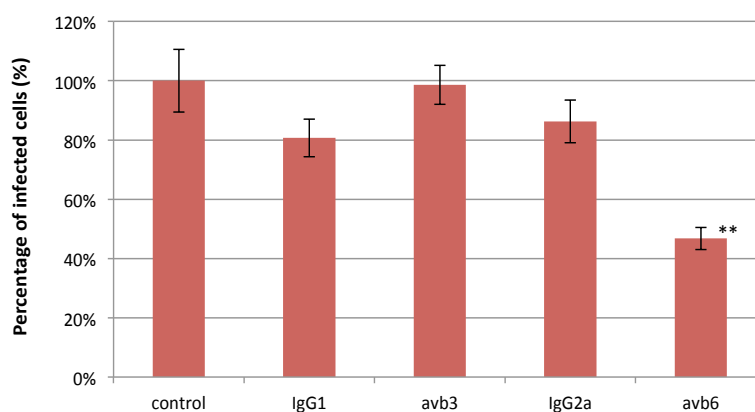
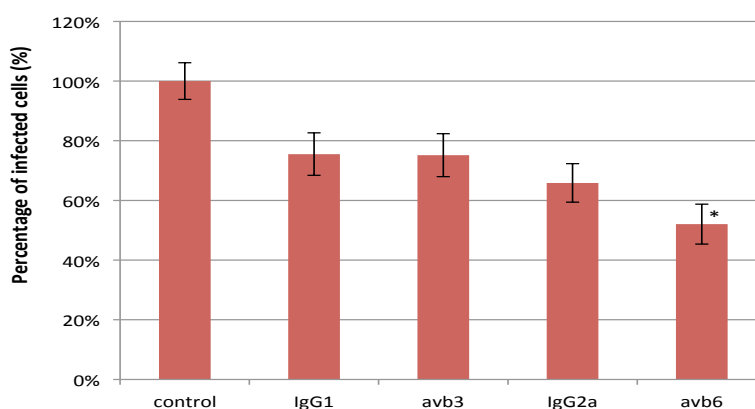
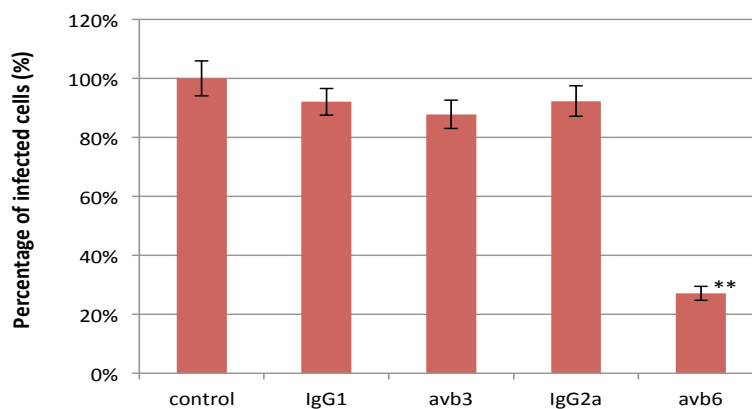
As it was found that the S2871R mutation was frequently found in A549/CVA9 Griggs adaptation experiments, it was interesting to find whether this affects infection. A previously engineered S2871R mutant was used. The mutations previously seen at the 3-fold axis (section 4.4) are also of interest. These are shown in Figure 4.21. Mutant D contains only a D2332N mutation. P2023S was previously genetically engineered from an infectious clone after being observed during adaptation experiments. Both these mutations cluster together in a striking position at the 3-fold axis. These mutations are distant from the S2871R (based on the nearest visible amino acid, position 2841).

### 4.5.2 Integrin $\alpha_v\beta_3$ and $\alpha_v\beta_6$ Antibody Blocking of Infections

In order to test whether adaptation was related to changes in receptor tropism, antibodies against the reported CVA9 cell receptors, integrins  $\alpha_v\beta_6$  and  $\alpha_v\beta_3$ , were used to block these molecules on A549 cells. Immunofluorescence analysis was done for CVA9 Griggs and the S2871R and P2023S mutants (Figure 4.22). Treatment with the  $\alpha_v\beta_6$  antibody reduced the infection of CVA9 Griggs and the mutants. The  $\alpha_v\beta_3$  antibody had no effect. This suggests that adaptation to A549 cells was not due to selection of an alternative receptor and  $\alpha_v\beta_6$  is still used. As previously reported for A549 cells,  $\alpha_v\beta_3$  does not seem to be a receptor for CVA9 Griggs and the mutants also do not seem to use this molecule (Williams *et al.*, 2004; Heikkila *et al.*, 2009).



**Figure 4.21** Close up view of a pore-like structure at the 3-fold axis formed by the amino acids **P2023S** and **D2332N**. D2332N (burgundy), P2023S (green) and S2871R (pink, 284 the closest position to 287). Mutations were mapped using Rasmol software.

**CVA9 Griggs****P2023S****S2871R**

**Figure 4.22 Effect of  $\alpha_v\beta_6$  and  $\alpha_v\beta_3$  antibodies on CVA9 infection of A549 cells.** 1.0  $\mu\text{g}$  of PE mouse IgG2a or IgG1 Isotype controls and 1.0  $\mu\text{g}$  of anti-integrin  $\alpha_v\beta_6$  and  $\alpha_v\beta_3$  antibodies were used to pre-treat A549 cells (30 min, 37°C) before infecting with CVA9 mutants. Infected cells were detected and counted using a CAV9 antibody and TRITC-labelled secondary. The control is cells without pre-treatment. 20 random fields were counted in each case and 5 of the control value is given, together with standard deviations. Significance level: \*\* = 0.01 \* = 0.05

### 4.5.3 Metal Ion-dependence ( $\text{Ca}^{2+}$ , $\text{Mg}^{2+}$ )

As integrin binding is dependent on divalent metal cations, virus binding to cells in the presence or absence of calcium chloride ( $\text{CaCl}_2$ ), and calcium plus magnesium chloride ( $\text{MgCl}_2$ ) was investigated. A549 cells were grown in 6-well plates and then washed with medium, TBS,  $\text{CaCl}_2$  or  $\text{CaCl}_2/\text{MgCl}_2$ , then diluted viruses (CVA9wt, S2871R and P2023S) were added to the cells for 1 hour on rocking platform at room temperature. Then the buffers and unbound virus were discarded and cells were washed twice with same buffers and plaque assay was performed in the presence of growth medium (Figure 4.23, 4.24). It can be seen that in the absence of calcium (TBS), CVA9 Griggs does not infect the cells. A few plaques are seen for S2871R, which may be due to HS interactions allowing the virus to bind to the cell surface. Surprisingly, the P2023S gives a similar number of plaques in the presence and absence of calcium, suggesting that an additional molecule can be used at the cell surface. Similar results are seen for the calcium and magnesium experiment, except that the additional magnesium enhances infectivity greatly (Figure 4.24).

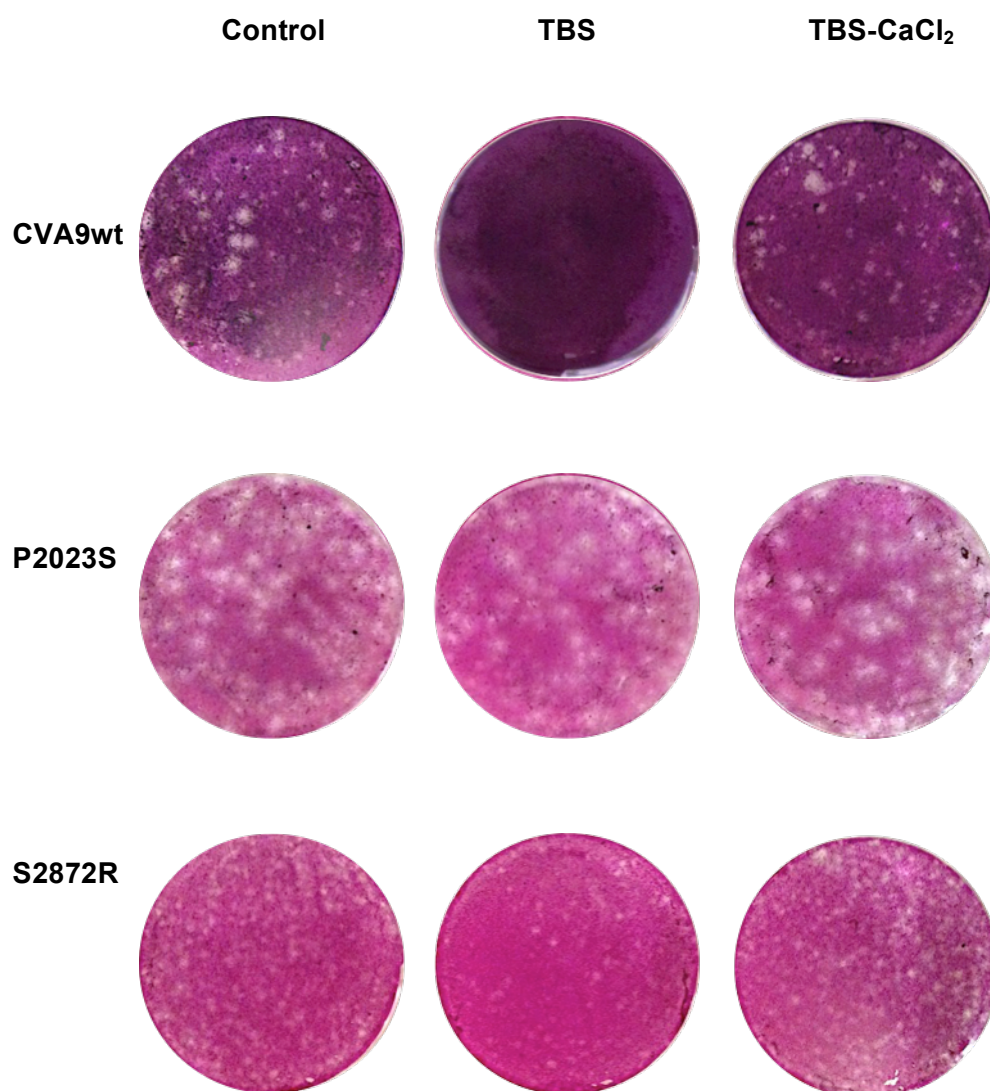


**Figure 4.23 Infection of CVA9 in the presence and absence of calcium.** A549 cells were washed with growth medium (contains calcium), TBS (no calcium) or TBS-CaCl<sub>2</sub>. Virus in the same solutions was added for 45 min and allowed to bind, then the solutions and unbound viruses were removed, the cells were washed with medium and the standard medium/CMC overlay was added. Cells were incubated for 3 days then stained with Crystal Violet.

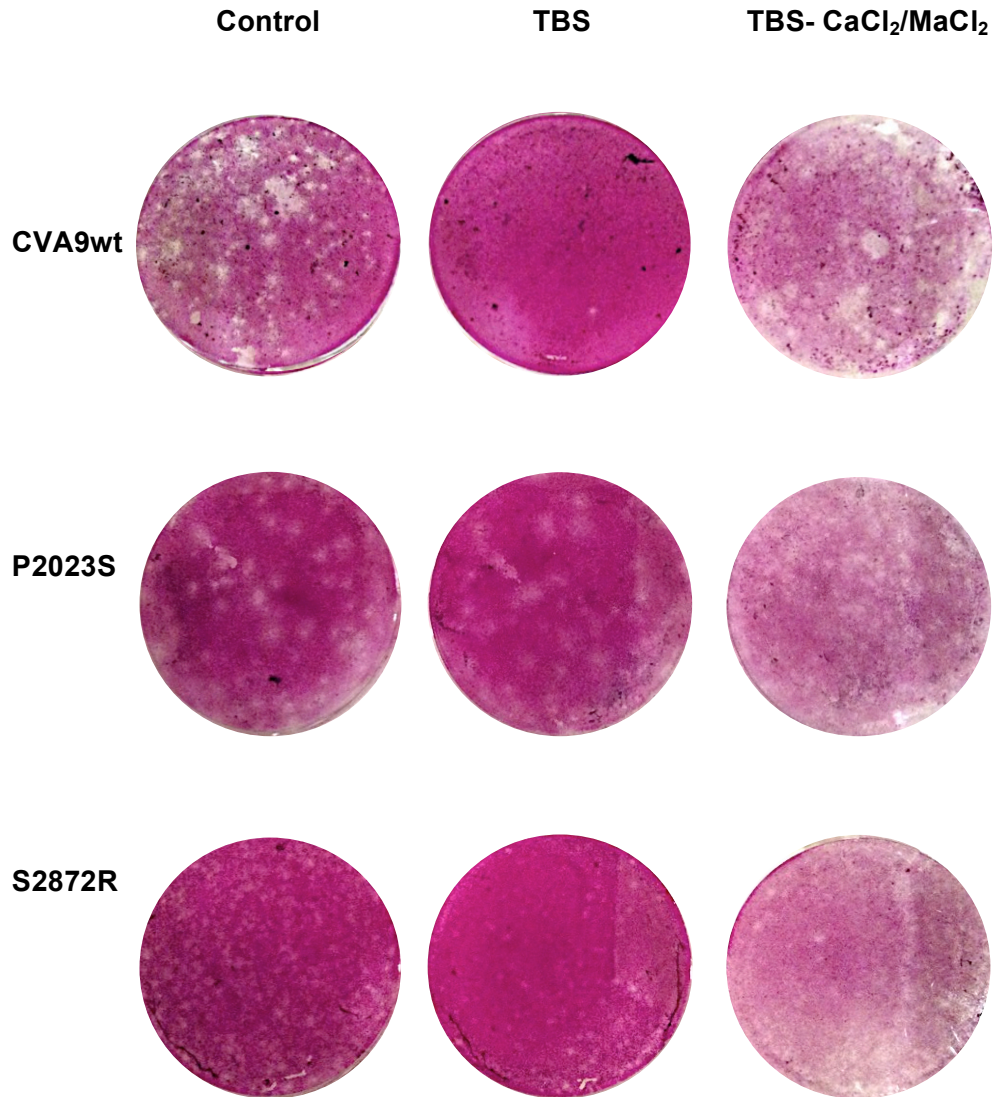


**Figure 4.24 Infection of CVA9 in the presence and absence of calcium plus magnesium.** A549 cells were washed with growth medium (contains calcium), TBS or TBS- $\text{CaCl}_2/\text{MgCl}_2$  Virus in the same solutions was added for 45 min and allowed to bind, then the solutions and unbound viruses were removed, the cells were washed with medium and the standard medium/CMC overlay was added. Cells were incubated for 3 days then stained with Crystal Violet.

#### 4.5.4 Temperature Sensitivity Assays

The location of the mutations in CVA9D and P2023S at the 3-fold axis and surrounding a pore, suggests that they could have an effect on the stability of the virus. Both the original CVA9wt and mutant viruses lost most of their infectivity when incubated for 1 hour at 37 °C before a plaque assay was performed and there was no clear difference (data not shown). The effect of temperature on virus growth was also studied. CVA9wt, D and P2023S variants were tested by performing plaque assays on A549 and GMK cells at 34°C, 37°C and 40°C (Figure 4.25 and 4.26). All the viruses showed plaques at 37 °C and there was little growth at 40°C. CVA9D seemed to be less affected by growing at 34 °C than CVA9wt on both cell lines, particularly A549 cells. However, the other mutant, CVA9 P2023S, showed no plaques at 34 °C, so the 3-fold axis mutations do not show a consistent effect.

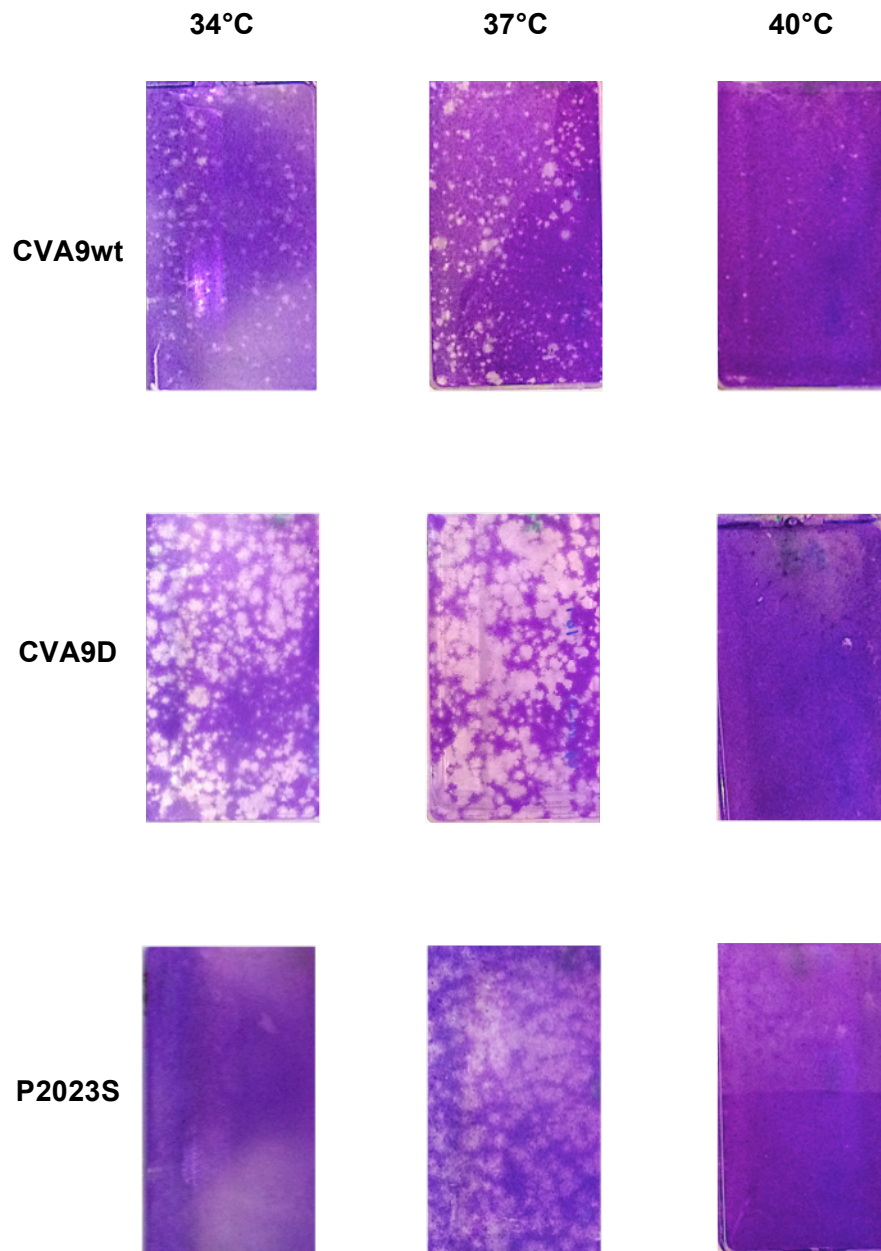


**Figure 4.25 Temperature sensitivity assay of CVA9wt, CVA9D and P2023S on A549 cells.** A normal plaque assay was performed, but after adding the overlay, the samples were incubated at 34°C, 37°C and 40°C for 3 days before being stained with Crystal violet.

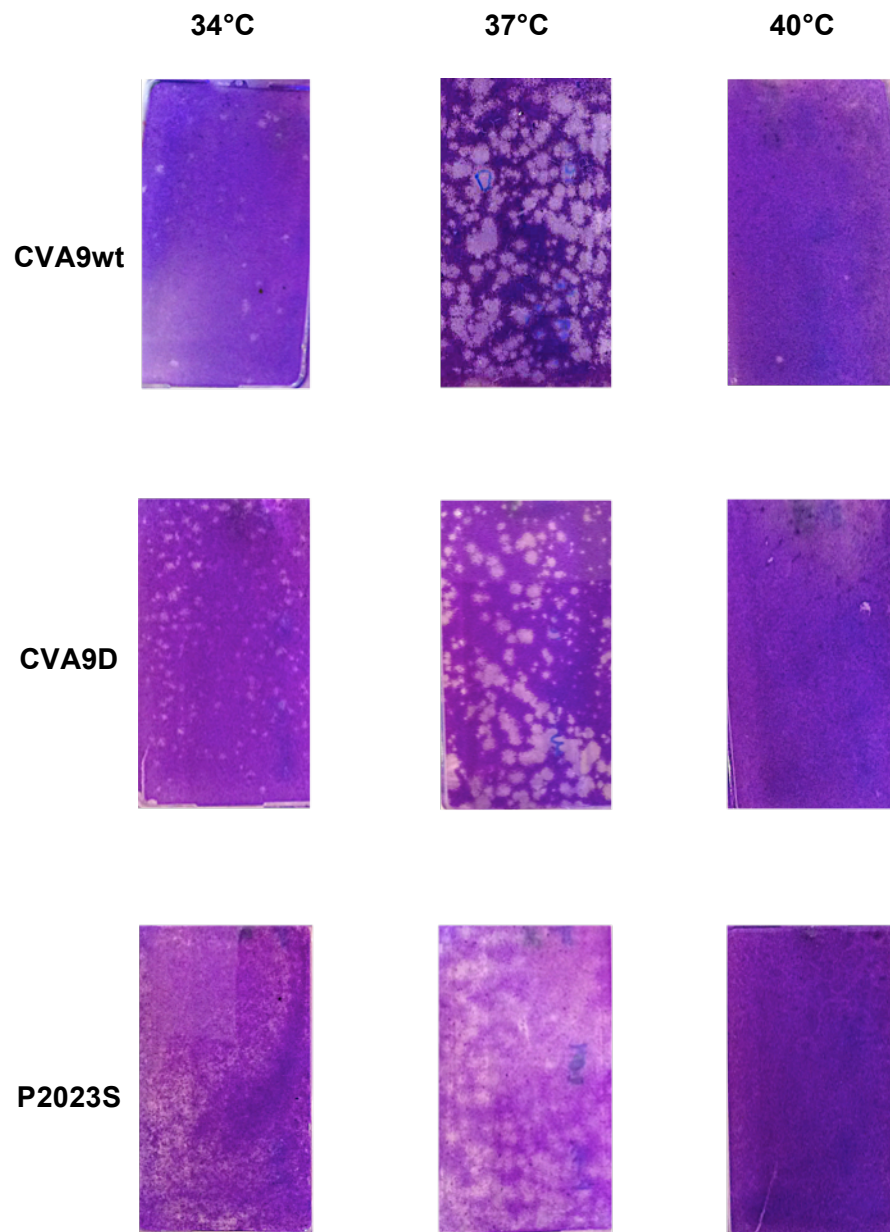


**Figure 4.26 Temperature sensitivity assay of CVA9wt, CVA9D and P2023S on GMK cells.** A normal plaque assay was performed, but after adding the overlay, the samples were incubated at 34°C, 37°C and 40°C for 3 days before being stained with Crystal violet.

## 4.6 Discussion

Virus receptors may be one of the determinants of virus host range and tissue tropism. Several receptors that are known to bind to CVA9 have been identified over the past few years. CVA9 is known to use a functional arginine-glycine-aspartic acid (RGD) motif to interact with cell surface integrin  $\alpha_v\beta_6$  during cell entry (Williams *et al.*, 2004; Heikkila *et al.*, 2009). In addition, some isolates of CVA9 and other enteroviruses have been identified which use heparan sulphate proteoglycan (HSPG) as a co-receptor for interaction of cells (McLeish *et al.*, 2012). It has been reported that foot-and-mouth disease virus (FMDV), in addition to binding to integrins, requires binding to heparan sulphate, suggesting that HSPG may interact with CVA9  $\alpha_v\beta_3$  on the cell surface promoting a specific binding of the virus (Jackson *et al.*, 1996).

HSPG is ubiquitously expressed by all cell types, and the expression varies on different cell types due to the variations in structure, differences in the sulphation degree, chain length and the position of the sulfate group (Tan *et al.*, 2013). Despite the functions of HSPG in animal development and homeostasis, HSPG is a potential target for the prevention of viral infection and pathogenicity of number of viruses. Moreover, an efficient interaction with HSPG can increase virulence and enhancing viral replication within specific host tissues (Zhu *et al.*, 2011).

Recently, it has been shown that CVA9 binds to HSPG by symmetry-related clustering of positive charges. Four CVA9 isolates (CO62, CO79, CO85, CO87) were studied previously. CO79 and CO85 infection were significantly inhibited in the presence of heparin, while CO62 and CO87 infections were not inhibited;

indeed, infection appeared to be enhanced (McLeish *et al.*, 2012) (Figure 4.1). Analysis of the HS-binding domain showed this is due to an arginine (R) at position 132 in the VP1 capsid protein of the inhibited isolates (CO79 and CO85), rather than a threonine (T) which is seen in the non-binding isolates. This forms tight clusters around the 5-fold axis of symmetry, generating a patch of a positively-charged area allowing interactions with HSPG (McLeish *et al.*, 2012) (Figures 4.6, 4.13, 4.16, 4.18 and 4.19).

To investigate HS binding further, 3 non-HS-binding isolates were passaged on the A549 human lung carcinoma cell line (Figure 4.3, 4.11 and 4.14). Variants were identified where infection found to be blocked by heparin, a HS analogue, suggesting HSPG involvement in infection. The results are summarised in Table 4.1. Sequence analysis suggest that at least two more classes of mechanisms can be involved in adaptation of CVA9 to A549, one where a mutation close to the RGD motif (SRRR>RRRR) gave either a linear HS-binding motif or a cluster of positive charges, and one with a mutation at position 59 in VP3 (Q593R). This mutation, observed in CO87N, CO87I and CO62H, does not give a linear motif but causes a change of the neutral amino acid Q (Glutamine) to a basic amino acid R (Arginine). Basic amino acids, lysine (K) or arginine (R), are often associated with binding to HSPG. The mutated position does not form a symmetry-related cluster, but an analysis of the three-dimensional structure based on the CVA9 Griggs, as in Figure 4.7, shows two adjacent basic amino acids in VP1, these are arginine position 275 (R275) and lysine position 276 (K276), so there is a conformationally-defined cluster of positive charge, which probably allows HSPG interactions. Thus, CVA9 binding to HSPG might occur by an additional mechanism to symmetry-related clustering.

Another possible mechanism that is utilized by CVA9 for HS-binding is a linear RRRR motif. This may correspond to the known motif BBXB, where B is a basic amino acid and X any neutral or hydrophobic amino acid (Cardin and Weintraub, 1989). This was observed by adaptation of CVA9 Griggs to A549 cells followed by a complete capsid sequence analysis of plaque-purified variants (CVA9GriggsN and CVA9GriggsS), which showed a mutation of S2871R (Figure 4.15). However, as RRRR is not neutral or hydrophobic, it may not be the linear motif but the additional positive charge close to the three already present in the Griggs RGD region, which is important. Unfortunately, VP1 position 287 cannot be seen in the three-dimensional structure based on the CVA9 Griggs, as it lies close to the C-terminus of VP1 where the structure was not determined (Hendry *et al.*, 1999). Position 284 on VP1, which is the closest amino acid that is visible in the structure, was mapped in Figures (4.16, 4.18 and 4.19). This is located relatively close to VP3 position 59 and VP1 positions 287-290 (SRRR). It could even more form a larger cluster with that centered on VP3 position 59. In addition to Q593R, CO62H has a Q to R mutation at position 286 (Figure 4.12). It is not clear if this also allows HSPG binding or if both mutations in CO62H are required. However, the location close to the RRRGD sequence (positions 288-292) and the fact that the mutation gives a basic amino acid suggests it could play a role.

An alignment of the C-terminus of VP1 of the isolates used in this work is shown in Figure 4.27. It can be seen that Griggs and CO62 are highly basic in this region due to the RRRGD sequence and this may explain why additional mutations that are close by (S2871R) or may be close by (Q2861R) are associated with HSPG binding. It is interesting that CO87 already has a run of 4 basic amino acids RKRRGD and yet is not blocked by heparin and does not

acquire further mutations in this region in mutating to blocked variants. It may be that K is less useful in giving HSPG-binding or due to conformational differences in the region.

The fact that S2871R lies close to the RGD motif that is used in CVA9 interaction with integrin  $\alpha_v\beta_6$  could be significant and the same could be true of the VP3 position 59, if this is close to the RGD motif. HSPG binding may be useful to the virus by making the interaction between the RGD and the integrin more efficient, possibly by the HSPG binding site on CVA9 binding to a cell surface molecule that is close to integrin  $\alpha_v\beta_6$ .

The blocking experiment using anti-integrin antibodies shows that the S2871R mutant is still blocked by the integrin  $\alpha_v\beta_6$ . This suggests that integrins are still needed for entry and that HSPG is not an alternative receptor. The other A549-adapting mutations, located at the 3-fold axis also do not seem to allow binding to an alternative receptor. The fact that binding is no longer dependent on calcium does though suggest that CVA9D and CVA9 P2023S can recognize another cell surface molecule. This interaction, like the one with HSPG, probably makes infection more efficient, and doesn't replace the need to interact with an integrin.

**Table 4.1 Summary of heparin blocked/non-blocked isolates.** Heparin blocked (grey) and non-blocked (green), CVA9 isolates and the amino acid differences (pink) probably giving the blocked phenotype.

Isolates	Mutations			
	VP3 59	VP1 132	VP1 287	VP1 286
CO75	Q	R	S	Q
CO79	Q	R	S	Q
CO87	Q	T	R	Q
CO87N	R	T	R	Q
CO87N1	R	T	R	Q
CO87N2	R	T	R	Q
CO87N3	R	T	R	Q
CO87N4	R	T	R	Q
CO87I	R	T	R	Q
CO87M1	R	T	R	Q
CO87M2	R	T	R	Q
CO62	Q	T	S	Q
CO62H	R	T	S	R
Griggs	Q	T	S	Q
GriggsN	Q	T	R	Q
GriggsS	Q	T	R	Q
GriggsS2871R*	Q	T	R	Q

\* Heparin-blocked viruses containing only the mutation highlighted. The GriggsS2871R mutant was engineered to contain only S2871R mutation.

```

Griggs      TDTRKDINTVTTVAQSRRRGGDMSTLNTH 867
GriggsN    TDTRKDINTVTTVAQRRRRGGDMSTLNTH 867
GriggsS    TDTRKDINTVTTVAQRRRRGGDMSTLNTH 867
CO87       TDTRKDINTVTTVAQRKRRGDLNTH 867
CO87N      TDTRKDINTVTTVAQRKRRGDLNTH 867
CO87I      TDTRKDINTVTTVAQRKRRGDLNTH 867
CO62       TDTRKDINTVTTIAQSRRRGGDMSTLNTH 867
CO62H      TDTRKDINTVTTIARSRRRGGDMSTLNTH 867
CO79       TDTRKDINTVTTIAQSGRRGDLNTH 867
CO85       TDTRKDINTVTTVAQSEHRGDLNTH 867
*****:*: :*:*: *

```

**Figure 4.27** The VP1 C-terminal sequences of the CVA9 isolates used in this thesis and the previous analysis of HSPG binding (McLeish *et al.*, 2012), together with heparin-blocked variants were aligned using ClustalW. Positions where all amino acid differences seen are highlighted in purple. The integrin binding RGD motif (highlighted in yellow) is observed in all CVA9 strains. Mutations in the variants are highlighted in red.

## **Chapter 5**

### **General Discussion and Future Work**

## 5.1 General Discussion

The purpose of this thesis was to understand coxsackievirus A9 (CVA9) and echovirus 11 (E11) cell tropism. This has been done by analyzing the infection of a panel of cell lines and flow cytometry analysis of one possible receptor, DAF. These viruses were then propagated on A549 cells, and in the case of E11, also on HeLa cells, and sequenced to reveal amino acid changes. These methods helped us to understand virus binding onto the cell surface and to determine if other possible mechanisms can be used on different cancer cell lines. A detailed understanding of virus infection and cell surface receptors will help to establish an efficient oncolytic virus cancer treatment based on these interactions.

Chapter 3 contains an analysis of how echovirus 11 (E11) can bind onto the cell surface and to determine if adapting this virus onto different cancer cell line can allow other possible mechanisms for binding. Several coxsackievirus A9 and echoviruses variants were tested in a panel of 8 cancer cell lines. Distinct patterns of infection were observed, but did not fully correlated with receptor expression, suggesting that other determinants also help to define tropism. To investigate this further, E11, (strain 7V-5A), was adapted by passaging on two cancer cell lines, A549 and HeLa, and mutations were observed after the 9 passage. Two mutations were seen in A549-adapted virus and these are both in regions most likely to be involved in DAF binding based on the structure of the DAF-binding footprint. These mutations are: VP2 position G145S in the SCR3 binding domains and VP3 position E59V in the SCR4 binding domain. It is not clear if these enhance or prevent DAF binding, but previous work suggests that adapting mutations selected by passaging in different cell lines can lead to a loss

of DAF binding (Stuart *et al.*, 2002b; Rezaikin *et al.*, 2009; Novoselov *et al.*, 2012). In HeLa-adapted virus, a single mutation was seen in VP4 position G16R. Mutations in VP4 have not previously been reported in adaptation experiments and so this observation is particularly interesting. The mutation may affect a later stage in cell entry, as it is known that VP4 is exposed after enteroviruses bind to receptors and that a VP4 mutant can bind to receptors but cannot enter the cell (Moscufo *et al.*, 1993).

Chapter 4 contains an analysis of the molecular basis of how heparin-blocked (and so assumed to be able to bind to HSPG) variants of coxsackievirus A9 (CVA9) bind onto the cell surface and to determine if there are other possible mechanisms can be used by adapting these viruses onto different cancer cell lines. To investigate CVA9 binding to HSPG, 3 isolates were propagated on A549 cells and heparin-blocked mutants were isolated. Although the isolates are diverse, the same mutation (VP3 Q59R) was seen in two isolates and probably gives a positively-charged cluster with adjacent amino acids. Other mutations were seen close to the RGD motif, where there is already a highly basic sequence. Together with a previous identification of a different mutation related to HSPG use, the results suggest multiple potential mechanisms for HSPG-binding (McLeish *et al.*, 2012). No clear differences in entry pathways were observed for CVA9 variants.

It is interesting that a mutation of the same amino acid (position 59 in VP3) is seen in E11 5V-7A adapted to A549 cells and CVA9 adapted on A549 cells followed by purification of a HSPG-binding variant. This may be coincidence, as VP3 position 59 is in a highly exposed part of the virus and likely to be able to

change without changing the structure of the particle significantly. The amino acid change in each case is different and in CVA9 HSPG binding results from the mutation, but this is not seen in E11 V5-7A. On the other hand this amino acid could be key to adapting different viruses to A549 cells. It would be interesting to adapt other viruses to A549 cells and compare the adapting mutations with those already seen.

## 5.2 Future Work

To extend the work already performed, several new experiments could be done.

- Haemagglutination assays of human red blood cells by E11 variants could be performed. Haemagglutination has been shown to be due to interaction of the virus with DAF and so this is a useful method of studying DAF binding. Blocking experiments with DAF antibodies could also be performed. These experiments should show whether the A549 variants still have the ability to bind to DAF or if it is made more efficient.
- The mutations observed could be built into an infectious E11 clone so that it is known that only these mutations are present and so are responsible for any changes in receptor interactions that are seen.
- Adapting E11 and CVA9 in different cancer cell lines to identify other possible mechanisms that can be used for cell tropism. Of particular interest is the adaptation of CVA9 to HeLa cells to find whether a VP4 change is also seen. The E11 VP4 change could be analysed further by seeing if this has an effect on the pore forming ability reported for VP4.

- Studying the entry pathways of these viruses and variants, to find if the alteration in receptor binding can allow the virus to enter cells by different mechanisms.

## References

Adams, M.J., King, A.M.Q. and Carstens, E.B. (2013). Ratification vote on taxonomic proposals to the International Committee on Taxonomy of Viruses (2013). *Archives of Virology*, **158**: 2023-2030.

Alberts, B., Johnson, A., Lewis, J., Raff, M., Roberts, K. and Walter, P. (2002). *Molecular Biology of the Cell*. 4<sup>th</sup> edition. New York: Garland Science.

Alexander, D. A., & Dimock, K. (2002). Sialic acid functions in enterovirus 70 binding and infection. *Journal of Virology*, **76**: 11265-11272.

Allen, M. D., Thomas, G. J., Clark, S., Dawoud, M. M., Vallath, S., Payne, S. J., Gomm, J. J., Dreger, S. A., Dickinson, S., Edwards, D. R., Pennington, C. J., Sestak, I., Cuzick, J., Marshall, J. F., Hart, I. R. and Jones, J. L. (2014). Altered microenvironment promotes progression of preinvasive breast cancer: myoepithelial expression of  $\alpha\beta 6$  integrin in DCIS identifies high-risk patients and predicts recurrence. *Clinical Cancer Research*, **20**: 344-357.

Artimo, P., Jonnalagedda, M., Arnold, K., Baratin, D., Csardi, G., de Castro, E., Duvaud, S., Flegel, V., Fortier, A., Gasteiger, E., Grosdidier, A., Hernandez, C., Ioannidis, V., Kuznetsov, D., Liechti, R., Moretti, S., Mostaguir, K., Redaschi, N., Rossier, G., Xenarios, I. and Stockinger, H. (2012). ExpPASy: SIB bioinformatics resource portal, *Nucleic Acids Research*, **40**: W597-W603.  
(<http://www.expasy.org/>)

Au, G. G., Lincz, L. F., Enno, A. and Shafren, D. R. (2007) Oncolytic Coxsackievirus A21 as a novel therapy for multiple myeloma. *British Journal of Haematology*, **137**: 133-141.

Bai, X., Bao, H., Li, P., Wei, W., Zhang, M., Sun, P., Cao, Y., Lu, Z., Fu, Y., Xie, B., Chen, Y., Li, D., Luo, J. and Liu, Z. (2014). Effects of two amino acid substitutions in the capsid proteins on the interaction of two cell-adapted PanAsia-1 strains of foot-and-mouth disease virus serotype O with heparan sulfate receptor. *Virology Journal*, **11**: 132.

Bandyopadhyay, A. and Raghavan, S. (2009). Defining the role of integrin  $\alpha\beta6$  in cancer. *Current Drug Targets*, **10**: 645-652.

Barth, H., Schnober, E. K., Zhang, F., Linhardt, R. J., Depla, E., Boson, B., Cosset, F., Patel, A. H., Blum, H. E. and Baumert, T. F. (2006) Viral and cellular determinants of the Hepatitis C Virus envelope-heparan sulfate interaction. *Journal of Virology*, **80**: 10579-10590.

Bergelson, J. M. (2010). Receptors, pp. 73-86 In Ehrenfeld, E., Domingo, E. and Roos, R. P., *The picornaviruses*. ASM Press, Washington, DC.

Bergelson, J. M., Chan, M., Solomon, K. R., John, N. F. ST., Lin, H. and Finberg R. W. (1994). Decay-accelerating factor (CD55), a glycosylphosphatidylinositol-anchored complement regulatory protein, is a receptor for several echoviruses. *Proceedings of the National Academy of Sciences*, **91**: 6245-6248.

Bergelson, J. M., Cunningham, J. A., Droguett, G., Kurt-Jones, E. A., Krithivas, A., Hong, J. S., Horwitz, M. S., Crowell, R. L. and Finberg, R. W. (1997). Isolation of a common receptor for Coxsackie B viruses and adenoviruses 2 and 5. *Science*, **275**: 1320-1323.

Berinstein, A., Roivainen, M., Hovi, T., Mason, P. W. and Baxt, B. (1995). Antibodies to the vitronectin receptor (integrin  $\alpha V\beta 3$ ) inhibit binding and infection of foot-and-mouth disease virus to cultured cells. *Journal of Virology*, **69**: 2664-2666.

Berry, L. J., Au, G. G., Berry, R. D. and Shafren, D. R. (2008) Potent oncolytic activity of human enteroviruses against human prostate cancer. *The Prostate*, **68**: 577-587.

Berryman, S., Clark, S., Kakker, N. K., Silk, R., Seago, J., Wadsworth, J., Chamberlain, K., Knowles, N. J. and Jackson, T. (2013). Positively charged residues at the five-fold symmetry axis of cell culture-adapted foot-and-mouth disease virus permit novel receptor interactions. *Journal of Virology*, **87**: 8735-8744.

Berryman, S., Clark, S., Monaghan, P. and Jackson, T. (2005). Early events in integrin  $\alpha\beta 6$ -mediated cell entry of foot-and-mouth disease virus. *Journal of Virology*, **79**: 8519-8534.

Bhella, D., Goodfellow, I.G., Roversi, P., Pettigrew, D., Chaudhry, Y., Evans, D.J., and Lea, S.M. (2004) The structure of echovirus type 12 bound to a two-domain fragment of its cellular attachment protein decay-accelerating factor (CD 55). *Journal of Biological Chemistry*, **279**: 8325-8332

Brooks, G. F., Carroll, K. C., Butel, J. S. and Morse, S. A. (2007). *Medical microbiology*. . 25<sup>th</sup> edition. United States, McGraw-Hill.

Byrnes, A. P. and Griffini, D. E. (1998) Binding of Sindbis Virus to cell surface heparan sulfate. *Journal of Virology*, **72**: 7349-7356.

Cancer Research UK (2012): [Cancer](http://www.cancerresearchuk.org/cancer-info/cancerstats/mortality/all-cancers-combined/#UK) in the UK report. Available from: <http://www.cancerresearchuk.org/cancer-info/cancerstats/mortality/all-cancers-combined/#UK> [Accessed: 6-4-2014].

Cann, A. J. (2009) *Principles of molecular virology*. 3<sup>th</sup> edition. UK, Academic Press, Elsevier.

Cann, A. J. (2011) *Principles of molecular virology*. 5<sup>th</sup> edition. UK, Academic Press, Elsevier.

Cardin, A. D. and Weintraub, H. J. (1989). Molecular modeling of protein-glycosaminoglycan interactions. *Arteriosclerosis, Thrombosis, and Vascular Biology*, **9**: 21-32.

Carter, J. and Saunders, V. (2007) *Virology: principles and applications*. UK, John Wiley & Sons.

Chang, K. H., Auvinen, P., Hyypiä, T. and Stanway, G. (1989). The nucleotide sequence of coxsackievirus A9; implications for receptor binding and enterovirus classification. *Journal of General Virology*, **70**: 3269-3280.

Chang, K. H., Day, C., Walker, J., Hyypiä, T. and Stanway, G. (1992). The nucleotide sequences of wild-type coxsackievirus A9 strains imply that an RGD motif in VP1 is functionally significant. *The Journal of General Virology*, **73**: 621-626.

Chen, L., Zhu, L., Zhou, Y. C., Xu, Z. W., Guo, W. Z. and Yang, W. Y. (2013). Molecular and phylogenetic analysis of the porcine kobuvirus VP1 region using infected pigs from Sichuan Province, China. *Virology Journal*, **10**: 281.

Chevaliez, S., Balanant, J., Maillard, P., Lone, Y. C., Lemonnier, F. A. and Delpeyroux, F. (2008). Role of class I human leukocyte antigen molecules in early steps of echovirus infection of rhabdomyosarcoma cells. *Virology*, **381**: 203-214.

Chevaliez, S., Szendrői, A., Caro, V., Balanant, J., Guillot, S., Berencsi, G. and Delpeyroux, F. (2004). Molecular comparison of echovirus 11 strains circulating in Europe during an epidemic of multisystem hemorrhagic disease of infants indicates that evolution generally occurs by recombination. *Virology*, **325**: 56-70.

Christianson, H. C. and Belting, M. (2014) Heparan sulfate proteoglycan as a cell-surface endocytosis receptor. *Matrix Biology*, **35**: 51-55.

Clarkson, N. A., Kaufman, R., Lublin, D. M., Ward, T., Pipkin, P. A., Minor, P. D., Evans, D. J. and Almond, J. W. (1995). Characterization of the echovirus 7 receptor: domains of CD55 critical for virus binding. *Journal of Virology*, **69**: 5497-5501.

Crooks, G. E., Hon, G., Chandonia, J. M. and Brenner, S. E. (2004). WebLogo: A sequence logo generator. *Genome Research*, **14**:1188-1190

Dalldorf, G. (1950). The Coxsackie Viruses\*. *American Journal of Public Health and the Nations Health*, **40**: 1508-1511.

Davis, M. P., Bottley, G., Beales, L. P., Killington, R. A., Rowlands, D. J. and Tuthill, T. J. (2008). Recombinant VP4 of human rhinovirus induces permeability in model membranes. *Journal of Virology*, **82**: 4169-4174.

DePalma, A. M., Vliegen, I., Clercq, E. D. and Neyts, J. (2008) Selective Inhibitors of Picornavirus Replication. *Medicinal Research Reviews*. **28**: 823-884.

Eager, R. M. and Nemunaitis, J. (2011) Clinical development directions in oncolytic viral therapy. *Cancer Gene Therapy*, **18**: 305-317.

Ehrenfeld, E., Domingo, E. and Roos, R. P. (2010) *The picornaviruses*. USA, ASM Press.

Escribano-Romero, E., Jimenez-Clavero, A. M., Gomes, P., Garcia-Ranea, J. A. and Ley, V. (2004) Heparan sulphate mediates swine vesicular disease virus attachment to the host cell. *Journal of General Virology*, **85**: 653-663.

Fernández-Miragall, O., Quinto, S. L. and Martínez-Salas, E. (2009) Relevance of RNA structure for the activity of Picornavirus IRES elements. *Virus Research*, **139**: 172-182.

Flint, S. J., Enquist, I. W., Racaniello, V. R. and Skalka, A. M. (2009) *Principle of Virology*: 3<sup>rd</sup> edition. USA, ASM Press.

Fry, E. E., Lea, S. M., Jackson, T., Newman, J. W., Ellard, F. M., Blakemore, W. E., Abu-Ghazaleh, R., Samuel, A., King, A. M. and Stuart, D. I. (1999). The structure and function of a foot-and-mouth disease virus–oligosaccharide receptor complex. *The EMBO Journal*, **18**: 543-554.

Goodfellow, I. G., Sioofy, A. B., Powell, R. M. and Evans, D. J. (2001). Echoviruses bind heparan sulfate at the cell surface. *Journal of Virology*, **75**: 4918-4921.

Goodman, S. L., Grote, H. J. and Wilm, C. (2012) Matched rabbit monoclonal antibodies against  $\alpha$ -series integrins reveal a novel  $\alpha\beta$ 3-LIBS epitope, and permit routine staining of archival paraffin samples of human tumors. *Biology Open*: 329-340.

Gullberg, M., Tolf, C., Jonsson, N., Polacek, C., Precechtelova, J., Badurova, M., Sojka, M., Mohlin, C., Israelsson, S., Johansson, K., Bopegamage, S., Hafenstein, S. and Lindberg, A. M. (2010). A single coxsackievirus B2 capsid residue controls cytolysis and apoptosis in rhabdomyosarcoma cells. *Journal of Virology*, **84**: 5868-5879.

Häcker, U., Nybakken, K., & Perrimon, N. (2005). Heparan sulphate proteoglycans: the sweet side of development. *Nature Reviews Molecular Cell Biology*, **6**: 530-541.

Harris, J. R. and Racaniello, V. R. (2005). Amino acid changes in proteins 2B and 3A mediate rhinovirus type 39 growth in mouse cells. *Journal of Virology*, **79**: 5363-5373.

Harvala, H., Kalimo, H., Bergelson, J., Stanway, G. and Hyypiä, T. (2005). Tissue tropism of recombinant coxsackieviruses in an adult mouse model. *Journal Of General Virology*, **86**: 1897-1907.

He, Y., Bowman, V. D., Mueller, S., Bator, C. M., Bella, J., Peng, X., Baker, T. S., Wimmer, E., Kuhn, R. J. and Rossmann, M. G. (2000). Interaction of the poliovirus receptor with poliovirus. *Proceedings of the National Academy of Sciences*, **97**: 79-84.

He, Y., Lin, F., Chipman, P. R., Bator, C. M., Baker, T. S., Shoham, M., Kuhn, R. J., Medof, M. E. and Rossmann, M. G. (2002). Structure of decay-accelerating factor bound to echovirus 7: a virus-receptor complex. *Proceedings of the National Academy of Sciences*, **99**: 10325-10329.

Heikkilä, O., Susi, P., Stanway, G. and Hyypiä, T. (2009). Integrin  $\alpha\beta 6$  is a high-affinity receptor for coxsackievirus A9. *Journal of General Virology*, **90**: 197-204.

Heikkilä, O., Susi, P., Tevaluoto, T., Härmä, H., Marjomäki, V., Hyypiä, T. and Kiljunen, S. (2010) Internalization of coxsackievirus A9 is mediated by  $\beta 2$ -microglobulin, dynamin, and arf6 but not by caveolin-1 or clathrin. *Journal of Virology*, **84**: 3666-3681.

Hendry, E., Hatanaka, H., Fry, E., Smyth, M., Tate, J., Stanway, G., Santti, J., Maaronen, M., Hyypiä, T. and Stuart, D. (1999). The crystal structure of coxsackievirus A9: new insights into the uncoating mechanisms of enteroviruses. *Structure*, **7**: 1527-1538.

Hughes, P. E., O'Toole, T. E., Yläne, J., Shattil, S. J. and Ginsberg, M. H. (1995). The conserved membrane-proximal region of an integrin cytoplasmic domain specifies ligand binding affinity. *Journal of Biological Chemistry*, **270**: 12411-12417.

Hughes, P. J. and Stanway, G. (2000). The 2A proteins of three diverse picornaviruses are related to each other and to H-rev107 family of proteins involved in the control of cell proliferation. *Journal of General Virology*, **81**: 201-207.

Hughes, P. J., Horsnell, C., Hyypiä, T. and Stanway, G. (1995). The coxsackievirus A9 RGD motif is not essential for virus viability. *Journal of Virology*, **69**: 8035-8040.

Huttunen, M., Waris, M., Kajander, R., Hyypiä, T. and Marjomäki, V. (2014). Coxsackievirus A9 infects cells via nonacidic multivesicular bodies. *Journal of Virology*, **88**: 5138-5151.

Hynes, R. O. (2002) Integrins: bidirectional, allosteric signaling machines. *Cell*, **110**: 673-687.

Israelsson, S., Gullberg, M., Jonsson, N., Roivainen, M., Edman, K. and Lindberg, A. M. (2010). Studies of Echovirus 5 interactions with the cell surface: heparan sulfate mediates attachment to the host cell. *Virus Research*, **151**: 170-176.

Jackson, T., Blakemore, W., Newman, J. W., Knowles, N. J., Mould, A. P., Humphries, M. J. and King, A. M. (2000b). Foot-and-mouth disease virus is a ligand for the high-affinity binding conformation of integrin  $\alpha 5\beta 1$ : influence of the leucine residue within the RGD motif on selectivity of integrin binding. *Journal of General Virology*, **81**: 1383-1391.

Jackson, T., Clark, S., Berryman, S., Burman, A., Cambier, S., Mu, D., Nishimura, S. and King, A. M. (2004). Integrin  $\alpha\beta 8$  functions as a receptor for foot-and-mouth disease virus: role of the  $\beta$ -chain cytodomain in integrin-mediated infection. *Journal of Virology*, **78**: 4533-4540.

Jackson, T., Ellard, F. M., Ghazaleh, R. A., Brookes, S. M., Blakemore, W. E., Corteyn, A. H., Stuart, D. I., Newman, J.W. and King, A. M. (1996). Efficient infection of cells in culture by type O foot-and-mouth disease virus requires binding to cell surface heparan sulfate. *Journal of Virology*, **70**: 5282-5287.

Jackson, T., King, A. M., Stuart, D. I. and Fry, E. (2003). Structure and receptor binding. *Virus Research*, **91**: 33-46.

Jackson, T., Mould, A. P., Sheppard, D. and King, A. M. (2002). Integrin  $\alpha\beta 1$  is a receptor for foot-and-mouth disease virus. *Journal of Virology*, **76**: 935-941.

Jackson, T., Sheppard, D., Denyer, M., Blakemore, W. and King, A. M. (2000a). The epithelial integrin  $\alpha\beta 6$  is a receptor for foot-and-mouth disease virus. *Journal of Virology*, **74**: 4949-4956.

James, D. G. (1952). The Coxsackie Viruses. *Postgraduate Medical Journal*, **28**: 637.

Jimenez-Clavero, M. A., Escribano-Romero, E., Ley, V. and Spiller, O. B. (2005). More recent swine vesicular disease virus isolates retain binding to coxsackie-adenovirus receptor, but have lost the ability to bind human decay-accelerating factor (CD55). *Journal of General Virology*, **86**: 1369-1377.

Jones, D. T., Taylor, W. R. and Thornton, J. M. (1992). The rapid generation of mutation data matrices from protein sequences. *Computer Applications in the Biosciences*, **8**: 275-282.

Kelly, E. and Russell, S. J. (2007) History of oncolytic viruses: genesis to genetic engineering. *Molecular Therapy*, **15**: 651-659.

Khan, A. G., Pichler, J., Rosemann, A. and Blaas, D. (2007). Human rhinovirus type 54 infection via heparan sulfate is less efficient and strictly dependent on low endosomal pH. *Journal of Virology*, **81**: 4625-4632.

King, A. M., Adams, M. J., & Lefkowitz, E. J. (Eds.). (2012). *Virus taxonomy: ninth report of the International Committee on Taxonomy of Viruses* (Vol. 9). USA, Academic Press, Elsevier.

King, R. J. B. and Robins, M. W. (2006) *Cancer biology*. 3<sup>rd</sup> edition. England. Pearson Education.

Knappe, M., Bodevin, S., Selinka, H. C., Spillmann, D., Streeck, R. E., Chen, X. S., Lindahl, U. and Sapp, M. (2007). Surface-exposed amino acid residues of HPV16 L1 protein mediating interaction with cell surface heparan sulfate. *Journal of Biological Chemistry*, **282**: 27913-27922.

Knowles, N. (2014). ICTV study group proposal: Creation of a new species (*Sicinivirus A*) in a new genus (*Sicinivirus*). 2014.018a-dV: (<http://www.ictvonline.org/proposals/2014.018a-dV.A.v3.Sicinivirus.pdf>)

[Accessed 31-3-2015].

Knowles, N.J., Hovi, T., Hyypiä, T., King, A.M.Q., Lindberg, A.M., Pallansch, M.A., Palmenberg, A.C., Simmonds, P., Skern, T., Stanway, G., Yamashita, T. and Zell, R. (2012). *Picornaviridae*. In: *Virus Taxonomy: Classification and Nomenclature of Viruses: Ninth Report of the International Committee on Taxonomy of Viruses*. Ed: King, A.M.Q., Adams, M.J., Carstens, E.B. and Lefkowitz, E.J. San Diego: Elsevier, pp. 855-880. [www.picornaviridae.com](http://www.picornaviridae.com) [Accessed: 28-02-2015]

Koretz, K., Brüderlein, S., Henne, C. and Möller, P. (1992). Decay-accelerating factor (DAF, CD55) in normal colorectal mucosa, adenomas and carcinomas. *British Journal Of Cancer*, **66**: 810-814.

La Monica, N. and Racaniello, V. R. (1989). Differences in replication of attenuated and neurovirulent polioviruses in human neuroblastoma cell line SH-SY5Y. *Journal of Virology*, **63**: 2357-2360.

Larkin, M. A., Blackshields, G., Brown, N. P., Chenna, R., McGettigan, P. A., McWilliam, H., Valentin, F., Wallace, I. M., Wilm, A., Lopez, R., Thompson, J. D., Gibson, T. J. and Higgins, D. G. (2007). ClustalW and ClustalX version 2. *Bioinformatics*, **23**: 2947-2948. (<http://www.ebi.ac.uk/Tools/msa/clustalw2/>)

Lim, H., Mulhaupt, H., & Couchman, J. R. (2015). Cell surface heparan sulfate proteoglycans control adhesion and invasion of breast carcinoma cells. *Molecular Cancer*, **14**: 15.

Lin, J. Y. and Shih, S. R. (2014) Cell and tissue tropism of enterovirus 71 and other enteroviruses infections. *Journal of Biomedical Science*, **21**: 18.

Lin, J., Chen, T., Weng, K., Chang, S., Chen, L. and Shih, S. (2009). Viral and host proteins involved in picornavirus life cycle. *Journal of Biomedical Science*, **16**:103.

Liu, J., Dong, W., Quan, X., Ma, C., Qin, C. and Zhang, L. (2012). Transgenic expression of human P-selectin glycoprotein ligand-1 is not sufficient for enterovirus 71 infection in mice. *Archives of Virology*, **157**: 539-543.

Liu, Y. and Rossmann, M. G. (2014). The cellular receptor for enterovirus 71. *Protein & Cell*, **5**: 655-657.

Liu, Z., Liu, H., Ma, T., Sun, X., Shi, J., Jia, B., Sun, Y., Zhan, J., Zhang, H., Zhu, Z. and Wang, F. (2014). Integrin  $\alpha\beta 6$ -Targeted SPECT Imaging for Pancreatic Cancer Detection. *Journal of Nuclear Medicine*, **55**: 989-994.

Loberg, R. D., Wojno, K. J., Day, L. L. and Pienta, K. J. (2005). Analysis of membrane-bound complement regulatory proteins in prostate cancer. *Urology*, **66**: 1321-1326.

Lukashev, A. N., Lashkevich, V. A., Koroleva, G. A., Ilonen, J. and Hinkkanen, A. E. (2004). Recombination in uveitis-causing enterovirus strains. *Journal of General Virology*, **85**: 463-470.

Maree, F. F., Blignaut, B., Aschenbrenner, L., Burrage, T. and Rieder, E. (2011). Analysis of SAT1 type foot-and-mouth disease virus capsid proteins: influence of receptor usage on the properties of virus particles. *Virus Research*, **155**: 462-472.

Maree, F. F., Blignaut, B., De Beer, T. A., Visser, N. and Rieder, E. A. (2010). Mapping of amino acid residues responsible for adhesion of cell culture-adapted foot-and-mouth disease SAT type viruses. *Virus Research*, **153**: 82-91.

Marlovits, T. C., Zechmeister, T., Gruenberger, M., Ronacher, B., Schwihla, H. and Blaas, D. (1998). Recombinant soluble low density lipoprotein receptor fragment inhibits minor group rhinovirus infection in vitro. *The FASEB Journal*, **12**: 695-703.

Martinez-Salas, E. (2008) The impact of RNA structure on Picornavirus IRES activity. *Trends in Microbiology*, **16**: 230-237.

Matrosovich, M., Herrler, G. and Klenk, H. D. (2013). Sialic Acid Receptors of Viruses. *Topics in Current Chemistry*, 1-28.

McLeish, N. J. (2010) Interaction of enteroviruses and parechoviruses with heparan sulfate and the effects of enterovirus infection on cellular proteins. PhD Thesis. University of Essex, UK

McLeish, N. J., Williams, Ç. H., Kaloudas, D., Roivainen, M. M. and Stanway, G. (2012). Symmetry-related clustering of positive charges is a common mechanism for heparan sulfate binding in enteroviruses. *Journal of Virology*, **86**: 11163-11170.

Meerani, S. and Yao, Y. (2010) Oncolytic viruses in cancer therapy. *European Journal of Scientific Research*, **40**: 156 -171.

Mercer, J. and Helenius, A. (2009). Virus entry by macropinocytosis. *Nature Cell Biology*, **11**: 510-520.

Mercer, J., Schelhaas, M. and Helenius, A. (2010) Virus entry by endocytosis. *Annual Review of Biochemistry*, **79**: 803-33.

Merilahti, P., Koskinen, S., Heikkilä, O., Karelehto, E. and Susi, P. (2012) Endocytosis of integrin-binding human picornaviruses. *Advances in Virology*, 2012.

Minor, P. D. (1996). Poliovirus biology. *Structure*, **4**: 775-778.

Moscufo, N., Yafal, A. G., Rogove, A., Hogle, J. and Chow, M. (1993). A mutation in VP4 defines a new step in the late stages of cell entry by poliovirus. *Journal of Virology*, **67**:5075-5078.

Mullen, J. T. and Tanabe, K. K. (2002) Viral oncolysis. *The Oncologist*, **7**: 106-119.

Murphy, A. M., Besmer, D. M., Moerdyk-Schauwecker, M., Moestl, N., Ornelles, D. A., Mukherjee, P. and Grdzlishvili, V. Z. (2012) Vesicular Stomatitis Virus as an oncolytic agent against pancreatic ductal adenocarcinoma. *Journal of Virology*, **86**: 3073-3087.

Nagy, P. D. and Pogany, J. (2012). The dependence of viral RNA replication on co-opted host factors. *Nature Reviews Microbiology*, **10**: 137-149.

Nakhaei<sup>1</sup>, P., Paz, S., Oliere, S., Tumilasci, V., Bell, J. C. and Hiscott, J. (2005) Oncolytic virotherapy of cancer with vesicular stomatitis virus. *Gene Therapy and Molecular Biology*, **9**: 269-280.

Nasu, J., Mizuno, M., Uesu, T., Takeuchi, K., Inaba, T., Ohya, S., Kawada, M., Shimo, K., Okada, H., Fujita, T. and Tsuji, T. (1998). Cytokine-stimulated release of decay-accelerating factor (DAF; CD55) from HT-29 human intestinal epithelial cells. *Clinical and Experimental Immunology*, **113**: 379-385.

Nelsen-Salz, B., Eggers, H. J. and Zimmermann, H. (1999). Integrin  $\alpha\text{v}\beta\text{3}$  (vitronectin receptor) is a candidate receptor for the virulent echovirus 9 strain Barty. *Journal of General Virology*, **80**: 2311-2313.

Newcombe, N. G., Beagley, L. G., Christiansen, D., Loveland, B. E., Johansson, E. S., Beagley, K. W. Barry, R. D. and Shafren, D. R. (2004). Novel role for decay-accelerating factor in coxsackievirus A21-mediated cell infectivity. *Journal of Virology*, **78**: 12677-12682.

Novoselov, A. V., Rezaykin, A. V., Sergeev, A. G., Fadeyev, F.A., Grigoryeva, J. V. and Sokolova, Z. I. (2012) A single amino acid substitution controls DAF-dependent phenotype of echovirus 11 in rhabdomyosarcoma cells. *Virus Research*, **166**: 87-96.

Núñez, J. I., Baranowski, E., Molina, N., Ruiz-Jarabo, C. M., Sánchez, C., Domingo, E. and Sobrino, F. (2001). A single amino acid substitution in nonstructural protein 3A can mediate adaptation of foot-and-mouth disease virus to the guinea pig. *Journal of Virology*, **75**: 3977-3983.

Olson, N. H., Kolatkar, P. R., Oliveira, M. A., Cheng, R. H., Greve, J. M., McClelland, A., Baker, T. S. and Rossmann, M. G. (1993). Structure of a human rhinovirus complexed with its receptor molecule. *Proceedings of the National Academy of Sciences of the United States of America*, **90**: 507-511.

Palmenberg, A., Neubauer, D. and Skern, T. (2010). Genome organization and encoded proteins, pp. 3-17 In Ehrenfeld, E., Domingo, E. and Roos, R. P., *The picornaviruses*. ASM Press, Washington, DC.

Panjwani, A., Strauss, M., Gold, S., Wenham, H., Jackson, T., Chou, J. J., Rowlands, D. J., Stonehouse, N. J., Hogle, J. M. and Tuthill, T. J. (2014). Capsid protein VP4 of human rhinovirus induces membrane permeability by the formation of a size-selective multimeric pore. *PLoS Pathogens*, **10**: e1004294.

Pasch, A., Küpper, J. H., Wolde, A., Kandolf, R. and Selinka, H. C. (1999). Comparative analysis of virus–host cell interactions of haemagglutinating and non-haemagglutinating strains of coxsackievirus B3. *Journal of General Virology*, **80**: 3153-3158.

Patel, M. R. and Kratzke, R. A. (2013) Oncolytic virus therapy for cancer: the first wave of translational clinical trials. *Translational Research*, **161**: 355-364.

Pathak, H. B., Arnold, J. J., Wiegand, P. N., Hargittai, M. R. S. and Cameron, C. E. (2007) Picornavirus genome replication: assembly and organization of the VPg uridylylation ribonucleicprotein (initiation) complex. *Journal of Biological Chemistry*, **282**: 16202-16213.

Plevka, P., Hafenstein, S., Harris, K. G., Cifuentes, J. O., Zhang, Y., Bowman, V. D., Chinman, P. R., Bator, C. M., Lin, F., Medof, M. E. and Rossmann, M. G. (2010). Interaction of decay-accelerating factor with echovirus 7. *Journal of Virology*, **84**: 12665-12674.

Porter, A. G. (1993) Minireview: Picornavirus nonstructural proteins: emerging roles in virus replication and inhibition of host cell functions. *Journal of Virology*, **67**: 6917-6921.

Powell, R. M., Schmitt, V., Ward, T., Goodfellow, I., Evans, D. J. and Almond, J. W. (1998). Characterization of echoviruses that bind decay accelerating factor (CD55): evidence that some haemagglutinating strains use more than one cellular receptor. *Journal of General Virology*, **79**: 1707-1713.

Qiagen (2006). QIAquick Spin Handbook For QIAquick PCR Purification Kit, QIAquick Nucleotide Removal Kit, QIAquick Gel Extraction Kit. Qiagen.

Qiagen (2010). QIAamp Viral RNA Mini Handbook for Purification of Viral RNA from Plasma serum, Cell-free Body Fluids, Cell-culture Supernatants. Qiagen.

Racaniello, V. R. (1996). Early events in poliovirus infection: virus-receptor interactions. *Proceedings of the National Academy of Sciences*, **93**: 11378-11381.

Ramsingh, A. I. and Collins, D. N. (1995). A point mutation in the VP4 coding sequence of coxsackievirus B4 influences virulence. *Journal of Virology*, **69**: 7278-7281.

Reddi, H. V., & Lipton, H. L. (2002). Heparan Sulfate Mediates Infection of High-Neurovirulence Theiler's Viruses. *Journal of Virology*, **76**: 8400-8407.

Reddy, P. S., Burroughs, K. D., Hales, L. M., Ganesh, S., Jones, B. H., Idamakanti, N., Hay, C., Li, S. S., Skele, K. L., Vasko, A. J., Yang, J., Watkins, D. N., Rudin, C. M. and Hallenbeck, P. L. (2007) Seneca Valley virus, a systemically

deliverable oncolytic picornavirus, and the treatment of neuroendocrine cancers. *Journal of the National Cancer Institute*, **99**: 1623-1633.

Reijmers, R. M., Spaargaren, M., & Pals, S. T. (2013). Heparan sulfate proteoglycans in the control of B cell development and the pathogenesis of multiple myeloma. *FEBS Journal*, **280**: 2180-2193.

Ren, R., and Racaniello, V. R. (1992). Human poliovirus receptor gene expression and poliovirus tissue tropism in transgenic mice. *Journal of Virology*, **66**: 296-304.

Rezaikin, A. V., Novoselov, A. V., Sergeev, A. G., Fadeyev, F. A. and Lebedev, S. V. (2009) Two clusters of mutations map distinct receptor-binding sites of echovirus 11 for the decay-accelerating factor (CD55) and for canyon-binding receptors. *Virus Research*, **145**: 74-79.

Rossmann, M. G., Arnold, E., Erickson, J. W., Frankenberger, E. A., Griffith, J. P., Hecht, H. J., Johnson J. E. and Mosser, A. G. (1985). Structure of a human common cold virus and functional relationship to other picornaviruses. *Nature*, **317**: 145-153

Rossmann, M. G., He, Y. and Kuhn, R. J. (2002). Picornavirus–receptor interactions. *Trends in Microbiology*, **10**: 324-331.

Rowlands, D. (2010). Picornaviruses. In: eLS. John Wiley & Sons Ltd, Chichester. <http://www.els.net/WileyCDA/ElsArticle/refId-a0001080.html> [Accessed: 3-3-2015].

Sarrazin, S., Lamanna, W. C. and Esko, J. D. (2011). Heparan sulfate proteoglycans. *Cold Spring Harbor Perspectives in Biology*, **3**: a004952.

Schneider-Schaulies, J. (2000). Cellular receptors for viruses: links to tropism and pathogenesis. *Journal of General Virology*, **81**: 1413-1429.

Schneider, T. D. and Stephens, R. M. (1990). Sequence Logos: A New Way to Display Consensus Sequences. *Nucleic Acids Research*, **18**: 6097-6100

Seitsonen, J., Susi, P., Heikkilä, O., Sinkovits, R. S., Laurinmäki, P., Hyypiä, T. and Butcher, S. J. (2010). Interaction of  $\alpha V\beta 3$  and  $\alpha V\beta 6$  integrins with human parechovirus 1. *Journal of Virology*, **84**: 8509-8519.

Semler, B. L. and Wimmer, E., (2002) *Molecular biology of picornavirus*. 1<sup>st</sup> edition. USA. ASM Press.

Shafren, D. R., Au, G. G., Nguyen, T., Newcombe, N. G., Haley, E. S., Beagley, L., Johansson, E. S., Hersey, P. and Barry, R. D. (2004) Systemic therapy of malignant human melanoma tumors by a common cold-producing Enterovirus, Coxsackievirus A21. *Clinical Cancer Research*, **10**: 53-60.

Shafren, D. R., Dorahy, D. J., Thorne, R. F., Kinoshita, T., Barry, R. D. and Burns, G. F. (1998) Antibody binding to individual short consensus repeats of decay-accelerating factor enhances Enterovirus Cell Attachment And Infectivity. *The Journal of Immunology*, **160**: 2318-2323.

Shafren, D. R., Sylvester, D., Johansson, E. S., Campbell, I. G. and Barry, R. D. (2005) Oncolysis of human ovarian cancers by Echovirus Type 1. *International Journal of Cancer*, **115**: 320-328.

Shakeel, S., Seitsonen, J. J., Kajander, T., Laurinmäki, P., Hyypiä, T., Susi, P. and Butcher, S. J. (2013). Structural and functional analysis of coxsackievirus A9 integrin  $\alpha\beta 6$  binding and uncoating. *Journal of Virology*, **87**: 3943-3951.

Shen, M., Reitman, Z. J., Zhao, Y., Moustafa, I., Wang, Q., Arnold, J. J., Pathak, H. B. and Cameron, C. E. (2008) Picornavirus genome replication: identification of the surface of the poliovirus (PV) 3C dimer that interacts with PV 3Dpol during VPg uridylylation and construction of a structural model for the PV 3C2-3Dpol complex. *Journal of Biological Chemistry*, **283**: 875-888.

Shieh, M. T., WuDunn, D., Montgomery, R. I., Esko, J. D. and Spear, P. G. (1992). Cell surface receptors for herpes simplex virus are heparan sulfate proteoglycans. *The Journal of Cell Biology*, **116**: 1273-1281.

Sieczkarski, S. B. and Whittaker, G. R. (2002) Dissecting virus entry via endocytosis. *The Journal of General Virology*, **83**: 1535-1545.

Smyth, M. S., & Martin, J. H. (2002). Picornavirus uncoating. *Molecular Pathology*, **55**: 214.

Smyth, M., Pettitt, T., Symonds, A. and Martin, J. (2003). Identification of the pocket factors in a picornavirus. *Archives of Virology*, **148**: 1225-1233.

Sobo, K., Rubbia-Brandt, L., Brown, T. D. K., Stuart, A. D. and McKee, T. A. (2011). Decay-accelerating factor binding determines the entry route of echovirus 11 in polarized epithelial cells. *Journal of Virology*, **85**: 12376-12386.

Solomon, T., Lewthwaite, P., Perera, D., Cardoso, M. J., McMinn, P. and Ooi, M. H. (2010). Virology, epidemiology, pathogenesis, and control of enterovirus 71. *The Lancet Infectious Diseases*, **10**: 778-790.

Stanway, G. (1990). Structure, function and evolution of picornaviruses. *Journal of General Virology*, **71**: 2483-2501.

Stanway, G. (2013). Molecular Biology and Classification of Enteroviruses, pp. 109-115 In Taylor, K. W., Hyöty, H., Toniolo, A. and Zuckerman, A. J., *Diabetes and Viruses*, Springer, New York.

Stanway, G. and Hyypia, T. (1999) Minireview: Parechoviruses. *Journal of Virology*, **73**: 5249-5254.

Ströh, L. J. and Stehle, T. (2014). Glycan engagement by viruses: receptor switches and specificity. *Annual Review of Virology*, **1**: 285-306.

Stuart, A. D., Eustace, H. E., McKee, T. A. and Brown, T. D. K. (2002a). A novel cell entry pathway for a DAF-using human enterovirus is dependent on lipid rafts. *Journal of Virology*, **76**: 9307-9322.

Stuart, A. D., McKee, T. A., Williams, P. A., Harley, C., Shen, S., Stuart, D. I., Brown, T. D. K. and Lea, S. M. (2002b) Determination of the structure of a decay accelerating factor-binding clinical isolate of echovirus 11 allows mapping of mutants with altered receptor requirements for infection. *Journal of Virology*, **76**: 7694-7704.

Svitkin, Y. V., Pestova, T. V., Maslova, S. V. and Agol, V. I. (1988). Point mutations modify the response of poliovirus RNA to a translation initiation factor: a comparison of neurovirulent and attenuated strains. *Virology*, **166**: 394-404.

Takada, Y., Ye, X. and Simon, S. (2007). The integrins. *Genome Biology*, **8**: 215.

Tamura, K., Stecher, G., Peterson, D., Filipski, A. and Kumar, S. (2013). MEGA6: Molecular Evolutionary Genetics Analysis version 6.0. *Molecular Biology and Evolution*, **30**: 2725-2729.

Tan, C. W., Poh, C. L., Sam, I. C. and Chan, Y. F. (2013). Enterovirus 71 uses cell surface heparan sulfate glycosaminoglycan as an attachment receptor. *Journal of Virology*, **87**: 611-620.

Toyoda, H., Yin, J., Mueller, S., Wimmer, E. And Cello, J. (2007) Oncolytic treatment and cure of neuroblastoma by a novel attenuated Poliovirus in a novel poliovirus-susceptible animal model. *Cancer Research*, **67**: 2857-2864.

Triantafyllou, K., Fradelizi, D., Wilson, K. and Triantafyllou, M. (2002). GRP78, a Coreceptor for Coxsackievirus A9, Interacts with Major Histocompatibility Complex Class I Molecules Which Mediate Virus Internalization. *Journal of Virology*, **76**: 633-643.

Tuthill, T. J., Gropelli, E., Hogle, J. M. and Rowlands, D. J. (2010). Picornaviruses. *Current Topics in Microbiology and Immunology*, **343**: 43-89.

Uncapher, C. R., Dewitt, C. M. and Colonno, R. J. (1991). The major and minor group receptor families contain all but one human rhinovirus serotype. *Virology*, **180**: 814-817.

Vlasak, M., Goesler, I. and Blaas, D. (2005). Human rhinovirus type 89 variants use heparan sulfate proteoglycan for cell attachment. *Journal of Virology*, **79**: 5963-5970.

Vuorinen, T., Vainionpaa, R., Heino, J. and Hyypia, T. (1999) Enterovirus receptors and virus replication in human leukocytes. *Journal of General Virology*, **80**: 921-927.

Wang, E. S., Dobrikova, E., Goetz, C., Dufresne, A. T. and Gromeier, M. (2011) Adaptation of an ICAM-1-tropic enterovirus to the mouse respiratory tract. *Journal of Virology*, **85**: 5606-5617.

Wang, X., Peng, W., Ren, J., Hu, Z., Xu, J., Lou, Z., Li, X., Yin, W., Shen, X., Porta, C., Walter, T. S., Evans, G., Axford, D., Owen, R., Rowlands, D. J., Wang, J., Stuart, D. I., Fry, E. E. and Rao, Z. (2012). A sensor-adaptor mechanism for enterovirus uncoating from structures of EV71. *Nature Structural & Molecular Biology*, **19**: 424-429.

Wang, Y. F. and Yu, C. K. (2014). Animal models of enterovirus 71 infection: applications and limitations. *Journal of Biomedical Science*, **21**: 31-41.

Wanger, E. K., Hewlett, M. J., Bloom, D. C. and Camerini, D. (2008) Basic Virology. 3rd edition. UK. Blackwell Publishing.

Ward, T., Pipkin, P. A., Clarkson, N. A., Stone, D. M., Minor, P. D. and Almond, J. W. (1994). Decay-accelerating factor CD55 is identified as the receptor for echovirus 7 using CELICS, a rapid immuno-focal cloning method. The *EMBO Journal*, **13**: 5070-5074.

Ward, T., Powell, R. M., Pipkin, P. A., Evans, D. J., Minor, P. D. and Almond, J. W. (1998). Role for  $\beta$ 2-microglobulin in echovirus infection of rhabdomyosarcoma cells. *Journal of Virology*, **72**: 5360-5365.

Whitton, J. L., Cornell, C. T. and Feuer, R. (2005) Host and virus determinants of picornavirus pathogenesis and tropism. *Nature Reviews Microbiology*, **3**: 765-776

Williams, C. H. (2002) Mutagenesis and virus blocking studies on virus-receptor interactions of Coxsackievirus A9. PhD Thesis. University of Essex, UK

Williams, C. H., Kajander, T., Hyypiä, T., Jackson, T., Sheppard, D. and Stanway, G. (2004). Integrin  $\alpha\beta$ 6 is an RGD-dependent receptor for coxsackievirus A9. *Journal of Virology*, **78**: 6967-6873.

Williams, C. H., Xeniou, O. and Stanway, G. Cell tropism determinants of Coxsackievirus A9 (unpublished).

Woo, P. C., Lau, S. K., Choi, G. K., Huang, Y., Teng, J. L., Tsoi, H. W., Tse, H., Yeung, M. L., Chan, K. H., Jin, D. Y. and Yuen, K. Y. (2012). Natural occurrence and characterization of two internal ribosome entry site elements in a novel virus, canine picodicrovirus, in the picornavirus-like superfamily. *Journal of Virology*, **86**: 2797-2808

Xiao, C., Bator, C. M., Bowman, V. D., Rieder, E., He, Y., Hébert, B., Bella, J., Baker, T. S., Wimmer, E., Kuhn, R. J. and Rossmann, M. G. (2001). Interaction of coxsackievirus A21 with its cellular receptor, ICAM-1. *Journal of Virology*, **75**: 2444-2451.

Xing, L., Huhtala, M., Pietiäinen, V., Käpylä, J., Vuorinen, K., Marjomäki, V., Heino, J., Johnson, M. S., Hyypiä, T. and Cheng, R. H. (2004). Structural and functional analysis of integrin  $\alpha 2$ I domain interaction with echovirus 1. *Journal of Biological Chemistry*, **279**: 11632-11638.

Yamashita, T., Sakae, K., Tsuzuki, H., Suzuki, Y., Ishikawa, N., Takeda, N., Miyamura, T. and Yamazaki, S. (1998). Complete Nucleotide Sequence and Genetic Organization of Aichi Virus, a Distinct Member of the Picornaviridae Associated with Acute Gastroenteritis in Humans. *Journal of Virology*, **72**: 8408-8412.

Yamayoshi, S., Ohka, S., Fujii, K. and Koike, S. (2013). Functional comparison of SCARB2 and PSGL1 as receptors for enterovirus 71. *Journal of Virology*, **87**: 3335-3347.

Yang, B., Chuang, H. and Yang, K. D. (2009). Sialylated glycans as receptor and inhibitor of enterovirus 71 infection to DLD-1 intestinal cells. *Virology Journal*, **6**: 141.

Ylipaasto, P., Eskelinen, M., Salmela, K., Hovi, T. and Roivainen, M. (2010). Vitronectin receptors,  $\alpha v$  integrins, are recognized by several non-RGD-containing echoviruses in a continuous laboratory cell line and also in primary human Langerhans' islets and endothelial cells. *Journal of General Virology*, **91**: 155-165.

Yoder, J. D., Cifuentes, J. O., Pan, J., Bergelson, J. M. and Hafenstein, S. (2012). The crystal structure of a coxsackievirus B3-RD variant and a refined 9-angstrom cryo-electron microscopy reconstruction of the virus complexed with decay-

accelerating factor (DAF) provide a new footprint of DAF on the virus surface. *Journal of Virology*, **86**: 12571-12581.

Zaini, Z., Phuektes, P. and McMinn, P. (2012) Mouse adaptation of a sub-genogroup B5 strain of human enterovirus 71 is associated with a novel lysine to glutamic acid substitution at position 244 in protein VP1. *Virus Research*, **167**: 86-96.

Zautner, A. E., Jahn, B., Hammerschmidt, E., Wutzler, P. and Schmidtke, M. (2006). N- and 6-O-sulfated heparan sulfates mediate internalization of coxsackievirus B3 variant PD into CHO-K1 cells. *Journal of Virology*, **80**: 6629-6636.

Zhu, W., Li, J. and Liang, G. (2011). How does cellular heparan sulfate function in viral pathogenicity?. *Biomedical and Environmental Sciences*, **24**: 81-87.

Zocher, G., Mistry, N., Frank, M., Hähnlein-Schick, I., Ekström, J. O., Arnberg, N. and Stehle, T. (2014). A sialic acid binding site in a human picornavirus. *PLoS Pathogens*, **10**: e1004401.

## **Appendices**





```

111/RD_2009 CNASKFHQGCLMVVCPPEAEMGCSQIDGTVNEHSLSEGETAKKFAATSTNGTNTVQSI VT 240
MorM-82_1982 CNASKFHQGCLLVVCPPEAEMGCSQIDGTVNEHSLSEGETAKKFAATSSNGQNVQSI VT 240
Gregory_1993 CNASKFHQGCLLVVCPPEAEMGCSQIDGTVNEHSLSEGETAKKFAATSTNGTNTVQSI VT 240
E11/7611_1993 CNASKFHQGCLMVVCPPEAEMGCSQIDGTVNEHSLSEGETAKKFAATSTNETNTVQSI VT 240
111/L41-431-1_2011 CNASKFHQGCLMVVCPPEAEMGCSQIDGTVNEHSLSEGETAKKFAATSTNGTNTVQSI VT 240
111/L41-431-6_2011 CNASKFHQGCLMVVCPPEAEMGCSQIDGTVNEHSLSEGETAKKFAATSTNGTNAVQSI VT 240
111/L41_2011 CNASKFHQGCLMVVCPPEAEMGCSQIDGTVNEHSLSEGETAKKFAATSTNGTNAVQSI VT 240
111/BGM_2009 CNASKFHQGCLMVVCPPEAEMGCSQIDGTVNEHSLSEGETAKKFAATSTNGTNTVQSI VT 240
111/Hep_2009 CNASKFHQGCLMVVCPPEAEMGCSQIDGTVNEHSLSEGETAKKFAATSTNGTNTVQSI VT 240
111/L41-431_2011 CNASKFHQGCLMVVCPPEAEMGCSQIDGTVNEHSLSEGETAKKFAATSTNGTNAVQSI VT 240
111/L41-311_2011 CNASKFHQGCLMVVCPPEAEMGCSQIDGTVNEHSLSEGETAKKFAATSTNGTNAVQSI VT 240
Gregory_1953 CNASKFHQGCLLVVCPPEAEMGCSQIDGTVNEHSLSEGETAKKFAATSTNGTNTVQTI VT 240
111/L41-211_2011 CNASKFHQGCLMVVCPPEAEMGCSQIDGTVNEHSLSEGETAKKFAATSTNGTNAVQSI VT 240
3123_2009 CNASKFHQGCLLVVCPPEAEMGCSQIDGTVNEHSLSEGETAKKFAATSTNGTNTVQTI VT 240
3123/70_2009 CNASKFHQGCLLVVCPPEAEMGCSQIDGTVNEHSLSEGETAKKFAATSTNGTNTVQTI VT 240
111/L41-121_2011 CNASKFHQGCLMVVCPPEAEMGCSQIDGTVNEHSLSEGETAKKFAATSTNGTNAVQSI VT 240
3123/28_2009 CNASKFHQGCLLVVCPPEAEMGCSQIDGTVNEHSLSEGETAKKFAATSTNGTNAVQTI VT 240
M07067754_2007 CNASKFHQGCLLVVCPPEAEMGCSQIDGTMNEHSLSEGETAKKFTNTPTNAANTVQSI VT 240
*****:*****. : **.:***** *: * : * : *::**

```

```

-----<
B2 --αB3--- =βF== =βG== =====βH=====
E11 V5-7A_2005 NAGMGVGVGNLTIFPHQWINLRTNNSATIVMPYINSVPMDNMFRRHNF T LMI I PFVSLDY 300
ROU-91_1991 NAGMGVGVGNLTIFPHQWINLRTNNSATIVMPYINSVPMDNMFRRHNF T LMI I PFVSLDY 300
D207_2008 NAGMGVGVGNLTIFPHQWINLRTNNSATIVMPYINSVPMDNMFRRHNF T LMI I PFVSLDY 300
Hun/90_1990 NAGMGVGVGNLTIFPHQWINLRTNNSATIVMPYINSVPMDNMFRRHNF T LMI I PFVSLDY 300
HUN-1108_1989 NAGMGVGVGNLTIFPHQWINLRTNNSATIVMPYINSVPMDNMFRRHNF T LMI I PFVSLDY 300
Kust-86_1986 NAGMGVGVGNLTIFPHQWINLRTNNSATIVIPYINSVPMDNMFRRHNF T LMI I PFVSLDY 300
FIN-0666_1989 NAGMGVGVGNLTIFPHQWINLRTNNSATIVIPYINSVPMDNMFRRHNF T LMI I PFVSLDY 300
Jena799_2002 NAGMGVGVGNLTIFPHQWINLRTNNSATIVMPYINSVPMDNMFRRHNF T LMI I PFVSLDY 300
Kar-87_1987 NAGMGVGVGNLTIFPHQWINLRTNNSATIVMPYINSVPMDNMFRRHNF T LMI I PFVSLDY 300
wv207_1983 NAGMGVGVGNLTIFPHQWINLRTNNSATIVMPYINNV P MDNMFRRHNF T LMI I PFVPLNY 300
20750473_2007 NAGMGVGVGNLTIFPHQWINLRTNNSATIVMPYINSVPMDNMFRRHNF T LMI I PFVSLDY 300
E11 18744_02_2002 NAGMGVGVGNLTIFPHQWINLRTNNSATIVMPYINNV P MDNMFRRHNF T LMI I PFVSLDY 300
61A3_2011 NAGMGVGVGNLTIFPHQWINLRTNNSATIVMPYINSVPMDNMFRRHNF T LMI I PFVSLDY 300
HUN_1300_1989 NAGMGVGVGNLTIFPHQWINLRTNNSATIVMPYINSVPMDNMFRRHNF T LMI I PFVSLDY 300
HUN_1337_1989 NAGMGVGVGNLTIFPHQWINLRTNNSATIVMPYINSVPMDNMFRRHNF T LMI I PFVSLDY 300
HUN_1335_1989 NAGMGVGVGNLTIFPHQWINLRTNNSATIVMPYINSVPMDNMFRRHNF T LMI I PFVSLDY 300
111/RD_2009 NAGMGVGVGNLTIFPHQWINLRTNNSATIVMPYINNV P MDNMFRRHNF T LMI I PFVPLDY 300
MorM-82_1982 NAGMGVGVGNLTIFPHQWINLRTNNSATIVMPYINNV P MDNMFRRHNF T LMI I PFVPLNY 300
Gregory_1993 NAGMGVGVGNLTIFPHQWINLRTNNSATIVMPYINNV P MDNMFRRHNF T LMI I PFVPLDY 300
E11/7611_1993 NAGMGVGVGNLTIFPHQWINLRTNNSATIVMPYINNV P MDNMFRRHNF T LMI I PFVPLDY 300
111/L41-431-1_2011 NAGMGVGVGNLTIFPHQWINLRTNNSATIVMPYINNV P MDNMFRRHNF T LMI I PFVPLDY 300
111/L41-431-6_2011 NAGMGVGVGNLTIFPHQWINLRTNNSATIVMPYINNV P MDNMFRRHNF T LMI I PFVPLDY 300
111/L41_2011 NAGMGVGVGNLTIFPHQWINLRTNNSATIVMPYINNV P MDNMFRRHNF T LMI I PFVPLDY 300
111/BGM_2009 NAGMGVGVGNLTIFPHQWINLRTNNSATIVMPYINNV P MDNMFRRHNF T LMI I PFVPLDY 300
111/Hep_2009 NAGMGVGVGNLTIFPHQWINLRTNNSATIVMPYINNV P MDNMFRRHNF T LMI I PFVPLDY 300
111/L41-431_2011 NAGMGVGVGNLTIFPHQWINLRTNNSATIVMPYINNV P MDNMFRRHNF T LMI I PFVPLDY 300
111/L41-311_2011 NAGMGVGVGNLTIFPHQWINLRTNNSATIVMPYINNV P MDNMFRRHNF T LMI I PFVPLDY 300
Gregory_1953 NAGMGVGVGNLTIFPHQWINLRTNNSATIVMPYINNV P MDNMFRRHNF T LMI I PFVPLDY 300
111/L41-211_2011 NAGMGVGVGNLTIFPHQWINLRTNNSATIVMPYINNV P MDNMFRRHNF T LMI I PFVPLDY 300
3123_2009 NAGMGVGVGNLTIFPHQWINLRTNNSATIVMPYINNV P MDNMFRRHNF T LMI I PFVPLDY 300
3123/70_2009 NAGMGVGVGNLTIFPHQWINLRTNNSATIVMPYINNV P MDNMFRRHNF T LMI I PFVPLDY 300
111/L41-121_2011 NAGMGVGVGNLTIFPHQWINLRTNNSATIVMPYINNV P MDNMFRRHNF T LMI I PFVPLDY 300
3123/28_2009 NAGMGVGVGNLTIFPHQWINLRTNNSATIVMPYINNV P MDNMFRRHNF T LMI I PFVPLDY 300
M07067754_2007 NAGMGVGVGNLTIFPHQWINLRTNNSATIVMPYINNV P MDNMFRRHNF T LMI I PFVPLNY 300
*****:*****. ****.:****. *****:*****. *: * : * : *::**

```

```

===βI=== =βI2=
E11 V5-7A_2005 SSDASTYVPI TVTVAPMCAEYNGRLRLATSLQGLPVMNTPGNSQFLTSDDFQSPSAMPQFD 360
ROU-91_1991 SSDASTYVPI TVTVAPMCAEYNGRLRLATSLQGLPVMNTPGNSQFLTSDDFQSPSAMPQFD 360
D207_2008 SSDASTYVPI TVTVAPMCAEYNGRLRLATSLQGLPVMNTPGNSQFLTSDDFQSPSAMPQFD 360
Hun/90_1990 SSDASTYVPI TVTVAPMCAEYNGRLRLATSLQGLPVMNTPGNSQFLTSDDFQSPSAMPQFD 360
HUN-1108_1989 SSDASTYVPI TVTVAPMCAEYNGRLRLATSLQGLPVMNTPGNSQFLTSDDFQSPSAMPQFD 360
Kust-86_1986 SSDASTYVPI TVTVAPMCAEYNGRLRLATSLQGLPVMNTPGNSQFVTSDDDFQSPSAMPQFD 360
FIN-0666_1989 SSDASTYVPI TVTVAPMCAEYNGRLRLATPLQGLPVMNTPGNSQFLTSDDFQSPSAMPQFD 360
Jena799_2002 ASDASTYVPI TVTVAPMCAEYNGRLRLATSLQGLPVMNTPGSTQFLTSDDFQSPSAMPQFD 360
Kar-87_1987 SSDASTYVPI TVTVAPMCAEYNGRLRLATSLQGLPVMNTPGNSQFLTSDDFQSPSAMPQFD 360
wv207_1983 SSDASTYVPI TVTVAPMCAEYNGRLRLATSLQGLPVMNTPGNSQFLTSDDFQSPSAMPQFD 360
20750473_2007 SSDASTYVPI TVTVAPMCAEYNGRLRLATSVQGLPVMNTPGNSQFLTSDDFQSPSAMPQFD 360
E11 18744_02_2002 SSDASTYVPI TVTVAPMCAEYNGRLRLATSLQGLPVMNTPGNSQFLTSDDFQSPSAMPQFD 360
61A3_2011 SSDASTYVPI TVTVAPMCAEYNGRLRLATSVQGLPVMNTPGNSQFLTSDDFQSPSAMPQFD 360
HUN_1300_1989 SSDASTYVPI TVTVAPMCAEYNGRLRLATSLQGLPVMNTPGNSQFLTSDDFQSPSAMPQFD 360
HUN_1337_1989 SSDASTYVPI TVTVAPMCAEYNGRLRLATSLQGLPVMNTPGNSQFLTSDDFQSPSAMPQFD 360
HUN_1335_1989 SSDASTYVPI TVTVAPMCAEYNGRLRLATSLQGLPVMNTPGNSQFLTSDDFQSPSAMPQFD 360

```



111/RD_2009	GLDNVFKHTLLGEILNYYAHWSGSIKLTFVFCGSAMATGKFLLAYAPPGANAPKSRKDM	480
MorM-82_1982	GLDGVFKHTLLGEILNYYAHWSGSIKLTFVFCGSAMATGKFLSAYAPPGANAPKSRKDM	480
Gregory_1993	GLDSVFKHTLLGEILNYYAHWSGSIKLTFVFCGSAMATGKFLLAYAPPGANAPKSRKDM	480
E11/7611_1993	GLDNVFKHTLLGEILNYYAHWSGSIKLTFVFCGSAMATGKFLLAYAPPGANAPKSRKDM	480
111/L41-431-1_2011	GLDNVFKHTLLGEILNYYAHWSGSIKLTFVFCGSAMATGKFLLAYAPPGANAPKSRKDM	480
111/L41-431-6_2011	GLDNVFKHTLLGEILNYYAHWSGSIKLTFVFCGSAMATGKFLLAYAPPGANAPKSRKDM	480
111/L41_2011	GLDNVFKHTLLGEILNYYAHWSGSIKLTFVFCGSAMATGKFLLAYAPPGANAPKSRKDM	480
111/BGM_2009	GLDNVFKHTLLGEILNYYAHWSGSIKLTFVFCGSAMATGKFLLAYAPPGANAPKSRKDM	480
111/Hep_2009	GLDNVFKHTLLGEILNYYAHWSGSIKLTFVFCGSAMATGKFLLAYAPPGANAPKSRKDM	480
111/L41-431_2011	GLDNVFKHTLLGEILNYYAHWSGSIKLTFVFCGSAMATGKFLLAYAPPGANAPKSRKDM	480
111/L41-311_2011	GLDNVFKHTLLGEILNYYAHWSGSIKLTFVFCGSAMATGKFLLAYAPPGANAPKSRKDM	480
Gregory_1953	GLDSVFKHTLLGEILNYYAHWSGSIKLTFVFCGSAMATGKFLLAYAPPGANAPKSRKDM	480
111/L41-211_2011	GLDNVFKHTLLGEILNYYAHWSGSIKLTFVFCGSAMATGKFLLAYAPPGANAPKSRKDM	480
3123_2009	GLDSVFKHTLLGEILNYYAHWSGSIKLTFVFCGSAMATGKFLLAYAPPGANAPKSRKDM	480
3123/70_2009	GLDSVFKHTLLGEILNYYAHWSGSIKLTFVFCGSAMATGKFLLAYAPPGANAPKSRKDM	480
111/L41-121_2011	GLDNVFKHTLLGEILNYYAHWSGSIKLTFVFCGSAMATGKFLLAYAPPGANAPKSRKDM	480
3123/28_2009	GLDSVFKHTLLGEILNYYAHWSGSIKLTFVFCGSAMATGKFLLAYAPPGANAPKSRKDM	480
M07067754_2007	GLENVFKHTLLGEILNYYAHWSGSIKLTFVFCGSAMATGKFLLAYAPPGANAPRTRKEAM	480

\*\*\*:\*\*\*\*\*:\*\*\*:\*\*\*\*\*:\*\*\*\*\*:\*\*\*\*\*:\*\*\*\*\*:\*\*\*\*\*:\*\*\*\*\*:\*\*\*:\*\*\*\*\*:\*\*\*:\*\*\*

E11 V5-7A_2005	- ==βF==	==βG==	==βH==	===	
ROU-91_1991	LGTHVVDVGLQSSCVLCIPWISQTHYRLVHQDEYTSAGNVTCWYQTGIVVPAGTPTSCS				540
D207_2008	LGTHI IWDVGLQSSCVLCIPWISQTHYRLVHQDEYTSAGNVTCWYQTGIVVPAGTPTSCS				540
Hun/90_1990	LGTHVVDVGLQSSCVLCIPWISQTHYRLVHQDEYTSAGNVTCWYQTGIVVPAGTPTSCS				540
HUN-1108_1989	LGTHVVDVGLQSSCVLCIPWISQTHYRLVHQDEYTSAGNVTCWYQTGIVVPAGTPTSCS				540
Kust-86_1986	LGTHI IWDVGLQSSCVLCIPWISQTHYRLVHQDEYTSAGNVTCWYQTGIVVPAGTPTSCS				540
FIN-0666_1989	LGTHI IWDVGLQSSCVLCIPWISQTHYRLVHQDEYTSAGNVTCWYQTGIVVPAGTPTSCS				540
Jena799_2002	LGTHVVDVGLQSSCVLCIPWISQTHYRLVHQDEYTSAGNVTCWYQTGIVVPAGTPTSCS				540
Kar-87_1987	LGTHI IWDVGLQSSCVLCIPWISQTHYRLVHQDEYTSAGNVTCWYQTGIVVPAGTPTSCS				540
wv207_1983	LGTHI IWDVGLQSSCVLCIPWISQTHYRLVQDEYTSAGNVTCWYQTGIVVPAGTPTSCS				540
20750473_2007	LGTHVVDVGLQSSCVLCIPWISQTHYRLVHQDEYTSAGNVTCWYQTGIVVPAGTPTSCS				540
E11_18744_02_2002	LGTHI IWDVGLQSSCVLCIPWISQTHYRLVQDEYTSAGNVTCWYQTGIVVPAGTPTSCS				540
61A3_2011	LGTHVVDVGLQSSCVLCIPWISQTHYRLVHQDEYTSAGNVTCWYQTGIVVPAGTPTSCS				540
HUN_1300_1989	LGTHVVDVGLQSSCVLCIPWISQTHYRLVHQDEYTSAGNVTCWYQTGIVVPAGTPTSCS				540
HUN_1337_1989	LGTHVVDVGLQSSCVLCIPWISQTHYRLVHQDEYTSAGNVTCWYQTGIVVPAGTPTSCS				540
HUN_1335_1989	LGTHVVDVGLQSSCVLCIPWISQTHYRLVHQDEYTSAGNVTCWYQTGIVVPAGTPTSCS				540
111/RD_2009	LGTHI IWDVGLQSSCVLCIPWISQTHYRLVQDEYTSAGNVTCWYQTGIVVPAGTPTSCS				540
MorM-82_1982	LGTHI IWDVGLQSSCVLCIPWISQTHYRLVQDEYTSAGNVTCWYQTGIVVPAGTPTSCS				540
Gregory_1993	LGTHI IWDVGLQSSCVLCIPWISQTHYRLVQDEYTSAGNVTCWYQTGIVVPAGTPTSCS				540
E11/7611_1993	LGTHI IWDVGLQSSCVLCIPWISQTHYRLVQDEYTSAGNVTCWYQTGIVVPAGTPTSCS				540
111/L41-431-1_2011	LGTHI IWDVGLQSSCVLCIPWISQTHYRLVQDEYTSAGNVTCWYQTGIVVPAGTPTSCS				540
111/L41-431-6_2011	LGTHI IWDVGLQSSCVLCIPWISQTHYRLVQDEYTSAGNVTCWYQTGIVVPAGTPTSCS				540
111/L41_2011	LGTHI IWDVGLQSSCVLCIPWISQTHYRLVQDEYTSAGNVTCWYQTGIVVPAGTPTSCS				540
111/BGM_2009	LGTHI IWDVGLQSSCVLCIPWISQTHYRLVQDEYTSAGNVTCWYQTGIVVPAGTPTSCS				540
111/Hep_2009	LGTHI IWDVGLQSSCVLCIPWISQTHYRLVQDEYTSAGNVTCWYQTGIVVPAGTPTSCS				540
111/L41-431_2011	LGTHI IWDVGLQSSCVLCIPWISQTHYRLVQDEYTSAGNVTCWYQTGIVVPAGTPTSCS				540
111/L41-311_2011	LGTHI IWDVGLQSSCVLCIPWISQTHYRLVQDEYTSAGNVTCWYQTGIVVPAGTPTSCS				540
Gregory_1953	LGTHI IWDVGLQSSCVLCIPWISQTHYRLVQDEYTSAGNVTCWYQTGIVVPAGTPTSCS				540
111/L41-211_2011	LGTHI IWDVGLQSSCVLCIPWISQTHYRLVQDEYTSAGNVTCWYQTGIVVPAGTPTSCS				540
3123_2009	LGTHI IWDVGLQSSCVLCIPWISQTHYRLVQDEYTSAGNVTCWYQTGIVVPAGTPTSCS				540
3123/70_2009	LGTHI IWDVGLQSSCVLCIPWISQTHYRLVQDEYTSAGNVTCWYQTGIVVPAGTPTSCS				540
111/L41-121_2011	LGTHI IWDVGLQSSCVLCIPWISQTHYRLVQDEYTSAGNVTCWYQTGIVVPAGTPTSCS				540
3123/28_2009	LGTHI IWDVGLQSSCVLCIPWISQTHYRLVQDEYTSAGNVTCWYQTGIVVPAGTPTSCS				540
M07067754_2007	LGTHI IWDVGLQSSCVLCIPWISQTHYRLVQDEYTSAGNVTCWYQTGIVVPAGTPTSCS				540

\*\*\*\*\*:\*\*\*\*\*:\*\*\*\*\*:\*\*\*\*\*:\*\*\*\*\*:\*\*\*\*\*:\*\*\*\*\*:\*\*\*\*\*:\*\*\*\*\*:\*\*\*\*\*:\*\*\*\*\*:\*\*\*\*\*

=βI====

>VP1

E11 V5-7A_2005	IMCFVSACNDFSVRLKDPFIEQSALLQGDVVEAIEGAVARVADTISSGPTNSQAVPAL	600
ROU-91_1991	IMCFVSACNDFSVRLKDPFIEQSALLQGDVVEAIEGAVARVADTISSGPTNSQAVPAL	600
D207_2008	IMCFVSACNDFSVRLKDPFIEQSALLQGDVVEAIEGAVARVADTISSGPTNSQAVPAL	600
Hun/90_1990	IMCFVSACNDFSVRLKDPFIEQSALLQGDVVEAIEGAVARVADTISSGPTNSQAVPAL	600
HUN-1108_1989	IMCFVSACNDFSVRLKDPFIEQSALLQGDVVEAIEGAVARVADTISSGPTNSQAVPAL	600
Kust-86_1986	IMCFVSACNDFSVRLKDPFIEQSALLQGDVVEAIEGAVARVADTISSGPTNSQAVPAL	600
FIN-0666_1989	MCMFVSACNDFSVRLKDPFIEQSALLQGDVVEAIEGAVARVADTISSGPTNSQAVPAL	600
Jena799_2002	LMCFVSACNDFSVRLKDPFIEQSALLQGDVVEAIEGAVARVADTISSGPTNSQAVPAL	600
Kar-87_1987	IMCFVSACNDFSVRLKDPFIEQSALLQGDVVEAIEGAVARVADTISSGPTNSQAVPAL	600
wv207_1983	IMCFVSACNDFSVRLKDPFIEQQAALLQGDVVEAVENAVARVADTISSGPTNSQAVPAL	600
20750473_2007	IMCFVSACNDFSVRLKDPFIEQSALLQGDVVEAIEGAVARVADTISSGPTNSQAVPAL	600
E11_18744_02_2002	IMCFVSACNDFSVRLKDPFIEQNALQGDVVEAVENAVARVADTISSGPTNSQAVPAL	600
61A3_2011	IMCFVSACNDFSVRLKDPFIEQSALLQGDVVEAIEGAVARVADTISSGPTNSQAVPAL	600
HUN_1300_1989	IMCFVSACNDFSVRLKDPFIEQSALLQGDVVEAIEGAVARVADTISSGPTNSQAVPAL	600
HUN_1337_1989	IMCFVSACNDFSVRLKDPFIEQSALLQGDVVEAIEGAVARVADTISSGPTNSQAVPAL	600
HUN_1335_1989	IMCFVSACNDFSVRLKDPFIEQSALLQGDVVEAIEGAVARVADTISSGPTNSQAVPAL	600
111/RD_2009	IMCFVSACNDFSVRLKDPFIEQTALLQGDVVEAVENAVARVADTISSGPTNSQAVPAL	600

MorM-82\_1982 IMCFVSACNDFSVRLLKDTPFIEQAALLQGDVVEAVENAVARVADTIGSGPNSQAVPAL 600  
 Gregory\_1993 IMCFVSACNDFSVRLLKDTPFIEQTALLQGDVVEAVENAVARVADTIGSGPNSQAVPAL 600  
 E11/7611\_1993 IMCFVSACNDFSVRLLKDTPFIEQTALLQGDVVEAVENAVARVADTIGSGPNSQAVPAL 600  
 111/L41-431-1\_2011 IMCFVSACNDFSVRLLKDTPFIEQTALLQGDVVEAVENAVARVADTIGSGPNSQAVPAL 600  
 111/L41-431-6\_2011 IMCFVSACNDFSVRLLKDTPFIEQTALLQGDVVEAVENAVARVADTIGSGPNSQAVPAL 600  
 111/L41\_2011 IMCFVSACNDFSVRLLKDTPFIEQTALLQGDVVEAVENAVARVADTIGSGPNSQAVPAL 600  
 111/BGM\_2009 IMCFVSACNDFSVRLLKDTPFIEQTALLQGDVVEAVENAVARVADTIGSGPNSQAVPAL 600  
 111/Hep\_2009 IMCFVSACNDFSVRLLKDTPFIEQTALLQGDVVEAVENAVARVADTIGSGPNSQAVPAL 600  
 111/L41-431\_2011 IMCFVSACNDFSVRLLKDTPFIEQTALLQGDVVEAVENAVARVADTIGSGPNSQAVPAL 600  
 111/L41-311\_2011 IMCFVSACNDFSVRLLKDTPFIEQTALLQGDVVEAVENAVARVADTIGSGPNSQAVPAL 600  
 Gregory\_1953 IMCFVSACNDFSVRLLKDTPFIEQTALLQGDVVEAVENAVARVADTIGSGPNSQAVPAL 600  
 111/L41-211\_2011 IMCFVSACNDFSVRLLKDTPFIEQTALLQGDVVEAVENAVARVADTIGSGPNSQAVPAL 600  
 3123\_2009 IMCFVSACNDFSVRLLKDTPFIEQTALLQGDVVEAVENAVARVADTIGSGPNSQAVPAL 600  
 3123/70\_2009 IMCFVSACNDFSVRLLKDTPFIEQTALLQGDVVEAVENAVARVADTIGSGPNSQAVPAL 600  
 111/L41-121\_2011 IMCFVSACNDFSVRLLKDTPFIEQTALLQGDVVEAVENAVARVADTIGSGPNSQAVPAL 600  
 3123/28\_2009 IMCFVSACNDFSVRLLKDTPFIEQTALLQGDVVEAVENAVARVADTIGSGPNSQAVPAL 600  
 M07067754\_2007 IMCFVSACNDFSVRLLKDTPFIEQDAILQGDVPGAVENVIVRVADTIGSGPNSQAVPAL 600  
 :\*\*\*\*\*:\* :\*:\*\*\*\*\* :\*..:\*\*\*\*\*..\*:\*\*\*\*\*

-αZ1- -αZ2- --αZ3-- ===βB=== =βC  
 E11 V5-7A\_2005 TAVETGHTSQVVPDGTMQTRHVKNYHSRSESTIENFLSRAACVYMGEYTTNTDETKRFA 660  
 ROU-91\_1991 TAVETGHTSQVVPDGTIQTRHVKNYHSRSESTIENFLSRSACVYMGEYTTNTDETKRFA 660  
 D207\_2008 TAVETGHTSQVVPDGTIQTRHVKNYHSRSESTIENFLSRSACVYMGEYTTNTDETKRFA 660  
 Hun/90\_1990 TAVETGHTSQVVPDGTMQTRHVKNYHSRSESTIENFLSRSACVYMGEYTTNTDETKRFA 660  
 HUN-1108\_1989 TAVETGHTSQVVPDGTMQTRHVKNYHSRSESTIENFLSRSACVYMGEYTTNTDETKRFA 660  
 Kust-86\_1986 TAVETGHTSQVVPDGTIQTRHVKNYHSRSESTIENFLSRSACVYMGEYTTNTDETKRFA 660  
 FIN-0666\_1989 TAVETGHTSQVVPDGTIQTRHVKNYHSRSESTIENFLSRSACVYMGEYTTNTDETKRFA 660  
 Jena799\_2002 TAVETGHTSQVVPDGTMQTRHVKNYHSRSESTIENFLSRSACVYMGEYTTNTDETKRFA 660  
 Kar-87\_1987 TAVETGHTSQVVPDGTIQTRHVKNYHSRSESTIENFLSRSACVYMGEYTTNTDETKRFA 660  
 wv207\_1983 TAVETGHTSQVTPSDTVQTRHVKNYHSRSESSIENFLSRSACVYMGEYHTTNSDQTKLFA 660  
 20750473\_2007 TAVETGHTSQVVPDGTMQTRHVKNYHSRSESTIENFLSRSACVYMGEYTTNTDETKRFA 660  
 E11\_18744\_02\_2002 TAVETGHTSQVTPSDTIQTRHVKNYHSRSESSIENFLSRSACVYMGEYTTNEDTSKLFA 660  
 61A3\_2011 TAVETGHTSQVVPDGTMQTRHVKNYHSRSESTIENFLSRSACVYMGEYTTNTDETKRFA 660  
 HUN\_1300\_1989 TAVETGHTSQVVPDGTMQTRHVKNYHSRSESTIENFLSRSACVYMGEYTTNTDETKRFA 660  
 HUN\_1337\_1989 TAVETGHTSQVVPDGTMQTRHVKNYHSRSESTIENFLSRSACVYMGEYTTNTDETKRFA 660  
 HUN\_1335\_1989 TAVETGHTSQVVPDGTMQTRHVKNYHSRSESTIENFLSRSACVYMGEYTTNTDETKRFA 660  
 111/RD\_2009 TAVETGHTSQVTPSDI IQTRHVKNYHSRSESSIENFLCRSACVYMGEYHTTNTDASKLFA 660  
 MorM-82\_1982 TAVETGHTSQVTPSDIMQTRHVKNYHSRSESSIENFLSRSACVYMGEYHTTNTDQTKLFA 660  
 Gregory\_1993 TAVETGHTSQVTPSDT MQTRHVKNYHSRSESSIENFLSRSACVYMGEYHTTNTDQTKLFA 660  
 E11/7611\_1993 TAVETGHTSQVTPSDI IQTRHVKNYHSRSESSIENFLCRSACVYMGEYHTTNTDASKLFA 660  
 111/L41-431-1\_2011 TAVETGHTSQVTPSDI IQTRHVKNYHSRSESSIENFLCRSACVYMGEYHTTNTDASKLFA 660  
 111/L41-431-6\_2011 TAVETGHTSQVTPSDI IQTRHVKNYHSRSESSIENFLCRSACVYMGEYHTTNTDASKLFA 660  
 111/L41\_2011 TAVETGHTSQVTPSDI IQTRHVKNYHSRSESSIENFLCRSACVYMGEYHTTNTDASKLFA 660  
 111/BGM\_2009 TAVETGHTSQVTPSDI IQTRHVKNYHSRSESSIENFLCRSACVYMGEYHTTNTDASKLFA 660  
 111/Hep\_2009 TAVETGHTSQVTPSDI IQTRHVKNYHSRSESSIENFLCRSACVYMGEYHTTNTDASKLFA 660  
 111/L41-431\_2011 TAVETGHTSQVTPSDI IQTRHVKNYHSRSESSIENFLCRSACVYMGEYHTTNTDASKLFA 660  
 111/L41-311\_2011 TAVETGHTSQVTPSDI IQTRHVKNYHSRSESSIENFLCRSACVYMGEYHTTNTDASKLFA 660  
 Gregory\_1953 TAVETGHTSQVTPSDT MQTRHVKNYHSRSESSIENFLSRSACVYMGGYRTTNTDQTKLFA 660  
 111/L41-211\_2011 TAVETGHTSQVTPSDI IQTRHVKNYHSRSESSIENFLCRSACVYMGEYHTTNTDASKLFA 660  
 3123\_2009 TAVETGHTSQVTPSDT MQTRHVKNYHSRSESSIENFLSRSACVYMGGYCTTNTDQTKLFA 660  
 3123/70\_2009 TAVETGHTSQVTPSDT MQTRHVKNYHSRSESSIENFLSRSACVYMGGYCTTNTDQTKLFA 660  
 111/L41-121\_2011 TAVETGHTSQVTPSDI IQTRHVKNYHSRSESSIENFLCRSACVYMGEYHTTNTDASKLFA 660  
 3123/28\_2009 TAVETGHTSQVTPSDT MQTRHVKNYHSRSESSIENFLSRSACVYMGGYCTTNTDQTKLFA 660  
 M07067754\_2007 TAAETGHTSQVTPSDTIQTRHVKNYHSRSESSIENFLCRSACVYMESYTTINSDITKLFV 660  
 \*\*.\* :\*:\*\*\*\*\* :\*..:\*\*\*\*\*..\*:\*\*\*\*\*

---αA--- =====βD===== ==βE===  
 E11 V5-7A\_2005 NWTINARRMVQMRKLEMFTYVRFDEVT FVITSKQDQGTQLGQDMPPLTHQIMYIPGG 720  
 ROU-91\_1991 NWTINARRMVQMRKLEMFTYVRFDEVT FVITSKQDQGTQLGQDMPPLTHQIMYIPGG 720  
 D207\_2008 NWTINARRMVQMRKLEMFTYVRFDEVT FVITSKQDQGTQLGQDMPPLTHQIMYIPGG 720  
 Hun/90\_1990 NWTINARRMVQMRKLEMFTYVRFDEVT FVITSKQDQGTQLGQDMPPLTHQIMYIPGG 720  
 HUN-1108\_1989 NWTINARRMVQMRKLEMFTYVRFDEVT FVITSKQDQGTQLGQDMPPLTHQIMYIPGG 720  
 Kust-86\_1986 NWTINARRMVQMRKLEMFTYVRFDEVT FVITSKQDQGTQLGQDMPPLTHQIMYIPGG 720  
 FIN-0666\_1989 NWTINARRMVQMRKLEMFTYVRFDEVT FVITSKQDQGTQLGQDMPPLTHQIMYIPGG 720  
 Jena799\_2002 NWTINARRMVQMRKLEMFTYVRFDEVT FVITSKQDQGTQLGQDMPPLTHQIMYIPGG 720  
 Kar-87\_1987 NWTINARRMVQMRKLEMFTYVRFDEVT FVITSKQDQGTQLGQDMPPLTHQIMYIPGG 720  
 wv207\_1983 SWTISARRMVQMRKLEIFTYVRFDEVT FVITSKQDQGTQLGQDMPPLTHQIMYIPGG 720  
 20750473\_2007 SWTINARRMVQMRKLEMFTYVRFDEVT FVITSKQDQGTQLGQDMPPLTHQIMYIPGG 720  
 E11\_18744\_02\_2002 SWTINARRMVQMRKLEMFTYVRFDEVT FVITSKQDQGTQLGQDMPPLTHQIMYIPGG 720  
 61A3\_2011 SWTINARRMVQMRKLEMFTYVRFDEVT FVITSKQDQGTQLGQDMPPLTHQIMYIPGG 720  
 HUN\_1300\_1989 NWTINARRMVQMRKLEMFTYVRFDEVT FVITSKQDQGTQLGQDMPPLTHQIMYIPGG 720  
 HUN\_1337\_1989 NWTINARRMVQMRKLEMFTYVRFDEVT FVITSKQDQGTQLGQDMPPLTHQIMYIPGG 720  
 HUN\_1335\_1989 NWTINARRMVQMRKLEMFTYVRFDEVT FVITSKQDQGTQLGQDMPPLTHQIMYIPGG 720  
 111/RD\_2009 SWTINARRMVQMRKLEMFTYVRFDEVT FVITSKQDQGTQLGQDMPPLTHQIMYIPGG 720  
 MorM-82\_1982 SWTISARRMVQMRKLEMFTYVRFDEVT FVITSRQDKGAKLQDMPPLTHQIMYIPGG 720



```

Gregory_1993 TLNHMGQIYVRHVNGSSPLPMTSTVRMYFKPKHVKAWVPRPRLCQYKNASTVNFTPTNV 840
E11/7611_1993 TLNRMGQIYVRHVNGSSPLPMTSTVRMYFKPKHVKVWVPRPRLCQYVNASTVNFKPTNI 840
111/L41-431-1_2011 TLNRMGQIYVRHVNGSSPLPMTSTVRMYFKPKHVKVWVPRPRLCQYVNASTVNFKPTNI 840
111/L41-431-6_2011 TLNRMGQIYVRHVNGSSPLPMTSTVRMYFKPKHVKVWVPRPRLCQYVNASTVNFKPTNI 840
111/L41_2011 TLNRMGQIYVRHVNGSSPLPMTSTVRMYFKPKHVKVWVPRPRLCQYVNASTVNFKPTNI 840
111/BGM_2009 TLNRMGQIYVRHVNGSSPLPMTSTVRMYFKPKHVKVWVPRPRLCQYVNASTVNFKPTNI 840
111/Hep_2009 TLNRMGQIYVRHVNGSSPLPMTSTVRMYFKPKHVKVWVPRPRLCQYVNASTVNFKPTNI 840
111/L41-431_2011 TLNRMGQIYVRHVNGSSPLPMTSTVRMYFKPKHVKVWVPRPRLCQYVNASTVNFKPTNI 840
111/L41-311_2011 TLNRMGQIYVRHVNGSSPLPMTSTVRMYFKPKHVKVWVPRPRLCQYVNASTVNFKPTNI 840
Gregory_1953 TLNHMGQIYVRHVNGSSPLPMTSTVRMYLKPCHKVAVVPRPRLCQYENASTVNFTPTNV 840
111/L41-211_2011 TLNRMGQIYVRHVNGSSPLPMTSTVRMYFKPKHVKVWVPRPRLCQYVNASTVNFKPTNI 840
3123_2009 TLNHMGQIYVRHVNGSSPLPMTSTVRMYLKPCHKVAVVPRPRLCQYENASTVNFTPTNV 840
3123/70_2009 TLNHMGQIYVRHVNGSSPLPMTSTVRMYLKPCHKVAVVPRPRLCQYENASTVNFTPTNV 840
111/L41-121_2011 TLNRMGQIYVRHVNGSSPLPMTSTVRMYFKPKHVKVWVPRPRLCQYVNASTVNFKPTNI 840
3123/28_2009 TLNHMGQIYVRHVNGSSPLPMTSTVRMYLKPCHKVAVVPRPRLCQYENASTVNFTPTNV 840
M07067754_2007 TLNMGQIYVRHVNGSPPLPMTSTVRIYFKPKHVKAWI PRPRLCQYVNASTVNFKPTNI 840
*** **:*:*.*.*.***** **:*:*****:.*:***** *****.*.*:

```

```

E11 V5-7A_2005 TDKRNSITYIPDTPVKPDVSNH 861
ROU-91_1991 TDKRDSITYVDPDTPVKPDVSNH 861
D207_2008 TDKRDSITYIPDTPVKPDVSNH 861
Hun/90_1990 TDKRDSITYIPDTPVKPDVSNH 861
HUN-1108_1989 TDKRDSITYIPDTPVKPDVSNH 861
Kust-86_1986 TDKRNSITYIPDTPVKPDVSNY 861
FIN-0666_1989 TDKRDSITYIPDTPVKPDVSNH 861
Jena799_2002 TDKRDSITYIPDTPVKPDVSNH 861
Kar-87_1987 TDKRDSITYIPDTPVKPDVSNH 861
wv207_1983 TDKRNSITYIPDTPVKPDVSNH 861
20750473_2007 TDKRDSITYIPDTPVKPDVSNY 861
E11 18744_02_2002 TEKRQSINYIPDTPVKPSVSTN 861
61A3_2011 TDKRDSITYIPDTPVKPDVSNY 861
HUN_1300_1989 TDKRDSITYIPDTPVKPDVSNH 861
HUN_1337_1989 TDKRDSITYIPDTPVKPDVSNH 861
HUN_1335_1989 TDKRDSITYIPHTVKPDVSNH 861
111/RD_2009 TEKRDSINYIPETVKPDVSTY 861
MorM-82_1982 TDKRDSITYIPETVVRPDVSNH 861
Gregory_1993 TDKRDSINYIPETVKPDLSNY 861
E11/7611_1993 TEKRDSINYIPETVKPDVSTY 861
111/L41-431-1_2011 TEKRDSINYIPETVKPDVSTY 861
111/L41-431-6_2011 TEKRDSINYIPETVKPDVSTY 861
111/L41_2011 TEKRDSINYIPETVKPDVSTY 861
111/BGM_2009 TEKRDSINYIPETVKPDVSTY 861
111/Hep_2009 TEKRDSINYIPETVKPDVSTY 861
111/L41-431_2011 TEKRDSINYIPETVKPDVSTY 861
111/L41-311_2011 TEKRDSINYIPETVVRPDVSTY 861
Gregory_1953 TDKRDSINYIPETVKPDLSNY 861
111/L41-211_2011 TEKRDSINYIPETV PDVSTY 861
3123_2009 TDKRDSINYIPETVKPDLSNY 861
3123/70_2009 TDKRDSINYIPETVKPDLSNY 861
111/L41-121_2011 TEKRDSINYIPETVVRPDVSTY 861
3123/28_2009 TDKRDSINYIPETVKPDLSNY 861
M07067754_2007 TEKRDSINYIPSTVKSVDVSTH 861
*:*: ** *:* *:*:..: .

```

**Appendix 2. Alignment of the sequence of the E11 5V-7A isolate with the E7 Wallace strain.** The structural domains of E7 are shown and the amino acids involved in binding to the DAF SCR domains are surrounded with: SCR2 in yellow, SCR3 in orange, SCR4 in red. Residues in contact with DAF are highlighted in grey (Plevka *et al.*, 2010)

```

>VP4
E7 Wallace      MGAQVSTQKTGAHETGLNASGNSIIHYTNINYYKDAASNSANRQDFTQDPGKFTEPVKDI 60
E11 V5-7A      MGTQVSTQKTGAHETGLNASGNSVIHYTNINYYKDAASNSANRQDFTQDPGKFTEPVKDI 60
                **.:*****.*****.*****.*****.*****.*****.*****.*****

                =βA1=  =βA2=

>VP2
E7 Wallace      MIKTMPALNSPSAEESGYSRVRSLTLGNSTITTQESANVVVGYGRWPEYLRDDEATAED 120
E11 V5-7A      MIKSMPALNSPSAEECGYSRVRSLTLGNSTITTQECANVVVAYGRWPEYLSDEEATAED 120
                ***.:*****.*****.*****.*****.*****.*****.*****.*****

                --αZ-  =βB  ==βC--αA1-  ----αA2----βD1=  =βD2=
E7 Wallace      QPTQPDVATCRFYTLESVQWEKNSAGWWWKFPPEALKDMGLFGQNMLYHYLGRAGYTIHVQ 180
E11 V5-7A      QPTQPDVATCRFYTLESVTWERESPGWWWKFPDALKDMGLFGQNMYYHYLGRAGYTIHVQ 180
                *****.***** **.:*.*****.*****.***** *****

                >-----PUFF-----
                ====βE====  --αB1-  -α
E7 Wallace      CNASKFHHQGCCLLVVCPPEAEMGCSQTDKEVAAMNLTKEEAHKFEPTKTNGEHTVQSIVC 240
E11 V5-7A      CNASKFHHQGCCLLVVCPPEAEMGCSVNVGVNEHGI SEGETAKKFSATASNGTHTVQSIVT 240
                *****:.* * .:::**:*.***. * :** *****

                -----<
                B2  --αB3--- =βF==  =βG==  =====βH=====
E7 Wallace      NAGMGVGVGNLTIIYPHQWINLRNNSCATIVMPYVNSVPMNMFRRHNFYTLMIIPFAPLDY 300
E11 V5-7A      NAGMGVGVGNLTIIYPHQWINLRNNSCATIVMPYINSVPMNMFRRHNFYTLMIIPFVSLDY 300
                *****:.*.*****.*****.*****:***.***

                ==βI==  =βI2=

                >VP3
E7 Wallace      AAQASEYVPVTVTIAPMCAEYNGRLRAY-QQGFVPLNTPGSNQFMTSDDFQSPSAMPQFD 359
E11 V5-7A      SSDASTYVPIITVTVAPMCAEYNGRLRLATSLQGLPVMNTPGSNQFLTSDDFQSPSAMPQFD 360
                :.* **.:**.:***** **.:**.:*****.*****.*****

                >----KNOB--<
                --αZ1-  αZ2-- -αZ3-  =βB  =βC=
E7 Wallace      VTPHMDIPGEVHNLMEIAEVDSVVPVNNIKVNLQSMDAYHIEVNTGNHQGEKIFAFQMOP 419
E11 V5-7A      VTPELDIPGEVKNLMEIAEVDSVVPVNNVEGKLDTMDIFRIPVQSGNQNTQVFGFQVQP 420
                ***.:*****:*****:.*:.* **.:**.:**.:**.:**.:**.:**.:**

                ---αA---  βD1  ==βD2==  ==βE==  ---αβ-
E7 Wallace      GLESVFKRTLMEIILNYYAHWSGSIKLTFTCGSAMATGKLLAYSPPGADVPAATRKQAM 479
E11 V5-7A      GLDSVFKHTLLGEIILNYYAHWSGVKLTFFVFCGSAMATGKFLAYSPPGANAPKTRKDAM 480
                **.:***:***:*****:****.*****:*****:.* **.:**

                - ==βF==  ==βG==  ==βH==  ==
E7 Wallace      LGTHMIWDIGLQSSCVLCIPWISQTHYRLVQQDEYTSAGNVTCWYQTGIVVPPGTPNKCVCV 539
E11 V5-7A      LGTHVVDVGLQSSCVLCIPWISQTHYRLVHQDEYTSAGNVTCWYQTGIVVPPAGTPTSCS 540
                ***.:**.:*****:*****:*****.*****.*****.***.***

```

```

=βI====
                                     >VP1
E7 Wallace      VLCFASACNDFSVRMLRDTPFIGQTALLQGDTEAIDNAIARVADTVASGPSNSTSIPAL 599
E11 V5-7A      IMCFVSACNDFSVRLKDTPFIEQSALLQGDVVEAIESAVARVADTISSGPTNSQAVPAL 600
                :*:.*.*****:*.***** *.*****. *:.*.*****:****:* :.*

    -αZ1-      -αZ2-      --αZ3--      ==βB====      =βC
E7 Wallace      TAVETGHTSQVEPSDTMQTRHVKNYHSRSESTVENFLSRACVYIEEYTKDQDNVNRYM 659
E11 V5-7A      TAVETGHTSQVVPDGTMQTRHVKNYHSRSESTIENFLSRAACVYMGEYTTNTDETKRFA 660
                ***** *.*****.*****:*****:****.* :.*.*:

                ---αA----      =====βD=====      ==βE====
E7 Wallace      SWTINARRMVQLRRKFELFTYMRFDMEITFVITSRQLPGTSIAQDMPPLTHQIMYIPPGG 719
E11 V5-7A      NWTINARRMVQMRKLEMFTYVRFDVEVTFVITSKQDQGTQLGQDMPPLTHQIMYIPPGG 720
                .*****:***:*.***:***:*.*****:*  **.:.*****

                ---αB-      =βF==      =βG1      βG2      βG3      =βG4 -α
E7 Wallace      PVPNSVTDFAWQTSTNPSIFWTEGNAPPRMSIPFISIGNAYSNFYDGWSHFSQNGVYGYN 779
E11 V5-7A      PIPKSTTDYAWQTSTNPSIFWTEGNAPPRMSIPFVSIGNAYSNFYDGWSHFSQNGVYGYN 780
                *:.*.*****:*****:*****:*****:*****:*****

                C-      ==βH==      =====βI=====
E7 Wallace      ALNNMGKLYARHVNKDTPYQMSSTIRVYFKPKHIRVWVPRPPRLSPYIKSSNVNFNPTNL 839
E11 V5-7A      TLNNMGQLYMRHVNGPSPLPMTSTVRVYFKPKHVKAWVPRPPRLCQYKNASTVNFSSNTNI 840
                :*****:*** ***: * *:*.*.*****:.******. * :*.*.*.*.*:

E7 Wallace      TDERSSITYVPDTIRPDVRTN 861
E11 V5-7A      TDKRNSITYIPDTVKPDVSNH 861
                **:.*.***:***:*** .:

```